An Adaptive Track Predictor for Ships

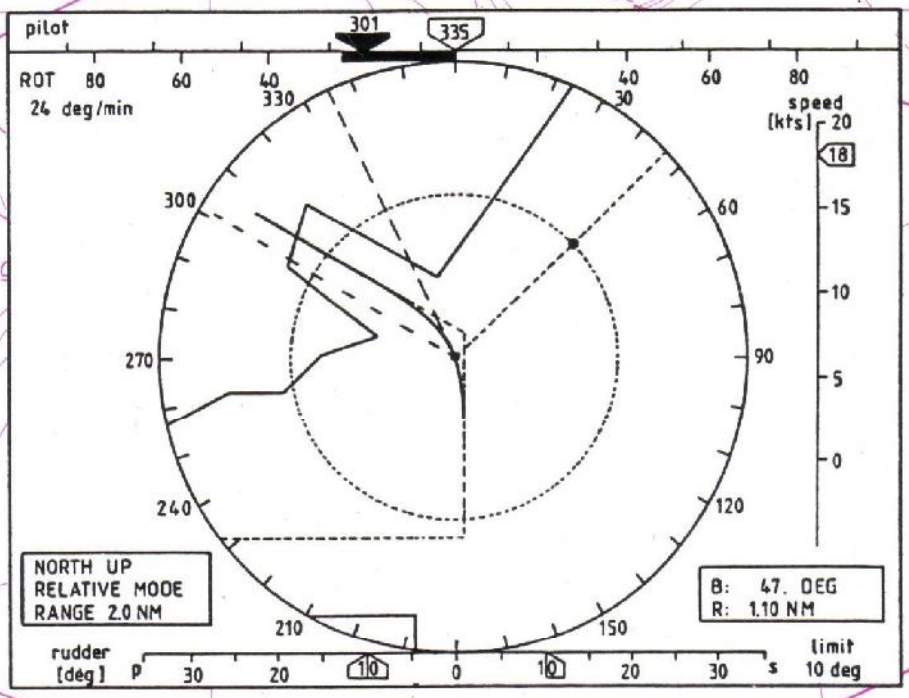

P.O. Passenier

AN ADAPTIVE TRACK PREDICTOR

FOR SHIPS

Photos and Figures 6.8, 6.9, 6.10, 6.16.a,b,c, 6.25 TNO Institute for Perception

AN ADAPTIVE TRACK PREDICTOR FOR SHIPS

PROEFSCHRIFT

Ter verkrijging van de graad van doctor
aan de Technische Universiteit Delft,
op gezag van de Rector Magnificus,
Prof.drs. P.A. Schenck,
in het openbaar te verdedigen
ten overstaan van een commissie
daartoe aangewezen door
het College van Dekanen
op dinsdag 28 november 1989 te 14.00 uur

door

Peter Otto Passenier

geboren te Sint Laurens,
elektrotechnisch ingenieur.

Dit proefschrift is goedgekeurd door de promotoren:

Prof.dr.ir. J. van Amerongen

en

Prof.dr.ir. P.P.J. van den Bosch

Aan Renée

Aan mijn ouders

The research reported in this thesis has been performed at the Delft University of Technology, Department of Electrical Engineering, Control Laboratory. The investigations were supported (in part) by the Netherlands Technology Foundation (STW).

SAMENVATTING

Dit proefschrift beschrijft het ontwerp van een baanpredictor voor schepen. Het voornaamste doel van deze baanpredictor is om de navigator tijdens het manoeuvreren te assisteren in zijn anticiperende vermogens, en zodoende een veiliger navigatie te bereiken.
Het werk is gestart als een vervolg op eerder onderzoek naar baanpredictie op het Laboratorium voor Regeltechniek van de Technische Universiteit Delft. Tevens werd op het Laboratorium voor Regeltechniek een aanzienlijke vooruitgang geboekt op het toepassen van adapterend regelen op het automatisch sturen van schepen. De behaalde resultaten zijn voornamelijk vastgelegd in het werk van Van Amerongen (1982) en van Van der Klugt (1987).

Vanwege bepaalde ontwikkelingen in de richting van integratie van manoeuvreer- en navigatiesystemen in combinatie met een nauwkeurig plaatsbepalingssysteem, is voor de ontwikkeling van het baanpredictiesysteem tevens gekozen voor een geïntegreerde opzet met betrekking tot navigatieinformatie en de stuurautomaat.

Het ontwerp van de feitelijke baanpredictor is gebaseerd op een relatief eenvoudig wiskundig model, dat wordt aangepast aan de variërende omstandigheden, in plaats van een meer complex, niet-lineair model, dat moeilijk is aan te passen.
Een geschikte methode voor het "on-line" identificeren en adapteren van de parameters van het predictiemodel en de verstoringen is bepaald door een structurele vergelijking van verschillende, bekende identificatiemethoden. Dit heeft geresulteerd in het toepassen van "extended-Kalman filtering" op het identificatie- en adaptatieprobleem. Hetzelfde concept blijkt ook toepasbaar te zijn op de koersregelaar, vergelijkbaar met de analogie tussen model referentie adapterend identificeren enerzijds en regelen anderzijds.

Voor wat betreft de presentatie van de predictieinformatie aan de navigator is gekozen voor een methode van directe superpositie van de voorspelde baan op een geïntegreerd manoeuvreer- en navigatiebeeldscherm, zoals ontwikkeld door het TNO Instituut voor Zintuigfysiologie. De invoer van gebruikerscommando's voor de predictor kon worden gerealiseerd door een kleine uitbreiding van de stuurautomaatconsole. Het blijkt dat, volgens deze geïntegreerde aanpak, de baanpredictor aan de scheepsbrug kan worden toegevoegd als een logische functie tussen navigatie (route planning) en manoeuvreren (het feitelijke koersveranderen).

Naast experimenten in een laboratoriumomgeving, voor het testen van de algoritmen voor predictie, identificatie en regeling, is met de experimentele baanpredictieopstelling een experiment uitgevoerd op de manoeuvreersimulator van het IZF-TNO in Soesterberg.
In dit experiment is de baanpredictor vergeleken met meer conventionele methoden van navigeren zoals "parallel indexen" en het gebruik van een grondsnelheidsvector. De met de baanpredictor behaalde nauwkeurigheid neemt in alle gevallen toe, maar de behaalde verbetering van de navigatieprestatie manifesteert zich vooral voor grote koersveranderingen. In dat geval wordt een reductie van de gemiddelde baanfout met 70% procent behaald, vergeleken met de conventionele condities.

SUMMARY

In this thesis the design of a track predictor for ships is reported. The principle purpose of this track predictor is to assist the navigator in his anticipating capabilities during manoeuvring, thus achieving safer navigation.
The work was originally started as a follow-up of previous research on this subject of track prediction at the Control Laboratory of Delft University of Technology. Also some considerable advances were made at the Control Laboratory in the field of applying adaptive control to the automatic steering of ships. The results are mainly reported in the work of Van Amerongen (1982) and of Van der Klugt (1987).

Because of certain developments towards the integration of manoeuvring and navigation systems in combination with an accurate positioning system, the development of the track-prediction system is based on an integrated approach with respect to the navigation information and the autopilot.

The design of the actual track predictor is based on a relatively simple mathematical model, which is adapted to the changing conditions, instead of using a more complex non-linear model, which is difficult to adapt.
A suitable method for on-line identification and adaptation of the prediction-model parameters and disturbances has been determined by a structural comparison of different, well-known, identification schemes. This has resulted in the application of Extended-Kalman filtering to the identification and adaptation problem. The same concept is shown also to be applicable to the course-changing controller, comparable to the analogy between Model-reference adaptive identification and control.

Regarding the presentation of the prediction information to the navigator, a straightforward method has been chosen of superimposing the predicted track on an integrated manoeuvring and navigation display, as designed by the TNO Institute for Perception. The input of user commands for the predictor could be obtained by a minor extension of the autopilot console. It appears that, for this integrated approach, the track predictor may be added to the ship's bridge as a logical function between navigation (track planning) and manoeuvring (actual course changing).

Besides experiments in a laboratory environment to test the algorithms for prediction, identification and control, a manoeuvring-simulator experiment was performed with the experimental track-prediction set-up at the TNO Institute for Perception in Soesterberg.
In this experiment the track predictor was tested against more conventional methods of navigation such as parallel indexing and the presentation of a ground-speed vector.
Although the overall accuracy is improved by using the track predictor, this improvement of the navigational performance especially manifests itself for large course changes. In these cases a reduction of the average track error with 70 % was obtained, compared to conventional conditions.

CONTENTS

LIST OF SYMBOLS

a_f, b_f	discrete parameters of the wave-colouring model
a_R, b_R	discrete parameters of the yaw reference model
a_s, b_s	discrete parameters of the first-order yaw transfer
A,B,C,D	matrices representing the discrete model
C_x, C_y, C_n	geometrical factors
F(k)	covariance matrix of the parameter estimation error
F_w	wind force
F_w^*	normalized wind force
g	acceleration of gravity
G	the ship's centre of gravity
H	observation matrix
I_{zz}	moment of inertia with respect to the z-axis
J_p, J_r	criterion functions
k	time index
K	gain of the first-order Nomoto yaw model
K^*	normalized gain of the Nomoto model
K(k)	gain matrix for the a-priori estimation
K_p, K_d	autopilot gains

K_R^*	normalized gain of the yaw reference model
K_u	gain of the first-order loss-of-speed model
K_u^*	normalized gain of the loss-of-speed model
$K_y(k)$	update gain for the estimated process output
$K_\vartheta(k)$	gain matrix for the estimated process parameters
$K_\rho(k)$	track scaling factor
L	length of the ship
m	mass of the ship
M(k)	covariance matrix of the a-priori estimation error
N	moment with respect to the ship's z-axis
N_w	additional input of the yaw model
P(k)	covariance matrix of the a-posteriori estimation error
Q	covariance matrix of the system noise
r	rate of turn or course-angular velocity
$\tilde{r}$	wave disturbed rate of turn
r^*	normalized rate of turn
R	covariance matrix of the observation noise
r_p	predicted rate of turn
r_p^*	normalized predicted rate of turn
s	travelled distance

s^*	normalized travelled distance
S	relevant area of the ship's superstructure
$S_\Theta(\omega)$	wave spectrum
T_s	time unit of the discrete system
u	speed in forward direction
$\tilde{u}$	measured forward speed
u^*	relative loss of forward speed
u_{cx}, u_{cy}	current speed in x_0- and y_0- direction
$\underline{u}(k)$	input of the discrete system
u_R	controller setpoint
$\underline{U}$	instantaneous speed vector
U_c	current speed
U_p	predicted forward speed
U_0	cruising speed
v	drift or sway speed
v^*	normalized sway speed
v_f	state of the wave-colouring model
$\underline{v}(k)$	observation-noise vector
v_p	predicted sway speed
v_p^*	normalized predicted sway speed

v_r	observation noise introduced by the rate-of-turn sensor
v_u	forward-speed observation noise
$\underline{v}_x$	position observation noise
v_ψ	observation noise introduced by the compass
V_w	wind speed
V_{wr}	relative wind speed
$\underline{w}(k)$	state system-noise vector
$\underline{w}_\Theta(k)$	parameter system-noise vector
$\underline{x}(k)$	state vector of the discrete system
$\tilde{\underline{x}}(k)$	a-priori estimation of the state vector
$\hat{\underline{x}}(k)$	a-posteriori estimation of the state vector
x,y	ship-fixed coordinate system
$\underline{x}_p$	ship's predicted position
$\underline{x}_p^*$	normalized predicted position
$\underline{x}_s$	ship's actual position
$\tilde{\underline{x}}_s$	observed ship's position
$\underline{x}_s^*$	normalized ship's position
x_0,y_0	space-fixed coordinate system
X,Y	forces in the x- or y- direction
$X_u,X_v,...$	hydrodynamic derivatives

X_0, Y_0	forces in the x_0- or y_0- direction
$\underline{y}$	process output
$\underline{z}(k)$	observation vector
$\underline{\tilde{z}}(k)$	noise-corrupted observation vector
β	drift angle
δ	rudder angle
δ_{max}	rudder limit
δ_{tmax}	trial rudder limit
Δu	loss of forward speed
$\Delta \underline{x}_u$	displacement due to the forward speed
$\Delta \underline{x}_v$	displacement due to the sway speed
ϵ	heading error
$\underline{\epsilon}$	prediction error
ϵ_p	predicted heading error
γ	drift or sway constant
γ^*	normalized drift or sway constant
γ_p	sway constant of the prediction model
γ_r	relative wind direction
γ_w	relative wave direction

λ	forgetting factor
Λ	interpolation matrix
$\underline{\vartheta}$	parameter vector
$\underline{\hat{\vartheta}}$	estimated parameter vector
$\underline{\vartheta}_c$	controller parameter vector
$\underline{\vartheta}_R$	reference-model parameter vector
τ	time constant of the first-order yaw model
τ^*	normalized time constant of the yaw model
τ_R^*	normalized time constant of the yaw reference model
τ_u	time constant of the loss-of-speed model
τ_u^*	normalized time constant of the loss-of-speed model
ω	relative wave frequency
ω_0	actual wave frequency
ψ	course angle or heading
$\tilde{\psi}$	wave-disturbed course angle
$\underline{\Psi}$	process signal vector
$\underline{\hat{\Psi}}$	estimated signal vector
$\underline{\Psi}_c$	controller signal vector
ψ_c	current direction
ψ_p	predicted course angle

ψ_r	heading setting
ψ_t	trial heading setting
ψ_w	wind direction

1 INTRODUCTION

1.1 Track prediction

During coastal navigation, the safety of the ship, the avoidance of groundings and collisions, is directly related to the accuracy of the own-ship's heading and position control (Kristiansen, 1980). To realize accurate control of the ship's motions relative to the ship's surroundings, the navigator should have anticipating capabilities with respect to the ship's actual track in relation to the planned track. Using this anticipation the future error between the planned (desired) track and the expected position may be minimized. The human behaviour to realize this minimization may be characterized by two elements (Schuffel, 1986):

- *Open-loop element*: the choice of manoeuvring actions on the basis of initial conditions and knowledge of the ship's manoeuvring properties (cognitive anticipation).
- *Closed-loop element*: corrections of manoeuvring actions on the basis of references. These references are used to judge the correctness of the actual track sailed with respect to the planned track (perceptive anticipation).

In his study on human control of ships, Schuffel showed that the open-loop element is not accurate, whereas the use of references (closed-loop element) can lead to accurate manoeuvring.

To improve the navigator's anticipating capabilities and thus the resulting accuracy of the ship's control, a track-prediction system can be useful. Previous research on this topic ranges from extrapolation methods (Bernotat, 1971) to prediction on the basis of a mathematical model of the process to be controlled (Kelley, 1968). A more practical study to demonstrate the possible advantages of track prediction for the accurate control of the ship's motions has been carried out by Van Berlekom (1977).

At the Control Laboratory of Delft University of Technology previous research has been carried out on possible structures of the mathematical prediction model to achieve an acceptable prediction of the ship's track (Nanninga, 1974; Reissenweber, 1975; Boonekamp, 1978; Van den Arend, 1979). Lack of display and computing power, however, prohibited the realization of an experimental set-up which could be tested in a realistic environment.

Since then there have been some important developments regarding the information presentation to the navigator:

- development of synthetic displays for the presentation of radar information,
- start of the development of an electronic chart for the presentation of navigation information,
- design of a bridge set-up for the 1990s with integration of manoeuvring and navigation information. This set-up should enable one-man-bridge ship steering (Van Breda et al., 1985).

Further, the availability of an accurate and world-wide positioning system such as the Global Positioning System (G.P.S.) opens further possibilities for automatic navigation such as a track-keeping system (Van Amerongen and Van Nauta Lemke, 1986).

1.2 The track-prediction project

In December 1984 new developments enabled a continuation of the former work on track prediction. The project "Track prediction of ships for safer navigation" was started at the Control Laboratory of the Delft University of Technology. This project was supported (in part) by the Netherlands Technology Foundation (STW). The aim of the project was to develop a track predictor as a manoeuvring aid for the navigator, in order to achieve safer navigation.

At the same time, considerable advances were made at the Control Laboratory in the field of applying adaptive control to the automatic steering of ships, which is mainly reported in the work of Van Amerongen (1982) and Van der Klugt (1987). Therefore, at the start of the track-prediction project, it was decided to adopt the following approach:

- apply the concepts of adaptive filtering and control to the track-prediction problem,
- realize an experimental set-up to test the contribution of the track predictor to the navigational performance.

Because of the developments with respect to integration of navigation and manoeuvring systems, the integration of the track predictor with the autopilot was taken as a starting point. In this way an integrated system could be obtained for accurate track keeping and changing from one straight track to another. Further,

an acceptable level of automation could be obtained with respect to the navigation tasks to be performed by the navigator.

The actual design of the track predictor was based on two elements which characterize the human steering behaviour:
prediction of the ship's track by a relatively simple mathematical model of the ship's manoeuvring behaviour (open-loop element), which is adapted on the basis of observations during manoeuvring (closed-loop element).

In the first phase of the project the research was devoted mainly to the development of the experimental set-up. This development consists of:

- research on simple mathematical prediction models which are sufficiently accurate to reflect the ship's dynamics, but may be identified and adapted to varying surroundings on the basis of measurements,
- research on the application and implementation of adaptive schemes into the predictor and autopilot,
- testing of the algorithms in a laboratory environment.

A suitable method for on-line identification of the prediction-model parameters and the disturbances on the basis of noise-corrupted measurements has been determined by a structural comparison of different, well-known, identification schemes. This has resulted in the application of Extended-Kalman filtering to the identification and adaptation problem. The same concept was shown also to be applicable to the course-changing controller, analogous to Model Reference Adaptive Control.

During the final phase of the project there was closer cooperation with the TNO Institute for Perception in Soesterberg. Because the usefulness of the predictor can only be judged when it is really used by the human operator in a realistic environment, the purpose of the cooperation with TNO was:

- To prepare and carry out a simulator experiment on the manoeuvring simulator of the TNO institute in order to demonstrate the effect of the track predictor on the navigational performance in tracking tasks.
- To determine how the interaction between the predictor and the navigator could take place in an efficient way. This resulted in an integration of the prediction information with a General Navigation Display as was designed by the TNO institute for the "Bridge '90" experiment (Boer and Schuffel, 1985) and a proposal for a user's console for the interaction with the predictor (Passenier, 1987).

The results of this simulator experiment are regarded as being a good indication as to whether the developed track predictor could be useful as a manoeuvring aid on board a real ship. The experiment indicates that the proposed predictor was quite successful.

1.3 Preview

This thesis describes the design of an adaptive track predictor, which is mainly based on the theory of Kalman filtering. The thesis is organized as follows:

Chapter two deals with the mathematical models of the ship's steering behaviour and their relation to the ship's track. Further, a mathematical description of the disturbances acting upon the ship will be given.

Chapter three describes the development of a relatively simple, basic prediction model for the prediction of the ship's track, which is sufficiently accurate. For this purpose a generalized description of the ship's track is presented as a tool for comparison between different prediction models.

Chapter four discusses the theoretical background of different schemes for on-line state and parameter estimation. This results in a unified description of both equation-error and output-error based identification schemes on the basis of the theory of Kalman filtering. Further, the unification is extended from identification to the field of Model-Reference Adaptive Control (MRAC).

In *Chapter five* the theory, presented in Chapter four, is applied to the actual track-prediction system. This yields different algorithms for filtering, identification, prediction and control.

Chapter six deals with the actual realization of the algorithms on an experimental set-up. Further, the results obtained with this experimental set-up are presented. Besides several experiments in a laboratory environment, in order to test the prediction and adaptation algorithms, a simulator experiment was performed on the manoeuvring simulator of the TNO Institute of Perception in Soesterberg. This controlled experiment was set up to investigate the usefulness of the track predictor as a manoeuvring aid.

Finally in *Chapter seven* conclusions are drawn and suggestions are given for further research.

2 MATHEMATICAL MODELLING

2.1 Introduction

Mathematical models which describe the motions of a manoeuvring ship cover a wide range of applications which can be divided into the following classes:

- *Ship design:*
  Improvement of the ship's manoeuvring properties in the design phase on the basis of mathematical models which relate the parameters of the ship design (for instance rudder surface) to the manoeuvring behaviour of the ship (for instance turning-circle diameter).
- *Simulation:*
  Description and improvement of the human steering behaviour, especially for large ships, by means of a manoeuvring simulator. The mathematical model implemented in this simulator should relate the steering actions to the resulting ship's motions as realistically as possible on a "real time basis". Detailed simulation studies of this type also provide the possibility of improving the dimensioning of the ship's restricted manoeuvring area in, for instance, coastal navigation.
- *Autopilot design:*
  Design of an autopilot for the accurate control of the ship's motions (course-keeping and track-keeping). Models for this purpose are usually identified for a specific ship on the basis of full-scale trials after which the suitable controller structure and parameters can be determined on the basis of this "control" model.

From this brief description of the different types of applications for the mathematical models it already has become clear that the structure of the mathematical model itself (the type of the model) depends largely on the application for which the model is intended:

- The mathematical models used to improve the ship's design are derived from the physical laws which govern the ship's motions. For this purpose the hydrodynamic forces which are exerted on the ship are divided into several components the coefficients of which may be determined from scale model tests in, for instance, a towing tank. By changing the design parameters of the ship, the relation between these parameters and the manoeuvring behaviour of the

ship can be determined. Because the mathematical models of this type are characterized by the hydrodynamic approach, these models will from now on be referred to as *hydrodynamic models* (see, for instance, Eda and Crane, 1965).
- For the realistic simulation of manoeuvres a mathematical model of the hydrodynamic type could be used, but this is no longer a necessity. In principle, a model which describes the empirical relations between the relevant variables of a manoeuvring ship would be sufficient. A proper structure for this *empirical model* may be obtained by the simplification of the complex hydrodynamic equations. Because the empirical models do not require the detailed knowledge of all the ship's hydrodynamic coefficients, model tuning can be achieved on the basis of the measured ship's response to properly chosen test signals at the input of the system during full-scale trials (Van Leeuwen, 1970).
- Transforming the linear part of an empirical model to the Laplace domain yields a set of (coupled) *transfer functions*. To account for the static non-linear relationship between the different variables, usually a non-linear part of the algebraic type is added. This yields a description of the ship's dynamics in a suitable form for the design of an autopilot, such as a course-keeping controller (for a survey on this type of model, see Van Amerongen, 1982).

Reviewing these different types of mathematical models it can be concluded that for a track-prediction application the analysis may be restricted to an empirical model. Such a model is able to give a sufficient description of the ship's manoeuvring behaviour without the need for an extensive identification procedure. Because the empirical model gives a relation between different signals, the variables of interest for a track-prediction system first have to be introduced (the term signals is used to emphasize the nature of the empirical model which relates different variables to each other on the basis of measurements).
The principle input signal for the manoeuvring ship is the rudder angle which has a direct dynamic relation to the ship's heading angle. This heading signal is, together with the ship's speed, related to the ship's path by kinematic relations. Other factors which cannot be instantaneously controlled but have an effect on the ship's manoeuvring behaviour are considered to be part of the ship's environment and are therefore classified as disturbances (Figure 2.1). These disturbances can be subdivided into two categories (Van Amerongen, 1982):

- disturbances which can be structurally incorporated into the model as additional input signals (*additive* disturbances).
- disturbances which influence the parameters of the model and are incorporated as multiplicative signals (*multiplicative* disturbances).

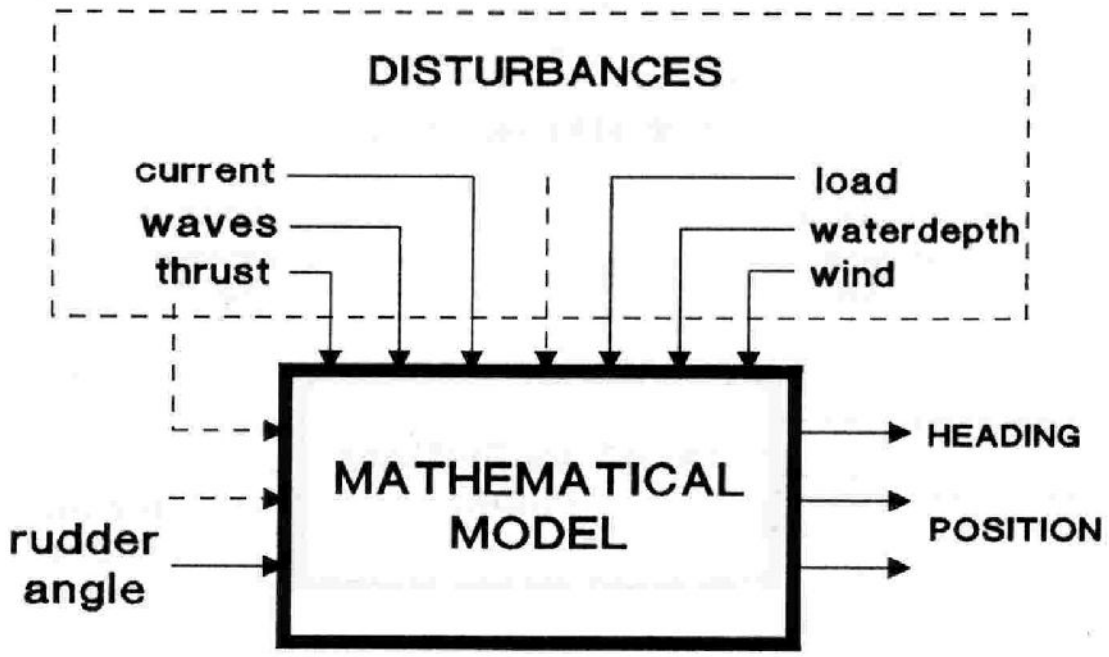

Fig. 2.1 Definition of the ship's input and disturbances

Note that in Figure 2.1 also the thrust is classified under the disturbances, because for prediction purposes, the thrust during a manoeuvre is considered to be constant and therefore any thrust deviation is regarded as a disturbance influencing the speed of the ship.

2.2 Mathematical models based on physical laws

In this section the ship's equations of motion are derived directly from Newton's law, after defining those ship's motions which are of interest to this study.

2.2.1 The ship's motions

To define the different ship's motions a coordinate system is introduced according to Figure 2.2. The origin of this ship-fixed axis system coincides with the ship's center of gravity G, from which the axes x, y and z are chosen along the ship's axes of symmetry.
Although in Figure 2.2 there are in total six degrees of freedom for the ship's motions (displacement along the x,y and z axis and rotations around these axes),

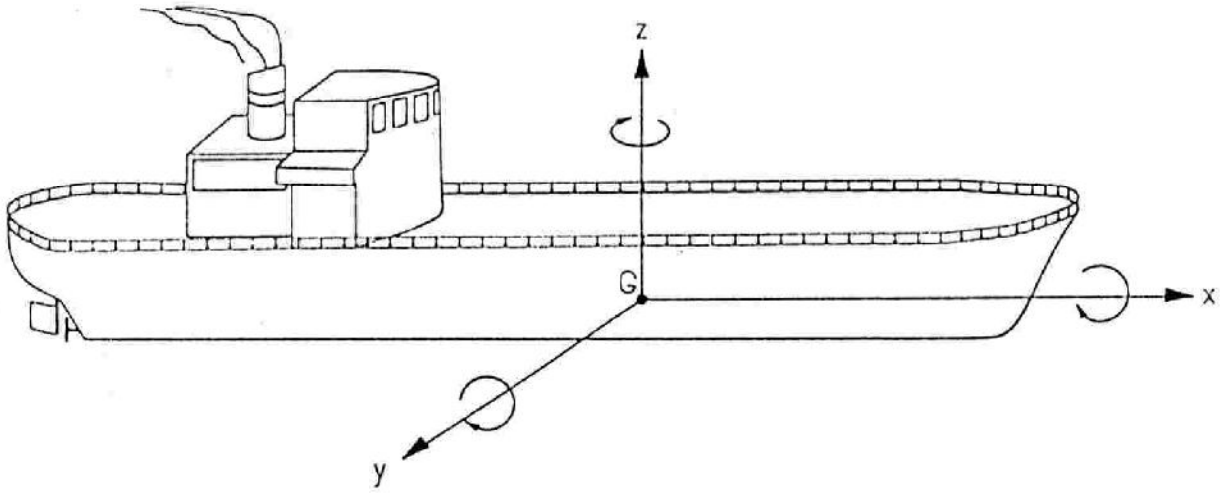

Fig. 2.2 Choice of the coordinate system

the only motions considered relevant to this study are those in the horizontal x,y plane, thus three motions of interest:

- Displacement along the x-axis (surge motion)
- Displacement along the y-axis (sway motion)
- Rotation around the z-axis (yaw motion)

2.2.2 The equations of motion

In order to apply Newton's law for the mathematical description of the ship's motions (surge, sway and yaw) a space-fixed coordinate system is defined according to Figure 2.3, with the variables of interest defined according to Table 2.1.

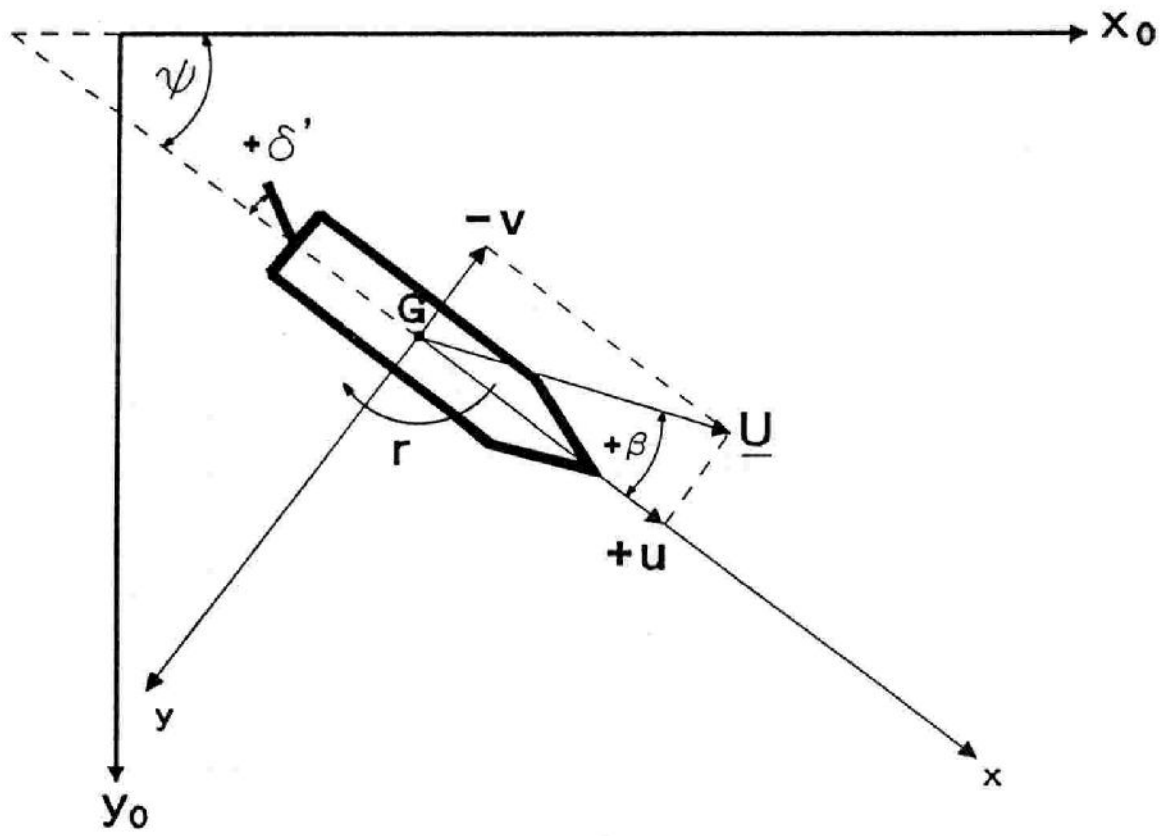

Fig. 2.3 The space-fixed coordinate system

Table 2.1 Definition of variables

x_0, y_0	space-fixed coordinate system
x,y	ship-fixed coordinate system
ψ	course angle or heading
$r = \dot{\psi} = d\psi/dt$	rate of turn or course-angular velocity
δ'	rudder angle
β	drift angle
G	ship's center of gravity
$\underline{U} = u - v$	instantaneous speed vector
$u = dx/dt$	speed in forward direction
$v = dy/dt$	drift or sway speed
X_0, Y_0	forces in the x_0- or y_0- direction
X,Y	forces in the x- or y- direction
N	moment with respect to the z-axis
m	mass of the ship
I_{zz}	moment of inertia with respect to the z-axis

Direct application of Newton's law on the moving object (ship) in this space-fixed coordinate system yields:

$$m \frac{d^2 x_0}{dt^2} = X_0 \qquad (2.1)$$

$$m \frac{d^2 y_0}{dt^2} = Y_0 \qquad (2.2)$$

$$I_{zz} \frac{d^2 \psi}{dt^2} = N \qquad (2.3)$$

To relate these general equations of motion to ship-fixed quantities such as propeller thrust, hull resistance and so on, it is convenient to transform (2.1)-(2.3) from the space-fixed coordinate system to the ship-fixed coordinate system, after which the ship's path relative to the space-fixed coordinate system can be determined by kinematic relations described in Section 2.4.
This transformation yields:

$$m (\dot{u} - vr) = X \qquad (2.4)$$

$$m (\dot{v} + ur) = Y \qquad (2.5)$$

$$I_{zz} \dot{r} = N \qquad (2.6)$$

where X and Y are the total forces on the ship's hull in the x- and the y-directions which cause the moment N around the z-axis.
The terms -mvr and +mur which appear in (2.4) and (2.5) describe the added resistance of the ship due to the turning (centripetal components). The effect of these components on the ship's path are treated in Section 2.4 where the kinematic relations are discussed. Although it is difficult to determine the exact relationship between X,Y and N and all the variables involved, a reasonable approximation may be obtained by a Taylor-series expansion.
For this purpose X,Y and Z are written as:

$$X = X(u,\dot{u},v,\dot{v},r,\dot{r},\delta',\dot{\delta}',u^2,v^2,r^2,.....) \qquad (2.7)$$

$$Y = Y(u,\dot{u},v,\dot{v},r,\dot{r},\delta',\dot{\delta}',u^2,v^2,r^2,.....) \qquad (2.8)$$

$$N = N(u,\dot{u},v,\dot{v},r,\dot{r},\delta',\dot{\delta}',u^2,v^2,r^2,.....) \qquad (2.9)$$

which for small variations $\Delta u,\Delta v,\Delta r,...$ yields:

$$\Delta X = X_u \Delta u + X_{\dot{u}} \Delta\dot{u} + X_v \Delta v + X_{\dot{v}} \Delta\dot{v} + X_r \Delta r + X_{\dot{r}} \Delta\dot{r} + \\ + X_{\delta'} \Delta\delta' + X_{\dot{\delta}'} \Delta\dot{\delta}' + \text{higher-order terms} \qquad (2.10)$$

$$\Delta Y = Y_u \Delta u + Y_{\dot{u}} \Delta\dot{u} + Y_v \Delta v + Y_{\dot{v}} \Delta\dot{v} + Y_r \Delta r + Y_{\dot{r}} \Delta\dot{r} + \\ + Y_{\delta'} \Delta\delta' + Y_{\dot{\delta}'} \Delta\dot{\delta}' + \text{higher-order terms} \qquad (2.11)$$

$$\Delta N = N_u \Delta u + N_{\dot{u}} \Delta\dot{u} + N_v \Delta v + N_{\dot{v}} \Delta\dot{v} + N_r \Delta r + N_{\dot{r}} \Delta\dot{r} + \\ + N_{\delta'} \Delta\delta' + N_{\dot{\delta}'} \Delta\dot{\delta}' + \text{higher-order terms} \qquad (2.12)$$

where X_u , X_v ,.... are the *hydrodynamic derivatives* of X with respect to variables u , v ,.....:

$$X_u = \frac{\delta X}{\delta u} \quad , \quad X_v = \frac{\delta X}{\delta v} \quad , \quad ..... \qquad (2.13)$$

Denoting the small variations $\Delta u,\Delta v,...$ as u,v,... and substituting this Taylor-series expansion for X, Y and N in (2.4)-(2.6) finally yields:

$$m(\dot{u} - vr) = X_u u + X_{\dot{u}}\dot{u} + X_v v + X_{\dot{v}}\dot{v} + X_r r + X_{\dot{r}}\dot{r} + X_{\delta,\delta'}\delta' + X_{\dot{\delta},\dot{\delta}'}\dot{\delta}' + \text{higher-order terms} \quad (2.14)$$

$$m(\dot{v} + ur) = Y_u u + Y_{\dot{u}}\dot{u} + Y_v v + Y_{\dot{v}}\dot{v} + Y_r r + Y_{\dot{r}}\dot{r} + Y_{\delta,\delta'}\delta' + Y_{\dot{\delta},\dot{\delta}'}\dot{\delta}' + \text{higher-order terms} \quad (2.15)$$

$$I_{zz}\dot{r} = N_u u + N_{\dot{u}}\dot{u} + N_v v + N_{\dot{v}}\dot{v} + N_r r + N_{\dot{r}}\dot{r} + N_{\delta,\delta'}\delta' + N_{\dot{\delta},\dot{\delta}'}\dot{\delta}' + \text{higher-order terms} \quad (2.16)$$

which are the general hydrodynamic equations for the surge, sway and yaw motions of the ship. To determine the hydrodynamic coefficients X_u, Y_u, N_u and so on, it is convenient to split the forces and the moment exerted on the ship into separate contributions of the hull (resistance), the propeller (thrust) and rudder (resistance and moment):

$$X = X_{hull} + X_{rudder} + X_{prop} \quad (2.17)$$

$$Y = Y_{hull} + Y_{rudder} \quad (2.18)$$

$$N = N_{hull} + N_{rudder} \quad (2.19)$$

By using superposition the coefficients of (2.17)-(2.19) can be determined independently.

The model (2.14)-(2.16) is a general approximation for the ship motions from which models for design improvement (Eda and Crane, 1965) as well as models for detailed simulation of manoeuvring (Abkowitz, 1964) can be derived. For control purposes the higher-order terms are in most cases disregarded, thus obtaining a linear model which in principle is only valid for small variations of the variables involved.

Neglecting these higher-order terms and assuming the forward speed to be constant, leads to the simple linear model of (2.20)-(2.21) which has been suggested by Davidson and Schiff (1946):

$$m\,(\dot{v} + ur) = Y_{\delta},\delta' + Y_v v + Y_{\dot{v}}\dot{v} + Y_r r + Y_{\dot{r}}\dot{r} \qquad (2.20)$$

$$I_{zz}\,\dot{r} = N_{\delta},\delta' + N_v v + N_{\dot{v}}\dot{v} + N_r r + N_{\dot{r}}\dot{r} \qquad (2.21)$$

Although it is difficult to determine the parameters of this model on the basis of full-scale trials, the model will be demonstrated to be a good starting point for the derivation of the empirical models in the following section.

2.3 Empirical models

As stated in the introduction, models which are based on the equations of motion are not attractive for control and prediction applications because of the complexity and the number of unknown parameters involved. Taking the underlying structure of these models as a starting point, however, rather simple models can be derived which are of an empirical nature, and may be described by transfer functions.

2.3.1 The transfer from rudder to rate of turn

Considering the model as suggested by Davidson and Schiff and eliminating the sway velocity v yields a very simple second-order model for the transfer from rudder to rate of turn, which again may be approximated by a first-order model according to (2.22) (Nomoto, 1957):

$$\tau\dot{r} + r = K\delta \qquad (2.22)$$

Note that in order to obtain a positive gain in the transfer functions from rudder angle to rate of turn, in (2.22) and in the following the rudder angle is defined as:

$$\delta = -\delta' \qquad (2.23)$$

The corresponding transfer function of (2.22) is given by:

$$\frac{r(s)}{\delta(s)} = \frac{K}{s\tau + 1} \qquad (2.24)$$

Because this model has been derived from the Davidson and Schiff model the first-order Nomoto model has, of course, the same limitations:

- Valid only for small rudder angles (The Davidson and Schiff equations became linear by neglecting the higher-order terms in the Taylor-series expansion).
- Valid only for a specific and constant forward speed (under this assumption the equation for the description of the forward speed vanishes).

Therefore, although for control applications such as course-keeping this model is still very attractive (Van Amerongen, 1982), for track-prediction purposes the limitations mentioned here have to be considered more carefully.
To examine the non-linearity of the transfer from rudder to rate of turn for large rudder angles, the spiral characteristic may be used, which describes the static relation between rudder angle and rate of turn for all rudder angles. From this spiral characteristic the *course stability* or *course unstability* of the ship can be seen. The phenomenon of course stability can be best illustrated by Figure 2.4, where a spiral characteristic for both types of ship is given.

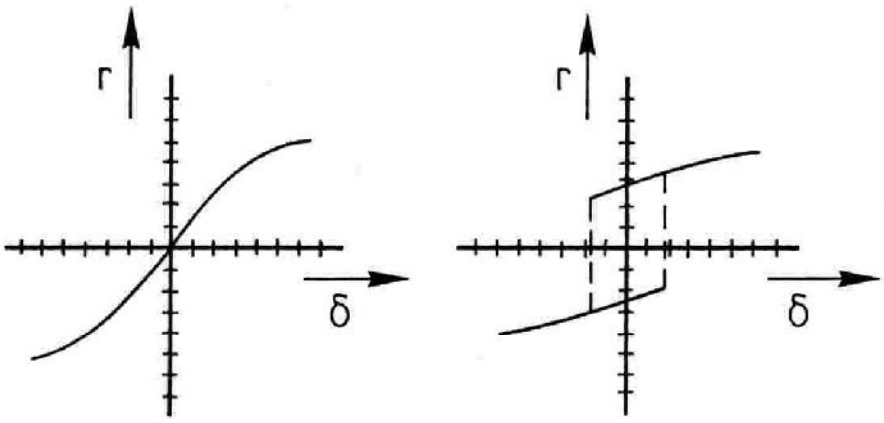

Course stable *Course unstable*

Fig. 2.4 Spiral characteristic for a course stable and unstable ship

In order to give a mathematical description of the phenomenon of course unstability and to get a better approximation for the non-linear relation between rudder and rate of turn for course-stable ships some authors suggest the addition of a non-linear component to the second-order Nomoto (Bech, 1969) or first-order Nomoto model (Norrbin, 1963) according to (2.25).

$$T\dot{r} + H(r) = K\delta \qquad (2.25)$$

where H(r) is a non-linear function of r.
From (2.25) it follows that the stationary relation ($\dot{r} = 0$) between rate of turn and rudder angle, which is called the reversed spiral characteristic, is given by:

$$H(r_{ss}) = K\delta \qquad (2.26)$$

with r_{ss} the stationary rate of turn.

This reversed spiral characteristic may, also for course-unstable ships, rather easily be determined on the basis of the *reversed spiral test* (Bech, 1968).
A suitable function for H(r) which enables, among others, the description of course unstability is in a general form:

$$H(r) = \alpha_3 r^3 + \alpha_2 r^2 + \alpha_1 r + \alpha_0 \qquad (2.27)$$

In (2.27) the coefficient α_0 can be used to describe the asymmetry of the ship (steady turning at zero degrees rudder) and a negative value of α_1 enables a good approximation for the reversed spiral characteristic of a course-unstable ship. To describe the reversed spiral characteristic of symmetrical ships a sufficient form of H(r) is given by (2.28), which together with (2.25) is Norrbin's model.

$$H_s(r) = \alpha_3 r^3 + \alpha_1 r \qquad (2.28)$$

The corresponding block-diagram is presented in Figure 2.5

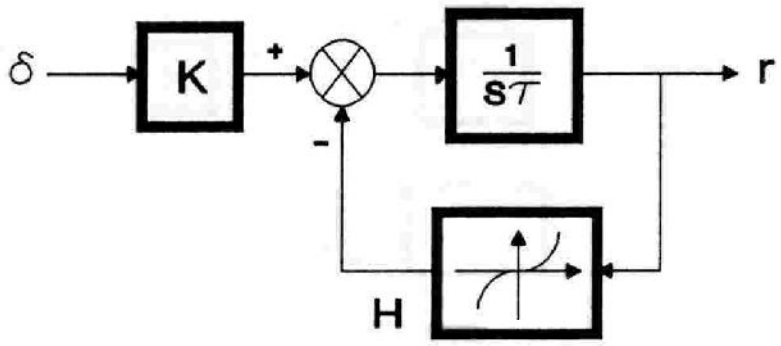

Fig. 2.5 Norrbin's model

Having eliminated the inability of the Nomoto model to describe the relation between rudder angle and rate of turn for large rudder angles, the fact remains that the resulting models of Bech and Norrbin are still only valid for a specific, constant value of the ship's thrust. Therefore, in order to apply (2.25) for different thrusts and to describe some characteristic phenomena which are caused by the loss of forward speed during a manoeuvre, in the following sections attention will be focussed on the empirical description of this forward speed for a manoeuvring

ship and the resulting effect on the ship's yaw motion.

2.3.2 Description of the ship's forward speed

In Section 2.2.2 an equation for the ship's forward speed was derived, based on the Newtonian equations of motion:

$$m(\dot{u} - vr) = X \approx X_{prop} + X_{hull} \qquad (2.29)$$

where the propeller thrust X_{prop} is related to the number of propeller revolutions by the *propeller thrust function* and the hull resistance X_{hull} is, among others, a function of the forward speed u.

For a non-manoeuvring ship (zero rate of turn) this implies that the ship is accelerated to a cruising speed U_0 at which the hull resistance equals the propeller thrust:

$$m\dot{u} = 0 = X_{prop} + X_{hull} \qquad (2.30)$$

$$u = U_0 \qquad (2.31)$$

For a manoeuvring ship (2.29) can be rewritten to (2.32) with $+mvr$ the added resistance due to the ship's turning:

$$m\dot{u} = X + mvr \qquad (2.32)$$

Carrying out a first-order Taylor expansion around $u = U_0$ yields:

$$\begin{aligned} m\dot{u} &= X_{(u=U_0)} - X_u\Delta u + mvr \\ &= 0 - X_u\Delta u + mvr \end{aligned} \qquad (2.33)$$

where

$$X_u = \left.\frac{\delta X}{\delta u}\right|_{(u=U_0)} \quad ; \quad \Delta u = U_0 - u \qquad (2.34)$$

Noting that $dU_0/dt = 0$, Eq. (2.33) may be written as an equation for Δu:

$$m\dot{\Delta u} = X_u\Delta u - mvr \qquad (2.35)$$

Approximating the sway velocity by $v = -\gamma r$ (Section 2.3.3) and noting that X_u is negative finally yields:

$$\frac{m}{\|X_u\|}\dot{\Delta u} = -\Delta u + \frac{m\gamma}{\|X_u\|} r^2 \qquad (2.36)$$

which by definition can be written as:

$$\tau_u \dot{\Delta u} + \Delta u = K_u r^2 \qquad (2.37)$$

This is a simple first-order relation with gain K_u and time constant τ_u between the loss of forward speed Δu during a manoeuvre and the rate of turn r. Following the same procedure as was carried out in Section 2.3.1 for the yaw motion, a non-linear term may be added to (2.37) to compensate for the neglecting of the higher-order terms in the Taylor-series expansion, resulting in:

$$\tau_u \dot{\Delta u} + H_u(\Delta u) = K_u r^2 \qquad (2.38)$$

where

$$H_u(\Delta u) = \Delta u + \beta_3 \Delta u^3 \qquad (2.39)$$

The block-diagram for (2.38) is presented in Figure 2.6

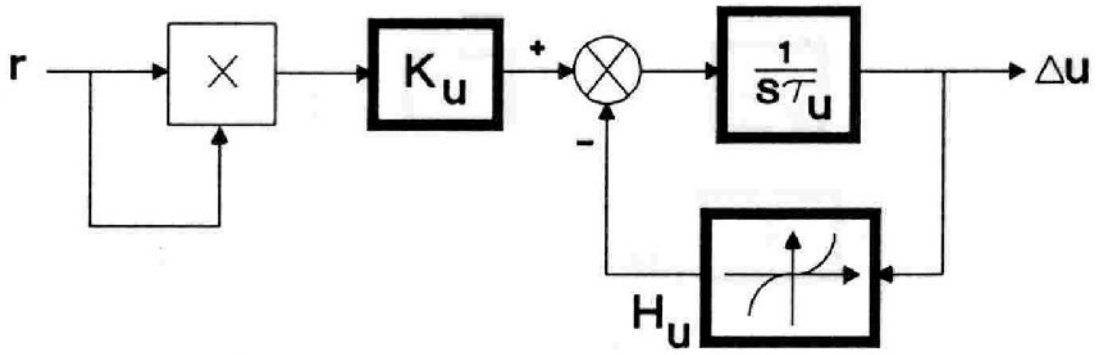

Fig. 2.6 Transfer from rate of turn to forward-speed loss

2.3.3 Generalizing the empirical relations

Although the limitation of the Davidson-and-Schiff model of a constant forward speed during a manoeuvre was eliminated in the previous section, the parameters of the transfer functions derived in Sections 2.3.1 and 2.3.2 for the rate of turn and the loss of forward speed are still only valid for a specific value of the ship's cruising speed U_0. Furthermore the characteristic overshoot in the ship's rate of

turn for a turning circle manoeuvre (Figure 2.7) cannot be reproduced by the linear first-order yaw model presented in Section 2.3.1.

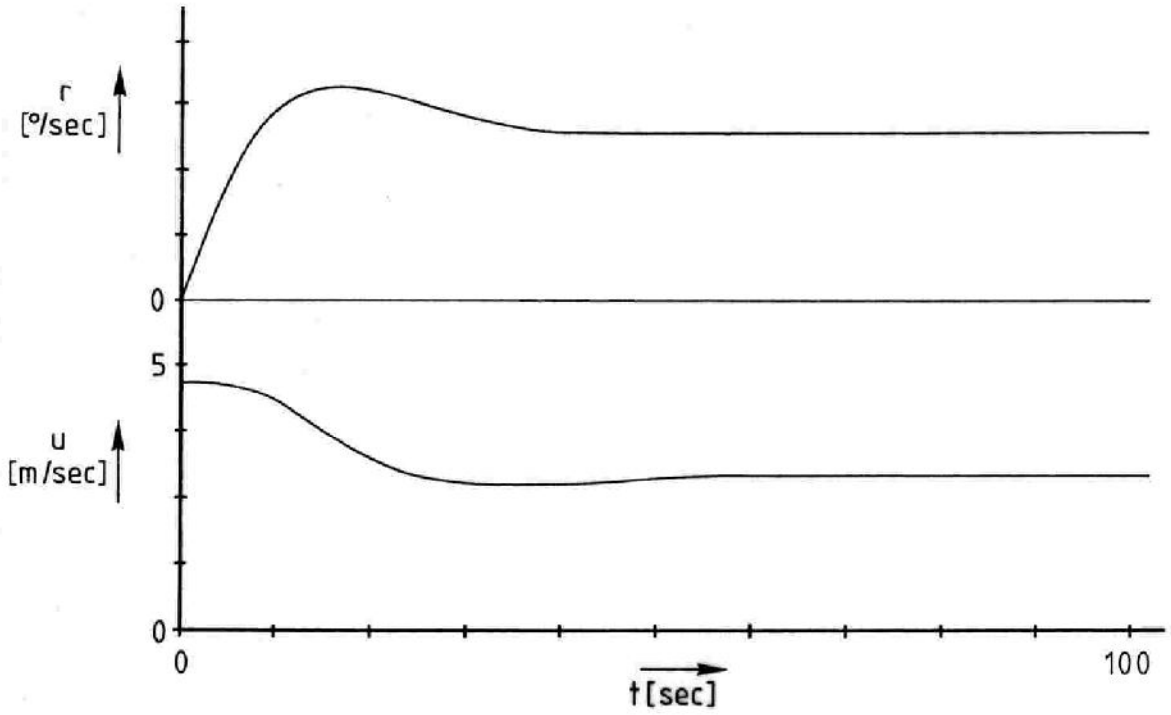

Fig. 2.7 Rate of turn and forward speed for a turning-circle manoeuvre

Van Leeuwen (1970) showed that these limitations could be eliminated by non-dimensionalizing the derived equations on the basis of the ship's forward speed u and length L. For this purpose he introduced the dimensionless variables:

$$r^* = \frac{L}{u} r \qquad (2.40)$$

$$u^* = \frac{\Delta u}{U_0} \qquad (2.41)$$

and

$$ds^* = \frac{u}{L} dt \qquad (2.42)$$

where L is the length of the ship and $u = U_0 - \Delta u$ is the instantaneous forward speed. By using the distance sailed by the ship instead of the time as the independent variable, the following rather simple relations could be derived for the dimensionless variables:

$$\tau^* \frac{dr^*}{ds^*} + H(r^*) = K^* \delta \qquad (2.43)$$

$$\tau_u^* \frac{du^*}{ds^*} + H_u(u^*) = K_u^* r^{*2} \qquad (2.44)$$

with

$$H(r^*) = \alpha_3^* r^{*3} + r^* \qquad (2.45)$$

$$H_u(u^*) = u^* \qquad (2.46)$$

Further an algebraic relation for the normalized sway velocity was derived:

$$v^* + H_v(r^*) = 0 \qquad (2.47)$$

with

$$v^* = \frac{v}{u} \qquad (2.48)$$

$$H_v(r^*) = \gamma_3^* r^{*3} + \gamma_1^* r^* \qquad (2.49)$$

Substituting (2.42) in (2.43) and (2.44) yields the time-dependent relations from which the rate of turn, the forward speed and the sway velocity can be calculated by (2.53):

$$\tau^* \frac{L}{u} \frac{dr^*}{dt} + H(r^*) = K^* \delta \qquad (2.50)$$

$$\tau_u^* \frac{L}{u} \frac{du^*}{dt} + H_u(u^*) = K_u^* r^{*2} \qquad (2.51)$$

$$v^* + H_v(r^*) = 0 \qquad (2.52)$$

and

$$r = \frac{u}{L} r^* \quad ; \quad u = U_0(1 - u^*) \quad ; \quad v = v^* u \qquad (2.53)$$

By relating the rate of turn to u and r^* according to (2.53) it follows that even for a first-order relation between r^* and δ an overshoot may appear in the rate of turn for a constant rudder angle, which according to (2.53) is caused by the loss of forward speed.
To obtain a model which obtained a better fit with experimental data (Van Amerongen; De Keizer, 1977), Eq. (2.50) was modified to (2.54) to introduce dynamics between variations in forward speed and rate of turn. This finally leads to the multivariable model of De Keizer (1977) which together with the drift equation of Van Leeuwen (2.52) gives a complete empirical description of the relevant ship motions during manoeuvring:

De Keizer:

$$\tau^* \frac{L}{u} \frac{dr}{dt} + \frac{u}{L} H(r^*) = K^* \frac{u}{L} \delta \qquad (2.54)$$

$$\tau_u^* \frac{L}{u} \frac{du^*}{dt} + H_u(u^*) = K_u^* r^{*2} \qquad (2.55)$$

Van Leeuwen:

$$\frac{v}{u} + H_v(r^*) = 0 \qquad (2.56)$$

with a minimal choice for the feedback polynomials:

$$H(r^*) = r^* \quad ; \quad H_u(u^*) = u^* \quad ; \quad H_v(r^*) = \gamma^* r^* \qquad (2.57)$$

For this minimal choice of the polynomials the equations become:

$$\tau \frac{dr}{dt} + r = K \delta \qquad (2.58)$$

$$\tau_u \frac{du^*}{dt} + u^* = K_u r^2 \qquad (2.59)$$

$$v = -\gamma r \qquad (2.60)$$

with the gain-scheduling formulas given by:

$$\tau = \tau^* \frac{L}{u} \quad ; \quad K = K^* \frac{u}{L} \tag{2.61}$$

$$\tau_u = \tau_u^* \frac{L}{u} \quad ; \quad K_u = K_u^* \left(\frac{L}{u} \right)^2 \tag{2.62}$$

$$\gamma = \gamma^* L \tag{2.63}$$

A block-diagram for the combined De Keizer and Van Leeuwen model is presented in Figure 2.8.

To summarize: the attractivity of using this multivariable model as a starting point for more specific research on the topic of track prediction lies in the following:

- applicability for different classes of ships,
- validity for different rudder angles and cruising speeds,
- limited number of parameters, especially in relation to the ability to describe quite complex phenomena such as loss of forward speed and overshoot in the rate of turn during a manoeuvre,
- parameters may be identified on the basis of full-scale trials.

2.3.4 The steering machine

To complete the mathematical description of the ship's dynamics, the dynamics of the steering machine have to be considered. This steering machine is a servomechanism which makes the actual rudder angle δ equal to the rudder angle δ_r , ordered by the helmsman or the autopilot. Without a further description of this, mainly hydraulic, device - for a more thorough description, Van Amerongen, 1982 may be consulted - the main parameters by which the steering machine can be characterized are:

- a rudder limiter which limits the ordered rudder angle δ_r to a maximum value of δ_{max} ;
- a speed limiter which reflects the limited speed with which the actual rudder angle can be changed (typical values range from 2.5 to 7 degrees per second).

This leads to the block-diagram of Figure 2.9 which has proved to be sufficiently accurate for simulation and control purposes (Van Amerongen, 1982; Van der Klugt, 1987).

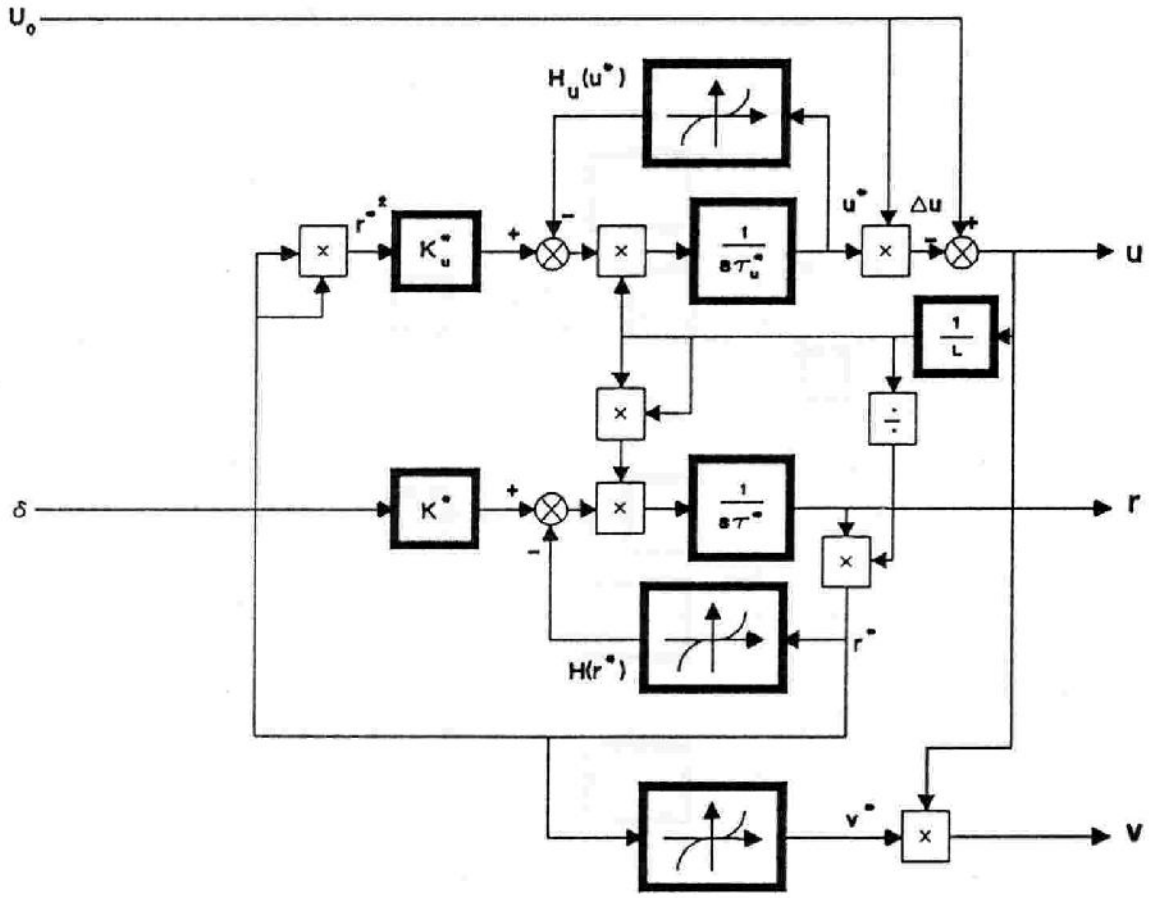

Fig. 2.8 The multivariable model of De Keizer and Van Leeuwen

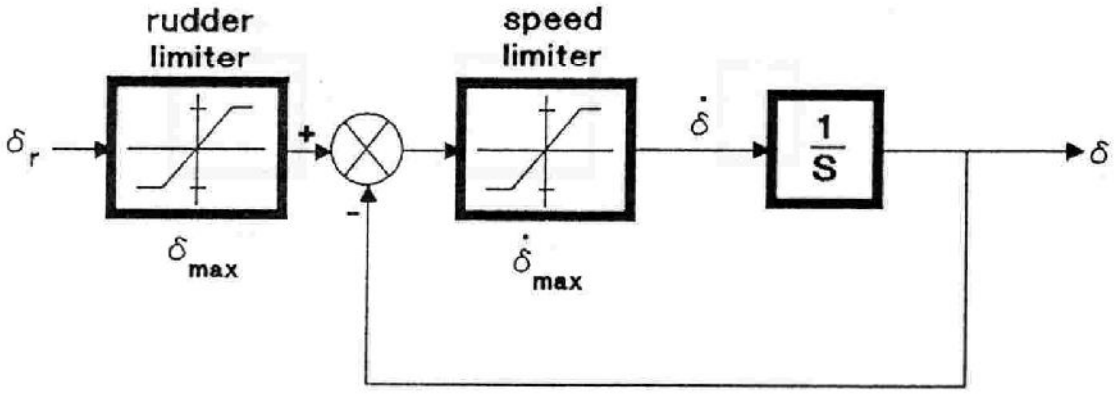

Fig. 2.9 Block-diagram of the steering machine

2.4 The kinematic relations

In the previous sections the equations of motion for the ship were derived after the transformation of Newton's law from the space-fixed coordinate system to the ship-fixed coordinate system. The effect of this transformation on the actual equations of motion was the introduction of two centripetal forces +mvr and -mur in the ship's x- and y-direction, due to the ship's turning.
To obtain the equations of the ship's path relative to the space-fixed coordinate system the inverse transformation has to be applied with respect to the ship-fixed variables, which yields the kinematic relations:

$$\dot{x}_s = u\cos\psi - v\sin\psi \qquad (2.64)$$

$$\dot{y}_s = u\sin\psi + v\cos\psi \qquad (2.65)$$

with x_s, y_s the ship's position in the space-fixed coordinate system x_0, y_0.
To describe the effect of the centripetal forces on the turning ship, Figure 2.10 was constructed for a steadily turning ship ($\dot{r} = 0$).
From Figure 2.10 it follows that the resulting ship's circular path can be constructed by the addition of two separate circular motions due to the ship's forward speed u and drift speed v, which are perpendicular with respect to each other. The angle between the ship's speed U along the path and the ship's forward speed u is defined as the drift angle β.

The kinematic relations for this combined circular motion are given by:

$$\dot{x}_s = U\cos\psi' \qquad (2.66)$$

$$\dot{y}_s = U\sin\psi' \qquad (2.67)$$

with $\psi' = \psi + \beta$

The diameter D of the resulting circular path may be determined by integrating the y-displacement from $t=0$ to $t=T_p/2$ (see Figure 2.10), with T_p the period of the circular motion, and substituting $\psi = \dot{\psi}t = rt$:

$$D = \Delta y = \int_0^{\frac{\pi}{r}} U\sin(rt)\,dt = \frac{2U}{r} \qquad (2.68)$$

and the radius R becomes:

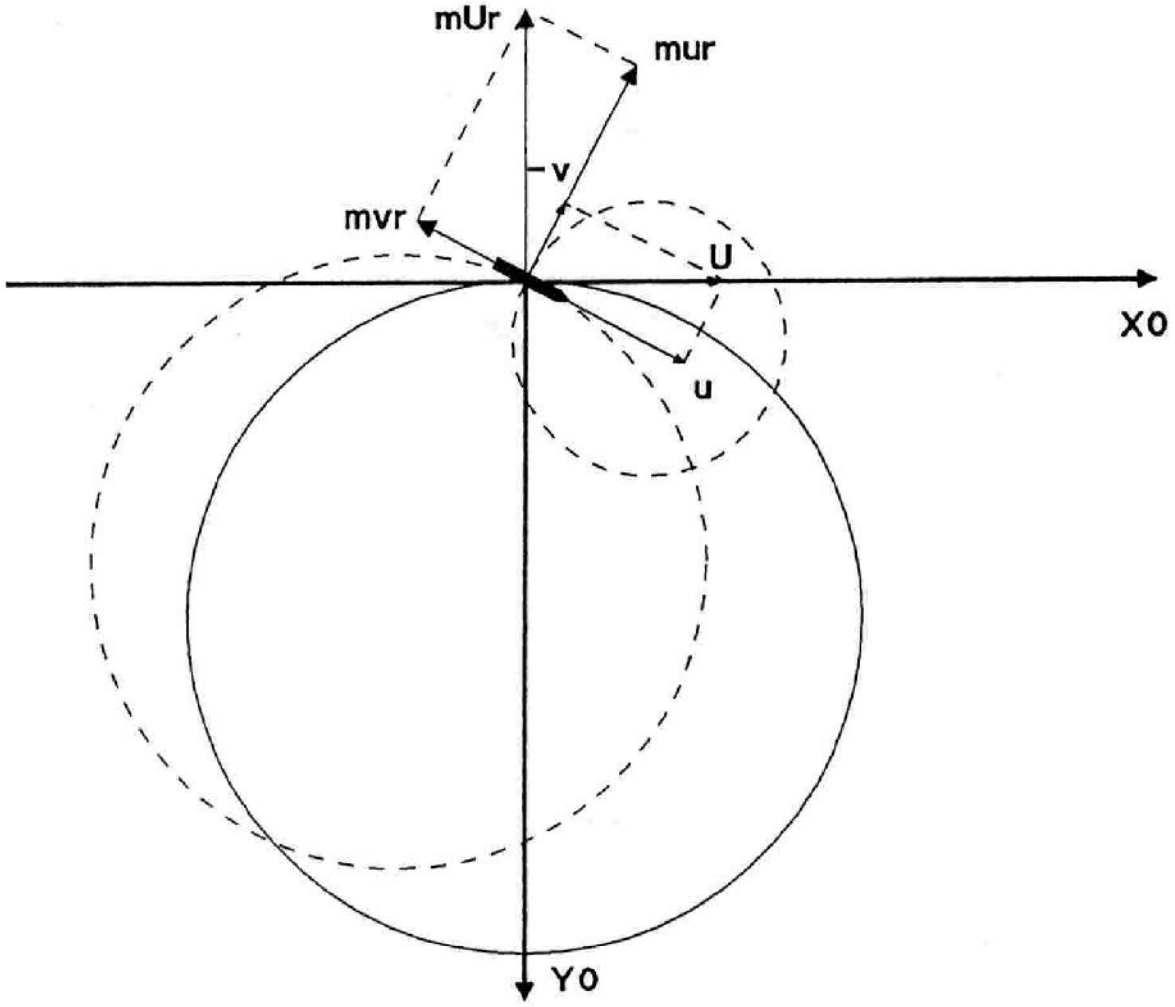

Fig. 2.10 Effect of centripetal forces

$$R = \frac{D}{2} = \frac{U}{r} \approx \frac{u}{r} \qquad (2.69)$$

Normalizing this relation with respect to the ship's length yields, together with (2.40), a geometrical interpretation of the normalized rate of turn r^* for the steadily turning ship:

$$\frac{R}{L} = \frac{u}{Lr} = \frac{1}{r^*} \qquad (2.70)$$

2.5 Disturbances

2.5.1 Introduction

In Section 2.1 the disturbances were defined as the factors which influence the manoeuvring behaviour of the ship but are of an uncontrollable nature and are therefore considered to be part of the ship's surroundings. The *additive disturbances* discussed in this section can be classified according to their principal effect on the mathematical description of the ship's motions:

- Additional factor in the kinematic relationships:
  current
- Additional factor in the equations of motion:
  wind, waves

2.5.2 Current

Although current of a non-uniform nature may influence the ship's rate of turn, the most characteristic influence of current is considered to be a change of the ship's speed vector with respect to the ground which causes the direction of this speed vector to differ from the ship's heading. Therefore the influence of this uniform current is modelled as an additional term to the kinematic relationships discussed in Section 2.4 according to Eqs. (2.71) and (2.72):

$$\dot{x}_s = u\cos\psi - v\sin\psi + U_c\cos\psi_c \qquad (2.71)$$

$$\dot{y}_s = u\sin\psi + v\cos\psi + U_c\sin\psi_c \qquad (2.72)$$

The current speed U_c and direction ψ_c are defined with respect to the space-fixed coordinate system according to Figure 2.11. In this figure also the wind speed V_w and direction ψ_w are defined.

2.5.3 Wind

Wind exerts an additional force on the ship which can be described by:

$$F_w = \frac{1}{2}\,\rho_l\, C_w(\gamma_r)\, V_{wr}^2\, S \qquad (2.73)$$

where

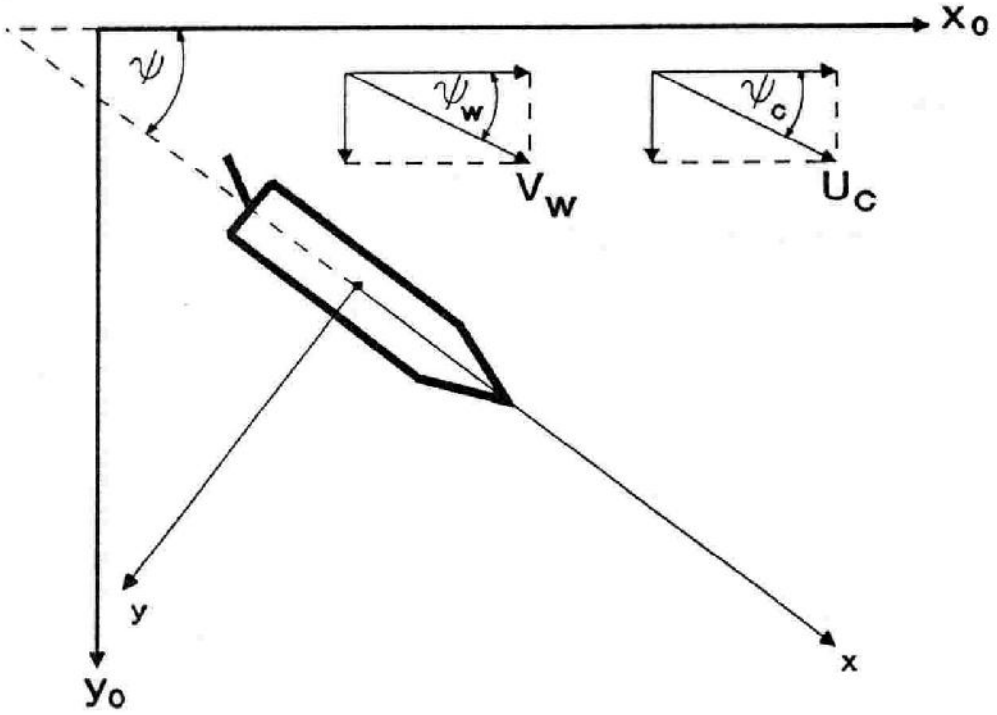

Fig. 2.11 Definition of current and wind speed and direction

ρ_l	is the air density
$C_w(\gamma_r)$	is a geometrical factor depending on the relative wind angle γ_r
V_{wr}	is the relative wind speed
S	is the relevant area of the ship's superstructure

The relative wind speed V_{wr} and wind angle γ_r (as would be measured on board the ship) may be determined by transforming the real wind speed and direction, as defined in Figure 2.11, to the ship-fixed coordinate system. In vector notation this yields:

$$\underline{V}_{wr} = \underline{V}_w - \underline{U} \qquad (2.74)$$

with $\underline{V}_{wr}$, $\underline{V}_w$ the relative and true wind speed vectors and $\underline{U}$ the ship's speed vector.

The resulting wind force given by (2.73) can be split into a force in the x-direction, the y-direction and an additional moment around the z-axis. The equations of motion for the ship-fixed coordinate system then become:

$$m\,(\dot{u} - vr) = X + X_{wind} \qquad (2.75)$$

$$m\,(\dot{v} + ur) = Y + Y_{wind} \qquad (2.76)$$

$$I_{zz}\dot{r} = N + N_{wind} \qquad (2.77)$$

These separate components of the wind forces and moment may be written in a more or less identical form to (2.73):

$$X_{wind} = \frac{1}{2}\rho_1 C_x(\gamma_r) V_{wr}^2 S_{wx} \qquad (2.78)$$

$$Y_{wind} = \frac{1}{2}\rho_1 C_y(\gamma_r) V_{wr}^2 S_{wy} \qquad (2.79)$$

$$N_{wind} = \frac{1}{2}\rho_1 C_n(\gamma_r) V_{wr}^2 S_{wy} L \qquad (2.80)$$

where S_{wx} and S_{wy} are determined by the projection of the ship's superstructure S at planes perpendicular to the x-axis and y-axis and L is the ship's length along the water line. The geometrical factors C_x , C_y and C_n can be approximated as a function of the relative wind angle γ_r by the following general formula (Schelling, 1977):

$$C_w(\gamma_r) = \sum_{k=0}^{\infty} a_k \cos(k\gamma_r) + b_k \sin(k\gamma_r) \qquad (2.81)$$

with k an integer and a_k and b_k specific for each ship.
For simulation purposes a simple approximation may be obtained by choosing (based on the experimental data of Wagner, 1967):

$$C_x(\gamma_r) = a_x \cos\gamma_r \qquad (2.82)$$

$$C_y(\gamma_r) = a_y \sin\gamma_r \qquad (2.83)$$

$$C_n(\gamma_r) = a_n \sin 2\gamma_r \qquad (2.84)$$

These approximations of the geometrical factors as a function of γ_r are sketched in Figure 2.12.
The additional wind moment around the z-axis and force in the x-direction may be incorporated into the Van Leeuwen model of Eqs. (2.43) and (2.44) according to (Schelling, 1977):

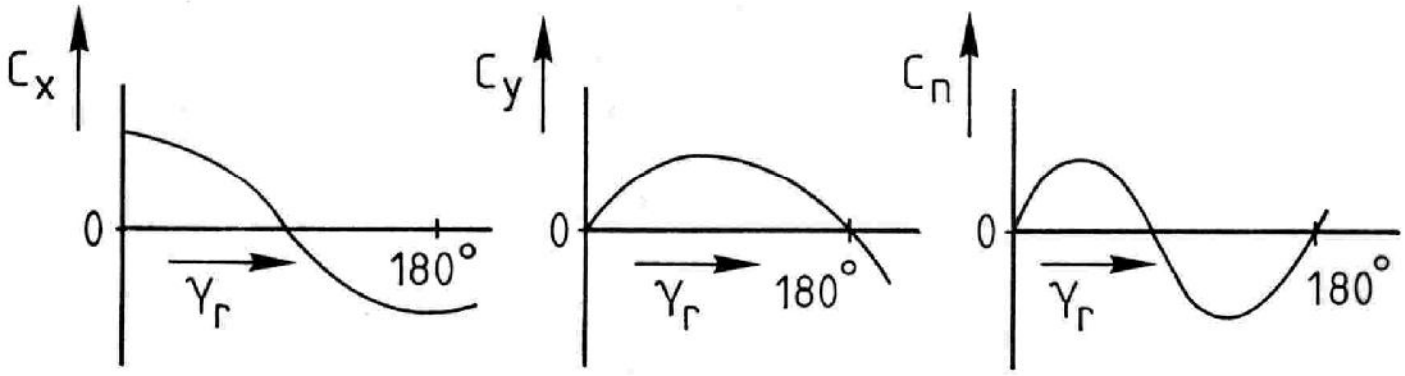

Fig. 2.12 The geometrical factors as a function of γ_r

$$\tau^* \frac{dr^*}{ds^*} + H(r^*) = K^* \delta + \tau^* N_w^* \qquad (2.85)$$

$$\tau_u^* \frac{du^*}{ds^*} + H_u(r^*) = K_u^* r^{*2} + \tau_u^* F_w^* \qquad (2.86)$$

In these equations the normalized wind moment and force are given by:

$$N_w^* = N_w' \left(\frac{L}{u}\right)^2 \sin 2\gamma_r \, V_{wr}^2 \qquad (2.87)$$

$$F_w^* = F_w' \left(\frac{L}{u^2}\right) \cos \gamma_r \, V_{wr}^2 \qquad (2.88)$$

with N_w' and F_w' specific and approximately constant for each ship.

The effect of turbulence may be reflected by adding a stochastic component with zero mean to V_{wr}.

2.5.4 Waves

Waves, which have quite different origins and characteristics (Groen and Dorrestein, 1976), cause an additional yaw motion of a high frequency and a negligible displacement.
Because of the stochastic nature of the wave influence, an analytical description has to be restricted to the frequency domain. For this purpose a description of the theoretical wave spectrum as a function of the wind speed or the significant wave height and the average period has been suggested by several authors (Pierson

and Moskovitz, 1964; Gerritsma, 1979). The general formula proposed by Gerritsma to relate the wave spectrum to the significant wave height and the average period is given by:

$$S_\theta(\omega) = A\omega^{-p}\exp(-B\omega^{-q}) \qquad (2.89)$$

where the coefficients A,B and p,q can be determined when statistical information is available on both the significant wave height and average period, which are approximately equal to the wave height and period as visually estimated by a human observer. For fully developed seas, the result of constant wind over a long period of time, the significant wave height and average period are directly related to the wind speed V_w.
For the influence on the ship's motions the relative wave frequency, which depends on the ship's speed and the angle between the ship's heading and the mean wave direction, has to be determined. The formula for this relative wave frequency is (Van Amerongen, 1982):

$$\omega(U,\gamma_w) = \omega_0 - \omega_0^2 U\cos(\gamma_w)/g \qquad (2.90)$$

with

ω_0	the actual wave frequency
U	the ship's speed
γ_w	the angle between the ship's heading and the wave direction
g	the acceleration of the gravity

In a manner analogous with the analysis of the yaw motions induced by the wind influence as discussed in the previous section, the wave influence can be treated as an additional input to the yaw model which may be approximated by:

$$N_g(\omega) = H_g(\omega)\sin 2\gamma_w \qquad (2.91)$$

with $H_g(\omega)$ a function of the relative wave frequency ω, depending on the shape of the hull, the water viscosity etc. and γ_w the angle of incidence of the waves relative to the ship.

For simulation purposes, a different approach may be followed by externally adding the wave influence to the undisturbed rate-of-turn signal (Van Amerongen, 1982) as sketched in Figure 2.13.
The wave disturbance signal can be generated by using a second-order shaping filter, driven by white noise according to Figure 2.14. The level of the white noise

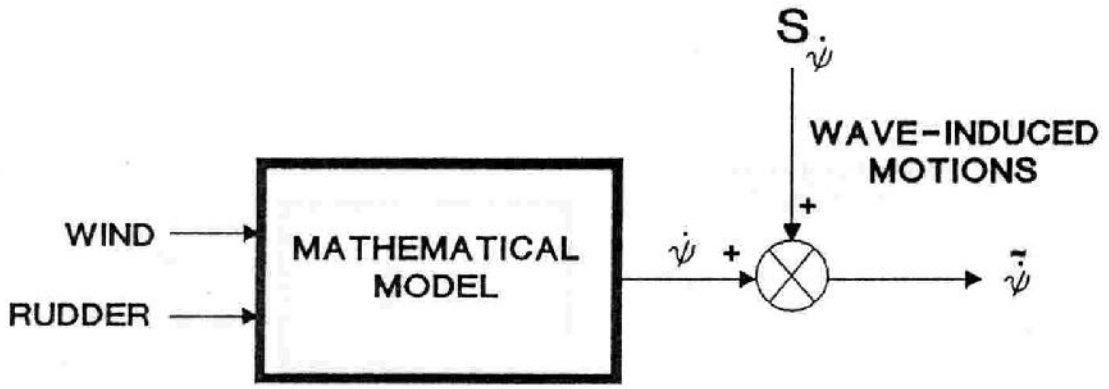

Fig. 2.13 Externally adding the wave disturbances

and the filter parameters ζ and ω_n, which are related to the sea-state parameters and the ship's dynamics, may be determined from full-scale measurements of the wave-disturbed rate-of-turn signal for a specific ship (Van Amerongen, 1982).

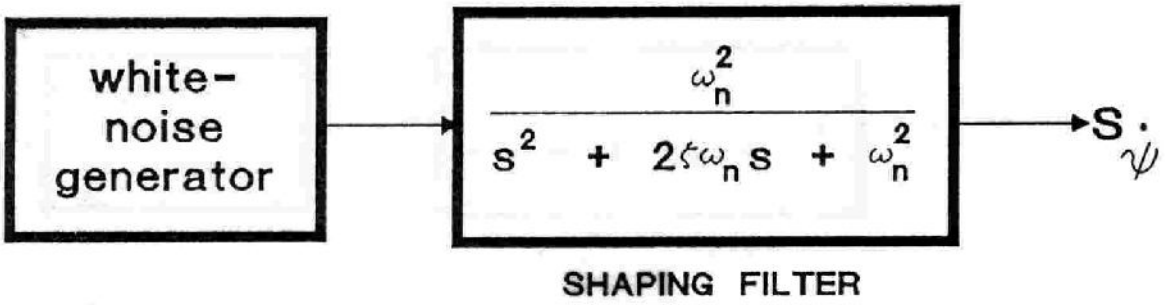

Fig. 2.14 Generation of wave motions

3 THE BASIC PREDICTOR

3.1 Introduction

The principle aim for the development of the track-prediction system is to assist the navigator during course-changing manoeuvres, in such a way that safety increases regarding groundings and collisions. Because, especially during coastal navigation, safety is directly related to the accuracy of the own ship's heading and position control (Kristiansen, 1980), research is directed towards the accurate control of the ship's motions.
In theory, two approaches may be followed to realize accurate position control with the assistance of a track predictor:

- *"Open-loop" approach*:
  Accurate prediction of the ship's track from the initial conditions before the execution of a manoeuvre, on the basis of a complex mathematical model of, for instance, the hydrodynamical type. With such a complex prediction model, adaptation to changing conditions and disturbances is difficult, if not impossible, to achieve.
- *"Closed-loop" approach*:
  Prediction of the ship's track on the basis of a relatively simple mathematical model which is adapted to changing conditions and disturbances during the execution of a manoeuvre on the basis of measurements. For this type of prediction model the empirical models as discussed in Chapter 2 are a good starting point, because these models were intended to relate the different relevant variables to each other on the basis of measured signals.

As to the feasibility of these two different approaches, it is obvious that the closed-loop approach offers the best perspective, just because of the required simplicity of the prediction model for this approach. Therefore, research on the prediction-model structure will be restricted to the mathematical models of an empirical nature, which may be provided with a closed-loop nature in combination with available techniques for on-line state and parameter estimation.

Previous research on the prediction-model structure was based on the second-order Bech model for the rate-of-turn prediction (Nanninga, 1974; Reissenweber, 1975) and on the first-order Nomoto model for the rate-of-turn prediction and a separate model for the loss-of-speed prediction (Boonekamp, 1978; Van der Arend,

1979). The underlying assumption in this approach was a demand for overall correspondence between real and predicted signals such as rate of turn and forward speed, which would guarantee track correspondence between real and predicted path. This track correspondence is defined as the matching of the ship's real path and its predicted path with respect to the ship's surroundings.

In the present study, the demand for track correspondence is taken as the single starting point for the development of the basic predictor structure, instead of simultaneous rate-of-turn and forward-speed correspondence, which is a more severe demand.
After the generalization of the mathematical track description in Section 3.2, the effect of the ship's speed on the ship's track is analyzed in Section 3.3.
As well as this prediction-oriented analysis of the ship's dynamics, the effects of the disturbances on the predicted track are analyzed in Section 3.4. After the presentation of some simulation results in Section 3.5, to back up the theoretical analysis, finally in Section 3.6 on the basis of these results some conclusions will be drawn regarding the basic predictor.

3.2 Generalized track description

3.2.1 Introduction

The kinematic relations, presented in Section 2.4, relate the relevant ship-fixed variables to the ship's path relative to a space-fixed coordinate system. For a correct path prediction, the ship's forward speed u(t), sway velocity v(t) and heading $\psi(t)$ are to be predicted:

$$x_s(t) = x_s(0) + \int_0^t u(\tau)\cos(\psi(\tau)) - v(\tau)\sin(\psi(\tau))\, d\tau \qquad (3.1)$$

$$y_s(t) = y_s(0) + \int_0^t u(\tau)\sin(\psi(\tau)) + v(\tau)\cos(\psi(\tau))\, d\tau \qquad (3.2)$$

The underlying demand for this approach is that the predicted track and real track correspond to each other on a time basis. This is reflected in the fact that the time is used as the independent variable for the description of the kinematic relations of (3.1) and (3.2).
A generalization of the track description may be achieved by examining the kinematic relations for different "independent" variables. In this way the underlying demand for correspondence on a time basis may be changed to a more general

demand for correspondence between the real path and the predicted path with respect to the ship's surroundings.
This is illustrated by Figure 3.1.a,b , where it is demonstrated that whereas the ship's rate of turn and speed are not correctly predicted as a function of the time (Figure 3.1.a), the resulting real and predicted path have a good track correspondence with respect to a space-fixed coordinate system (Figure 3.1.b).
Achieving the generalization will yield more insight into the demands which are minimally to be satisfied by the predictor in order to guarantee the desired track correspondence. The analysis shows a direct link with the work of Van Leeuwen (1970) presented in Section 2.3, where some empirical relations for the relevant ship motions were derived after changing the independent variable from time to distance covered by the ship.

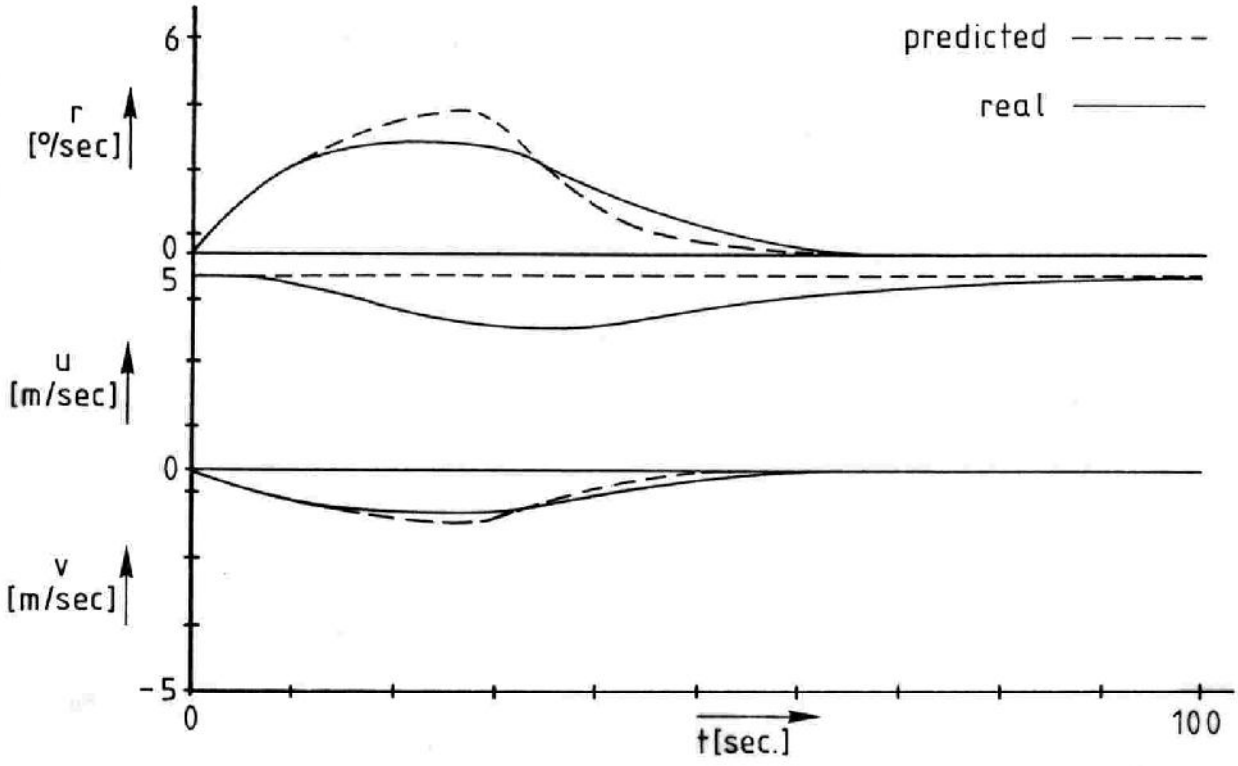

Fig. 3.1.a Real and predicted rate of turn and speed

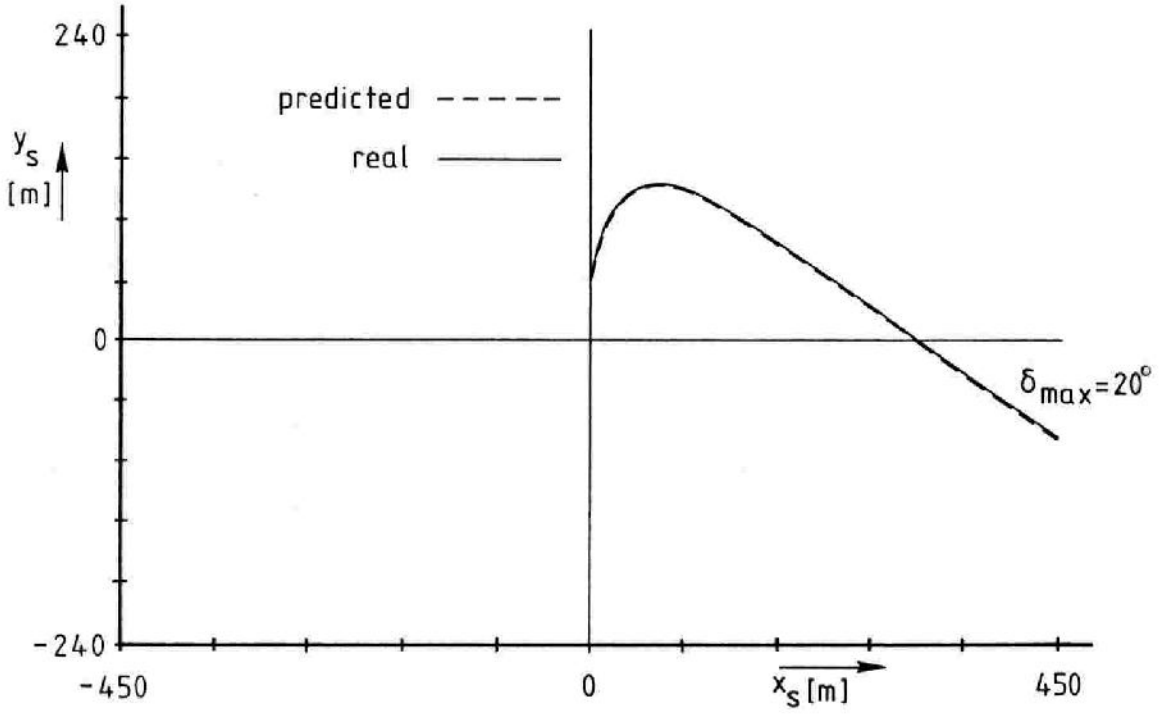

Fig. 3.1.b Corresponding real and predicted track

3.2.2 General kinematic relations

The relations for the determination of the ship's path relative to the space-fixed coordinate system are given in their most general form by:

$$x_s = \int_0^{\Delta x_u} dx_u + \int_0^{\Delta x_v} dx_v \qquad (3.3)$$

$$y_s = \int_0^{\Delta y_u} dy_u + \int_0^{\Delta y_v} dy_v \qquad (3.4)$$

with

x_s, y_s	the ship's position,
$\Delta x_u, \Delta y_u$	the ship's displacement due to the forward speed,
$\Delta x_v, \Delta y_v$	the ship's displacement due to the sway speed,
dx_u, dy_u	infinitesimal position change due to the forward speed,
dx_v, dy_v	infinitesimal position change due to the sway speed.

and, without loss of generality, the initial value of the ship's position is assumed to be zero.
According to these relations, the ship's motion may be divided into separate contributions from the forward speed and from the sway velocity. For now, the analysis is continued for the forward speed only. The influence of the sway velocity can be examined in a similar way.
The displacement due to the forward speed may be rewritten as (3.5)-(3.6), which is illustrated by Figure 3.2 for an arbitrary ship path.

$$\Delta x_u(s) = \int_0^s \cos(\psi(\sigma))\, d\sigma \qquad (3.5)$$

$$\Delta y_u(s) = \int_0^s \sin(\psi(\sigma))\, d\sigma \qquad (3.6)$$

with ψ the ship's heading and s the distance travelled by the ship.
The relation between ds, u and dt is given by:

$$ds = u(t)\, dt \qquad (3.7)$$

where u is the forward speed of the ship.
After substitution in Eqs. (3.5) and (3.6) this yields the time-dependent kinematic relations. Instead of doing this, ds is written as:

$$ds = L\, ds^* \qquad (3.8)$$

with s^* the distance travelled by the ship, normalized with respect to the ship's length, as introduced by Van Leeuwen:

$$ds^* = \frac{ds}{L} = \frac{u(t)}{L}\, dt \qquad (3.9)$$

After substitution of (3.8) in Eqs. (3.5) and (3.6), these equations become:

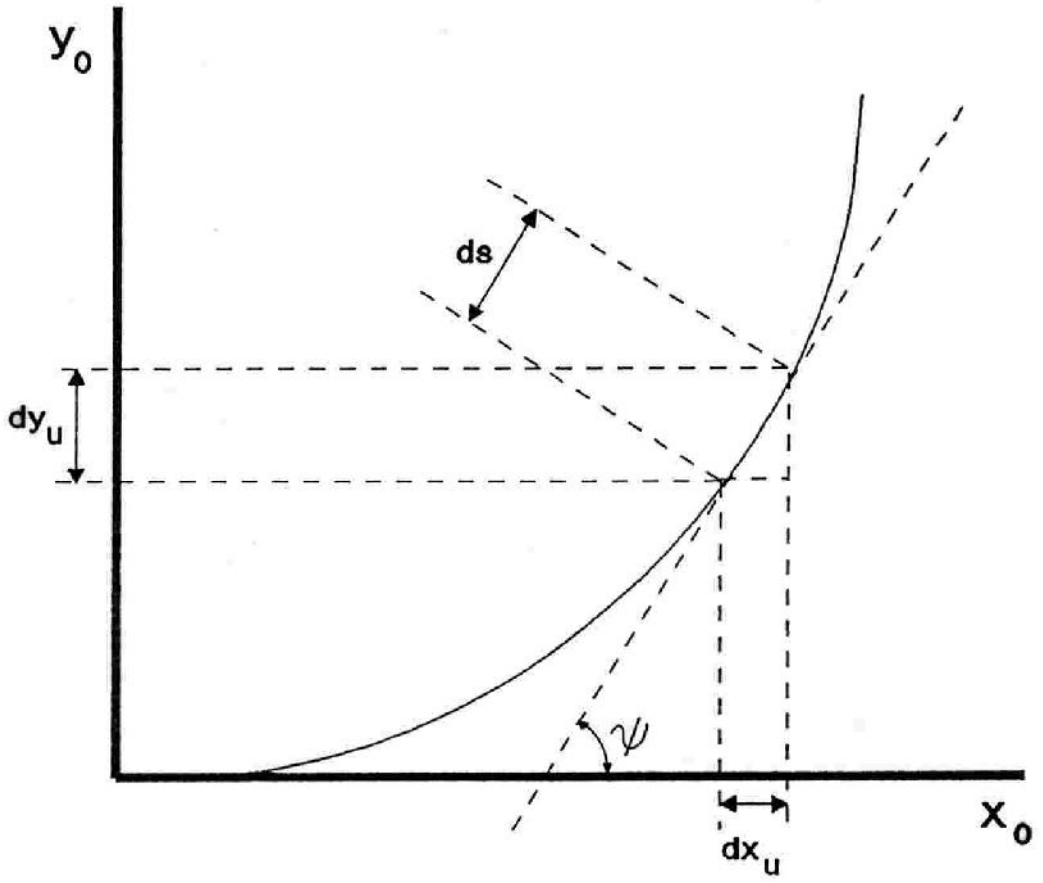

Fig. 3.2 Relation between position and distance travelled by the ship

$$\Delta x_u^*(s^*) = \int_0^{s^*} \cos(\psi(\sigma^*)\, d\sigma^* \qquad (3.10)$$

$$\Delta y_u^*(s^*) = \int_0^{s^*} \sin(\psi(\sigma^*)\, d\sigma^* \qquad (3.11)$$

where Δx_u^* , Δy_u^* is the ship's normalized displacement:

$$\Delta x_u^* = \frac{\Delta x_u}{L} \quad ; \quad \Delta y_u^* = \frac{\Delta y_u}{L} \qquad (3.12)$$

To determine a sufficient condition for track correspondence, the ship's heading ψ has to be expressed as a function of the newly chosen independent variable s^*. This can be achieved by writing:

$$\psi(s^*) = \int_0^{\Delta\psi} d\psi = \int_0^{s^*} \frac{d\psi}{d\sigma^*}\, d\sigma^* = \int_0^{s^*} r^*(\sigma^*)\, d\sigma^* \qquad (3.13)$$

with $r^*(s^*)$ the ship's normalized rate of turn as a function of s^*.
Just as for the position, the initial value of the ship's heading is assumed to be zero.
Substituting (3.13) in Eqs. (3.10) and (3.11) yields:

$$\Delta x_u^*(s^*) = \int_0^{s^*} \cos\left(\int_0^{\sigma^*} r^*(\sigma_2^*)d\sigma_2^* \right) d\sigma^* \qquad (3.14)$$

$$\Delta y_u^*(s^*) = \int_0^{s^*} \sin\left(\int_0^{\sigma^*} r^*(\sigma_2^*)d\sigma_2^* \right) d\sigma^* \qquad (3.15)$$

Evaluating this expression for the ship's normalized displacement, which is dependent on r^* only, it follows that track correspondence between the ship's real and its predicted path is guaranteed by demanding:

$$r_s^*(s^*) = r_p^*(s^*) \quad \forall \; s^* \in [0, s_e^*] \qquad (3.16)$$

with s_e^* the normalized travelled distance for the prediction horizon and r_s^* and r_p^* the real and predicted normalized rate of turn as a function of s^*.
In this case it also holds:

$$\psi_s^*(s^*) = \psi_p(s^*) \quad \forall \; s^* \in [0, s_e^*] \qquad (3.17)$$

To complete this general analysis, the contribution of the sway velocity has to be considered. Carrying out this analysis in the s^* domain, the expression for this sway contribution is given by (analogous to Eqs. (3.10) and (3.11)):

$$\Delta x_v^*(s_v^*) = -\int_0^{s_v^*} \sin(\psi(\sigma_v^*))\, d\sigma_v^* \qquad (3.18)$$

$$\Delta y_v^*(s_v^*) = \int_0^{s_v^*} \cos(\psi(\sigma_v^*))\, d\sigma_v^* \qquad (3.19)$$

with the relation between ds_v^*, v and dt given by:

$$ds_v^* = \frac{v(t)}{L}\,dt \qquad (3.20)$$

Combining (3.20) with (3.9) yields:

$$ds_v^* = \frac{v}{u}\,ds^* = v^*\,ds^* \qquad (3.21)$$

where v^* equals the normalized sway velocity, as introduced by Van Leeuwen. Substituting (3.21) in Eqs. (3.18) and (3.19), the normalized sway displacement as a function of the normalized travelled distance due to the forward speed becomes:

$$\Delta x_v(s^*) = -\int_0^{s^*} \sin(\psi(\sigma^*))\; v^*(\sigma^*)\; d\sigma^* \qquad (3.22)$$

$$\Delta y_v^*(s^*) = \int_0^{s^*} \cos(\psi(\sigma^*))\; v^*(\sigma^*)\; d\sigma^* \qquad (3.23)$$

In the case of track correspondence with respect to the forward speed it must hold that $\psi_s(s^*) = \psi_p(s^*)$ by condition (3.17). The remaining condition for track correspondence with respect to the sway displacement then becomes:

$$v_s^*(s^*) = v_p^*(s^*) \quad \forall\ s^* \in [0, s_e^*] \qquad (3.24)$$

Adding the normalized displacements with respect to the forward speed and the sway speed, yields for the ship's normalized position:

$$\underline{x}_s^*(s^*) = \underline{\Delta x}_u^*(r^*(s^*)) + \underline{\Delta x}_v^*(r^*(s^*), v^*(s^*)) \qquad (3.25)$$

with $\underline{x}_s^*$ given by $(x_s^*\ ,\ y_s^*)^T$.
In summary, it may be stated that track correspondence between the real path and the predicted path is guaranteed if the two normalized variables r^* and v^* are correctly predicted as a function of s^*.

3.2.3 Translation criteria

During the execution of a manoeuvre the predicted track needs to be adjusted according to the distance already covered by the ship since the start of the manoeuvre. Therefore a method of translating the predicted track during the

execution of a manoeuvre has to be determined in such a way that the track correspondence between the ship's real path and its predicted path is preserved. This translation problem can be formulated so as to determine the predicted normalized position x_p^* , y_p^* for which it holds that (see also Figure 3.3):

$$\int_0^{s^*} d\sigma^* = \int_0^{s_p^*} d\sigma_p^* \qquad (3.26)$$

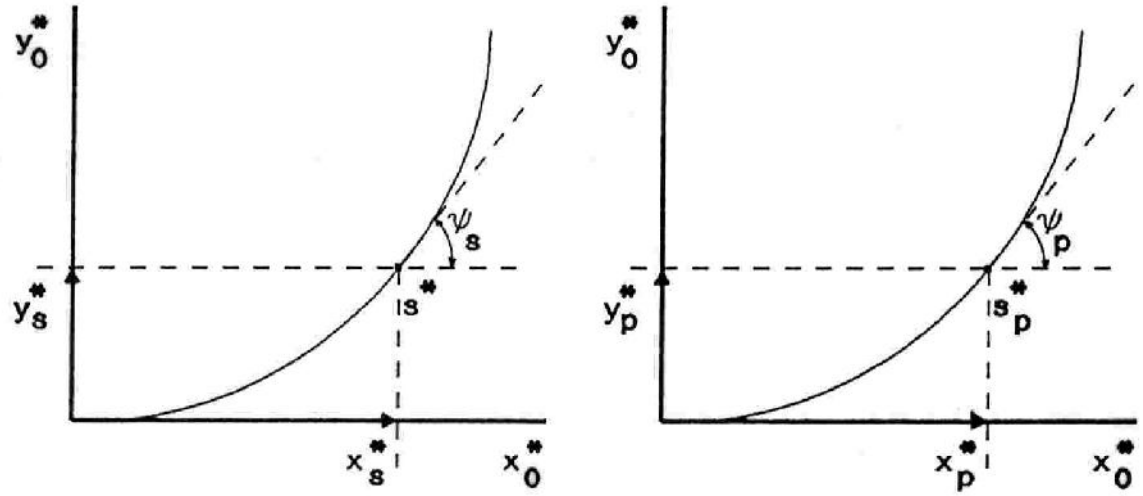

Fig. 3.3 Determination of the translation point

To solve this problem (3.26) is transformed to the course domain:

$$\int_0^{\psi_s} R_s^*(\psi)\, d\psi = \int_0^{\psi_p} R_p^*(\psi)\, d\psi \qquad (3.27)$$

with

$$R^*(\psi) = \frac{ds^*(\psi)}{d\psi} \qquad (3.28)$$

In the case of track correspondence between the real and the predicted path the following condition is satisfied:

$$R_s^*(\psi) = R_p^*(\psi) \quad \forall \quad \psi \in [0, \psi_e] \tag{3.29}$$

which is the equivalent of (3.16) for the course domain.
Because of this condition, (3.27) can only be satisfied by selecting:

$$\psi_p = \psi_s \tag{3.30}$$

This implies that, also in the case of an unknown speed of the ship, a correct translation method is provided by selecting the ship's predicted position x_p , y_p for which (3.30) is satisfied as the translation origin for the predicted track. Only in the case where both the speed of the ship and the ship's heading are known, can the time also be used as a means of translating the predicted track.
In that case it must hold:

$$\int_0^{t_s} \frac{ds^*}{d\tau}\, d\tau = \int_0^{t_p} \frac{ds_p^*}{d\tau}\, d\tau \tag{3.31}$$

or:

$$\int_0^{t_s} u_s(\tau)\, d\tau = \int_0^{t_p} u_p(\tau)\, d\tau \tag{3.32}$$

Therefore

$$t_p = t_s \tag{3.33}$$

because

$$u_s(t) = u_p(t) \quad \forall \quad t \in [0, t_e] \tag{3.34}$$

In the following sections the influence of the speed of the ship and the disturbances on the ship's track will be investigated more explicitly on the basis of the generalized track description.

3.3 Influence of the speed of the ship

3.3.1 Introduction

To examine the influence of the speed of the ship on the ship's track, the following aspects are considered:

- influence of the ship's cruising speed U_0, which is the ship's speed before the start of a manoeuvre,
- influence of the loss of forward speed Δu during the execution of a manoeuvre, due to the ship's turning,
- influence of the sway speed v during the execution of a manoeuvre.

For this analysis a simple prediction model with constant forward speed U_p is compared in the s^* domain to three empirical models in which the aspect under consideration is incorporated. By following this approach the aspect to be analyzed may be examined in an undisturbed way.
For the aspects mentioned here, the empirical models are chosen as:

- First-order Nomoto model with gain scheduling with respect to U_0 for the analysis of the cruising-speed influence,
- Non-linear Van Leeuwen model for the analysis of the influence of the loss of forward speed,
- Van Leeuwen model for the analysis of the influence of the sway speed.

The corresponding investigation scheme is presented in Figure 3.4.

3.3.2 Influence of the cruising speed

For the analysis of the cruising-speed influence on the ship's track, the transfer from rudder to rate of turn is examined in Section 3.3.2.1 (open-loop analysis). Further this analysis will be extended to the closed-loop system (ship supplied with a course-changing controller) in Section 3.3.2.2.

3.3.2.1 The open-loop configuration

The first-order Nomoto model describes the ship's transfer from rudder angle to rate of turn for a fixed cruising speed U_0. It is given by:

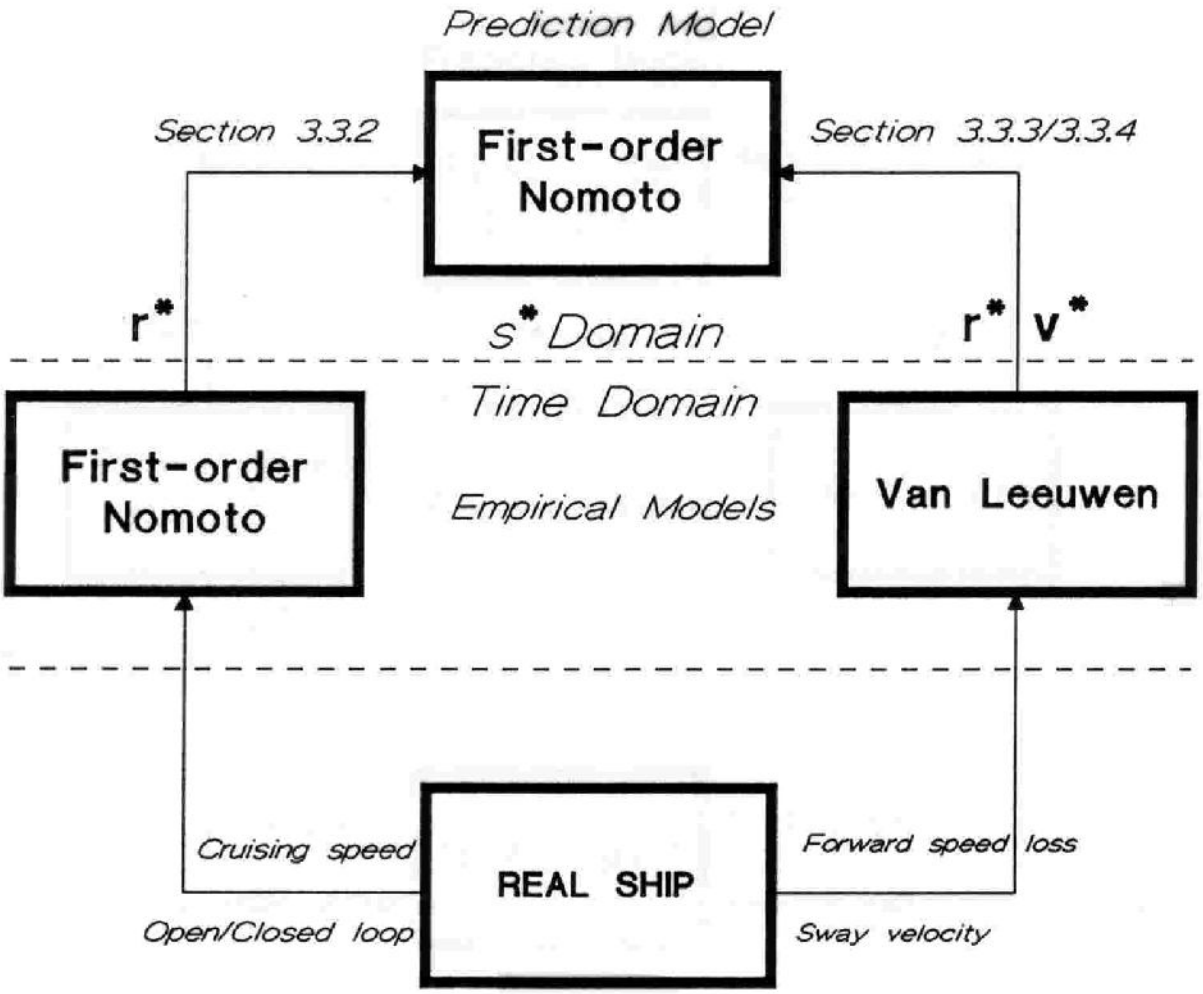

Fig. 3.4 Influence of the speed of the ship

$$\tau^* \frac{L}{U_0} \frac{dr}{dt} + r = K^* \frac{U_0}{L} \delta \qquad (3.35)$$

which is the time-domain relation for r.
Assuming the parameters τ^* , K^* and the ship's length L to be known but the cruising speed U_0 to be unknown, the prediction model is chosen as:

$$\tau^* \frac{L}{U_p} \frac{dr_p}{dt} + r_p = K^* \frac{U_p}{L} \delta \qquad (3.36)$$

with U_p the predicted velocity.

To carry out the analysis for the comparison of the ship's "real" path, corresponding to (3.35), and the ship's predicted path according to (3.36), these equations are transformed to the s^* domain by substituting:

$$ds^* = \frac{U_0}{L}\,dt \qquad (3.37)$$

$$ds_p^* = \frac{U_p}{L}\,dt \qquad (3.38)$$

This yields:

$$\tau^* \frac{dr^*}{ds^*} + r^* = K^* \delta \qquad (3.39)$$

and

$$\tau^* \frac{dr_p^*}{ds_p^*} + r_p^* = K^* \delta \qquad (3.40)$$

for the predictor,

with

$$r^* = \frac{d\psi}{ds^*} = \frac{L}{U_0}\,\frac{d\psi}{dt} \qquad (3.41)$$

and

$$r_p^* = \frac{d\psi_p}{ds^*} = \frac{L}{U_p}\,\frac{d\psi_p}{dt} \qquad (3.42)$$

Because (3.39) and (3.40) are identical relations the following equivalence condition is satisfied:

$$r^*(s^*) = r_p^*(s_p^*) \qquad (3.43)$$

which is a sufficient condition for track correspondence with respect to the forward speed according to (3.16). Note that knowledge of the cruising speed U_0 is irrelevant. This implies that knowledge of τ^* , K^* is sufficient to give an exact prediction of the ship's normalized track, while knowledge of the ship's length

can be used to denormalize this predicted track to the actual ship positions x_s , y_s on the basis of (3.12).

3.3.2.2 The closed-loop configuration

The same analysis as performed in the previous section can be carried out for the closed-loop configuration, when the ship is supplied with a course-changing controller according to Figure 3.5

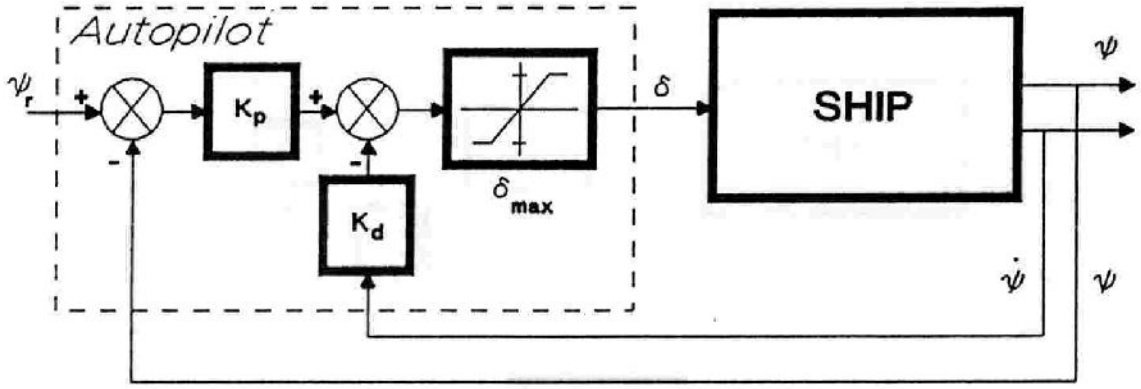

Fig. 3.5 Ship with course-changing controller

The basic course-changing controller is characterized by two gains K_p and K_d and a rudder limit δ_{max}. For the analysis the course-changing manoeuvre is divided into two parts:

- Stationary part, for which the rudder angle equals the maximum value as given by the rudder limiter.
- Counter-rudder part at the end of the manoeuvre.

During the stationary part the rudder angle is given by:

$$\delta = \delta_{max} \qquad (3.44)$$

and the open-loop analysis of the previous section may be referred to.

For the counter-rudder part δ is given by:

$$\delta = K_p (\psi_r - \psi) - K_d \dot{\psi} \qquad (3.45)$$

with ψ_r the new course setting.
Because the autopilot gains K_p and K_d are known, Eq. (3.45) may be substituted as well in (3.35) as in (3.36), which yields:

$$\tau^* \left(\frac{L}{U_0}\right)^2 \ddot{\psi} + \frac{L}{U_0} \dot{\psi} = K^* K_p(\psi_r - \psi) - K^* K_d \dot{\psi} \qquad (3.46)$$

for the "real" ship and

$$\tau^* \left(\frac{L}{U_p}\right)^2 \ddot{\psi}_p + \frac{L}{U_p} \dot{\psi}_p = K^* K_p(\psi_r - \psi_p) - K^* K_d \dot{\psi}_p \qquad (3.47)$$

for the prediction.
To transform these equations to the s^* domain the last terms of (3.46) and (3.47) are written as:

$$K^* K_d \dot{\psi} = K^* K_d \frac{U_0}{L} \frac{L}{U_0} \dot{\psi} = K^* K_d \frac{U_0}{L} r^* \qquad (3.48)$$

$$K^* K_d \dot{\psi}_p = K^* K_d \frac{U_p}{L} \frac{L}{U_p} \dot{\psi}_p = K^* K_d \frac{U_p}{L} r_p^* \qquad (3.49)$$

and thus:

$$\tau^* \frac{dr^*}{ds^*} + r^* = K^* K_p(\psi_r - \psi) - K^* K_d \frac{U_0}{L} r^* \qquad (3.50)$$

$$\tau^* \frac{dr_p^*}{ds^*} + r_p^* = K^* K_p(\psi_r - \psi_p) - K^* K_d \frac{U_p}{L} r_p^* \qquad (3.51)$$

These relations for the real and the predicted normalized rate of turn are not identical because of the last term, and therefore the track-correspondence condition cannot be satisfied. This problem may, however, be solved if, instead of using a fixed derivative gain, K_d is chosen according to:

$$K_d = K_d^* \frac{L}{U_s} \tag{3.52}$$

with U_s given by the forward speed u for the real ship and the predicted speed U_p for the predictor. This choice for K_d is in accordance with suggestions found in literature (see, for instance, Van Amerongen, 1982).
Noting that, for now, the forward speed of the ship is considered to be constant and equal to the cruising speed U_0, the values for K_d for the real autopilot and for the predictor are given by:

$$K_d = K_d^* \frac{L}{U_0} \tag{3.53}$$

$$K_{dp} = K_d^* \frac{L}{U_p} \tag{3.54}$$

After substituting these values for K_d in Eqs. (3.50) and (3.51) the final equations become:

$$\tau^* \frac{dr^*}{ds^*} + r^*(s^*) = K^* K_p \varepsilon(s^*) - K^* K_d^* r^*(s^*) \tag{3.55}$$

$$\tau \frac{dr_p^*}{ds^*} + r_p^*(s^*) = K^* K_p \varepsilon_p(s^*) - K^* K_d^* r_p^*(s^*) \tag{3.56}$$

with

$$\varepsilon(s^*) = \psi_r - \psi(s^*) \tag{3.57}$$

$$\varepsilon_p(s^*) = \psi_r - \psi_p(s^*) \tag{3.58}$$

Examining (3.55) and (3.56), the relations for the description of r^* and r_p^* in the s^* domain have become identical again, so track correspondence is guaranteed. Therefore from this closed-loop analysis it can be concluded that, whereas forward-speed information remains irrelevant for the predictor, this information should be available for correct gain-scheduling of the autopilot gains according to (3.52).

3.3.3 Influence of the loss of forward speed

In the previous sections the influence of a constant forward speed U_0 on the ship's track was examined. To analyze the influence of the loss of forward speed, due to the ship's turning, the equations proposed by Van Leeuwen for the mathematical description of the ship's normalized yaw and surge motions are reconsidered (Section 2.3.3):

$$\tau^* \frac{dr^*}{ds^*} + H(r^*) = K^* \delta \qquad (3.59)$$

$$\tau_u^* \frac{du^*}{ds^*} + H_u(r^*) = K_u^* r^{*2} \qquad (3.60)$$

with u^* the relative speed loss and a minimal choice for the polynomials:

$$H(r^*) = r^* \quad ; \quad H_u(u^*) = u^* \qquad (3.61)$$

Considering the main cause of the non-linearity in the transfer from rudder to rate of turn to be the loss of forward speed, a sufficient model for the description of this effect becomes:

$$\tau^* \frac{dr^*}{ds^*} + r^* = K^* \delta \qquad (3.62)$$

$$\tau_u^* \frac{du^*}{ds^*} + H_u(r^*) = K_u^* r^{*2} \qquad (3.63)$$

Comparing (3.62) with the first-order prediction model of the previous section:

$$\tau^* \frac{dr_p^*}{ds^*} + r_p^* = K^* \delta \qquad (3.64)$$

it may be concluded that r^* as a function of s^* can be exactly predicted by this model. This implies that the track-correspondence condition is satisfied, regardless of Eq. (3.63) for the description of the loss of forward speed. Therefore, the simple prediction model of (3.64) is also sufficient to deal with the non-linearities, introduced by the loss of forward speed.

3.3.4 Influence of the sway speed

Van Leeuwen proposed the normalized sway speed v* as a function of the normalized rate of turn r^*:

$$v^* + H_v(r^*) = 0 \qquad (3.65)$$

with $v^* = v/u$ and a minimal choice for the polynomial:

$$H_v(r^*) = \gamma^* r^* \qquad (3.66)$$

Assuming the sway velocity for the predictor to be proportional to the predicted rate of turn, the prediction relation becomes:

$$v_p = - \gamma_p r_p \qquad (3.67)$$

Normalizing this relation with respect to the constant forward speed of the predictor U_p yields:

$$v_p^* + \frac{\gamma_p}{L} r_p^* = 0 \qquad (3.68)$$

with

$$v_p^* = \frac{v_p}{U_p} \qquad (3.69)$$

In the case of track correspondence with respect to the forward speed ($r^*(s^*) = r^*_p(s^*)$), the prediction relation (3.68) for the normalized sway velocity is rendered equivalent to relation (3.65) in combination with (3.66) by choosing:

$$\gamma_p = \gamma^* L \qquad (3.70)$$

Because for this choice of γ_p the condition $v^*(s^*) = v^*_p(s^*)$ is satisfied, by (3.24) this implies that overall track correspondence is guaranteed.

Summarizing the results of these sections regarding the speed analysis, the following conclusions may be drawn:

- *Section 3.3.2.1:*

A sufficient prediction model for the open-loop prediction of the ship's track for different cruising speeds U_0 (as described by the Nomoto model) is:

$$\tau^* \frac{L}{U_p} \dot{r}_p + r_p = K^* \frac{U_p}{L} \delta \qquad (3.71)$$

with the predicted speed U_p arbitrary.

- *Section 3.3.2.2:*

The gain scheduling for the derivative gain K_d of the autopilot for correct closed-loop prediction for different cruising speeds U_0 should be:

$$\text{Ship:} \qquad K_d = K_d^* \frac{L}{U_0} \qquad (3.72)$$

$$\text{Predictor:} \qquad K_{dp} = K_d^* \frac{L}{U_p} \qquad (3.73)$$

with the predicted speed U_p arbitrary.

- *Section 3.3.3:*

The prediction model of (3.71) with constant predicted speed U_p is also sufficient for the prediction of the ship's track with loss of forward speed, due to the ship's turning (as described by the Van Leeuwen model).

- *Section 3.3.4:*

A sufficient prediction model for the correct prediction of the sway contribution to the ship's track (as described by the Van Leeuwen model) is:

$$v_p = - \gamma_p r_p \qquad (3.74)$$

in combination with (3.71) and $\gamma_p = \gamma^* L$.

To sum up: a prediction model for the correct prediction of the ship's track has been derived which does not require predictability of the ship's instantaneous speed vector $\underline{U} = (u,v)^T$ during manoeuvring.

3.4 Disturbances

Having examined the predictability of the ship's path by a first-order Nomoto model on the basis of the generalized track description, in this section the influence of the disturbances will be analyzed. The disturbances under consideration are wind and current.

3.4.1 Wind

To carry out the analysis for the wind influence, this influence is incorporated into the Van Leeuwen model as suggested by Schelling (1977):

$$\tau^* \frac{dr^*}{ds^*} + H(r^*) = K^* \delta + \tau^* N_w^* \qquad (3.75)$$

For prediction purposes the additional displacement of the ship, due to the wind force, is treated as current influence.
In (3.75) the normalized wind moment is given by:

$$N_w^* = N_w' \left(\frac{L}{u} \right)^2 \sin(2\gamma_r) V_{wr}^2 \qquad (3.76)$$

with γ_r and V_{wr} the relative wind angle and speed and N_w' specific and approximately constant for each ship. Denoting the normalized relative wind speed as:

$$V_{wr}^* = \frac{V_{wr}}{u} \qquad (3.77)$$

an alternative form for the normalized wind moment becomes:

$$N_w^* = N_w'' \sin(2\gamma_r) V_{wr}^{*2} \qquad (3.78)$$

From (3.75) it follows that for a correct prediction of r^* as a function of s^* - which guarantees track correspondence - knowledge about N_w^* and therefore by (3.78) knowledge about V_{wr}^* and γ_r is required. Because both these quantities depend on the ship's instantaneous speed vector $\underline{U}$ along the ship's path, exact prediction becomes impossible without information on the ship's forward speed u

and sway speed v.
However, global information about the wind effect on the ship's yawing behaviour may be incorporated into the predictor by writing:

$$\tau^* \frac{dr_p^*}{ds^*} + r_p^* = K^* \delta + N_{wp}^* \sin(2\gamma_{rp}) \qquad (3.79)$$

with N_{wp}^* based on the maximum rudder angle necessary to compensate for the wind influence according to:

$$N_{wp}^* = K^* \delta_{wmax} \qquad (3.80)$$

and γ_{rp} the angle between the absolute wind direction and the ship's predicted heading:

$$\gamma_{rp} = \psi_w - \psi_p \qquad (3.81)$$

Another possible approach is to compensate for the wind influence by the course-changing controller according to Eqs. (3.82) and (3.83):

$$K^* \frac{dr^*}{ds^*} + H(r^*) = K^* \delta' + \tau^* N_w^* \qquad (3.82)$$

where

$$\delta' = \delta - \frac{\tau^*}{K^*} \hat{N}_w^* \qquad (3.83)$$

and $\hat{N}_w^*$ is provided by an on-line estimation procedure on the basis of the measured relative wind angle and speed.
In the case of a first-order polynomial for $H(r^*)$, substitution of this choice for δ' in (3.82) yields for the description of the ship's normalized yaw motion r^*:

$$\tau^* \frac{dr^*}{ds^*} + r^* = K^* \delta \qquad (3.84)$$

and track correspondence is guaranteed for the first-order prediction model without wind influence:

$$\tau^* \frac{dr_p^*}{ds^*} + r_p^* = K^* \delta \qquad (3.85)$$

3.4.2 Current

The effect of uniform current may be added to the kinematic relations in the time domain according to (Section 2.5.2) :

$$x_s(t) = \int_0^t u \cos(\psi) d\tau - \int_0^t v \sin(\psi) d\tau + \int_0^t U_c \cos(\psi_c) d\tau \qquad (3.86)$$

$$y_s(t) = \int_0^t u \sin(\psi) d\tau + \int_0^t v \cos(\psi) d\tau + \int_0^t U_c \sin(\psi_c) d\tau \qquad (3.87)$$

with U_c and ψ_c the current speed and direction. Adding this current influence to the predictor, the equations for the predicted track in the time domain become:

$$x_p(t) = \int_0^t U_p \cos(\psi_p) d\tau - \int_0^t v_p \sin(\psi_p) d\tau + \int_0^t U_c \cos(\psi_c) d\tau \qquad (3.88)$$

$$y_p(t) = \int_0^t U_p \sin(\psi_p) d\tau + \int_0^t v_p \cos(\psi_p) d\tau + \int_0^t U_c \sin(\psi_c) d\tau \qquad (3.89)$$

Comparing (3.86)-(3.87) with (3.88)-(3.89) it follows that in the time domain the influence of the current is identical for the real and the predicted path, regardless of U_p , v_p and ψ_p. This, however, does not imply track correspondence between the real and the predicted path, as can be seen by transforming the equations to the s^* domain. This yields, for instance, for the x-coordinate:

$$x_s^* = \int_0^{s^*} \cos(\psi) d\sigma^* - \int_0^{s^*} \sin(\psi)\, v^* d\sigma^* + \int_0^{s_c^*} \cos(\psi_c) d\sigma_c^* \qquad (3.90)$$

$$x_p^* = \int_0^{s^*} \cos(\psi_p) d\sigma^* - \int_0^{s^*} \sin(\psi_p)\, v_p^* d\sigma^* + \int_0^{s_c^*} \cos(\psi_c) d\sigma_c^* \qquad (3.91)$$

where

$$ds_c^* = \frac{U_c}{L} dt = \frac{U_c}{u_n} ds^* = U_c^* ds^* \qquad (3.92)$$

and $u_n = u$ for (3.90), $u_n = U_p$ for (3.91).
substituting (3.92) in Eqs. (3.90) and (3.91) yields:

$$x_s^* = \int_0^{s^*} \cos(\psi) d\sigma^* - \int_0^{s^*} \sin(\psi) v^* d\sigma^* + \int_0^{s^*} \cos(\psi_c) \frac{U_c}{u} d\sigma^* \qquad (3.93)$$

$$x_p^* = \int_0^{s^*} \cos(\psi_p) d\sigma^* - \int_0^{s^*} \sin(\psi_p) v_p^* d\sigma^* + \int_0^{s^*} \cos(\psi_c) \frac{U_c}{U_p} d\sigma^* \qquad (3.94)$$

Examining the current-dependent parts of Eqs. (3.93) and (3.94) it may be concluded that for track correspondence between the real and the predicted path, regarding the current contribution, the following condition must be satisfied:

$$\frac{U_c}{u} = \frac{U_c}{U_p} \quad \text{or} \quad U_p(s^*) = u(s^*) \qquad (3.95)$$

Therefore information about the ship's forward speed becomes essential for a correct prediction.
An approximation may be obtained by selecting:

$$U_p = U_0 \qquad (3.96)$$

with U_0 the ship's cruising speed before the start of a manoeuvre.

3.5 Simulation results

To illustrate the theoretical conclusions on the basis of the generalized track description some simulations were carried out. These simulations were performed with the Interactive Simulation Package PSI, which was developed at the Control Laboratory (Van den Bosch, 1981). For this purpose the basic prediction scheme was compared to the non-linear De Keizer model of the "ROV Zeefakkel", a naval training vessel for which this model had been identified on the basis of full-scale trials (De Keizer, 1977). The simulations were performed both with and without

the influence of uniform current.

3.5.1 Results for different rudder limits

The closed-loop prediction scheme, described in Section 3.3.2.2, was tested for a large course change of 120 degrees for 3 different rudder limits at a cruising speed of 9 knots (4.5 m/s), which was also the value for the constant predicted speed. The results for the ship's "real" (according to the De Keizer model) and predicted rate of turn, forward speed and sway velocity for a rudder limit of 10,20 and 30 degrees are presented in Figures 3.6, 3.7 and 3.8:

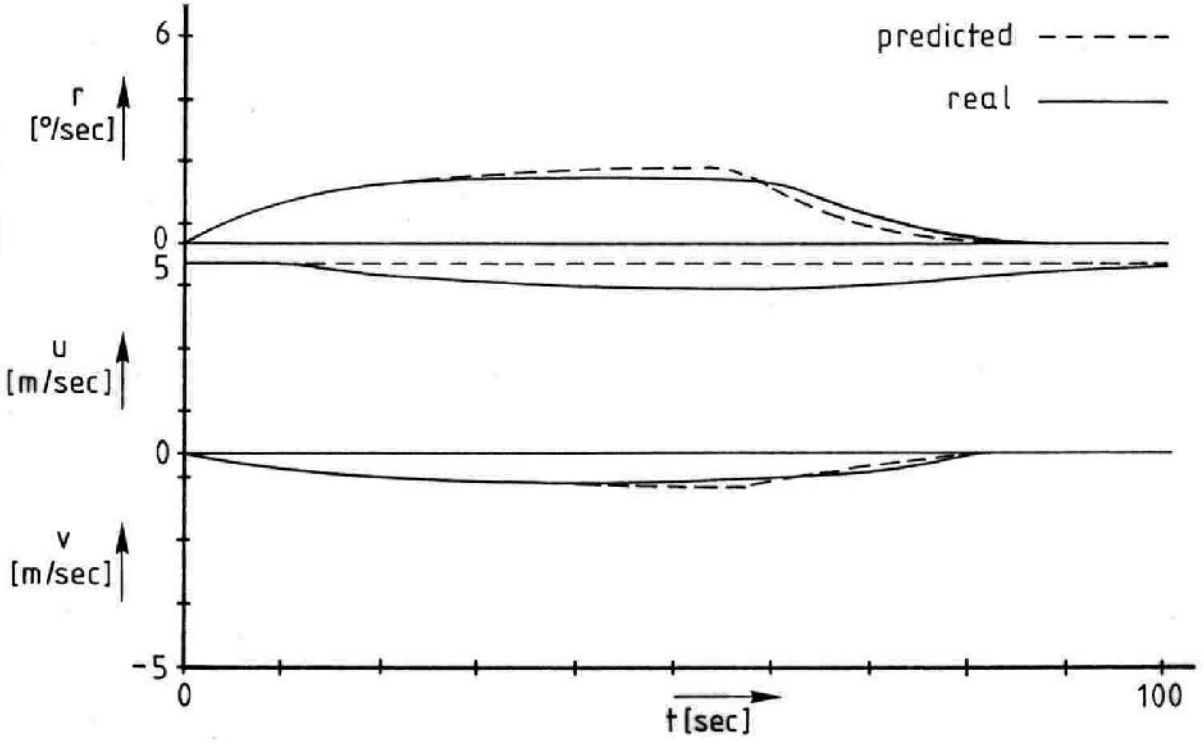

Fig. 3.6 Results for a rudder limit of 10 degrees

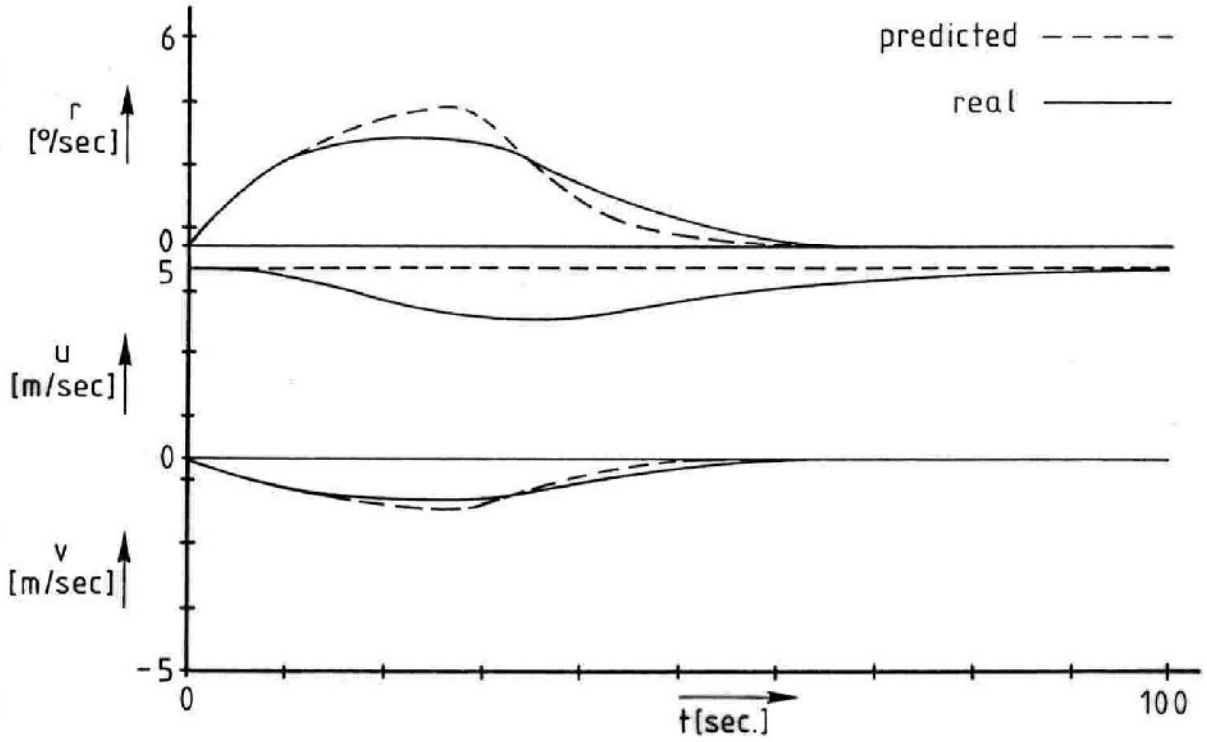

Fig. 3.7 Results for a rudder limit of 20 degrees

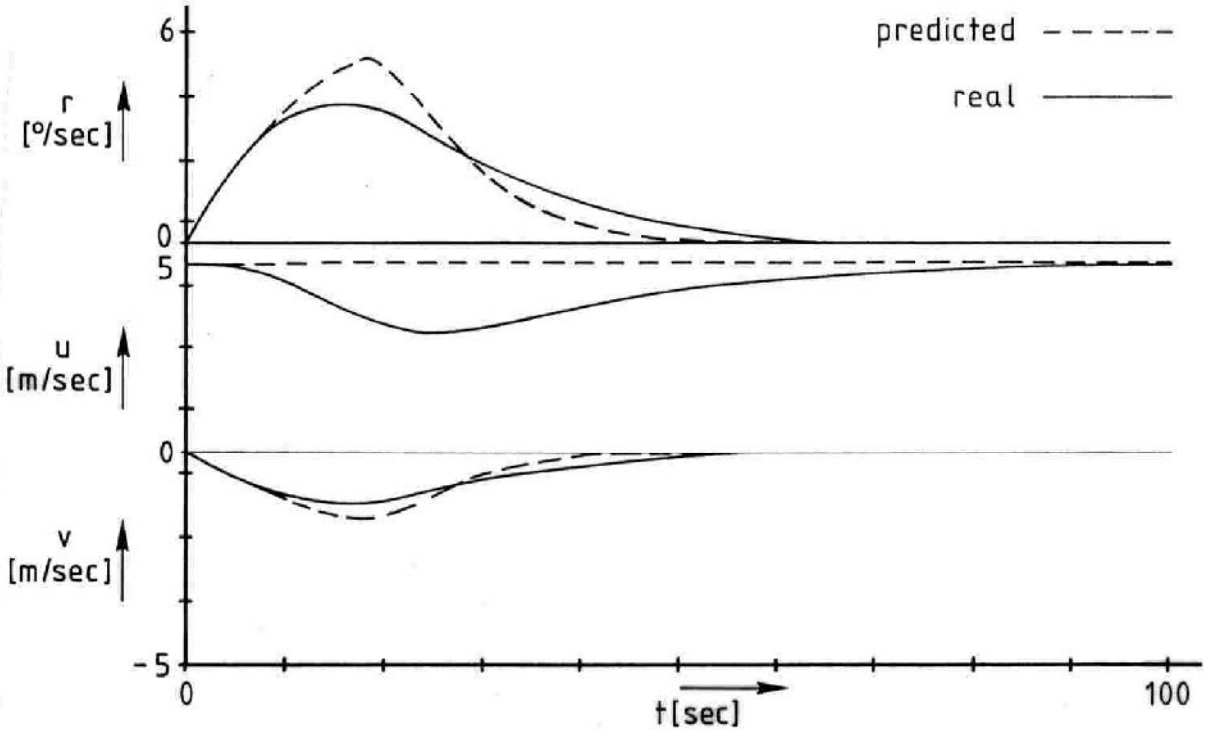

Fig. 3.8 Results for a rudder limit of 30 degrees

From these results it may already be concluded that the real and predicted tracks certainly cannot correspond on a time basis because of the deviations between the

real and predicted rate-of-turn and speed signals. To analyze the track correspondence between the real and the predicted paths, in Figures 3.9, 3.10 and 3.11 the ship's real and predicted normalized rate of turn r^* and sway velocity v^* are presented for the different rudder limits as a function of s^*.

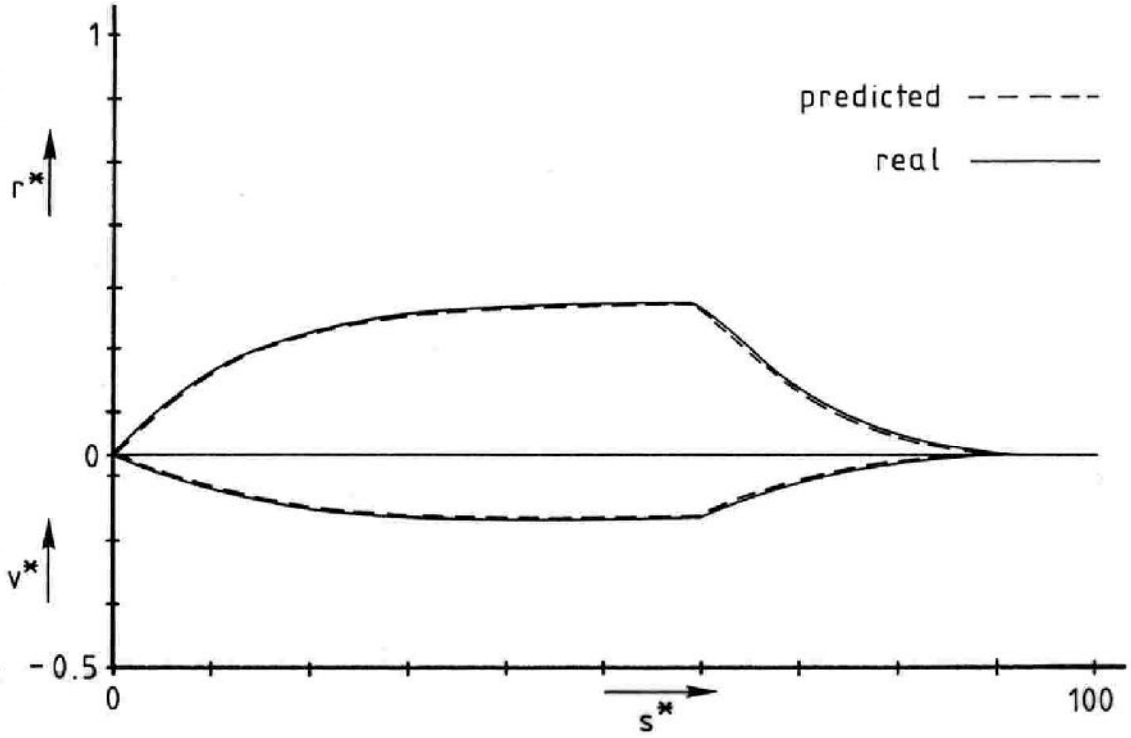

Fig. 3.9 Normalized results for a rudder limit of 10 degrees

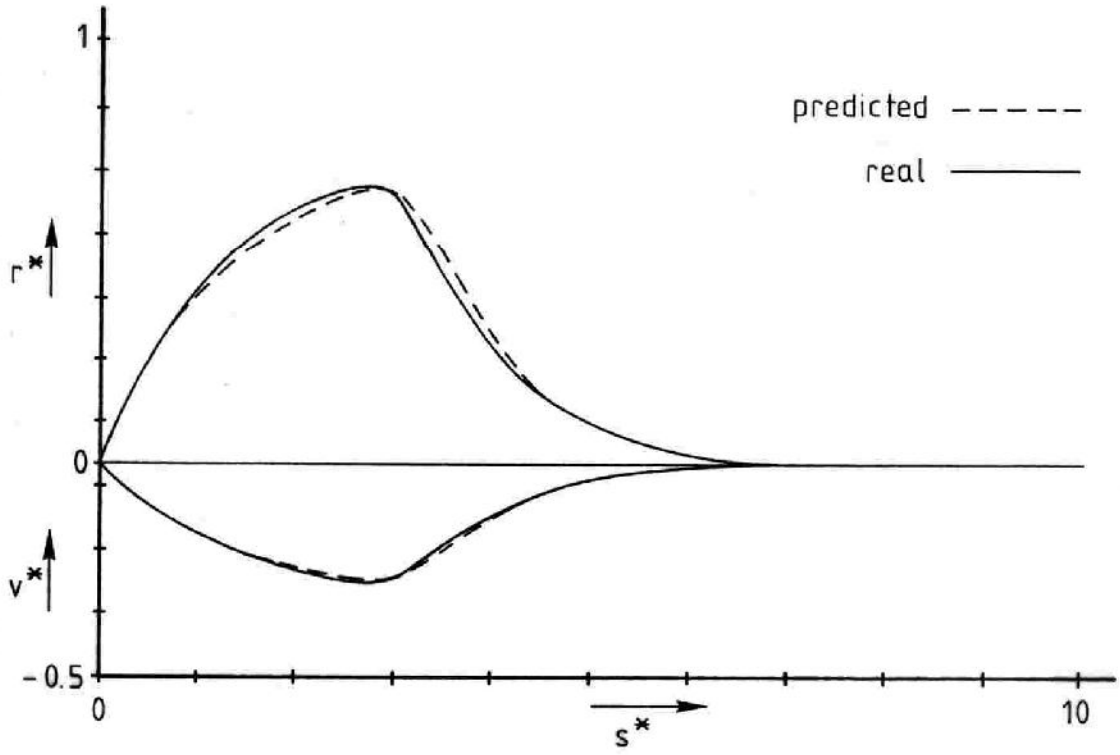

Fig. 3.10 Normalized results for a rudder limit of 20 degrees

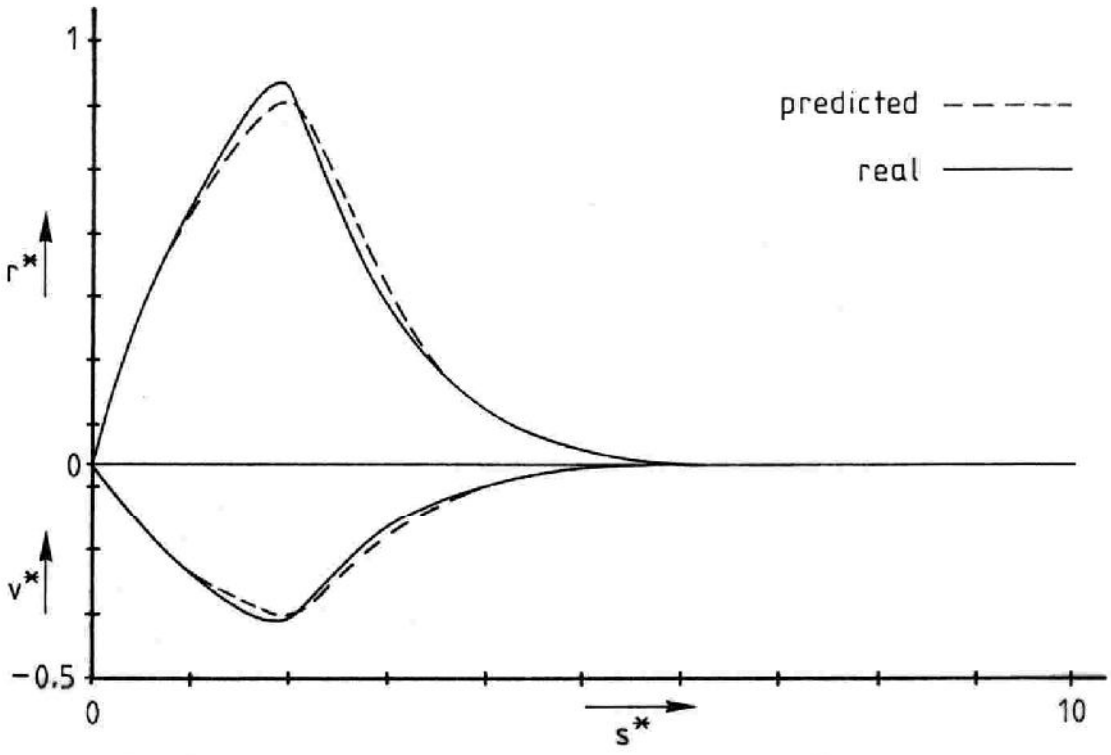

Fig. 3.11 Normalized results for a rudder limit of 30 degrees

Comparing these real and predicted normalized signals to each other, a reasonable correspondence between the real and predicted values may be observed. This leads to the conclusion of a reasonable track correspondence between the real and the

predicted path on the basis of the generalized track description. This is confirmed by Figure 3.12, where the real and predicted tracks are presented for the three rudder limits.

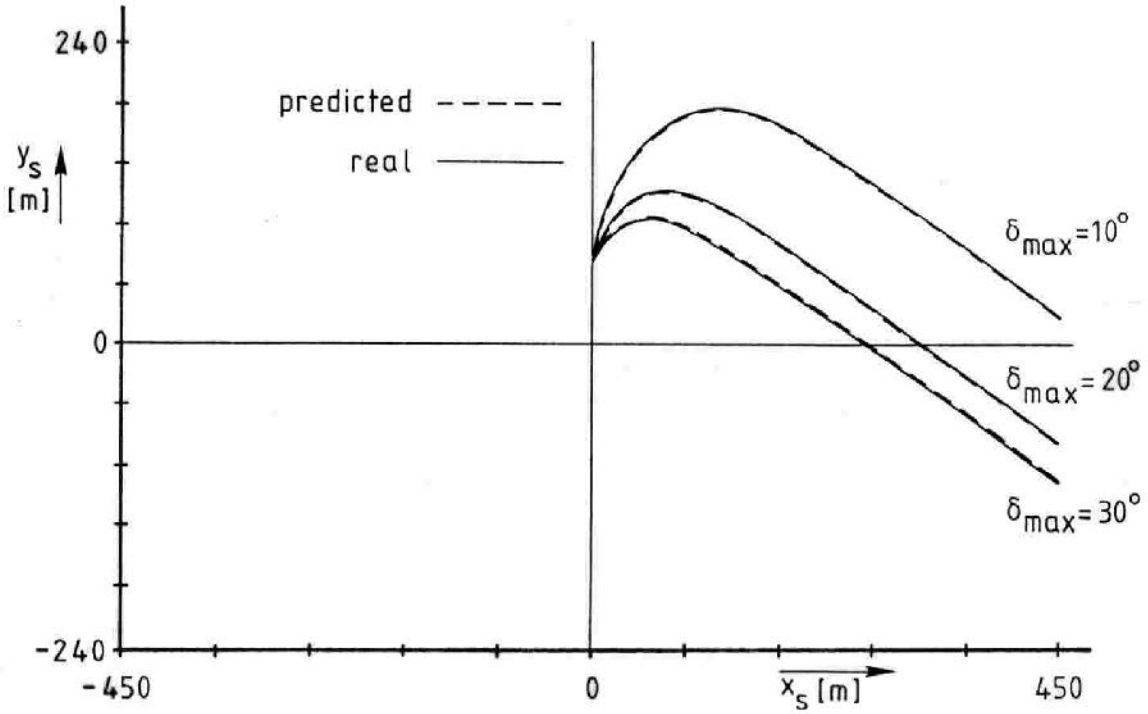

Fig. 3.12 Real and predicted tracks for the different rudder limits

3.5.2 Results in the presence of uniform current

To demonstrate the effect of adding the influence of uniform current to a predicted path with reasonable track correspondence in the absence of disturbances, the experiment described in the previous section was repeated for a rudder limit of 20 degrees, both with and without the influence of current. The current direction and speed were 315 degrees and 3 knots. The results obtained without and with current influence are presented simultaneously in Figure 3.13, to enable a direct comparison.

From this figure the conclusion of Section 3.4.2 is confirmed in that, although there is an exact track correspondence between the real and the predicted path in the absence of current, and although the current speed and direction are exactly known, a deviation between the real and the predicted path will occur under the influence of current, because of the incorrect prediction of the ship's forward speed. However, the results also confirm that a reasonable track correspondence may still be obtained by choosing for the predicted speed U_p the ship's cruising speed U_0.

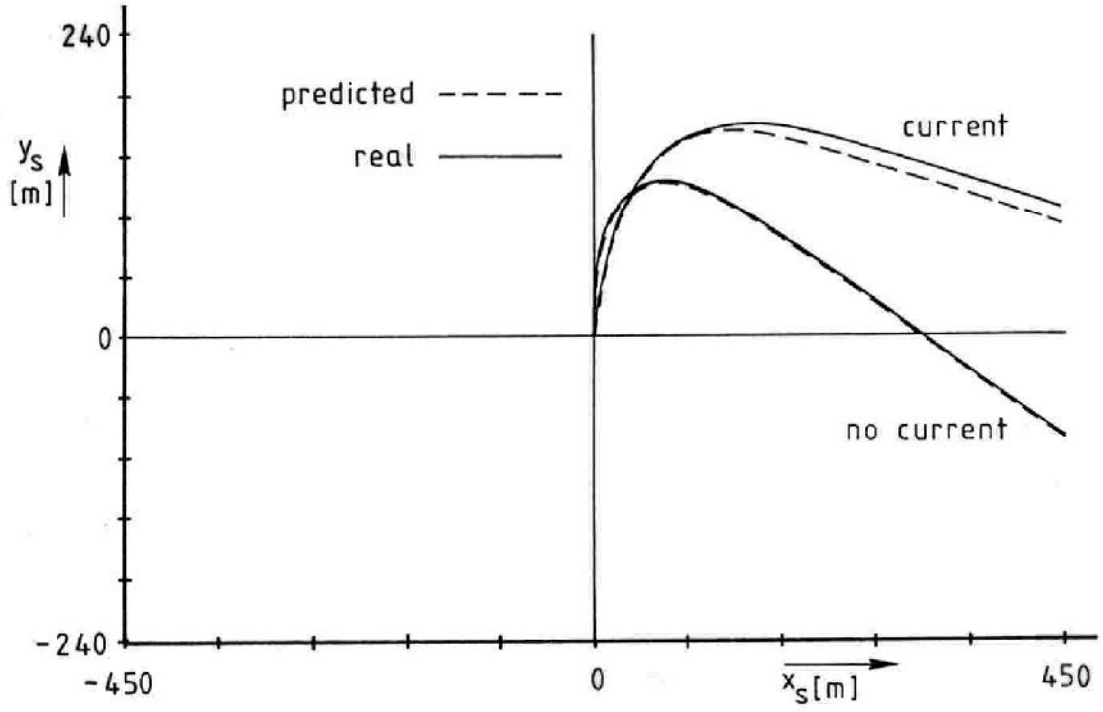

Fig. 3.13 Real and predicted tracks without and with current

3.6 Discussion

In this chapter a generalized track description has been derived on the basis of which a correct translation method was proved to be a translation of the predicted track on the basis of a correspondence between the real and the predicted course (Section 3.2).

Using the generalized track description, in Section 3.3 the predictability of the ship's track by a first-order Nomoto model with regard to the ship's dynamics was examined.
The main conclusion, which is confirmed by the simulation results in Section 3.5, is that a sufficient prediction scheme is provided by the linear first-order model of Figure 3.14 if the only demand for the predictor is one of track correspondence between the real and the predicted path.

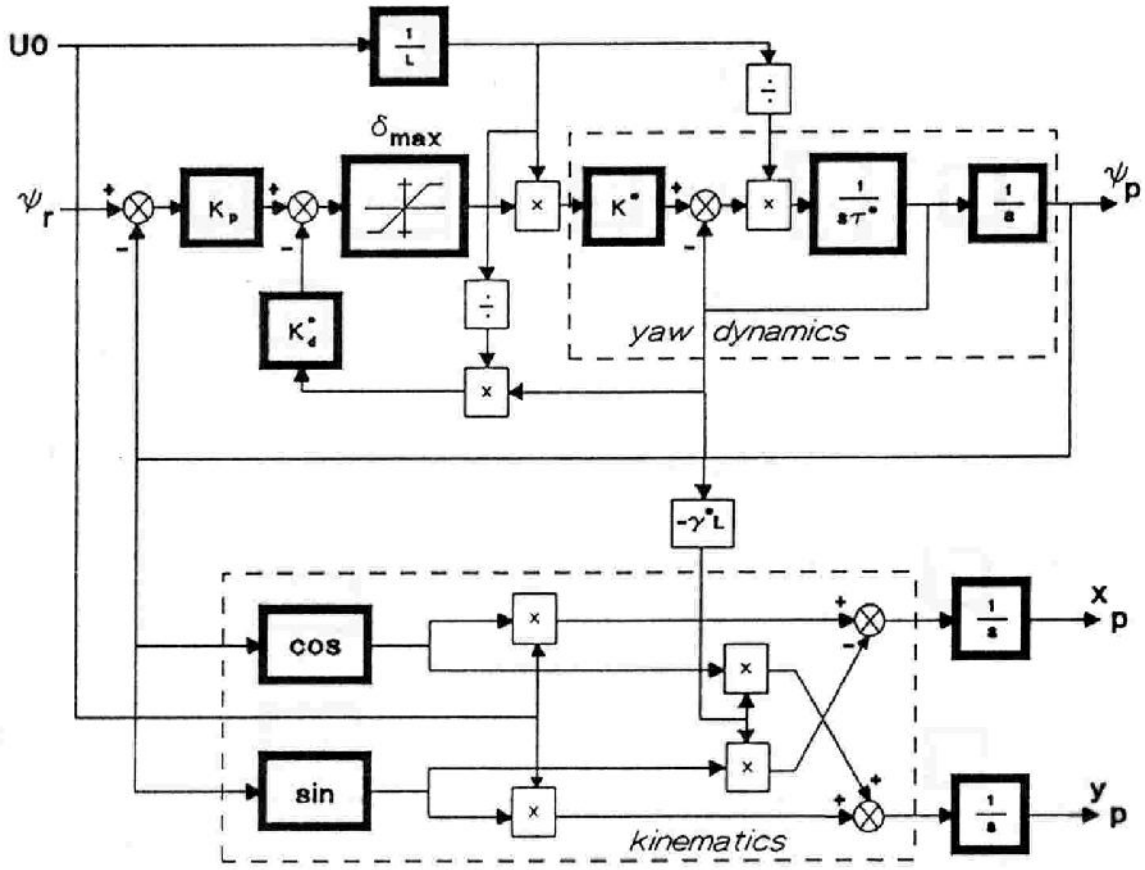

Fig. 3.14 The basic prediction scheme

with parameters K^* , τ^* and γ^* for the ship's dynamics,

K_p , K_d^* for the autopilot,

U_0 and L for the scheduling of these parameters

For the incorporation of the disturbances like wind and current into the predictor it was demonstrated that knowledge about the ship's forward speed u becomes essential for exact prediction. However, an approximation may be obtained by selecting the predicted speed equal to the ship's cruising speed U_0 (Section 3.4).

4 IDENTIFICATION AND ADAPTATION

4.1 Introduction

In Chapter 3 an approach to predicting the ship's track on the basis of a relatively simple mathematical model which is adapted to changing conditions was discussed. This closed-loop approach requires a method for on-line identification and adaptation of the model parameters. This chapter will concentrate on the available theory regarding on-line state and parameter estimation and adaptive control.
Because of the crucial role which the measurements play in the chosen approach, in Section 4.2 attention will be focussed on the optimal interpretation of measurements by following a statistical approach. This can be applied to both static and dynamic measurement problems.
As an extension of this analysis, the Kalman filter will be derived for state estimation by treating dynamic model knowledge as a-priori information for the optimal measurement-filtering scheme (Section 4.3).
Regarding the estimation of the model parameters, in Section 4.4 the theories of discrete MRAS and Least Squares identification will be unified by analyzing them both from the optimal measurement-reconstruction point of view.
For a combined estimation of the model state and parameters, the principle of Kalman filtering may be extended to the parameter domain. This results in a non-linear filtering problem, which after linearization yields the relations for the Extended Kalman filter (Section 4.5).
Further, the analogy between MRAS identification and control will be extended to the field of Kalman filtering in Section 4.6.
Finally, in Section 4.7 some conclusions will be drawn regarding the applicability of the theory presented here to the development of the actual track-prediction system.

4.2 Optimal measurement interpretation

To clarify the basic concept behind Kalman filtering, in this section attention will be focussed on the optimal estimation of variables on the basis of inexact observations (measurements). Put formally, this problem can be stated as the determination of the probability density function of a stochastic process, by using

the observations of another, related, stochastic process (Maybeck, 1979).
For the present study a distinction will be made between the optimal filtering (Section 4.2.1) and reconstruction of variables (Section 4.2.2).

4.2.1 Measurement filtering

To make the distinction between the filtering of measurements and the reconstruction, a linear statistical model of the type of Eq. (4.1) is assumed for the description of the inaccurate measurement:

$$\tilde{\underline{z}} = \underline{z} + \underline{v} = H\underline{x} + \underline{v} \qquad (4.1)$$

where $\underline{x}$ is the vector quantity to be estimated, $\underline{x} \in \mathbb{R}^n$
$\underline{z}$ is the observation of $\underline{x}$ through the observation matrix H, $\underline{z} \in \mathbb{R}^{n_z}$, $H \in \mathbb{R}^{n_z} \times \mathbb{R}^n$
$\underline{v}$ is observation noise, $\underline{v} \in \mathbb{R}^{n_z}$
$\tilde{\underline{z}}$ is the noise-corrupted measurement of $\underline{x}$, $\tilde{\underline{z}} \in \mathbb{R}^{n_z}$

This model will be referred to as the measurement model. The linear measurement model can be rewritten to Eq. (4.2), where the variable $\underline{x}$ is separated into a directly observable part $\underline{x}_d$ and an indirectly observable part $\underline{x}_i$ (see also Figure 4.1):

$$\tilde{\underline{z}} = (H_d \quad 0)\ (\ \underline{x}_d^T,\ \underline{x}_i^T\ )^T + \underline{v} \qquad (4.2)$$

where $\underline{x}_d \in \mathbb{R}^{n_d}$, $\underline{x}_i \in \mathbb{R}^{n_i}$ and $H_d \in \mathbb{R}^{n_z} \times \mathbb{R}^{n_d}$, $n_z \geq n_d$

The problem of determing $\underline{x}_d$ from $\tilde{\underline{z}}$, which now is defined as the filtering problem, will be treated in this section, whereas the problem of determing the indirectly observable part $\underline{x}_i$ from the measurements, which is defined as the reconstruction problem, will be deferred to in the next section.

The measurement of the directly observable part of $\underline{x}$ may be written as:

$$\tilde{\underline{z}} = H_d\ \underline{x}_d + \underline{v} \qquad (4.3)$$

If information on $\underline{x}_d$ is available before the measurement $\tilde{\underline{z}}$ is known (based on,

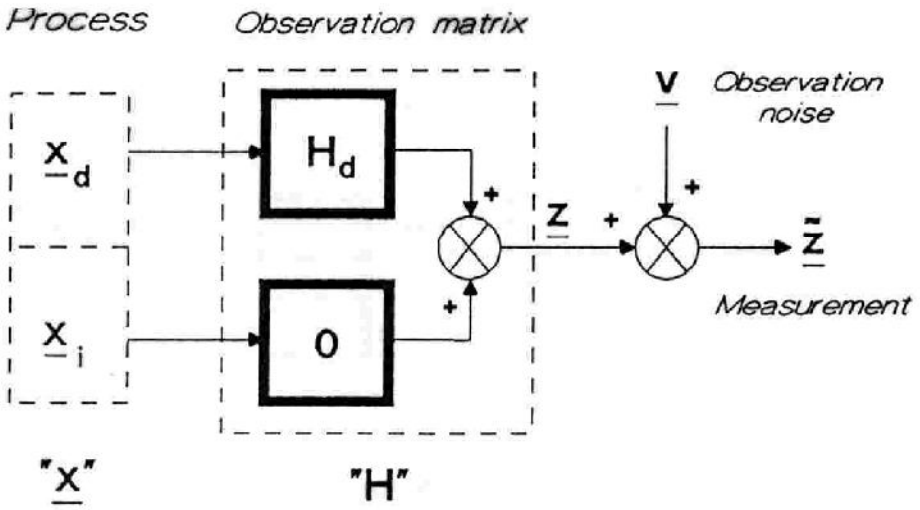

Fig. 4.1 Measurement model for the observation of $\underline{x}$

for instance, previous measurements) the estimation of $\underline{x}_d$ on the basis of this information is called the a-priori estimation of $\underline{x}_d$. In the same way the a-posteriori estimation of $\underline{x}_d$ is the estimation of $\underline{x}_d$, once the measurement $\tilde{\underline{z}}$ is known:

$$a\ priori:\ \bar{\underline{x}}_d \quad + \quad measurement:\ \tilde{\underline{z}} \quad \longrightarrow \quad a\ posteriori:\ \hat{\underline{x}}_d$$

In accordance with this measurement scheme the optimal filtering problem may be reformulated to determine the optimal a-posteriori estimation of $\underline{x}_d$ on the basis of the measurement $\tilde{\underline{z}}$ and the a-priori information on $\underline{x}_d$.
For a definition of the term "optimal" the statistics of the observation noise $\underline{v}$ have to be considered:
In the case of unknown statistics of $\underline{v}$ (which also implies the accuracy of the measurement to be unknown), the measurement $\tilde{\underline{z}}$ does not provide any reliable new information about $\underline{x}_d$, and the optimal a-posteriori estimation obviously reduces to the a-priori estimation:

$$\hat{\underline{x}}_d = \bar{\underline{x}}_d \qquad (4.4)$$

When some of the statistics of $\underline{v}$ are known in the form of, for instance, a probability-density function, an optimal choice of the a-posteriori estimation is possible.
Knowledge of this probability density function of $\underline{v}$ can be used for the determination of the probability density function of the a-posteriori estimation, once the measurement $\tilde{\underline{z}}$ is known. The statistically optimal choice for this a-posteriori estimation of $\underline{x}_d$ would then be given by the conditional mean:

$$\hat{\underline{x}}_d = E\{ \underline{x}_d / \tilde{\underline{z}} \} \qquad (4.5)$$

When, for instance, a Gaussian model for $\underline{v}$ is assumed, knowledge of the mean value and covariance of $\underline{v}$ is sufficient for the description of the Gaussian probability density function. The mean and covariance of $\underline{v}$ are defined as:

$$E\{\underline{v}\} = \bar{\underline{v}} \qquad (4.6)$$

$$E\{ (\underline{v} - \bar{\underline{v}})(\underline{v} - \bar{\underline{v}})^T \} = R \qquad (4.7)$$

According to the notation of (4.6), $E\{\underline{v}\}$ may also be regarded as the a-priori estimation of $\underline{v}$, which of course is correct because $E\{\underline{v}\}$ is by definition the statistical expectation of $\underline{v}$.
In this case of a Gaussian density it can be shown that the conditional mean of (4.5) also maximizes the conditional probability density function of $\underline{x}_d$, which is referred to as the maximum-a-posteriori choice:

$$\hat{\underline{x}}_d = E\{ \underline{x}_d / \tilde{\underline{z}} \} = \max_{\underline{x}_d} p(\underline{x}_d / \tilde{\underline{z}}) \qquad (4.8)$$

Without loss of generality, in the following it will be assumed that $\underline{v}$ has zero mean. Further, the separate components of this noise vector are assumed to be statistically independent of each other, which reduces the covariance matrix R to a diagonal matrix:

$$E\{ \underline{v} \} = \underline{0} \qquad (4.9)$$

$$r_{ij} = \sigma_i^2 \quad ; \quad i=j \qquad (4.10)$$

$$r_{ij} = 0 \quad ; \quad i \neq j \qquad (4.11)$$

with r_{ij} an element of R and σ_i^2 the variance of v_i.
For the comparison of the a-priori and a-posteriori estimations of $\underline{x}_d$, the covariance matrices of these estimations are introduced. The a-priori covariance matrix M and a-posteriori covariance matrix P are defined as:

$$M = E\{ (\underline{x}_d - \bar{\underline{x}}_d)(\underline{x}_d - \bar{\underline{x}}_d)^T \} \qquad (4.12)$$

$$P = E\{ (\underline{x}_d - \hat{\underline{x}}_d)(\underline{x}_d - \hat{\underline{x}}_d)^T \} \qquad (4.13)$$

An alternative form for the problem of determing the optimal a-posteriori estima-

tion which is equivalent to (4.8) is then given by:

$$\min_{\hat{\underline{x}}_d}! \ \text{trace}\ \{P(\hat{\underline{x}}_d)\} \qquad (4.14)$$

with trace {P} the summation of the diagonal elements of the a-posteriori covariance matrix P, given by (4.13).
For the solution of (4.14), two extremes of this minimization problem are considered:

- In the case of large measurement noise (large variance R) the solution of (4.14) becomes trivial (just as in the case where no information about the reliability of $\tilde{\underline{z}}$ is available):

$$\hat{\underline{x}}_d = \bar{\underline{x}}_d \qquad (4.15)$$

$$P_{min} = M \qquad (4.16)$$

  with P_{min} the minimal value of P
- In the absence of measurement noise ($\underline{v} = \underline{0}$, R = 0), on the basis of the measurement model (4.3) the corresponding trivial solution of (4.14) becomes:

$$\hat{\underline{x}}_d = H_d^{-1}\tilde{\underline{z}} = H_d^{-1}\underline{z} \qquad (4.17)$$

$$P_{min} = 0 \qquad (4.18)$$

  with H_d^{-1} the inverse or pseudo inverse of the observation matrix H_d, depending on the redundancy of the measurement vector $\tilde{\underline{z}}$. The observation matrix H_d is invertible because $\underline{x}_d$ is by definition directly observable from $\tilde{\underline{z}}$.

Now for arbitrary R, the a-posteriori estimation of $\underline{x}_d$ is written as a linear interpolation between the 2 extreme solutions of (4.15) and (4.17):

$$\hat{\underline{x}}_d = \bar{\underline{x}}_d + \Lambda(H_d^{-1}\tilde{\underline{z}} - \bar{\underline{x}}_d) \quad ; \quad \Lambda \in \mathbb{R}^{n_d} \times \mathbb{R}^{n_d} \qquad (4.19)$$

or

$$\hat{\underline{x}}_d = \bar{\underline{x}}_d + K_d (\tilde{\underline{z}} - H_d \bar{\underline{x}}_d) \qquad (4.20)$$

$$K_d = \Lambda H_d^{-1} \qquad (4.21)$$

The extreme solutions of (4.15) and (4.17) are obtained by choosing for the interpolation matrix $\Lambda = 0$ or $\Lambda = I$.
Substituting the measurement model of (4.3) for $\tilde{\underline{z}}$ in (4.20) yields a relation between the *a-posteriori* and *a-priori* estimation error:

$$(\hat{\underline{x}}_d - \underline{x}_d) = (I - K_d H_d)(\bar{\underline{x}}_d - \underline{x}_d) + K_d \underline{v} \qquad (4.22)$$

and together with Eqs. (4.7), (4.12) and (4.13):

$$P = (I - K_d H_d) M (I - K_d H_d)^T + K_d R K_d^T \qquad (4.23)$$

by treating the a-posteriori error as the summation of two statistically independent variables.
This expression for P may be written as:

$$P = (I - K_d H_d) M + (K_d (H_d M H_d^T + R) - M H_d^T) K_d^T \qquad (4.24)$$

The choice for K_d which minimizes trace $\{P\}$ is given by:

$$K_{dopt} = M H_d^T (H_d M H_d^T + R)^{-1} \qquad (4.25)$$

By (4.24) the a-posteriori covariance matrix P for this choice of K_d reduces to:

$$P_{min} = (I - K_d H_d) M = (I - \Lambda) M \qquad (4.26)$$

Because of the assumed Gaussian density for $\underline{v}$ the a-posteriori estimation for $\underline{x}_d$ given by (4.20) in combination with (4.25) also maximizes the conditional probability density function for $\underline{x}_d$. Further, it equals the conditional mean of this density function, which is, from a statistical viewpoint, the best estimation available for $\underline{x}_d$, once the measurement $\tilde{\underline{z}}$ is known.
Resuming, an optimal filtering of the measurement $\tilde{\underline{z}}$ is provided by:

$$\hat{\underline{x}}_d = \bar{\underline{x}}_d + K_d(\tilde{\underline{z}} - H_d\bar{\underline{x}}_d) \qquad (4.27)$$

$$K_d = MH_d^T(H_dMH_d^T + R)^{-1} \qquad (4.28)$$

In this case the a-posteriori and a-priori covariance matrices P and M are related by:

$$P = (I - K_dH_d)M \qquad (4.29)$$

The block-diagram for the optimal update of the a-priori estimation to the a-posteriori estimation on the basis of the measurements is presented in Figure 4.2.

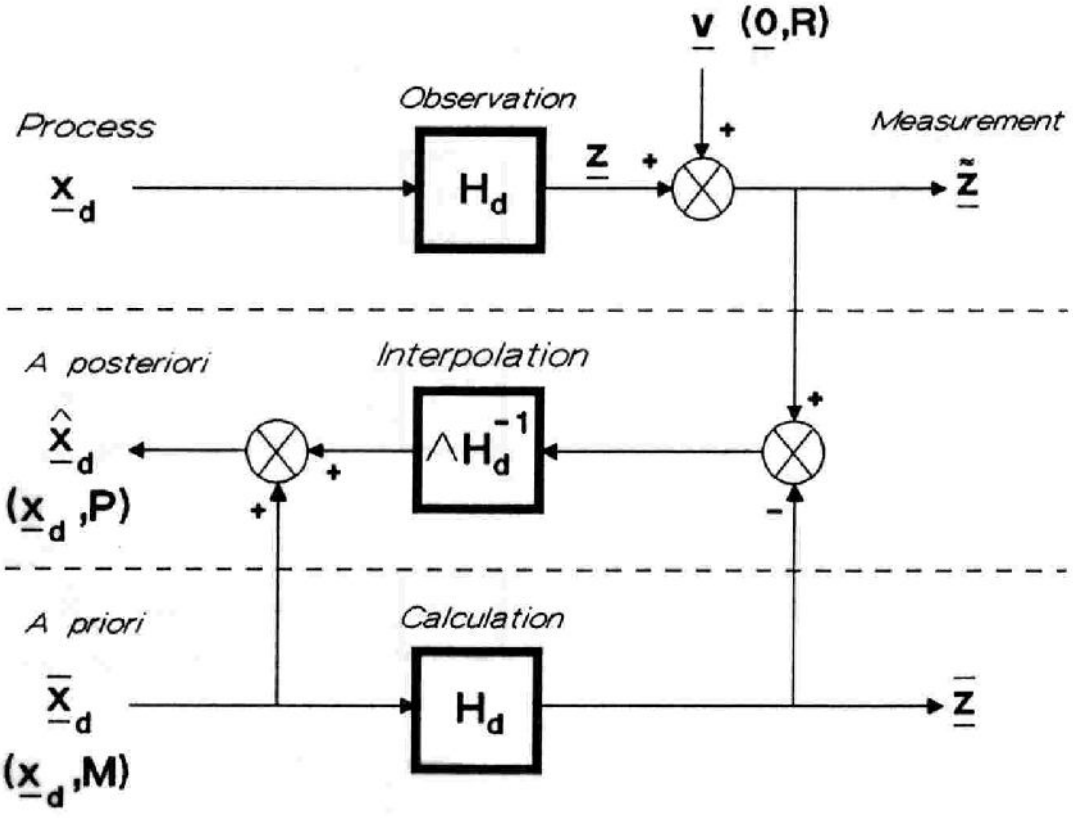

Fig. 4.2 Measurement filtering by optimal interpolation

The notation $\underline{v}$ ($\underline{0}$,R) is introduced to state that $\underline{v}$ has zero mean and covariance R.

4.2.2 Measurement reconstruction

As defined in the previous section, by measurement reconstruction the estimation of not directly observable variables from the measurements is meant. This implies that the observation matrix H equals zero for these variables, according to (4.30):

$$\underline{\tilde{z}} = (H_d \quad 0)(\underline{x}_d^T, \underline{x}_i^T)^T + \underline{v} \qquad (4.30)$$

where $\underline{x}_i$ is the indirectly observable part of $\underline{x} = (\underline{x}_d^T , \underline{x}_i^T)^T$.
Assuming a-priori information on $\underline{x}_i$ to be available, the overall a-priori estimation for $\underline{x}$ becomes:

$$\underline{\bar{x}} = (\underline{\bar{x}}_d^T, \underline{\bar{x}}_i^T)^T \qquad (4.31)$$

and the covariance matrix M :

$$M = E\{(\underline{x} - \underline{\bar{x}})(\underline{x} - \underline{\bar{x}})^T\} = \begin{bmatrix} M_{dd} & M_{di} \\ M_{id} & M_{ii} \end{bmatrix} \qquad (4.32)$$

with the submatrices:

$$M_{dd} = E\{(\underline{x}_d - \underline{\bar{x}}_d)(\underline{x}_d - \underline{\bar{x}}_d)^T\} \qquad (4.33)$$

$$M_{di} = E\{(\underline{x}_d - \underline{\bar{x}}_d)(\underline{x}_i - \underline{\bar{x}}_i)^T\} \qquad (4.34)$$

$$M_{id} = E\{(\underline{x}_i - \underline{\bar{x}}_i)(\underline{x}_d - \underline{\bar{x}}_d)^T\} = M_{di}^T \qquad (4.35)$$

$$M_{ii} = E\{(\underline{x}_i - \underline{\bar{x}}_i)(\underline{x}_i - \underline{\bar{x}}_i)^T\} \qquad (4.36)$$

Noting that M_{id} and M_{dd} can be treated as regression coefficients for $\underline{x}_i$ with respect to $\underline{x}_d$, these variables are related to each other by:

$$(\underline{x}_i - \underline{\bar{x}}_i) = M_{id}M_{dd}^{-1}(\underline{x}_d - \underline{\bar{x}}_d) \qquad (4.37)$$

Substituting the best estimation for $\underline{x}_d$ after the measurement, obtained by optimal measurement filtering, yields for the a-posteriori estimation of the indirectly observable part:

$$(\hat{\underline{x}}_i - \bar{\underline{x}}_i) = M_{id}M_{dd}^{-1}(\hat{\underline{x}}_d - \bar{\underline{x}}_d) \qquad (4.38)$$

or

$$\hat{\underline{x}}_i = \bar{\underline{x}}_i + M_{id}M_{dd}^{-1}(\hat{\underline{x}}_d - \bar{\underline{x}}_d) \qquad (4.39)$$

where by (4.27) :

$$\hat{\underline{x}}_d = \bar{\underline{x}}_d + \Lambda H_d^{-1}(\tilde{\underline{z}} - H_d\,\bar{\underline{x}}_d) \qquad (4.40)$$

Thus a combined update scheme for the estimation of both the directly and the indirectly observable parts of $\underline{x}$ on the basis of the measurement $\tilde{\underline{z}}$ is obtained:

$$\hat{\underline{x}} = \bar{\underline{x}} + K(\tilde{\underline{z}} - H\bar{\underline{x}}) \qquad (4.41)$$

with

$$K = \begin{bmatrix} I \\ M_{id}M_{dd}^{-1} \end{bmatrix} K_d \qquad (4.42)$$

and K_d given by (4.28).
Substituting (4.28) in (4.42) finally yields for the overall update gain K:

$$K = MH^T(HMH^T + R)^{-1} \qquad (4.43)$$

Concluding, for the linear measurement model, the combined solution of the overall filtering and reconstruction problem becomes:

$$\hat{\underline{x}} = \bar{\underline{x}} + K(\tilde{\underline{z}} - H\bar{\underline{x}}) \qquad (4.44)$$

with K given by (4.43).

This combined filtering scheme in this case can be treated as the result of linear interpolation for the directly observable part $\underline{x}_d$ of $\underline{x}$ and linear regression for the indirectly observable part $\underline{x}_i$ (see Figure 4.3).

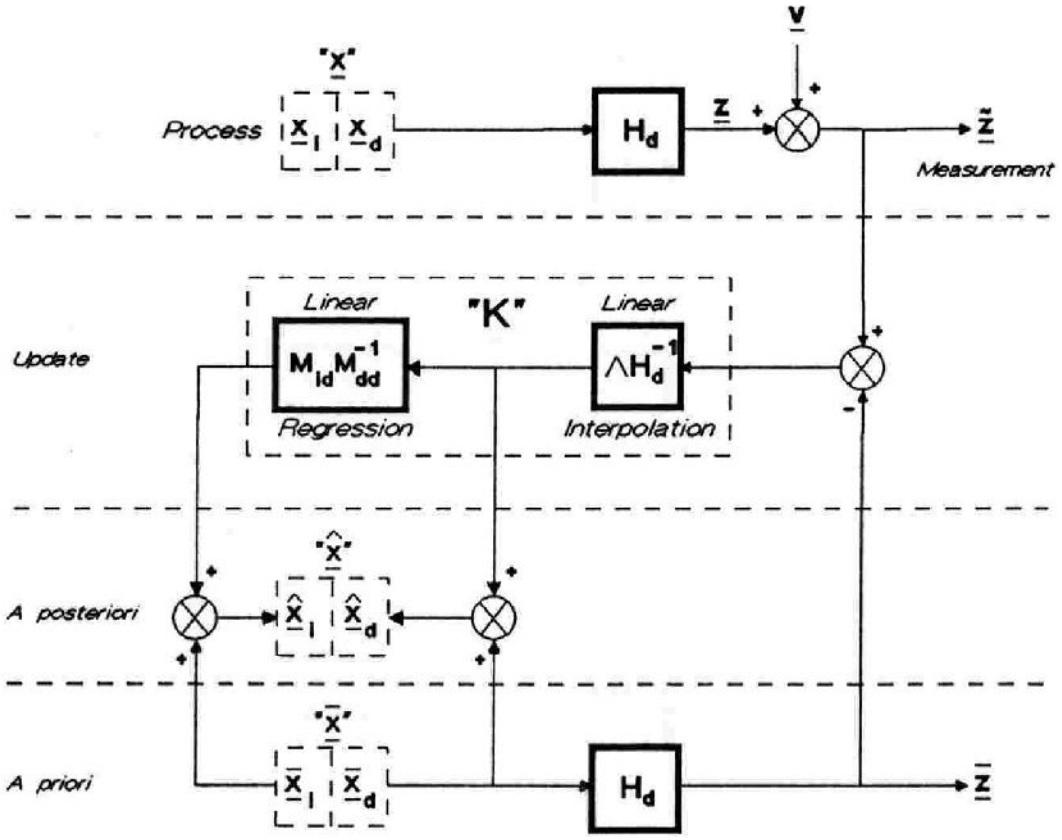

Fig. 4.3 The combined optimal filtering and reconstruction scheme

Combining the update of the a-priori estimation on the basis of optimal interpolation and linear regression results in the equivalent block-diagram of Figure 4.4, where the combined update is called innovation.

4.3 State estimation: theory of Kalman filtering

In the previous section it was assumed that besides the measurements some a-priori knowledge was available on the variables to be estimated. For some applications, especially in the field of control and systems engineering, this a-priori information is available in the form of a dynamic model. In the discrete case a common choice for the structure of the dynamic model is a first-order Markov chain, given by:

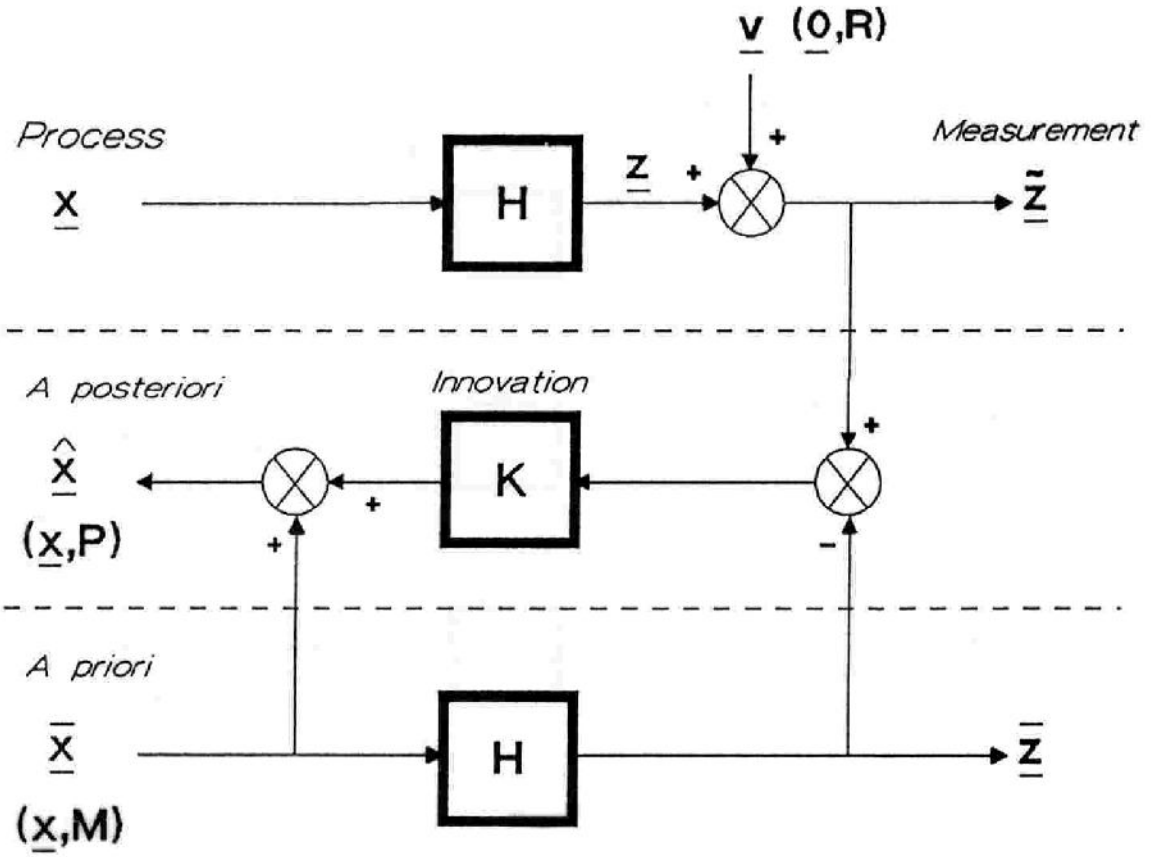

Fig. 4.4 Equivalent scheme for Figure 4.3

$$\underline{x}(k) = A\underline{x}(k-1) + B\underline{u}(k-1) + D\underline{w}(k-1) \qquad (4.45)$$

where $\underline{x}(k)$ is the variable to be estimated (model state),
$\underline{u}(k)$ stands for external signals which influence the state, but are known (model input),
$\underline{w}(k)$ are unknown external influences of a statistical nature, incorporated as (white) system noise,
and A,B and D are the known model parameters

at time $t = k.T_s$, with T_s the time unit of the discrete system.

For the estimation of the state of this discrete model, measurements are performed which may be described in a form identical to the general linear measurement model introduced in Section 4.2:

$$\tilde{\underline{y}}(k) = \underline{y}(k) + \underline{v}(k) = C(k)\underline{x}(k) + \underline{v}(k) \qquad (4.46)$$

with $\underline{y}(k)$ the noise-free and $\tilde{\underline{y}}(k)$ the noise-corrupted process output (measurement),
$\underline{v}(k)$ white measurement noise with zero mean and covariance R,
$C(k)$ the (time-dependent) observation matrix.

Once an a-priori estimation of $\underline{x}(k)$ is available, the a-posteriori estimation can be calculated as discussed in the previous section:

$$\hat{\underline{x}}(k) = \bar{\underline{x}}(k) + K(\tilde{\underline{y}}(k) - C(k)\bar{\underline{x}}(k)) \qquad (4.47)$$

with K provided by (4.43).

Assuming that the state-estimation scheme is performed in a recursive way, the a-posteriori estimation at $t = (k-1).T_s$ and the dynamic model of (4.45) are available for the a-priori estimation at $t = k.T_s$. Obviously, because by definition the white system noise $\underline{w}(k-1)$ is unknown, the best choice for this a-priori estimation would be:

$$\bar{\underline{x}}(k) = A\hat{\underline{x}}(k-1) + B\underline{u}(k-1) \qquad (4.48)$$

Finally, for the determination of the update gain K according to optimal measurement filtering, the covariance matrix M for the a-priori estimation error is needed. By combining (4.48) with (4.45) this a-priori estimation error is given by:

$$(\underline{x}(k) - \bar{\underline{x}}(k)) = A(\underline{x}(k-1) - \hat{\underline{x}}(k-1)) + D\underline{w}(k-1) \qquad (4.49)$$

Treating Eq. (4.49) as the summation of two statistically independent variables, the propagation equation for the covariance matrix M in time becomes:

$$M(k) = AP(k-1)A^T + DQD^T \qquad (4.50)$$

where Q is the covariance matrix of the white Gaussian system noise and P(k-1) is the covariance matrix of the previous a-posteriori estimation error.
This results in the following equations for the estimation of the model state $\underline{x}(k)$ on the basis of the measurements $\tilde{\underline{y}}(k)$, which are a combination of dynamic model knowledge and optimal measurement filtering:

a priori:

$$\bar{\underline{x}}(k) = A\hat{\underline{x}}(k-1) + B\underline{u}(k-1) \qquad (4.51)$$

$$M(k) = AP(k-1)A^T + DQD^T \qquad (4.52)$$

measurement:

$$\tilde{\underline{y}}(k) = C(k)\underline{x}(k) + \underline{v}(k) \qquad (4.53)$$

a posteriori:

$$K(k) = M(k)C(k)^T(C(k)M(k)C(k)^T + R)^{-1} \qquad (4.54)$$

$$\hat{\underline{x}}(k) = \bar{\underline{x}}(k) + K(k)(\tilde{\underline{y}}(k) - C(k)\bar{\underline{x}}(k)) \qquad (4.55)$$

$$P(k) = (I - K(k)C(k))M(k) \qquad (4.56)$$

This is the Kalman filter (Kalman, 1960; Kalman and Bucy, 1961) for state estimation on the basis of the measured process output $\tilde{\underline{y}}$.
The corresponding block-diagram for this combination of a-priori model knowledge with optimal measurement filtering is presented in Figure 4.5.
An equivalent form for this filter is presented in Figure 4.6, where the nature of the Kalman filter, that of being a matching filter between process and model, is emphasized.

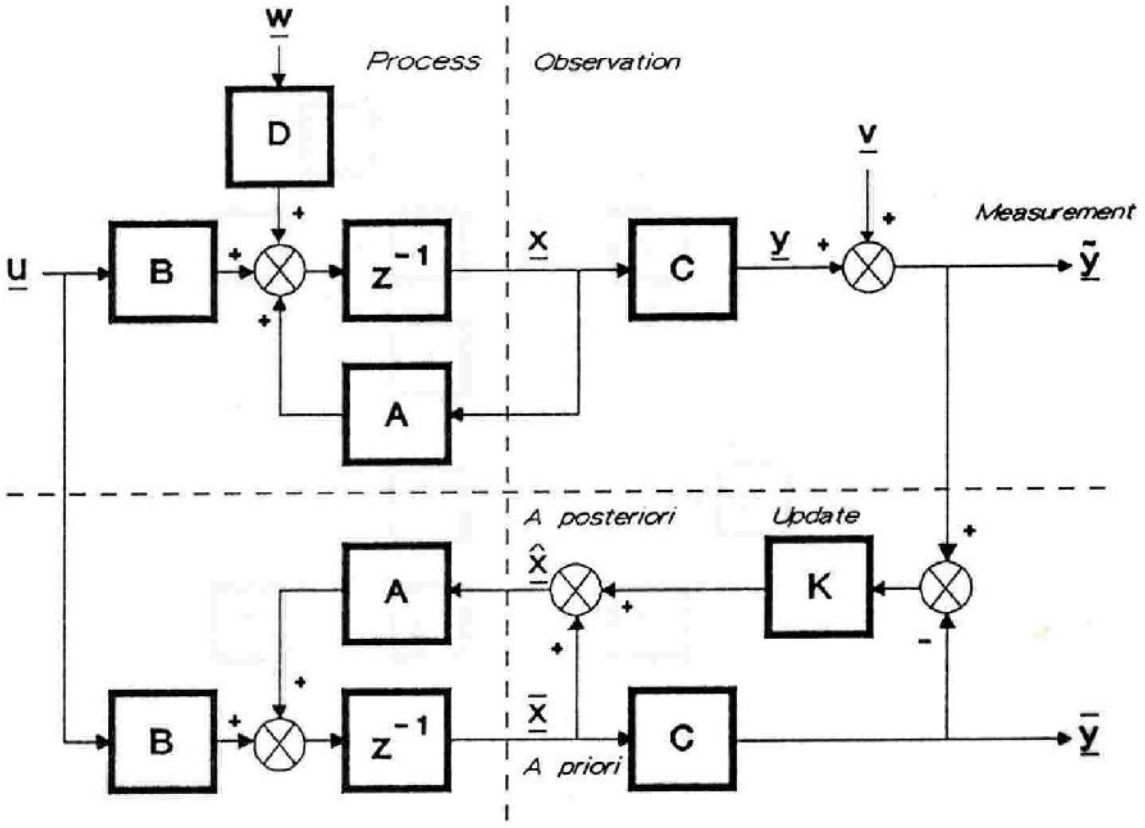

Fig. 4.5 Adding dynamic model knowledge to the measurement scheme

4.4 Parameter estimation: theory of MRAS

The theory of Model Reference Adaptive Systems (MRAS) has a wide range of applications both in the field of adaptive control and that of system identification (see, for instance, Van Amerongen, 1982).

Identification schemes, which are based on MRAS theory, can be divided into two categories, namely Series-Parallel MRAS and Parallel MRAS, which refer to the way the adjustable model is updated. Depending on the application, both schemes have their specific advantages (for instance, better noise-rejecting properties for the Parallel MRAS scheme (Landau, 1976; Dugard and Landau, 1980), high convergence speed for the Series-Parallel scheme).

In this section the basic equations of discrete MRAS identification schemes, which are structurally identical both for Parallel and Series-Parallel MRAS, will be

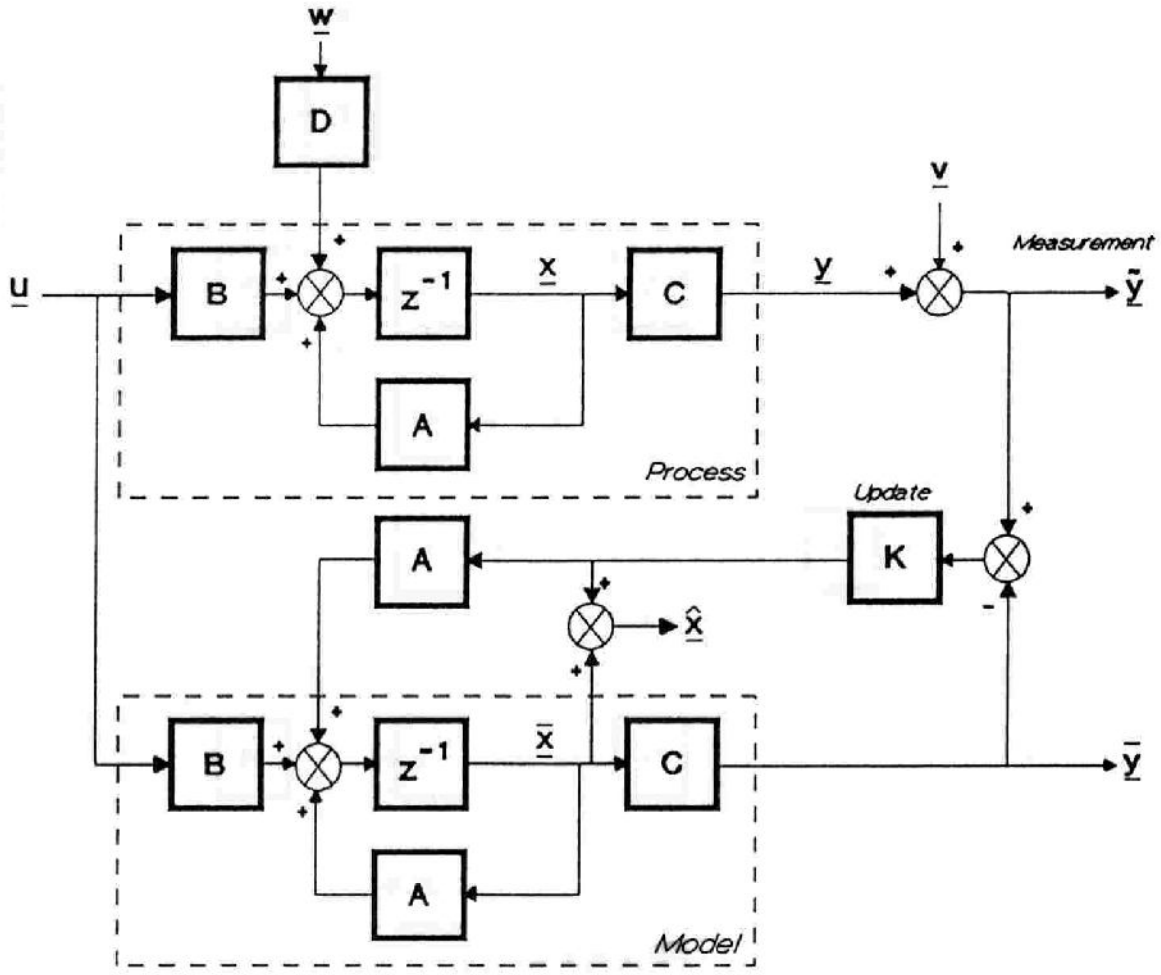

Fig. 4.6 The Kalman filter for state estimation

analyzed from the point of view of optimal measurement filtering and reconstruction, as described in Section 4.2.
Further, on the basis of this approach, it will be demonstrated in a heuristic way how the advantages of Series-Parallel and Parallel MRAS identification can be unified into one, combined, identification scheme. In Section 4.5 this combined identification scheme will be shown to be a simplified version of the Extended Kalman filter.

4.4.1 The general equations of the recursive identification scheme

Both in the case of discrete Series-Parallel and Parallel MRAS identification, the unknown parameters of a process are estimated by minimizing a criterion V, which

is based on the difference between the observed output of the process and the one-step-ahead predicted output of a model, where model and process have the same input. For identification purposes the model prediction or a-priori estimation of the process output y at $t = k.T_s$ is commonly written as:

$$\bar{y}(k) = \hat{\underline{\psi}}^T(k)\hat{\underline{\theta}}(k-1) \qquad (4.57)$$

with

$\hat{\underline{\psi}}^T(k) = (\hat{y}(k-1),\hat{y}(k-2),\ldots,u(k),u(k-1),\ldots)$

$\hat{\underline{\theta}}(k-1)$ the estimated parameter vector at $t = (k-1).T_s$

$u(k)$ the input for both process and model at $t = k.T_s$

$\hat{y}(k)$ to be defined in the following.

After the measurement $\tilde{y}(k)$ at $t = k.T_s$ the prediction error $\varepsilon(k)$ is defined as:

$$\varepsilon(k) = \tilde{y}(k) - \bar{y}(k) \qquad (4.58)$$

This prediction error is used to update the estimation of the parameter vector according to:

$$\hat{\underline{\theta}}(k) = \hat{\underline{\theta}}(k-1) + F(k)\hat{\underline{\psi}}(k)\varepsilon(k) \qquad (4.59)$$

with

$$F(k) = F(k-1) - \frac{F(k-1)\hat{\underline{\psi}}(k)\hat{\underline{\psi}}^T(k)F(k-1)}{(1 + \hat{\underline{\psi}}^T(k)F(k-1)\hat{\underline{\psi}}(k))} \qquad (4.60)$$

This is a recursive formulation of the solution to the Least Squares problem, which minimizes the criterion (see, for instance, Mendel, 1973):

$$V(k) = \sum_{i=1}^{k} \varepsilon^2(i) \qquad (4.61)$$

In the case of Series-Parallel MRAS $\hat{y}(k-1)$ in $\hat{\underline{\psi}}^T(k)$ is replaced by $\tilde{y}(k-1)$:

$$\hat{y}(k-1) = \tilde{y}(k-1) \qquad (4.62)$$

In this case the prediction error, given by (4.58), is commonly referred to as the *equation error.*
For Parallel MRAS the prediction is based on the previous *model* output, by substituting:

$$\hat{y}(k-1) = \bar{y}(k-1) \qquad (4.63)$$

The corresponding prediction error is called the *output error.*
Besides this single difference, the equations for Least Squares or Series-Parallel and Parallel MRAS identification are identical.
Because, from the MRAS point of view, F(k) is the adaptive gain, with (4.60) the adaptation to changing parameters will decrease. To ensure permanent adaptation after the initial estimation has converged, there are several possibilities. One of them is the introduction of a *forgetting factor* λ according to (see, for instance, Lammers, 1983):

$$F(k) = \frac{1}{\lambda}\left(F(k-1) - \frac{F(k-1)\hat{\underline{\psi}}(k)\hat{\underline{\psi}}^T(k)F(k-1)}{(\lambda + \hat{\underline{\psi}}^T(k)F(k-1)\hat{\underline{\psi}}(k))}\right) \qquad (4.64)$$

$$\text{with} \quad 0 < \lambda \leq 1$$

A choice of $\lambda < 1$ prevents F(k) from becoming zero, and therefore permanent adaptation is ensured. For the following analysis, without loss of generality, λ is assumed to be one.

4.4.2 Analysis from the optimal measurement point of view

In order to analyze the performance of both Series-Parallel and Parallel MRAS identification schemes in the presence of observation noise, the parameter-estimation problem will be considered as a problem of optimal measurement filtering. For this purpose the process equations are written as:

$$y(k) = \underline{\psi}^T(k)\underline{\theta} \qquad (4.65)$$

$$\tilde{y}(k) = y(k) + v(k) \qquad (4.66)$$

with
- $y(k)$ the noise-free process output,
- $\underline{\psi}^T(k)$ = (y(k-1), y(k-2),..., u(k), u(k-1),...),
- $\underline{\theta}$ the constant process parameter vector and
- $v(k)$ the observation noise, Gaussian (0,R).

Eqs. (4.65) and (4.66) can be combined to:

$$\tilde{y}(k) = \underline{\psi}^T(k)\underline{\theta} + v(k) \qquad (4.67)$$

Comparing this equation for $\tilde{y}(k)$ to the linear measurement model:

$$\underline{\tilde{z}}(k) = H(k)\underline{x}(k) + \underline{v}(k) \qquad (4.68)$$

with $\underline{x}$ the variable to be estimated from the measurement $\underline{\tilde{z}}$, it follows that (4.67) can be regarded as a measurement equation for the process parameters $\underline{\theta}$ through the observation vector $\underline{\psi}^T(k)$ and observation noise v(k).
For the optimal estimation of the parameters from the measurements an a-priori estimation of the output y(k) is required, which of course is the model prediction:

$$\bar{y}(k) = \underline{\psi}^T(k)\underline{\bar{\theta}}(k) \qquad (4.69)$$

$$\text{with} \quad \underline{\bar{\theta}}(k) = \underline{\hat{\theta}}(k-1) \qquad (4.70)$$

This yields for the optimal estimation of the process parameters:

a priori:

$$\underline{\bar{\theta}}(k) = \underline{\hat{\theta}}(k-1) \qquad (4.71)$$

$$M(k) = F(k-1) \qquad (4.72)$$

measurement:

$$\tilde{y}(k) = \underline{\psi}^T(k)\underline{\theta} + v(k) \qquad (4.73)$$

a posteriori:

$$K_\theta(k) = F(k-1)\underline{\psi}(k)(\underline{\psi}(k)^T F(k-1)\underline{\psi}(k) + 1)^{-1} \qquad (4.74)$$

$$\hat{\theta}(k) = \hat{\theta}(k-1) + K_\theta(k)(\tilde{y}(k) - \underline{\psi}^T(k)\underline{\hat{\theta}}(k-1)) \qquad (4.75)$$

$$F(k) = (I - K_\theta \underline{\psi}^T(k))F(k-1) \qquad (4.76)$$

by substituting P(k) = F(k) and setting R = 1 in the basic equations for optimal

measurement filtering.
These equations are equivalent to the general equations (4.57)-(4.60) of the recursive identification scheme described in the previous section by substituting in (4.74)-(4.76):

$$\underline{\psi}(k) = \hat{\underline{\psi}}(k) \qquad (4.77)$$

This implies that these general equations can be regarded as the result of applying optimal measurement filtering to the parameter estimation problem, where for the observation vector $\underline{\psi}(k)$ an estimate according to (4.77) is substituted (See Figure 4.7).

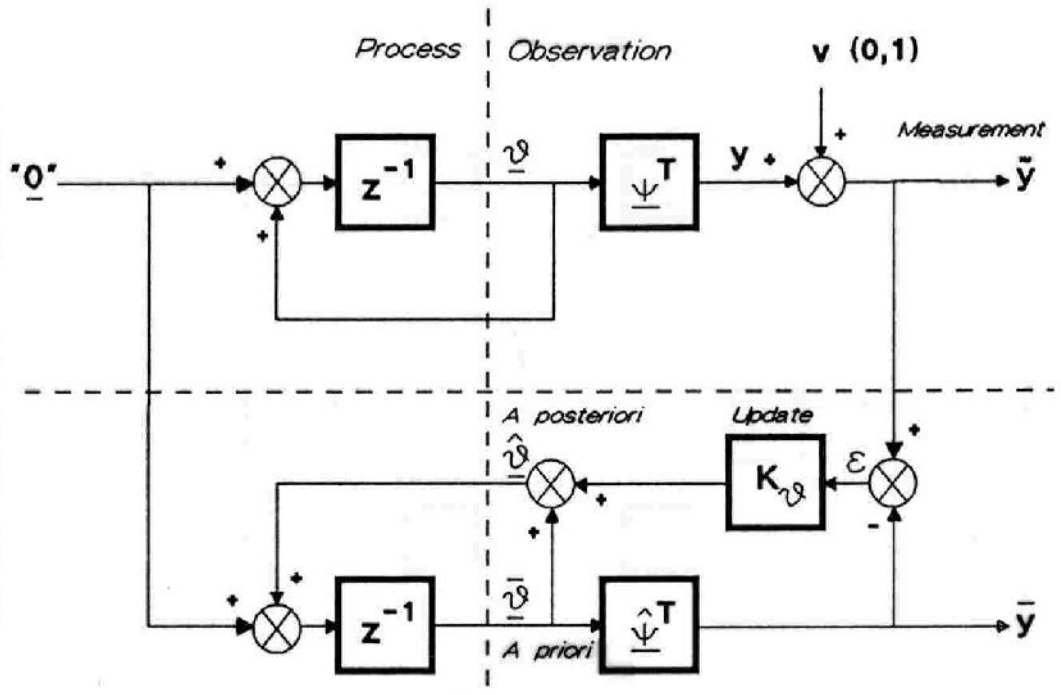

Fig. 4.7 Measurement scheme for MRAS identification

The effect of the substitution of (4.77) for the different choices of the estimated observation vector in the case of Series-Parallel and Parallel MRAS in the presence of observation noise will be discussed in the next section.

4.4.3 Performance in the presence of observation noise

To analyze the noise-rejecting performance of both the Series-Parallel and Parallel MRAS identification schemes, which are both characterized by a different choice for the estimation of the observation vector $\underline{\psi}(k)$, the simple case is considered for which this observation vector is given by ($u = 0$):

$$\underline{\psi}(k) = y(k-1) \qquad (4.78)$$

This simple first-order case will be sufficient for the qualitative noise analysis to come.
The estimation of the observation vector then becomes:

$$\hat{\underline{\psi}}(k) = \hat{y}(k-1) \qquad (4.79)$$

with

$$\hat{y}(k-1) = \tilde{y}(k-1) \qquad (4.80)$$

for the Series-Parallel identifier and

$$\hat{y}(k-1) = \bar{y}(k-1) \qquad (4.81)$$

for the Parallel MRAS identifier.
Combining these different estimations for the observation vector with the parameter estimation scheme of Figure 4.7, yields the equivalent filtering scheme of Figure 4.8. In this figure $K_{sp} = 1$ for the Series-Parallel identifier and $K_{sp} = 0$ for the Parallel identifier.
From Figure 4.8 it follows that for the Series-Parallel identifier ($K_{sp} = 1$) in the absence of observation noise the estimated observation vector becomes:

$$\hat{\underline{\psi}}(k) = \underline{\psi}(k) \qquad (4.82)$$

which for the Parallel identifier will only be the case after convergence of the estimator. Therefore, for small observation noise v, the Series-Parallel scheme is to be preferred above the Parallel scheme, for which both the estimation of the parameters and the observation vector have to converge.
However, in the presence of considerable observation noise, for the Series-Parallel scheme an unacceptable biasing of the estimated parameter vector may occur, which can be explained by examining part of Figure 4.8 (see Figure 4.9).

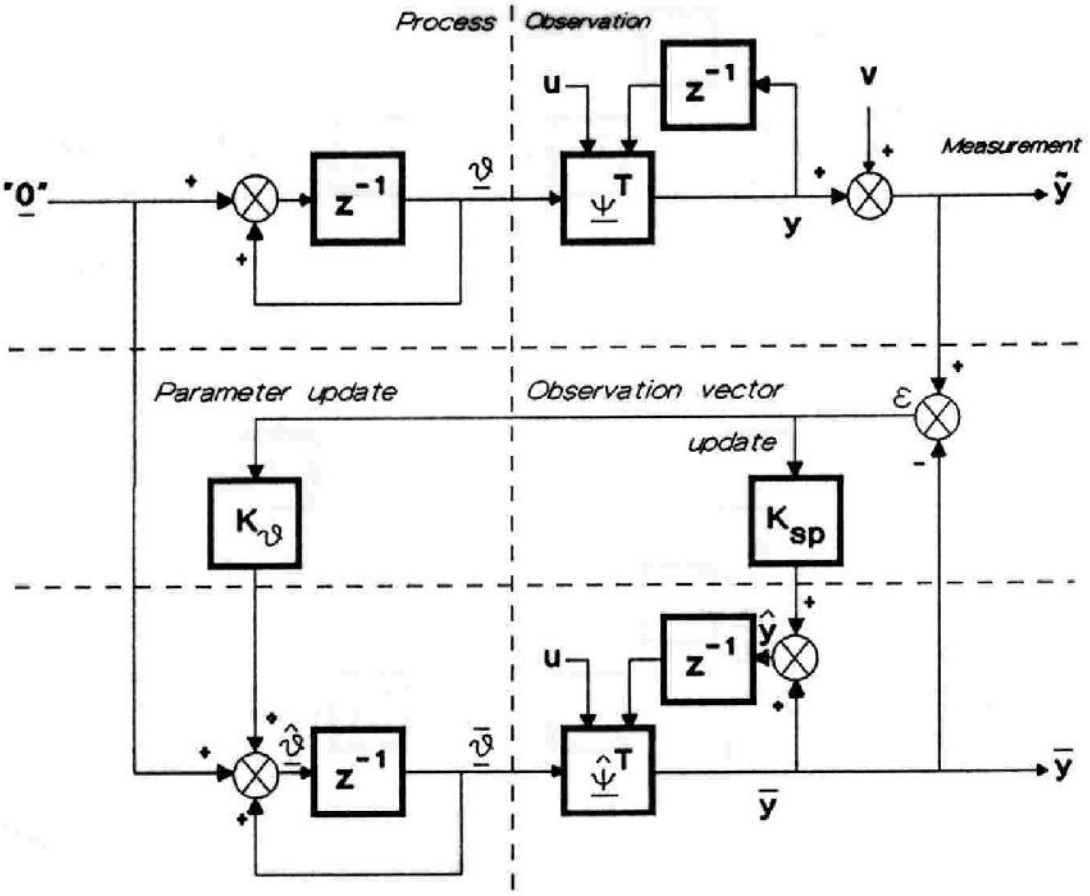

Fig. 4.8 Equivalent filtering scheme for MRAS identification

For this situation in the a-priori estimation of the process output y a cross term caused by v(k-1) will occur, which will have a non-zero mean value. This again will cause the parameter estimation to be biased after convergence.
For the Parallel identifier Figure 4.8 reduces to Figure 4.10 (K_{sp} = 0) and therefore the cross term will not exist.
As a result of this structural analysis it may be concluded that the Parallel MRAS identifier has better noise-rejecting properties but has a slower convergence when compared to the Series-Parallel identifier. This is confirmed by the simulation results presented in Chapter 6.
In the next section it will be shown, in a heuristic way, how to combine these specific advantages for both methods into one identification scheme.

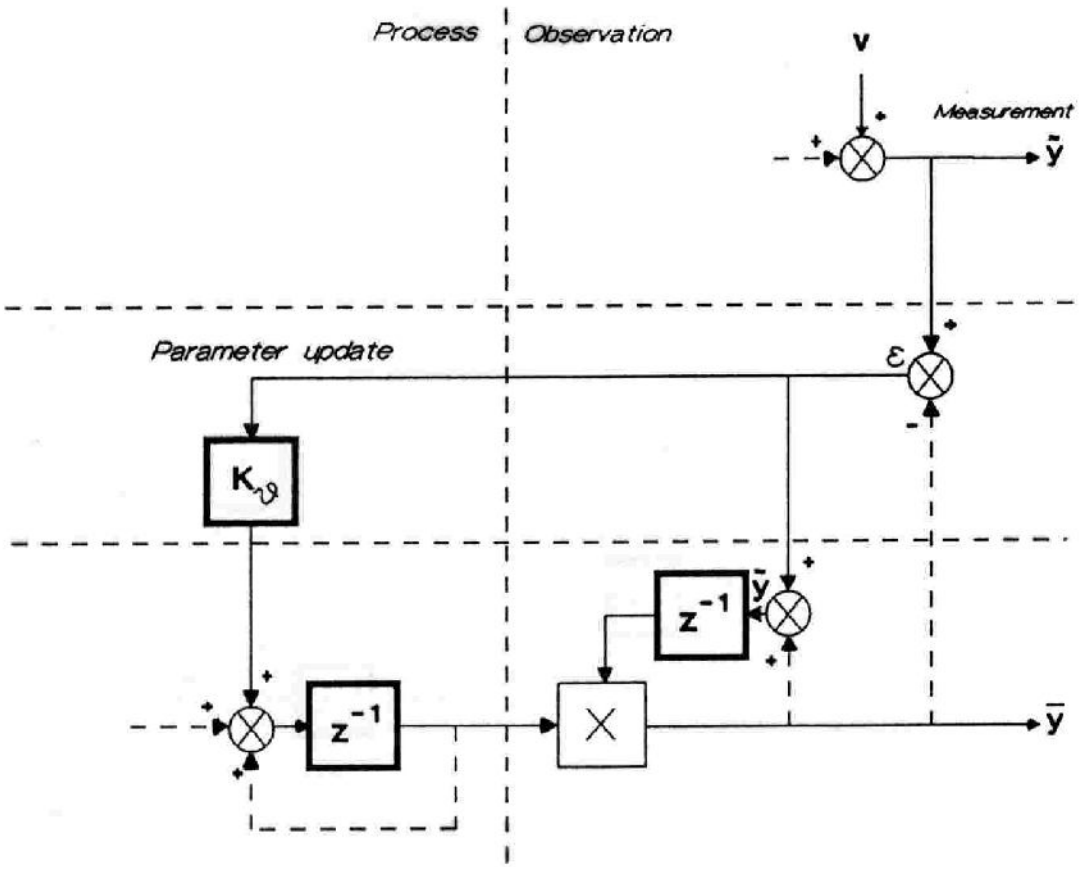

Fig. 4.9 Biasing problem for the Series-Parallel identifier

4.4.4 A combined approach

To combine the advantages of Series-Parallel (faster convergence) and Parallel MRAS (better noise rejection), the filtering scheme of Figure 4.8 is reconsidered. Without loss of generality, the relations for the estimation of the observation vector $\underline{\psi}(k)$ are given for the first-order case:

$$\hat{\underline{\psi}}^T(k) = (\hat{y}(k-1), u(k)) \qquad (4.83)$$

$$\bar{y}(k) = \hat{\underline{\psi}}^T(k)\bar{\underline{\theta}}(k) \qquad (4.84)$$

$$\hat{y}(k) = \bar{y}(k) + K_{sp}(\tilde{y}(k) - \bar{y}(k)) \qquad (4.85)$$

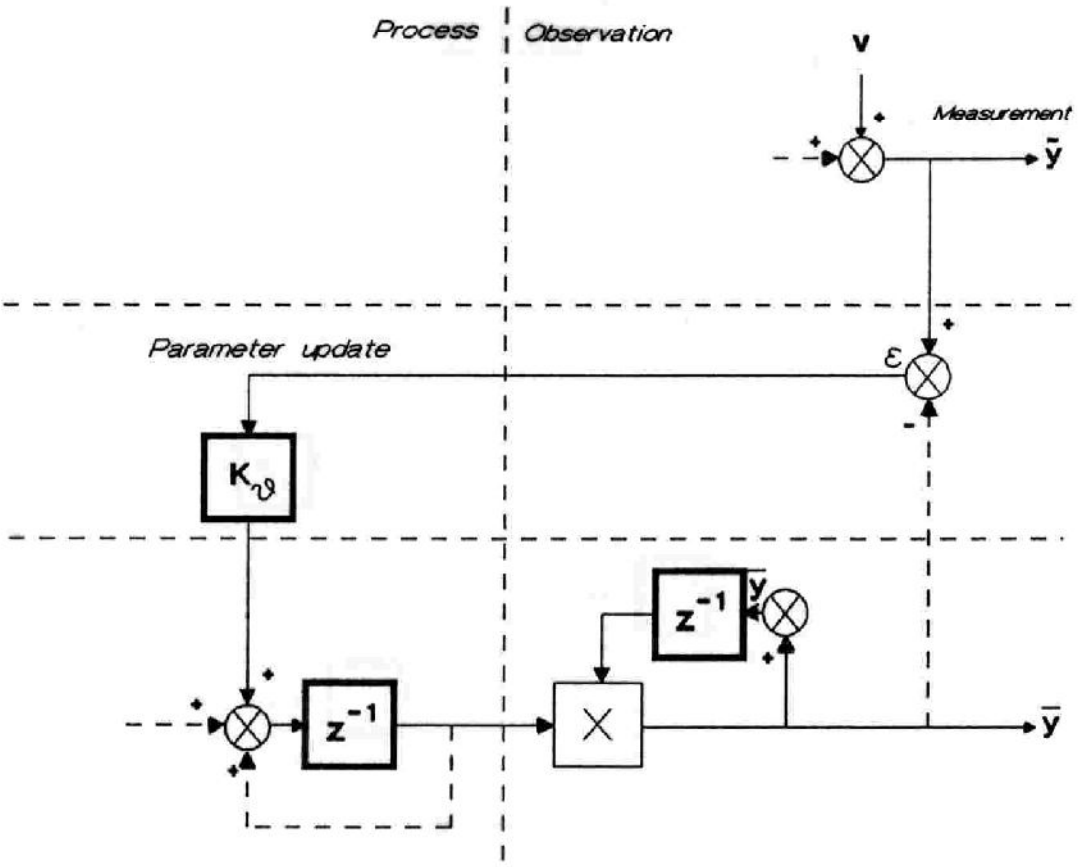

Fig. 4.10 Equivalent scheme for the Parallel identifier

where $K_{sp} = 1$ for Series-Parallel ($\hat{y}(k) = \tilde{y}(k)$)and $K_{sp} = 0$ for Parallel MRAS ($\hat{y}(k) = \bar{y}(k)$). Examining these choices for K_{sp}, Eq. (4.85) can be regarded as an extreme form of updating the estimated observation vector, given by (4.83). For a more sophisticated choice for the update gain K_y , a separate filtering scheme for the optimal estimation of the observation vector $\underline{\psi}(k)$ can be set up according to Figure 4.11.

Applying optimal measurement filtering again, an optimal choice for K_y is provided by (4.43) if the a-priori covariance M_y of y is available. In this case K_y is given by:

$$K_y(k) = \frac{M_y(k)}{M_y(k) + R} \qquad (4.86)$$

with R the variance of the measurement noise.

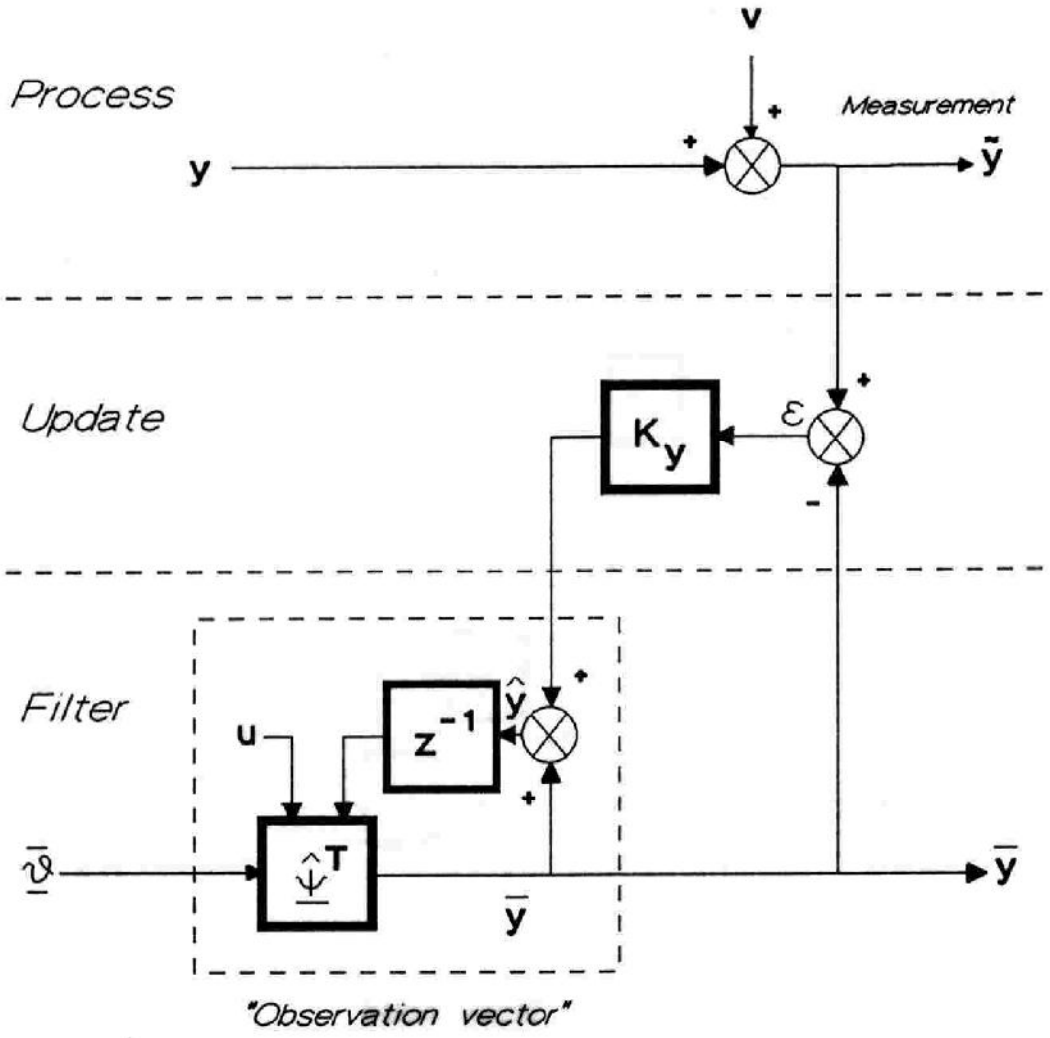

Fig. 4.11 Separate filtering scheme for the observation vector $\underline{\Psi}(k)$

The a-posteriori covariance of y then reduces to:

$$P_y(k) = (1 - K_y(k))M_y(k) \qquad (4.87)$$

or

$$P_y(k) = \frac{M_y(k)}{M_y(k) + R} \cdot R \qquad (4.88)$$

To determine the a-priori covariance, the prediction step of the estimator is

examined:

$$\bar{y}(k) = \hat{\underline{\psi}}^T(k)\bar{\underline{\theta}}(k) \qquad (4.89)$$

which may be approximated by:

$$\bar{y}(k) \approx \underline{\psi}^T(k)\underline{\theta} + \hat{\underline{\psi}}^T(k)(\bar{\underline{\theta}}(k) - \underline{\theta}) + \bar{\underline{\theta}}^T(k)(\hat{\underline{\psi}}(k) - \underline{\psi}(k)) \qquad (4.90)$$

or

$$(\bar{y}(k) - y(k)) \approx \hat{\underline{\psi}}^T(k)(\bar{\underline{\theta}}(k) - \underline{\theta}) + \bar{\underline{\theta}}^T(k)(\hat{\underline{\psi}}(k) - \underline{\psi}(k)) \qquad (4.91)$$

Treating (4.91) as the summation of 2 statistically independent variables, and thus neglecting all cross terms, the a-priori covariance matrix becomes:

$$M_y(k) = \hat{\underline{\psi}}^T(k)F(k-1)\hat{\underline{\psi}}(k) + \bar{\underline{\theta}}^T(k)M_{\psi}(k)\bar{\underline{\theta}}(k) \qquad (4.92)$$

By writing the model prediction as:

$$\bar{y}(k) = (\hat{y}(k-1), u)\ (\bar{\theta}_y(k), \bar{\theta}_u(k))^T \qquad (4.93)$$

and noting that the uncertainty in the model input u is zero, (4.92) is equivalent to:

$$M_y(k) = \hat{\underline{\psi}}^T(k)F(k-1)\hat{\underline{\psi}}(k) + \bar{\theta}_y(k)P_y(k-1)\bar{\theta}_y(k) \qquad (4.94)$$

The resulting equation (4.94) for $M_y(k)$ consists of two components due to the a-priori parameter and state uncertainty, with F(k) given by (4.76) and $P_y(k)$ by (4.87).

By giving F(k) and $P_y(k)$ high starting values, thus stating high initial uncertainty on both the estimated parameters and state, from (4.86) and (4.94) it follows that $K_y(0) = 1$, and therefore the combined algorithm starts up as a Series-Parallel identifier (prediction based entirely on measurements). Further, because of the decreasing uncertainty both $P_y(k)$ and F(k) will decrease and become zero for large k, which will cause the nature of the combined algorithm to change from a Series-Parallel identifier to a Parallel identifier (prediction based entirely on the model). Thus a reasonable estimation of both the state and the parameters will be obtained after convergence, also in the presence of considerable observation noise, because of the noise rejecting properties of the Parallel MRAS identifier. This

combined identification scheme may be adjusted to the level of the observation noise by choosing an appropriate value for R in (4.86), which stands for the variance of the observation noise. The filtering scheme for this combined Series-Parallel / Parallel MRAS identifier is presented in Figure 4.12.

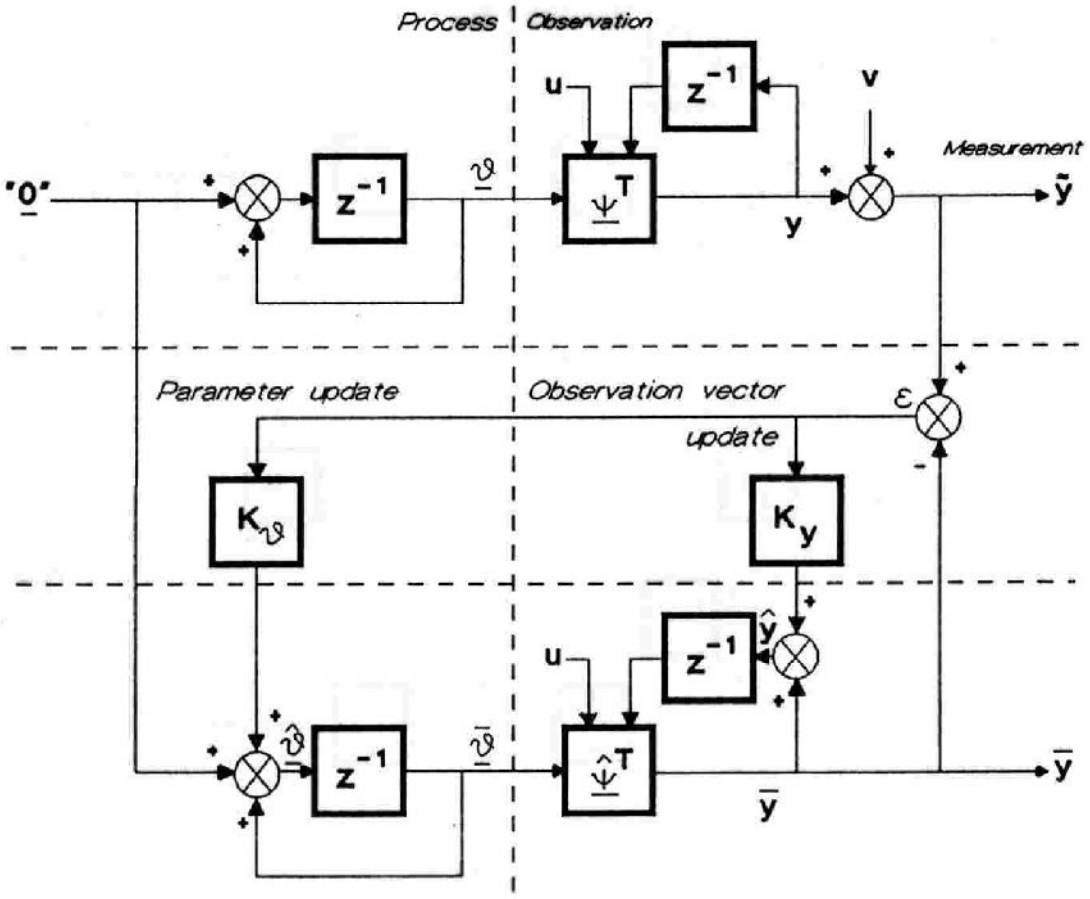

Fig. 4.12 The combined filtering scheme

After this rather heuristic derivation of a combined state and parameter estimation scheme from the discrete MRAS identifier, a more formal and general presentation of the theory of combined state and parameter estimation will be carried out in the next section on the basis of the theory of Extended Kalman filtering.

4.5 Combined state and parameter estimation

In the previous sections attention has been focussed on the separate estimation of the model state, for which optimal measurement filtering was applied to the state space (Section 4.3), and the estimation of the model parameters, for which measurement filtering was applied to the parameter space (Section 4.4). However, it has also been demonstrated in a heuristic way that an improvement of the parameter estimation could be achieved by combining parameter-space information with state-space information, thus yielding a combined state and parameter estimator. The more formal and general derivation of the combined state- and parameter-estimation scheme, which can be formulated as a non-linear filtering problem, will be treated in this section.

4.5.1 Theory of Extended Kalman filtering

As has been demonstrated in Section 4.3, the Kalman filter may be derived by adding a-priori information in the form of dynamic model knowledge to the optimal measurement-filtering scheme, where for ordinary Kalman filtering the model is supposed to be linear.
In the case of a non-linear model, the model can be linearized by using a Taylor-series expansion, after which ordinary Kalman filtering may be applied again. To carry out this linearization the general form of the state-space equations is supposed to be:

$$\underline{x}(k) = \underline{\Phi}(\underline{x}(k-1),k-1) + B(k-1)\underline{u}(k-1) + G(k-1)\underline{w}(k-1) \qquad (4.95)$$

$$\underset{\sim}{\underline{z}}(k) = \underline{h}(\underline{x}(k),k) + \underline{v}(k) \qquad (4.96)$$

with $\underline{\Phi}$ and $\underline{h}$ the non-linear vector functions describing the system dynamics and the observations. Further, it is assumed that a discrete state trajectory $\underline{x}(k)$ can be generated. The state-space equations may then be written as:

$$\begin{aligned}\underline{x}(k) = {} & [\underline{\Phi}(\underline{x}(k-1),k-1) - \underline{\Phi}(\bar{\underline{x}}(k-1),k-1)] + \\ & + \underline{\Phi}(\bar{\underline{x}}(k-1),k-1) + B(k-1)\underline{u}(k-1) + G(k-1)\underline{w}(k-1)\end{aligned} \qquad (4.97)$$

$$\underset{\sim}{\underline{z}}(k) = [\underline{h}(\underline{x}(k),k) - \underline{h}(\bar{\underline{x}}(k),k)] + \underline{h}(\bar{\underline{x}}(k),k) + \underline{v}(k) \qquad (4.98)$$

For a small deviation from the trajectory a Taylor-series expansion yields:

$$\underline{\Phi}(\underline{x}(k-1),k-1) - \underline{\Phi}(\bar{\underline{x}}(k-1),k-1) \approx \Phi(\bar{\underline{x}}(k-1),k-1)[\underline{x}(k-1) - \bar{\underline{x}}(k-1)] \quad (4.99)$$

$$\underline{h}(\underline{x}(k),k) - \underline{h}(\bar{\underline{x}}(k),k) \approx H(\bar{\underline{x}}(k),k)[\underline{x}(k) - \bar{\underline{x}}(k)] \quad (4.100)$$

with Φ and H the matrices of partial derivatives of $\underline{\Phi}$ and $\underline{h}$ with respect to $\underline{x}$ for $\underline{x} = \bar{\underline{x}}$

By substituting (4.99)-(4.100) in (4.97)-(4.98), the non-linear system is approximated by the linear system:

$$\underline{x}(k) = \Phi(\bar{\underline{x}}(k-1),k-1)\underline{x}(k-1) - \Phi(\bar{\underline{x}}(k-1),k-1)\bar{\underline{x}}(k-1) + \underline{\Phi}(\bar{\underline{x}}(k-1),k-1) + B(k-1)\underline{u}(k-1) + G(k-1)\underline{w}(k-1) \quad (4.101)$$

$$\tilde{\underline{z}}(k) = H(\bar{\underline{x}}(k),k)\underline{x}(k) - H(\bar{\underline{x}}(k),k)\bar{\underline{x}}(k) + \underline{h}(\bar{\underline{x}}(k),k) + \underline{v}(k) \quad (4.102)$$

to which the equations of ordinary Kalman filtering can be applied for the estimation of $\underline{x}(k)$ from the measurements $\tilde{\underline{z}}(k)$.
For the generation of the discrete state trajectory there are several possibilities, one of them being:

$$\bar{\underline{x}}(k) = \underline{\Phi}(\bar{\underline{x}}(k-1),k-1) + B(k-1)\underline{u}(k-1) \quad (4.103)$$

$$\bar{\underline{x}}(0) = \hat{\underline{x}}(0) \quad (4.104)$$

where the trajectory is completely determined by the initial estimate of the system state. This estimator is called the linearized Kalman filter.
To adapt the a-priori determined state trajectory to the observations along the trajectory another possibility for the generation of this trajectory could be:

$$\bar{\underline{x}}(k) = \underline{\Phi}(\hat{\underline{x}}(k-1),k-1) + B(k-1)\underline{u}(k-1) \quad (4.105)$$

Because of this adaptation of the trajectory to the observations, large initial estimation errors will not be allowed to propagate in time. The choice of (4.105) for the state trajectory in combination with the Kalman-filtering equations applied to (4.101)-(4.102) is called the Extended Kalman filter (Heemink, 1986).

4.5.2 Application to combined state and parameter estimation

A specific example of a non-linear filtering problem is the estimation of the state and the parameters of a dynamic model (Eykhoff, 1974). To apply the theory of Extended Kalman filtering to the state- and parameter-estimation problem, the state-space equations introduced in Section 4.4 are written as:

$$y(k) = \underline{\psi}^T(k)\underline{\theta}(k-1) + w_y(k-1) \qquad (4.106)$$

$$\tilde{y}(k) = y(k) + v(k) \qquad (4.107)$$

with $\underline{\theta}(k)$ the time-varying process parameters,
$\underline{\psi}^T(k)$ the observation vector,
$w_y(k)$ and $v(k)$ the system and observation noise with zero mean and variance Q_y and R.

For the combined estimation of y(k) and $\underline{\theta}(k)$ on the basis of $\tilde{y}(k)$, the system state is extended with $\underline{\theta}(k)$:

$$\underline{\theta}(k) = \underline{\theta}(k-1) + \underline{w}_\theta(k-1) \qquad (4.108)$$

The white system-noise component $\underline{w}_\theta$ is added to state permanent uncertainty about the process parameters, thereby achieving permanent adaptation to the time-varying parameters.
To obtain a linear model, the deterministic part of (4.106) is written as:

$$\begin{aligned} y(k) = {} & \hat{\underline{\psi}}^T(k)\hat{\underline{\theta}}(k-1) + (\underline{\psi}^T(k) - \hat{\underline{\psi}}^T(k))\hat{\underline{\theta}}(k-1) + \\ & + \hat{\underline{\psi}}^T(k)(\underline{\theta}(k-1) - \hat{\underline{\theta}}(k-1)) + \\ & + (\underline{\psi}^T(k) - \hat{\underline{\psi}}^T(k))(\underline{\theta}(k-1) - \hat{\underline{\theta}}(k-1)) \end{aligned} \qquad (4.109)$$

Neglecting the last term, a linear approximation is obtained:

$$\begin{aligned} y(k) \approx {} & \hat{\underline{\psi}}^T(k)\hat{\underline{\theta}}(k-1) + (\underline{\psi}^T(k) - \hat{\underline{\psi}}^T(k))\hat{\underline{\theta}}(k-1) + \\ & + \hat{\underline{\psi}}^T(k)(\underline{\theta}(k-1) - \hat{\underline{\theta}}(k-1)) \end{aligned} \qquad (4.110)$$

Together with (4.107) and (4.108) the combined linear state-space equations

become:

$$\begin{bmatrix} y(k) \\ \underline{\vartheta}(k) \end{bmatrix} = \begin{bmatrix} \underline{\hat{\vartheta}}^T(k-1) & \underline{\hat{\psi}}^T(k) \\ 0 & I \end{bmatrix} \begin{bmatrix} \underline{\psi}(k) \\ \underline{\vartheta}(k-1) \end{bmatrix} - \begin{bmatrix} \underline{\hat{\psi}}^T(k)\underline{\hat{\vartheta}}(k-1) \\ \underline{0} \end{bmatrix} + \begin{bmatrix} w_y(k-1) \\ \underline{w}_\vartheta(k-1) \end{bmatrix} \qquad (4.111)$$

$$\tilde{y}(k) = (1 \quad \underline{0}^T) \begin{bmatrix} y(k) \\ \underline{\vartheta}(k) \end{bmatrix} + v(k)$$

and, for simplicity but without loss of generality, $\underline{\psi}^T(k) = (y(k-1)\ ,\ u(k))$

For the Extended Kalman filter the a-priori estimations are generated by:

$$\begin{bmatrix} \bar{y}(k) \\ \underline{\bar{\vartheta}}(k) \end{bmatrix} = \begin{bmatrix} \hat{\psi}^T(k)\hat{\vartheta}(k-1) \\ \underline{\hat{\vartheta}}(k-1) \end{bmatrix} \qquad (4.112)$$

with a-priori covariance matrix M(k):

$$M(k) = \begin{bmatrix} M_{yy} & M_{y\vartheta} \\ M_{\vartheta y} & M_{\vartheta\vartheta} \end{bmatrix}_k$$

$$= \begin{bmatrix} \underline{\bar{\vartheta}}^T & \underline{\hat{\psi}}^T \\ 0 & I \end{bmatrix}_k \begin{bmatrix} P_{\psi\psi} & P_{\psi\vartheta} \\ P_{\vartheta\psi} & P_{\vartheta\vartheta} \end{bmatrix}_{k-1} \begin{bmatrix} \underline{\bar{\vartheta}} & 0 \\ \underline{\hat{\psi}} & I \end{bmatrix}_k + \begin{bmatrix} Q_y & 0 \\ 0 & \underline{Q}_\vartheta \end{bmatrix} \qquad (4.113)$$

$$= \begin{bmatrix} \underline{\bar{\vartheta}}_y & \underline{\hat{\psi}}^T \\ 0 & I \end{bmatrix}_k \begin{bmatrix} P_{yy} & P_{y\vartheta} \\ P_{\vartheta y} & P_{\vartheta\vartheta} \end{bmatrix}_{k-1} \begin{bmatrix} \underline{\bar{\vartheta}}_y & 0 \\ \underline{\hat{\psi}} & I \end{bmatrix}_k + \begin{bmatrix} Q_y & 0 \\ 0 & \underline{Q}_\vartheta \end{bmatrix} \qquad (4.114)$$

by substituting $\underline{\psi}^T(k) = (y(k-1)\ ,\ u(k))$ and $\underline{\vartheta}^T = (\vartheta_y\ ,\ \vartheta_u)$.
Calculation of the Kalman update gains by (4.54) yields:

$$\begin{bmatrix} K_y(k) \\ K_\vartheta(k) \end{bmatrix} = \frac{1}{(M_{yy}(k) + R)} \begin{bmatrix} M_{yy}(k) \\ M_{\vartheta y}(k) \end{bmatrix} \qquad (4.115)$$

According to the principles of optimal measurement filtering and reconstruction, discussed in Section 4.2, this may be written as:

$$\begin{bmatrix} K_y(k) \\ K_\vartheta(k) \end{bmatrix} = \begin{bmatrix} 1 \\ M_{\vartheta y}(k)/M_{yy}(k) \end{bmatrix} \lambda_y(k) \qquad (4.116)$$

with the optimal interpolation coefficient $\lambda_y(k)$ for the directly observable process output y given by:

$$\lambda_y(k) = \frac{M_{yy}(k)}{(M_{yy}(k) + R)} \qquad (4.117)$$

The a-posteriori estimation then becomes:

$$\begin{bmatrix} \hat{y}(k) \\ \hat{\underline{\vartheta}}(k) \end{bmatrix} = \begin{bmatrix} \bar{y}(k) \\ \bar{\underline{\vartheta}}(k) \end{bmatrix} + \begin{bmatrix} 1 \\ M_{\vartheta y}(k)/M_{yy}(k) \end{bmatrix} \lambda_y(k)(\tilde{y}(k) - \bar{y}(k)) \qquad (4.118)$$

with covariance matrix P(k):

$$P(k) = \begin{bmatrix} P_{yy} & P_{y\vartheta} \\ P_{\vartheta y} & P_{\vartheta\vartheta} \end{bmatrix}_k = \begin{bmatrix} (1-K_y)M_{yy} & (1-K_y)M_{y\vartheta} \\ (1-K_y)M_{\vartheta y} & M_{\vartheta\vartheta} - K_\vartheta M_{y\vartheta} \end{bmatrix}_k \qquad (4.119)$$

The corresponding filtering scheme for this combined state and parameter estimator is presented in Figure 4.13.

In this figure the white system-noise component $w_y(k)$ is written as $w_y'(k)$, to show the structural correspondence between process and filter. The relation is given by: $w_y'(k) = w_y(k)/\vartheta_y(k)$

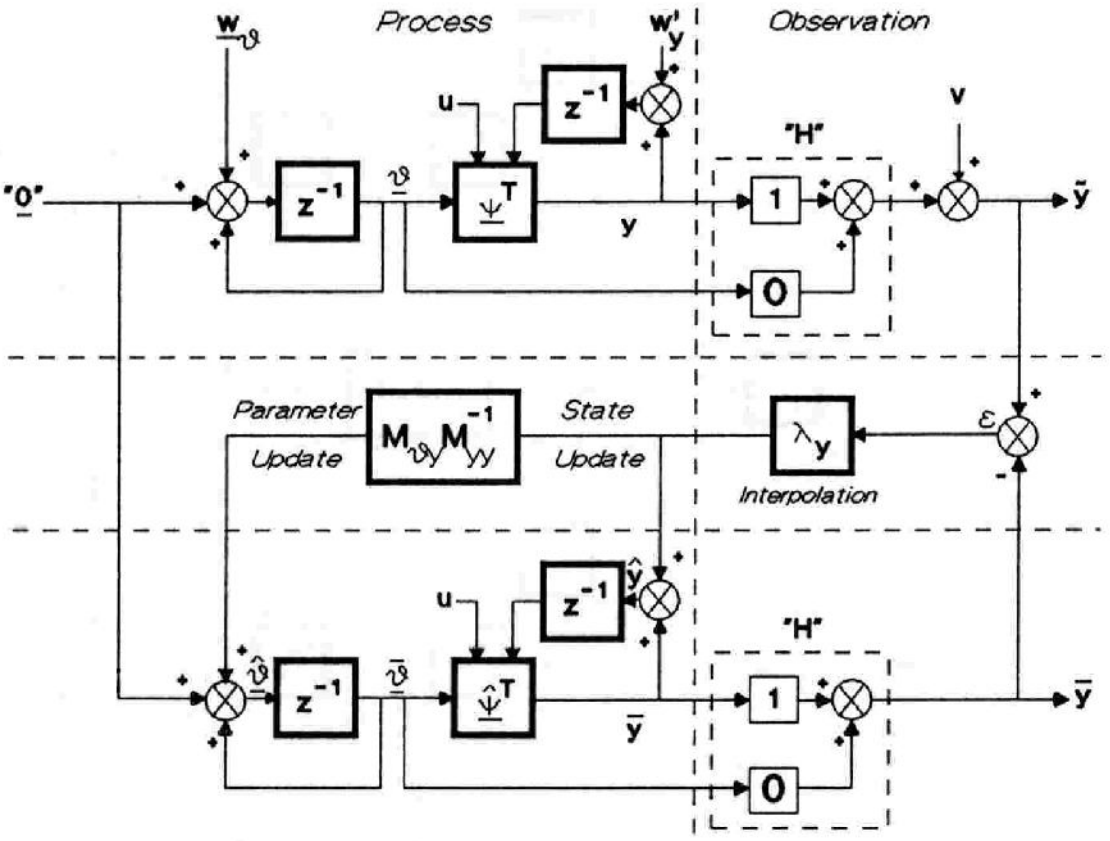

Fig. 4.13 The Extended Kalman filter for state and parameter estimation

4.5.3 Relation with other methods

To demonstrate the relationship of Extended Kalman filtering for combined state and parameter estimation with the methods presented in Section 4.4, the equations for the update gains of the model state and parameters are considered in the absence of system noise:

$$\begin{bmatrix} K_y(k) \\ K_\vartheta(k) \end{bmatrix} = \frac{1}{(M_{yy}(k) + R)} \begin{bmatrix} M_{yy}(k) \\ M_{\vartheta y}(k) \end{bmatrix} \qquad (4.120)$$

with M_{yy} and $M_{\vartheta y}$ components of the a-priori covariance matrix:

$$M(k) = \begin{bmatrix} M_{yy} & M_{y\theta} \\ M_{\theta y} & M_{\theta\theta} \end{bmatrix}_k$$

M(k) is related to the a-posteriori covariance matrix P(k-1) of the previous measurement:

$$P(k-1) = \begin{bmatrix} P_{yy} & P_{y\theta} \\ P_{\theta y} & P_{\theta\theta} \end{bmatrix}_{k-1}$$

by relation (4.114).
Neglecting the cross terms $P_{y\theta}$ and $P_{\theta y}$ in P(k-1) it is assumed that correlation between the a-priori estimates of y and $\underline{\theta}$ at interval k is mainly due to the model relation (4.114) for the propagation of the covariance matrices in time. Applying (4.114) for this special choice of P(k-1), M(k) becomes:

$$M_{yy}(k) = \bar{\theta}_y(k) P_{yy}(k-1) \bar{\theta}_y(k) + \hat{\underline{\psi}}^T(k) P_{\theta\theta}(k-1) \hat{\underline{\psi}}(k) \quad (4.121)$$

$$M_{\theta y}(k) = M_{y\theta}^T(k) = P_{\theta\theta}(k-1) \hat{\underline{\psi}}(k) \quad (4.122)$$

$$M_{\theta\theta}(k) = P_{\theta\theta}(k-1) \quad (4.123)$$

The non-zero terms of the a-posteriori covariance matrix P at interval k are given by:

$$P_{yy}(k) = (1 - K_y(k))\, M_{yy}(k) \quad (4.124)$$

$$P_{\theta\theta}(k) = (I - K_\theta(k) \hat{\psi}^T) M_{\theta\theta}(k) = (I - K_\theta(k) \hat{\psi}^T) P_{\theta\theta}(k-1) \quad (4.125)$$

Combining this with the relations for $K_y(k)$, $K_\theta(k)$ results in the filtering scheme:

<u>a priori</u>:

$$M_{yy}(k) = \bar{\theta}_y(k) P_{yy}(k-1) \bar{\theta}_y(k) + \hat{\underline{\psi}}^T(k) P_{\theta\theta}(k-1) \hat{\underline{\psi}}(k) \quad (4.126)$$

$$M_{\theta y}(k) = M_{y\theta}^T(k) = P_{\theta\theta}(k-1) \hat{\underline{\psi}}(k) \quad (4.127)$$

$$M_{\theta\theta}(k) = P_{\theta\theta}(k-1) \quad (4.128)$$

update gains:

$$K_y(k) = \frac{M_{yy}(k)}{M_{yy}(k) + R} \qquad (4.129)$$

$$K_\vartheta(k) = \frac{M_{\vartheta\vartheta}(k)\hat{\underline{\psi}}(k)}{M_{yy}(k) + R} \qquad (4.130)$$

a posteriori:

$$P_{yy}(k) = (1 - K_y(k))M_{yy}(k) \qquad (4.131)$$

$$P_{\vartheta\vartheta}(k) = (I - K_\vartheta(k)\hat{\underline{\psi}}^T(k))M_{\vartheta\vartheta}(k) \qquad (4.132)$$

These equations are equivalent to the basic combined filtering scheme, derived in Section (4.4.4) by substituting:

$$M_{yy}(k) = M_y(k) \; ; \; P_{yy}(k) = P_y(k) \; ; \; P_{\vartheta\vartheta}(k) = F(k) \qquad (4.133)$$

The simplification of the a-posteriori covariance matrix P(k) of the Extended Kalman filter may be continued by also assuming, in addition to $P_{y\vartheta} = 0$, that $P_{yy} = 0$. Thus it is stated that the uncertainty about the model state after the measurement has become zero.
Combining this with the choice for $K_y(k) = K_{sp}$, where $K_{sp} = 0$ or $K_{sp} = 1$, the filtering relations further reduce to:

a priori:

$$M_{yy}(k) = \hat{\psi}^T(k)P_{\vartheta\vartheta}(k-1)\hat{\psi}(k) \qquad (4.134)$$

$$M_{\vartheta y}(k) = M_{y\vartheta}^T(k) = P_{\vartheta\vartheta}(k-1)\hat{\underline{\psi}}(k) \qquad (4.135)$$

$$M_{\vartheta\vartheta}(k) = P_{\vartheta\vartheta}(k-1) \qquad (4.136)$$

update gains:

$$K_y(k) = K_{sp} = 0 \quad \text{or} \quad 1 \tag{4.137}$$

$$K_\theta(k) = \frac{M_{\theta\theta}(k)\hat{\underline{\psi}}(k)}{M_{yy}(k) + R} \tag{4.138}$$

a posteriori:

$$P_{\theta\theta}(k) = (I - K_\theta(k)\hat{\underline{\psi}}^T(k))M_{\theta\theta}(k) \tag{4.139}$$

For $K_{sp} = 1$ and writing $P_{\theta\theta}(k)$ as $F(k)$ this filtering scheme yields the relations for the *Minimum Variance* (MV) or *Markov* parameter estimator (Söderström and Stoica, 1989).

As a final simplification it is assumed that no knowledge on the observation-noise variance is available. Substituting $R = 1$ in (4.137) leads to the Series-Parallel MRAS or Least-Squares filtering scheme for $K_{sp} = 1$ and to the Parallel MRAS parameter-estimation scheme for $K_{sp} = 0$, as discussed in Section 4.4.1.

Regarding the adaptation of these filtering schemes it may be concluded that by the introduction of system noise on the parameters, according to Eq. (4.108), adaptation to time-varying parameters is inherently achieved. Therefore no additional measures, such as the introduction of a forgetting factor, are required to obtain adaptation. The system noise manifests itself as an additive component to the parameter covariance matrix F(k), instead of the multiplicative nature of the forgetting factor as described in Section 4.4.1.

Finally, to conclude this structural comparison of the different methods for state and parameter estimation an overview is constructed, which summarizes the basic correspondence between the different methods.

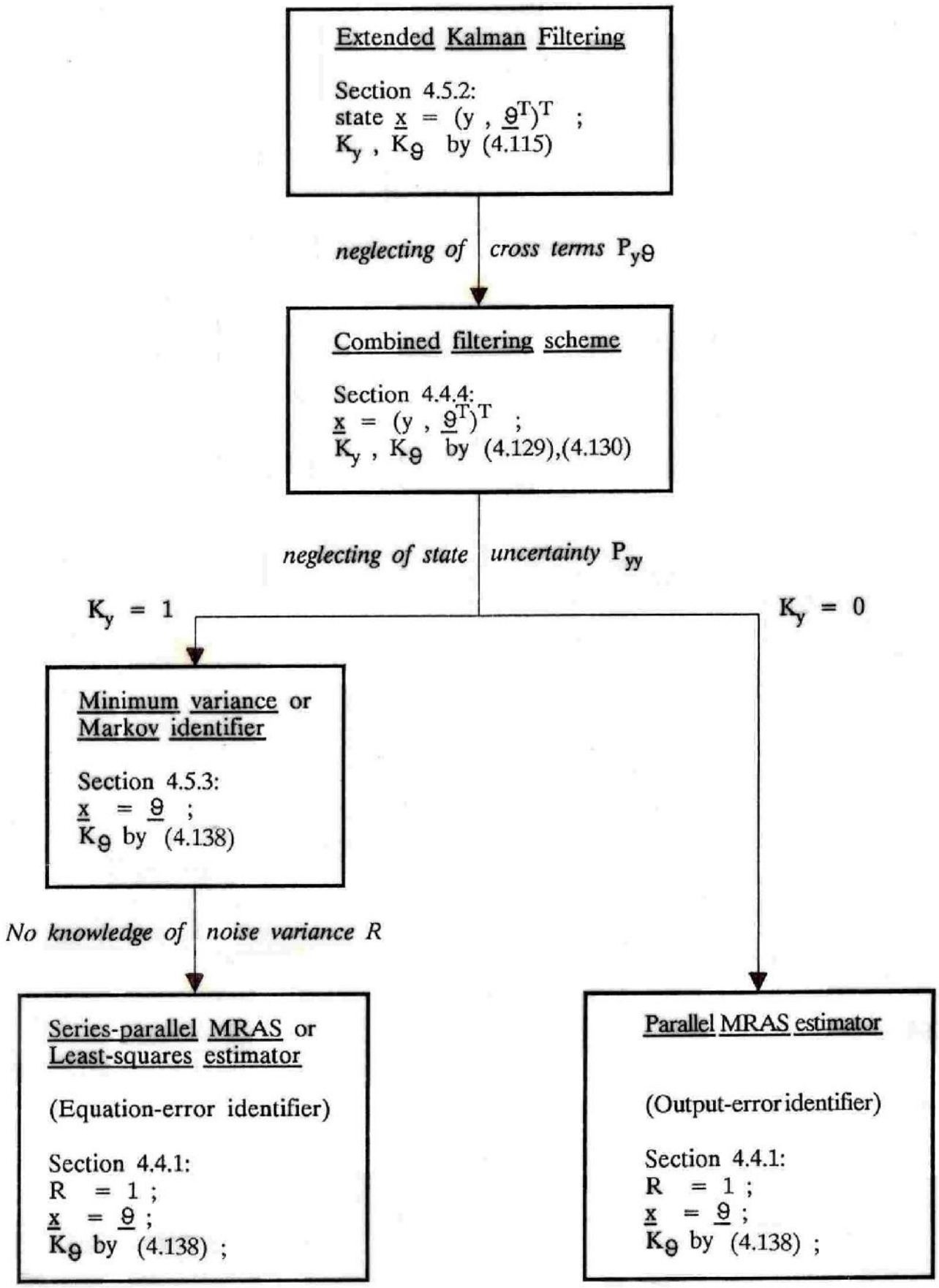
Extended Kalman Filtering
Section 4.5.2:
state $\underline{x} = (y , \underline{\vartheta}^T)^T$;
K_y , K_ϑ by (4.115)
neglecting of cross terms $P_{y\vartheta}$
Combined filtering scheme
Section 4.4.4:
$\underline{x} = (y , \underline{\vartheta}^T)^T$;
K_y , K_ϑ by (4.129),(4.130)
neglecting of state uncertainty P_{yy}
$K_y = 1$
$K_y = 0$
Minimum variance or Markov identifier
Section 4.5.3:
$\underline{x} = \underline{\vartheta}$;
K_ϑ by (4.138)
No knowledge of noise variance R
Series-parallel MRAS or Least-squares estimator
(Equation-error identifier)
Section 4.4.1:
R = 1 ;
$\underline{x} = \underline{\vartheta}$;
K_ϑ by (4.138) ;
Parallel MRAS estimator
(Output-error identifier)
Section 4.4.1:
R = 1 ;
$\underline{x} = \underline{\vartheta}$;
K_ϑ by (4.138) ;

4.6 Adaptive control

In the previous sections attention has been focussed on the identification of a process on the basis of noise-corrupted measurements. The resulting estimated parameters and filtered process state may be combined with a controller, designed for the deterministic case, as will be described in Section 4.6.1.

An alternative scheme for the control of a noise-corrupted process is based on the analogy between identification and control, as this exists for MRAS theory. This underlying analogy between identification and model-reference control will be applied to the field of Kalman filtering in Section 4.6.2.

4.6.1 Indirect adaptive control

For the control of a noise-corrupted process, the schemes for state and parameter estimation as discussed in the previous sections may, in principle, be combined with a controller designed for the deterministic case according to:

$$u = \hat{\underline{\psi}}_c^T \underline{\theta}_c \qquad (4.140)$$

$$\underline{\theta}_c = P(\hat{\underline{\theta}}) \qquad (4.141)$$

with $\underline{\theta}_c$ the controller parameters, which are determined on the basis of the estimated process parameters by, for instance, a pole-placement algorithm P, and u the process input based on the feedback of the estimated process output in combination with the controller parameters. In (4.140) the estimated process output is combined with the controller setpoint u_R according to:

$$\hat{\underline{\psi}}_c^T = (\hat{y}(k), \hat{y}(k-1), \ldots, u_R(k), u_R(k-1), \ldots) \qquad (4.142)$$

Because in the case of changing process parameters, $\hat{\underline{\theta}}$ will be adapted on the basis of the parameter-estimation algorithm, after which the controller parameters $\underline{\theta}_c$ will be adapted according to (4.141), the control scheme (4.140)-(4.141) is of an indirect adaptive nature.

4.6.2 Model-reference control

To obtain a scheme of direct adaptive control, the process and model relations for the Extended-Kalman-filter state and parameter estimator are reexamined:

Process:

$$y(k) = \underline{\psi}^T(k)\underline{\theta}(k-1) \qquad (4.143)$$

$$\tilde{y}(k) = y(k) + v(k) \qquad (4.144)$$

Model:

$$\bar{y}(k) = \hat{\underline{\psi}}^T(k)\hat{\underline{\theta}}(k-1) \qquad (4.145)$$

The a-priori estimation of the process state may be written as:

$$\bar{y}(k) = \hat{\underline{\psi}}^T(k)\underline{\theta}_R + \hat{\underline{\psi}}^T(k)(\hat{\underline{\theta}}(k-1) - \underline{\theta}_R) \qquad (4.146)$$

or

$$\bar{y}(k) = \hat{\underline{\psi}}^T(k)\underline{\theta}_R + \hat{\underline{\psi}}^T(k)\Delta\hat{\underline{\theta}}(k-1) \qquad (4.147)$$

with $\underline{\theta}_R$ an a-priori chosen value of the parameter vector and $\Delta\hat{\underline{\theta}}(k-1)$ the difference between this a-priori choice and the estimated process parameters. For the direct adaptive control it is assumed that an additional input signal $\Delta u(k)$ is available:

$$y(k) = \underline{\psi}^T(k)\underline{\theta} + \Delta u(k) \qquad (4.148)$$

$$\bar{y}(k) = \hat{\underline{\psi}}^T(k)\underline{\theta}_R + \hat{\underline{\psi}}^T(k)\Delta\hat{\underline{\theta}}(k-1) + \Delta u(k) \qquad (4.149)$$

Because the additional input signal $\Delta u(k)$ is common to process and model, the equations for the Extended Kalman filter remain unaffected.
A suitable choice for this input signal is provided by:

$$\Delta u(k) = -\hat{\underline{\psi}}^T(k)\Delta\hat{\underline{\theta}}(k-1) \qquad (4.150)$$

For this choice the relations for process and model modify to:

$$y(k) = \underline{\psi}^T(k)\underline{\theta}(k-1) - \hat{\underline{\psi}}^T(k)\Delta\hat{\underline{\theta}}(k-1) \qquad (4.151)$$

$$\bar{y}(k) = \hat{\underline{\psi}}^T(k)\underline{\theta}_R \qquad (4.152)$$

Because the Kalman filter minimizes the difference between process and model output, it implies that the process is controlled according to (4.152), which has become a reference model.
Of course, the direct-adaptive control scheme (4.151)-(4.152) in combination with the Kalman-filtering relations for K_y and K_θ can be regarded as an extension of discrete Model-Reference Adaptive Control (MRAC) on the basis of either a Series-Parallel model or a completely Parallel model, to a combined reference model (comparable to the "model update method", Van Amerongen, 1980).
The analogy between identification and control with a Kalman filter is demonstrated in Figure 4.14.a,b for a first-order system.
For this first-order system the different variables are given by:

$$\underline{\theta} = (a_p , b_p)^T, \quad \underline{\theta}_R = (a_R , b_R)^T,$$
$$\underline{\psi}^T = (y(k-1) , u(k-1)),$$
$$K_\theta = (K_a , K_b)^T.$$

4.7 Discussion

The theory presented in this chapter on the basis of optimal measurement filtering (Section 4.2) has provided insight into some fundamental techniques for on-line state (Section 4.3) and parameter (Sections 4.4 and 4.5) estimation of a noise-corrupted process by using a Kalman filter.
Further, a modified Kalman-filtering scheme for direct adaptive control of a process has been considered (Section 4.6) on the basis of the analogy between MRAS identification and control.
Possible applications of this theory to the problems related to track-prediction are:

- removing of the high-frequency wave motions from the measured heading or rate-of-turn signal, which is a measurement-filtering problem,
- filtering of the position fixes and estimation of the current influence from these measurements, which is a measurement-filtering and reconstruction problem,
- estimation and adaptation of the prediction model parameters, which is an identification problem,
- design of the course-changing controller on the basis of the model-reference

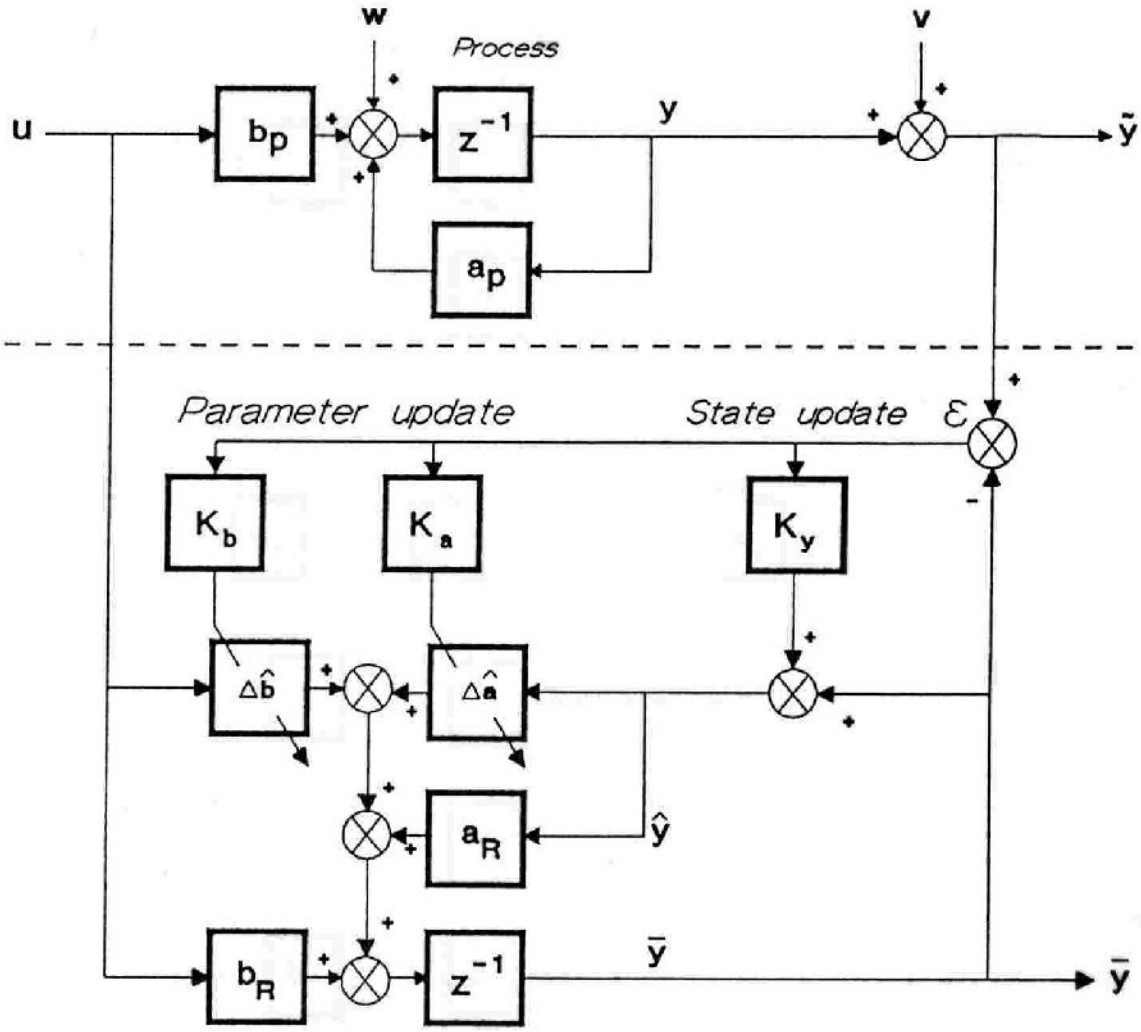

Fig. 4.14.a Using the Kalman filter for identification

techniques described in this chapter.

The applicability of the theory will be treated in the next chapter.

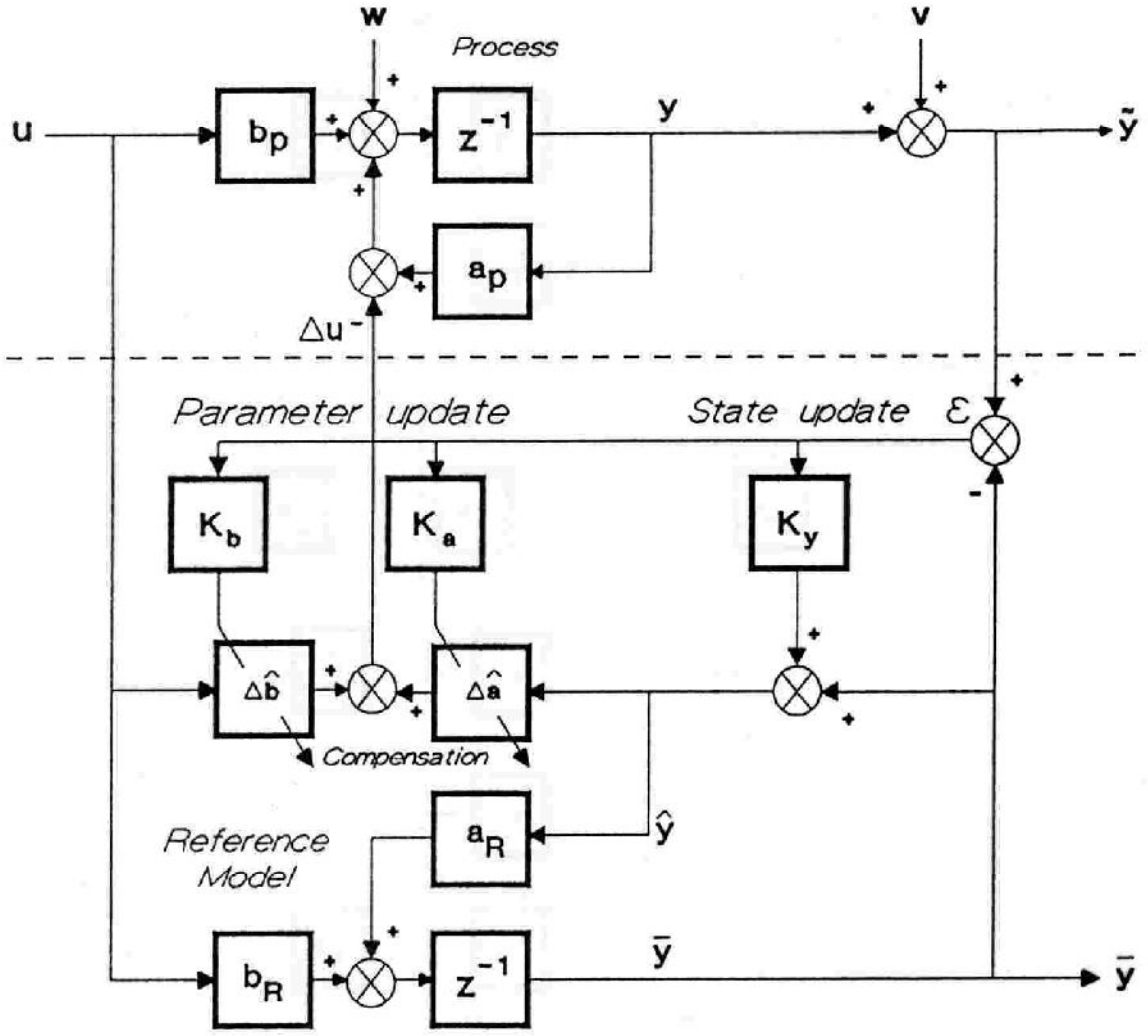

Fig. 4.14.b Using the Kalman filter for control

5 APPLICATION OF THE THEORY TO TRACK PREDICTION

5.1 Introduction

The prediction model, derived in Chapter 3, has a limited number of parameters which have to be adapted to the ship's changing dynamics. For this purpose a method for on-line identification and adaptation is required.
Besides the parameters of the prediction model, the influence of the disturbances also has to be estimated from the measurements in order to achieve adaptation to changing conditions. In terms of Chapter 4 this is a reconstruction problem.
Further, the signals which are considered to be part of the ship's state are to be estimated from the noisy measurements. These states construct the initial state of the prediction model on the basis of which the prediction is calculated. The estimation of this initial state may be formulated as a filtering problem.

In order to apply techniques of optimal measurement filtering to solving these problems, in Section 5.2 the parameters and relevant variables for the track-prediction system will be defined in relation to the available measurements. This allows a separate treatment of the filtering problem of the yaw motions in Section 5.3 and the ship's position in Section 5.4, resulting in a yaw filter and a position filter.

In Section 5.5 possible levels of integration of the yaw filter with the course-changing controller will be discussed on the basis of model-reference techniques in combination with Kalman filtering as described in the previous chapter.
The combination of the yaw and the position filter with the actual track predictor will be treated in Section 5.6. Further, direct adaptation of the predicted track during the execution of a manoeuvre will be discussed in this section. This will provide the track predictor with the closed-loop element, as described in Chapter 1.

The chapter will be concluded with a review (Section 5.7), in which the main points of application of the theory of Chapter 4 to track prediction are summarized.

5.2 Definition of the measurement structure

For track prediction, the ship's motions have to be considered in respect to a space-fixed coordinate system. These motions are related to the motions with respect to a ship-fixed coordinate system by the kinematic relations described in Section 2.4.
The ship-fixed motions of interest (displacement and rotation) for this purpose are those in the horizontal x,y plane (Section 2.2.1):

- displacement along the x-axis (surge motion),
- displacement along the y-axis (sway motion),
- rotation around the z-axis (yaw motion).

The most important disturbances and their effects were considered to be (Section 2.5):

- *current:* additional displacement and yaw motion,
- *wind:* additional yaw motion of the ship and displacement,
- *waves:* additional yaw motion of a stochastic nature and a negligible displacement.

For the on-line reconstruction of these disturbing influences, a distinction is made only between additional yawing ("wind influence") and displacement ("current influence") of the ship. Further, the high-frequency yaw motions ("wave influence") of the ship are regarded as undesirable, and have to be filtered (Van Amerongen, 1982; Van der Klugt, 1987).

For the observation of the motions of interest, the following signals are considered to be available:

- the ship's heading ψ and rate of turn r (provided by the compass after differentiation or from a rate gyro),
- the ship's forward speed u (provided by the log),
- the ship's position $\underline{x}_s$ (provided by a positioning system).

Together with the measured rudder angle δ, which is the input signal for the ship, the diagram of Figure 5.1 for the disturbances, the ship's motions and the monitoring of these motions on the basis of the measurements can be constructed.
The wave influence is classified as system noise, causing high-frequency components

in the measured rate-of-turn and heading signal.

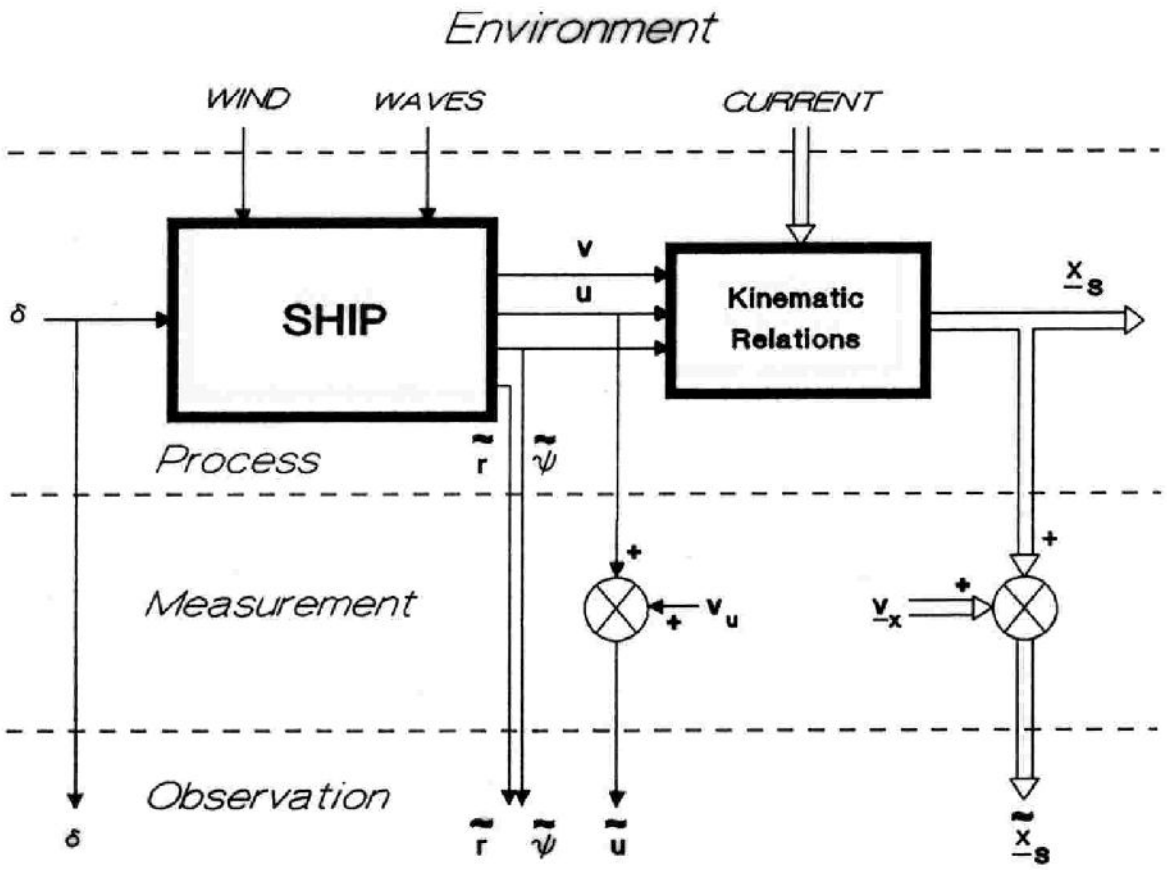

Fig. 5.1 Measurement diagram for the ship's motions

In Figure 5.1 v_u is the measurement noise on the measured forward speed and $\underline{v}_x$ is the measurement noise on the position fixes.
The measurement diagram can be separated into two substructures, according to the yaw motions (resulting in the ship's heading) and kinematics (resulting in the ship's position).
This separation has the following advantages for the filter design and implementation:

- The non-linearity, introduced by the terms sinψ and cosψ in the kinematic relations to relate the ship-fixed quantities to the space-fixed quantities, has been eliminated because these terms have become an input signal for this substructure. The same applies to the role which the forward speed u plays for the gain scheduling of the yaw-model parameters.
- Decrease of computational complexity, which will be considered in Section 5.4.

This yields the separate measurement diagram of Figure 5.2.a for the filtering of the ship's rate-of-turn and heading signal and estimation of the wind influence, and the measurement diagram of Figure 5.2.b for the filtering of the measured forward speed and position and reconstruction of the sway velocity and current influence.

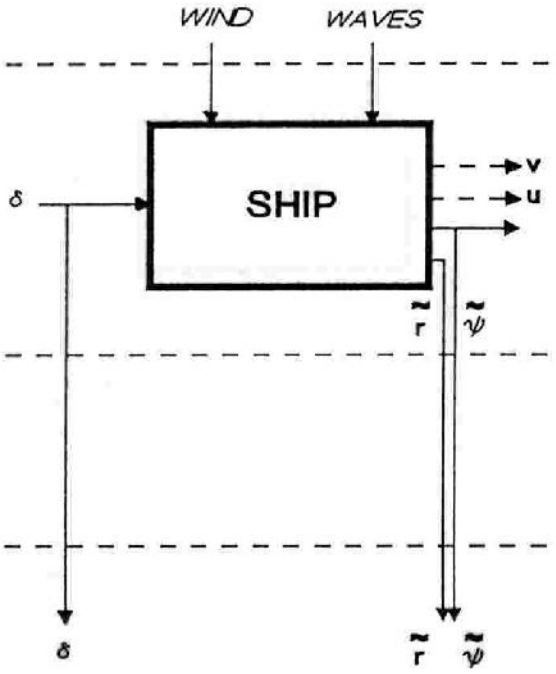

Fig. 5.2.a Yaw motions

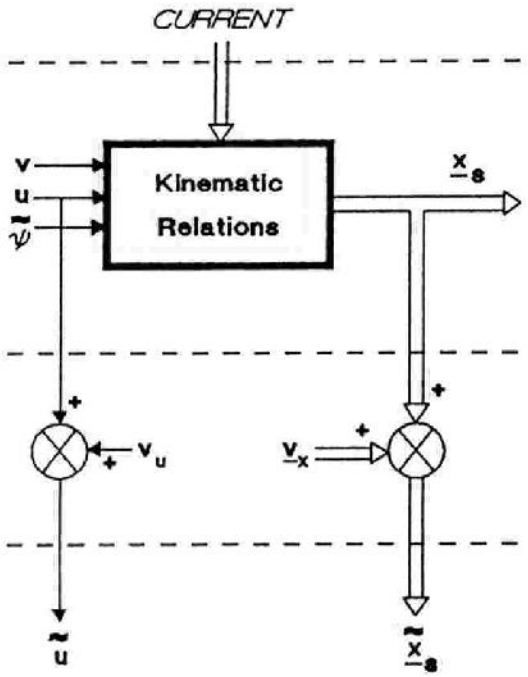

Fig. 5.2.b Kinematics

The application of optimal measurement filtering theory to these two separate filtering and reconstruction problems will be described in the following sections.

5.3 The yaw filter

According to the concepts of discrete optimal filtering and reconstruction discussed in Chapter 4, two types of information on the quantity to be filtered should be available, namely *a-priori information* and *measurement information*. For the optimal filtering of the rate-of-turn signal (the filter for this purpose will be referred to as the yaw filter) the two types of information become:

- *a-priori information*:
  provided by a dynamic model of the ship's yaw motions,
- *measurement information:*

provided according to the measurement diagram of Figure 5.2.a

Focussing attention on the filtering problem for the moment, and therefore disregarding the estimation of the wind influence which is a reconstruction problem, the combination of model knowledge and measurement information yields the filter structure of Figure 5.3 for the filtering of the wave motions:

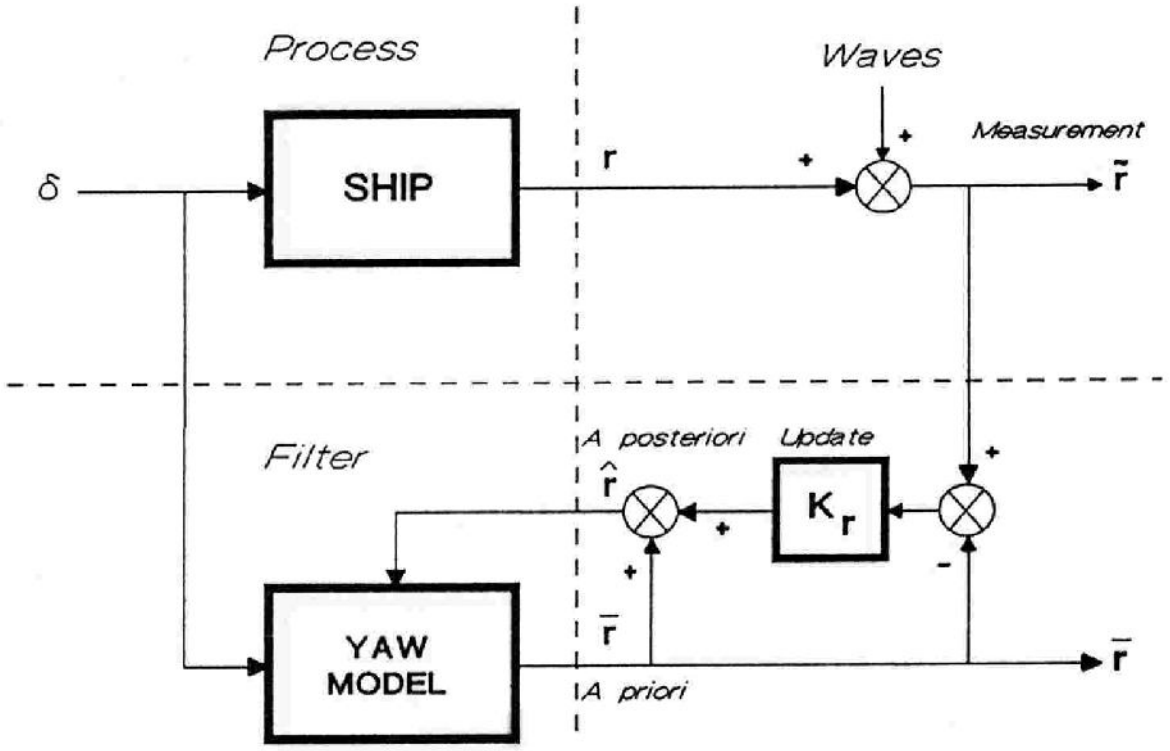

Fig. 5.3 Structure of the yaw filter

For the filter design the wave influence is treated as measurement noise, which has to be filtered from the measured rate-of-turn signal.
To determine the filter gain K_r for the update of the rate-of-turn estimation on the basis of optimal filtering theory, the structure of the yaw model has to be considered in more detail.
The continuous-time De Keizer model for the description of the yaw motions is given by:

$$\tau^* \frac{L}{u} \dot{r} + r = K^* \frac{u}{L} \delta \qquad (5.1)$$

with u the forward speed and L the length of the ship and δ the rudder angle. To obtain a discrete relation, there are several possibilities:

- z-transformation
- numerical integration, for instance Euler, Tustin, Runge Kutta 2 etc.

Assuming the sampling frequency to be sufficiently high, the second approach may be followed by using a first-order Euler approximation for the calculation of r:

$$r(k) = r(k-1) + T_s \dot{r}(k-1) \qquad (5.2)$$

with T_s the sampling interval.

Combining this with (5.1) yields the discrete relation:

$$r(k) = a_s r(k-1) + b_s \delta(k-1) \qquad (5.3)$$

with the discrete parameters related to the continuous-time parameters by:

$$a_s = 1 - T_s/\tau^* . \frac{u}{L} \qquad (5.4)$$

$$b_s = K^*/\tau^* \; T_s \left(\frac{u}{L} \right)^2 \qquad (5.5)$$

The discrete equations for the process become:

process:

$$r(k) = a_s r(k-1) + b_s \delta(k-1) + w_r(k-1) \qquad (5.6)$$

$$\tilde{r}(k) = r(k) + v(k) \qquad (5.7)$$

where $w_r(k)$ is white system noise, introduced to represent model uncertainty, and v(k) represents the wave influence which, for now, is assumed to be white measurement noise.
A suitable form for the a-priori estimation of the rate-of-turn signal may then be obtained by combining (5.6) with the a-posteriori estimation at $t = (k-1).T_s$:

a priori:

$$\bar{r}(k) = a_s \hat{r}(k-1) + b_s \delta(k-1) \qquad (5.8)$$

Applying the Kalman-filtering theory for state estimation, presented in Section 4.3, and using Eqs. (5.6)-(5.8) yields for the covariance $m_r(k)$ of the a-priori estimation

error:

$$m_r(k) = a_s^2 \, p_r(k-1) + \sigma_w^2 \qquad (5.9)$$

with $p_r(k-1)$ the covariance of the a-posteriori estimation error at $t = (k-1).T_s$, and σ_w^2 the variance of the system noise.
If the variance of the wave influence is known, which may be provided by an on-line estimation procedure proposed by Van Amerongen (1982) and worked out in more detail by Van der Klugt (1987), the optimal gain for the update of the a-priori estimation on the basis of the measurement becomes:

$$K_r(k) = \frac{m_r(k)}{m_r(k) + \sigma_v^2} \qquad (5.10)$$

with σ_v^2 the variance of the wave influence.
This yields for the a-posteriori estimation:

a posteriori:

$$\hat{r}(k) = \bar{r}(k) + K_r(k)(\tilde{r}(k) - \bar{r}(k)) \qquad (5.11)$$

with covariance:

$$p_r(k) = (1 - K_r(k)) \, m_r(k) \qquad (5.12)$$

The more detailed structure of this yaw filter is presented in Figure 5.4.
In the case of unknown parameters of the discrete yaw model, the filter structure of Figure 5.4 may be extended to a filtering and reconstruction scheme on the basis of the Extended-Kalman-filtering approach, described in the previous chapter. The wind influence may also be estimated by modelling this influence as an additional input N_w to the yaw model (Section 2.5.3).

The relations for the a-priori estimation, process and measurement and a-posteriori estimation are for this purpose extended to:

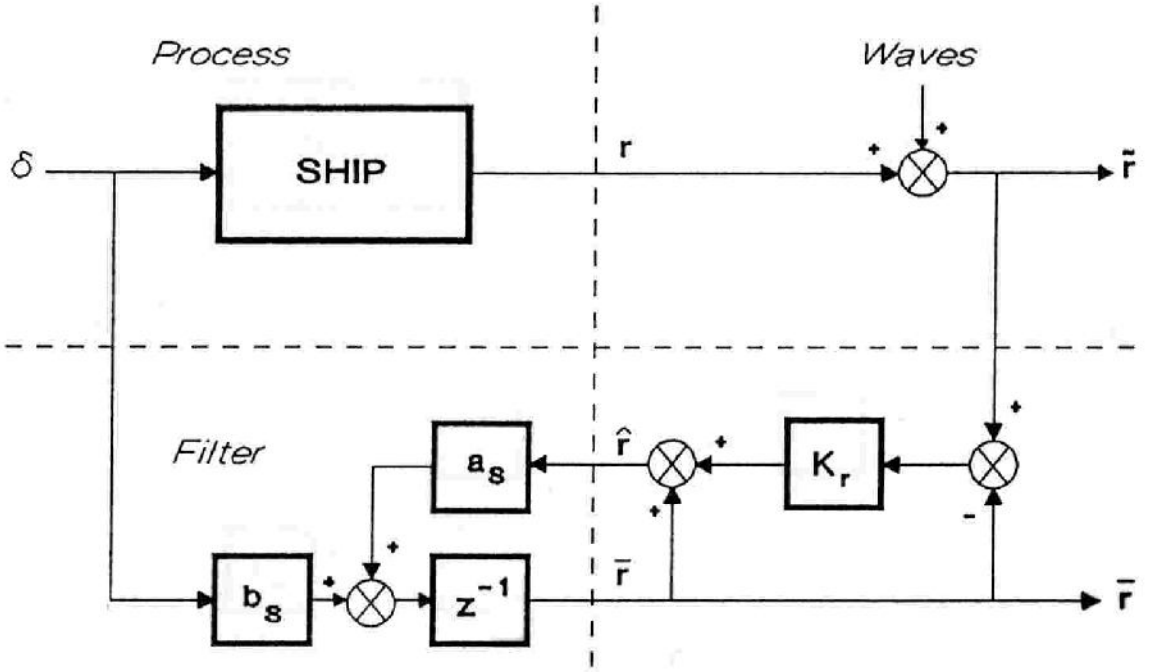

Fig. 5.4 Kalman filter for the yaw motions

a priori:

$$\bar{r}(k) = \hat{a}_s(k-1)\hat{r}(k-1) + \hat{b}_s(k-1)\delta(k-1) + \hat{N}_w(k-1) \qquad (5.13)$$

$$\bar{a}_s(k) = \hat{a}_s(k-1) \qquad (5.14)$$

$$\bar{b}_s(k) = \hat{b}_s(k-1) \qquad (5.15)$$

$$\bar{N}_w(k) = \hat{N}_w(k-1) \qquad (5.16)$$

process:

$$r(k) = a_s(k-1)r(k-1) + b_s(k-1)\delta(k-1) + N_w(k-1) + w_r(k-1) \qquad (5.17)$$

$$a_s(k) = a_s(k-1) + w_a(k-1) \qquad (5.18)$$

$$b_s(k) = b_s(k-1) + w_b(k-1) \qquad (5.19)$$

$$N_w(k) = N_w(k-1) + w_n(k-1) \qquad (5.20)$$

where the parameters a_s , b_s and N_w are modelled as constants to which white system noise $w_i(k)$ is added to achieve adaptation.

measurement:

$$\tilde{r}(k) = r(k) + v(k) \qquad (5.21)$$

which yields the prediction error:

$$\epsilon(k) = \tilde{r}(k) - \bar{r}(k) \qquad (5.22)$$

a posteriori:

$$\hat{r}(k) = \bar{r}(k) + K_r(k)\epsilon(k) \qquad (5.23)$$

$$\hat{a}_s(k) = \bar{a}_s(k) + K_a(k)\epsilon(k) \qquad (5.24)$$

$$\hat{b}_s(k) = \bar{b}_s(k) + K_b(k)\epsilon(k) \qquad (5.25)$$

$$\hat{N}_w(k) = \bar{N}_w(k) + K_n(k)\epsilon(k) \qquad (5.26)$$

The update gains $K_r(k)$, $K_a(k)$, $K_b(k)$ and $K_n(k)$ are provided by the Kalman-filtering relations in such a way that for the given a-priori covariances m_r, m_a, m_b, m_n and measurement-noise variance σ_v^2, the a-posteriori covariances p_r, p_a, p_b, p_n of the estimation errors become minimal, comparable to (5.9)-(5.12).
Together with Eqs. (5.4) and (5.5) the update equations (5.24)-(5.25) for the discrete parameters a_s and b_s may be transformed to an expression for the update of the continuous normalized parameters K^* and τ^* :

$$(1/\hat{\tau}^*)_k = (1/\hat{\tau}^*)_{k-1} - K_a/T_s.(L/\hat{u}(k)).\epsilon(k) \qquad (5.27)$$

$$(\hat{K}^*/\hat{\tau}^*)_k = (\hat{K}^*/\hat{\tau}^*)_{k-1} + K_b/T_s.(L/\hat{u}(k))^2.\epsilon(k) \qquad (5.28)$$

In these equations the ship's forward speed u is replaced by a best estimation, to be calculated by the position filter.

To complete the design of the yaw filter, the colouring of the measurement noise, which up to now has been assumed to be white, has to be considered.
A possible discrete first-order description for the colouring of the wave motions,

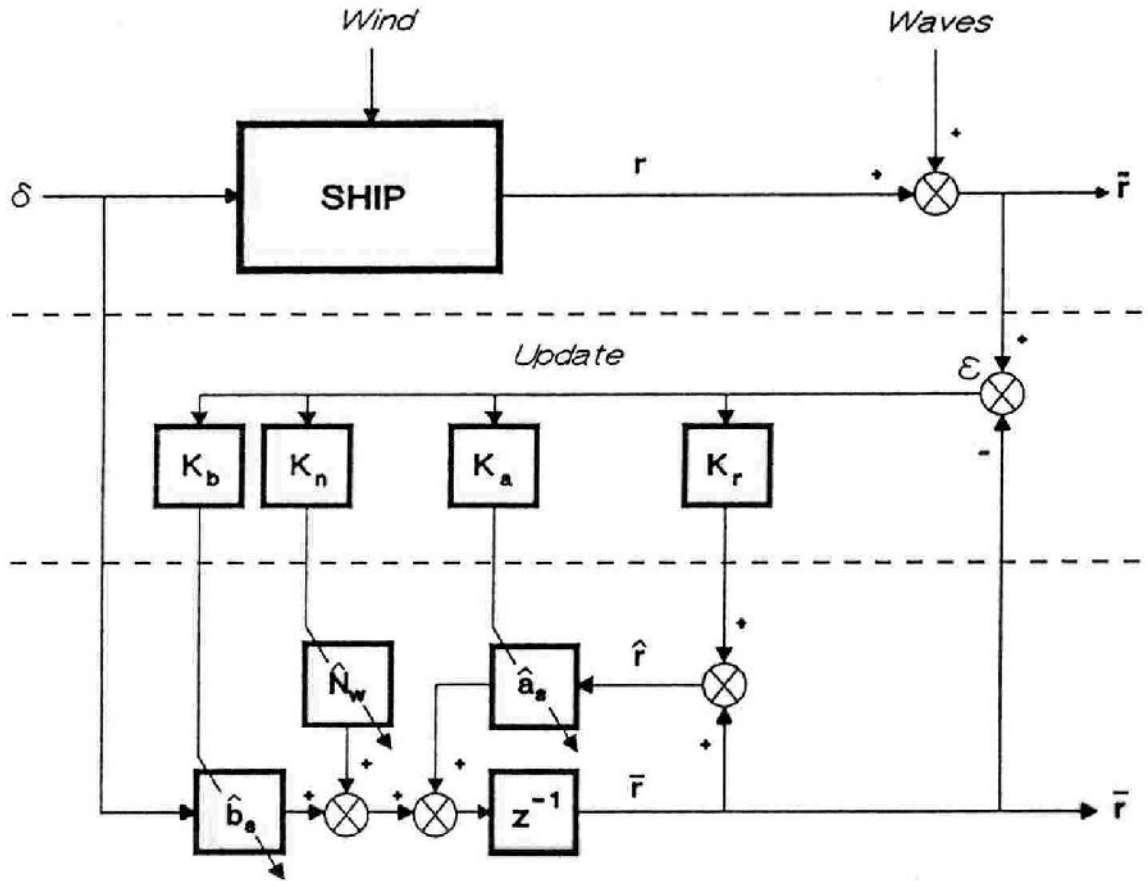

Fig. 5.5 Extended Kalman filter for estimation of yaw-model parameters

based on the proposal by Van der Klugt (1987), is:

$$v_f(k) = a_f v_f(k-1) + b_f w(k-1) \qquad (5.29)$$

$$v(k) = w(k) - v_f(k) \qquad (5.30)$$

with w(k) white noise and v(k) the wave influence, added to the rate-of-turn signal (instead of to the heading signal, as was worked out by Van der Klugt):

$$\tilde{r}(k) = r(k) + v(k) \qquad (5.31)$$

The discrete parameters of (5.29), which is a first-order filter for w(k), are related to the time constant of the continuous-time filter by (using Euler): $a_f = 1 - T_s/\tau_f$ and $b_f = T_s/\tau_f$.
By using the colouring model of (5.29)-(5.30), high-frequency components in the

rate-of-turn signal (selected by the filter time constant τ_f) are regarded as measurement noise in the observation equation (5.31), and therefore are filtered.

This colouring of the wave motions may be incorporated into the yaw filter by extending the filter state with $v_f(k)$. This yields the following extensions for the filter equations:

a priori:

$$\bar{v}_f(k) = a_f \hat{v}_f(k-1) \qquad (5.32)$$

measurement:

$$\tilde{r}(k) = r(k) - v_f(k) + w(k) + v_r(k) \qquad (5.33)$$

with $v_r(k)$ the additional measurement error, introduced by the rate-of-turn sensor.

a posteriori:

$$\hat{v}_f(k) = \bar{v}_f(k) + K_v(k)\varepsilon(k) \qquad (5.34)$$

with $K_v(k)$ provided by the Kalman-filtering scheme and the prediction error $\varepsilon(k)$:

$$\varepsilon(k) = \tilde{r}(k) - (\bar{r}(k) - \bar{v}_f(k)) \qquad (5.35)$$

This substructure of the yaw filter is given in Figure 5.6.
In this figure r_w is the wave-disturbed rate-of-turn signal, before the measurement noise v_r of the rate-of-turn sensor is added.
As a final extension, heading information (provided by the compass) is added to the yaw filter. By this extension of the filter a configuration is obtained for the filtering of the undesirable high-frequency wave influence from the heading signal. Further, if no rate-of-turn sensor is available, the filter can still provide a reasonable estimation of the rate-of-turn signal on the basis of the measured heading signal.
For this purpose the measured heading signal is written as:

$$\tilde{\psi}(k) = \psi(k) + \psi_v(k) + v_\psi(k) \qquad (5.36)$$

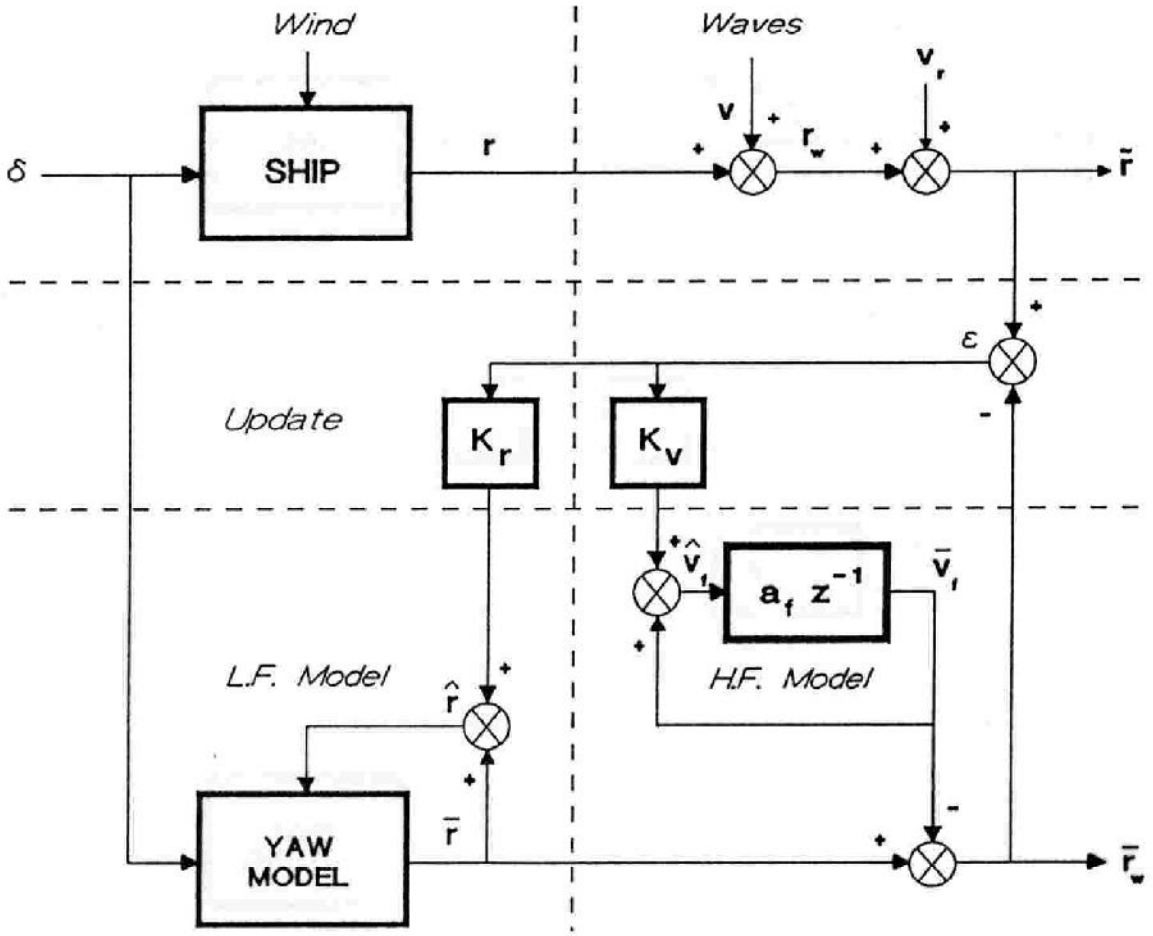

Fig. 5.6 Yaw-filter substructure for the coloured wave influence

with $\psi(k)$ the low-frequency component, $\psi_v(k)$ the wave influence and $v_\psi(k)$ the measurement error of the compass.
Together with the relations for the rate-of-turn signal, these quantities may be expressed as:

$$\psi(k) = \psi(k-1) + T_s r(k-1) \qquad (5.37)$$

$$\psi_v(k) = \psi_v(k-1) + T_s(w(k-1)-v_f(k-1)) \qquad (5.38)$$

which yields the following process and measurement equations for $\psi(k)$ and $\psi_v(k)$:

process:

$$\psi(k) = \psi(k-1) + T_s r(k-1) \qquad (5.39)$$

$$\psi_v(k) = \psi_v(k-1) - T_s v_f(k-1) + T_s w(k-1) \qquad (5.40)$$

measurement:

$$\tilde{\psi}(k) = \psi(k) + \psi_v(k) + v_\psi(k) \qquad (5.41)$$

For the a-priori estimation, the previous a-posteriori estimations of the rate-of-turn filter are substituted in the process relations, thus obtaining:

a priori:

$$\bar{\psi}(k) = \hat{\psi}(k-1) + T_s \hat{r}(k-1) \qquad (5.42)$$

$$\bar{\psi}_v(k) = \hat{\psi}_v(k-1) - T_s \hat{v}_f(k-1) \qquad (5.43)$$

which together with the equations of the rate-of-turn filter provide sufficient information for the calculation of the optimal updates on the basis of the prediction error, which now has become a vector:

a posteriori:

$$\hat{\psi}(k) = \bar{\psi}(k) + K_\psi(k)\underline{\varepsilon}(k) \qquad (5.44)$$

$$\hat{\psi}_v(k) = \bar{\psi}_v(k) + K_h(k)\underline{\varepsilon}(k) \qquad (5.45)$$

The prediction error vector $\underline{\varepsilon}(k) = (\varepsilon_r(k) , \varepsilon_\psi(k))^T$ is given by:

$$\varepsilon_r(k) = \tilde{r}(k) - (\bar{r}(k) - \bar{v}_f(k)) \qquad (5.46)$$

$$\varepsilon_\psi(k) = \tilde{\psi}(k) - (\bar{\psi}(k) + \bar{\psi}_v(k)) \qquad (5.47)$$

The substructure for this extension of the yaw filter for the filtering of the heading signal is presented in Figure 5.7.

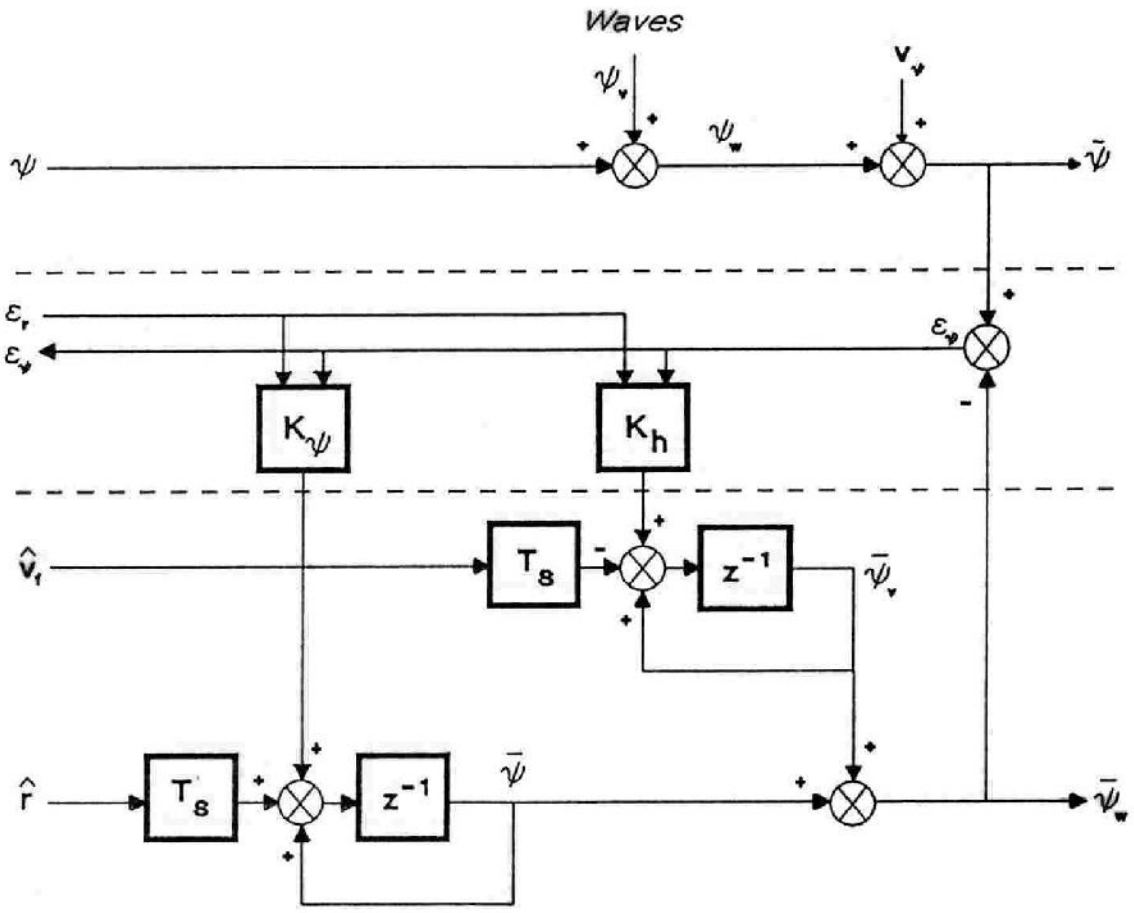

Fig. 5.7 Extension of the yaw filter for filtering of the heading

Resuming, the yaw filter is a Kalman filter for the estimation of a seven-dimensional state vector:

$$\hat{\underline{x}}_y^T = (\hat{a}_s, \hat{b}_s, \hat{N}_w, \hat{r}, \hat{v}_f, \hat{\psi}, \hat{\psi}_v)$$

where the subscript y stands for yaw filter.
The filter input consists of: $(\delta, \hat{u})^T$, with δ the actual rudder angle and $\hat{u}$ the estimated forward speed provided by the position filter, to be described in the next section.

The required measurements are:

$$\tilde{\underline{y}}_y^T = (\tilde{r}, \tilde{\psi})$$

The main parameter of the filter is the variance of the high-frequency wave motions, which may be provided by an on-line estimation procedure in combination with a first-order filter with discrete parameter a_f or time constant τ_f (Van Amerongen, 1982; Van der Klugt 1987). In this way the filter becomes adaptive with respect to the sea state.
The variance of the different system-noise components on the parameters has to be chosen in such a way that an acceptable performance (adaptation) of the filter is obtained (calibration of the filter).
The variance of the measurement noise reflects the expected accuracy of the sensors (compass and rate-of-turn gyro).

5.4 The position filter

As described in Section 5.2, for the determination of the ship's position and the influence of uniform current (Section 2.5.2), it is assumed that position fixes are provided by a positioning system. Further, information on the forward speed u is considered to be available, provided by the log, to enable gain scheduling of the predictor and autopilot parameters (a separate speed filter for this purpose has been described by Van der Klugt, 1987). Assuming information on the sway velocity v to be determined from the position fixes, the measurement diagram of Figure 5.2.b was obtained.
Because the variables mentioned here are, together with the ship's heading ψ, related to each other by the kinematic relations (Section 2.4), these kinematic relations may be added to the measurement diagram as a-priori information. This results in the filter structure of Figure 5.8, which has a filtering part (position and forward speed, update gain K_f) and a reconstruction part (current and sway speed, update gain K_c). In this figure $\underline{x}_s$ is the ship's position: $\underline{x}_s = (x_s , y_s)^T$, related by the kinematic relations to the forward speed u, the sway velocity v and the current speed $\underline{u}_c = (u_{cx} , u_{cy})^T$.
The measurement noise of the positioning system and the log is given by $\underline{v}_x$ and v_u.

Additional a-priori knowledge may be incorporated into the filter by assuming the ship's sway velocity proportional to the rate of turn (Section 2.3.3):

$$v = -\gamma r \qquad (5.48)$$

Considering no a-priori information to be available on the forward speed of the ship and the current influence, for filtering purposes these quantities are modelled

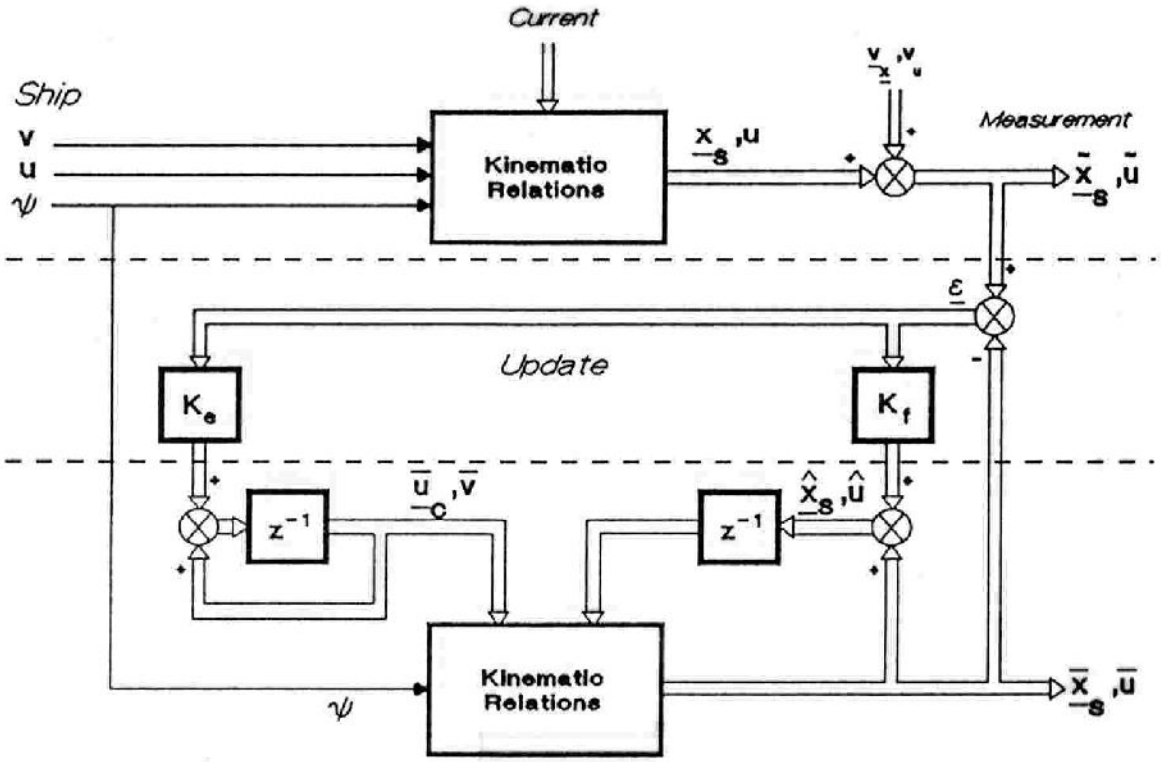

Fig. 5.8 Structure of the position filter

as a constant, to which system noise is added to achieve adaptation. Resuming, the relations for the process become:

process:

ship-fixed: forward speed u and sway velocity v

$$u(k) = u(k-1) + w_u(k) \qquad (5.49)$$

$$\gamma(k) = \gamma(k-1) + w_\gamma(k) \qquad (5.50)$$

$$v(k) = -\gamma(k)\, r(k) \qquad (5.51)$$

space-fixed: current speed in x and y direction

$$u_{cx}(k) = u_{cx}(k-1) + w_{cx}(k) \qquad (5.52)$$

$$u_{cy}(k) = u_{cy}(k-1) + w_{cy}(k) \qquad (5.53)$$

kinematic relations: ship speed in x and y direction

$$u_{sx}(k-1) = u(k-1)\cos\psi(k-1) - v(k-1)\sin\psi(k-1) + u_{cx}(k-1) \quad (5.54)$$

$$u_{sy}(k-1) = u(k-1)\sin\psi(k-1) + v(k-1)\cos\psi(k-1) + u_{cy}(k-1) \quad (5.55)$$

position:

$$x_s(k) = x_s(k-1) + T_s\, u_{sx}(k-1) \quad (5.56)$$

$$y_s(k) = y_s(k-1) + T_s\, u_{sy}(k-1) \quad (5.57)$$

with the process state consisting of: u, γ, u_{cx} , u_{cy}, x_s and y_s .
The relations are written in this specific order to show how the ship-fixed and space-fixed quantities are related to each other by the kinematic relations, which yield the ship's position.
The corresponding equations for the a-priori estimations of the position filter become:

a priori:

ship fixed: forward speed and sway velocity

$$\bar{u}(k) = \hat{u}(k-1) \quad (5.58)$$

$$\bar{\gamma}(k) = \hat{\gamma}(k-1) \quad (5.59)$$

$$\hat{v}(k-1) = \hat{\gamma}(k-1)\hat{\psi}(k-1) \quad (5.60)$$

space fixed: current speed in x and y direction

$$\bar{u}_{cx}(k) = \hat{u}_{cx}(k-1) \quad (5.61)$$

$$\bar{u}_{cy}(k) = \hat{u}_{cy}(k-1) \quad (5.62)$$

kinematic relations: ship speed in x and y direction

$$\hat{u}_{sx}(k-1) = \hat{u}(k-1)\cos\hat{\psi}(k-1) - \hat{v}(k-1)\sin\hat{\psi}(k-1) + \hat{u}_{cx}(k-1) \quad (5.63)$$

$$\hat{u}_{sy}(k-1) = \hat{u}(k-1)\sin\hat{\psi}(k-1) + \hat{v}(k-1)\cos\hat{\psi}(k-1) + \hat{u}_{cy}(k-1) \quad (5.64)$$

position:

$$\bar{x}_s(k) = \hat{x}_s(k-1) + T_s\,\hat{u}_{sx}(k-1) \quad (5.65)$$

$$\bar{y}_s(k) = \hat{y}_s(k-1) + T_s\,\hat{u}_{sy}(k-1) \quad (5.66)$$

In this a-priori estimation scheme the estimations of the ship's rate of turn and heading are provided by the yaw filter, described in the previous section.

After the a-priori estimation, the measurement is performed:

measurement:

$$\tilde{u}(k) = u(k) + v_u(k) \quad (5.67)$$

$$\tilde{x}_s(k) = x_s(k) + v_x(k) \quad (5.68)$$

$$\tilde{y}_s(k) = y_s(k) + v_y(k) \quad (5.69)$$

with $\tilde{u}$ and $\tilde{x}_s,\tilde{y}_s$ the measured forward speed and the ship's position, and v_u , v_x and v_y the corresponding observation noise.
Finally, the a-priori estimations are updated on the basis of the prediction error vector $\underline{\varepsilon}(k)$:

$$\underline{\varepsilon}(k) = ((\tilde{u} - \bar{u}),\ (\tilde{x}_s - \bar{x}_s),\ (\tilde{y}_s - \bar{y}_s))^T_k \quad (5.70)$$

This yields the a-posteriori estimations:

a posteriori:

speed:

$$\hat{u}(k) = \bar{u}(k) + K_u^T \underline{\varepsilon}(k) \qquad (5.71)$$

$$\hat{\gamma}(k) = \bar{\gamma}(k) + K_\gamma^T \underline{\varepsilon}(k) \qquad (5.72)$$

$$\hat{u}_{cx}(k) = \bar{u}_{cx}(k) + K_{cx}^T \underline{\varepsilon}(k) \qquad (5.73)$$

$$\hat{u}_{cy}(k) = \bar{u}_{cy}(k) + K_{cy}^T \underline{\varepsilon}(k) \qquad (5.74)$$

position:

$$\hat{x}_s(k) = \bar{x}_s(k) + K_x^T(k)\, \underline{\varepsilon}(k) \qquad (5.75)$$

$$\hat{y}_s(k) = \bar{y}_s(k) + K_y^T(k)\, \underline{\varepsilon}(k) \qquad (5.76)$$

with the update gains K_u, K_γ, ... provided again by the Kalman-filtering equations, which minimize the a-posteriori covariances p_u , p_γ and so on.

The estimated sway constant may be normalized with respect to the ship's length L by:

$$\hat{\gamma}^*(k) = \hat{\gamma}(k)/L \qquad (5.77)$$

Resuming, the position filter is a Kalman filter for the estimation of a six-dimensional state vector:

$$\underline{\hat{x}}_p^T = (\hat{u}\ ,\hat{\gamma}\ ,\hat{u}_{cx},\hat{u}_{cy},\ \hat{x}_s,\ \hat{y}_s)$$

where the subscript p stands for position filter.

The filter input consists of: $(\hat{r}\ ,\ \hat{\psi})^T$, with r the filtered rate of turn and ψ the filtered heading, provided by the yaw filter.

The required measurements are:

$$\underset{\sim}{y}_p^T = (\tilde{u}, \tilde{x}_s, \tilde{y}_s)$$

The main parameter of the filter is the variance of the position-fix measurement error, which is a characteristic of the positioning system. The variances of the various system noise components have to be chosen in such a way that an acceptable adaptation of the filter to changing current is obtained.

Computational aspects

In this and the previous section two separate Kalman filters have been derived for the filtering of the ship's heading (the yaw filter described in Section 5.3) and the ship's position (the filter described in this section). This resulted in an on-line estimation scheme of a seven-dimensional and a six-dimensional state vector on the basis of the measurements (Figure 5.9).
To judge the computational complexity of these Kalman filters, the number of elements of the covariance matrices, necessary for the calculation of the update gains, is considered to be a good indication (see also Van der Klugt, 1987).
Because these covariance matrices are symmetrical, the number of elements corresponding to an n-dimensional state vector is given by: $n.(n+1)/2$
For the 7-dimensional yaw filter this yields: $N_y = 7.(7+1)/2 = 28$
and for the 6-dimensional position filter: $N_p = 6.(6+1)/2 = 21$
which yields a total amount of $28 + 21 = 49$ elements.
If the two separate filters would be combined into one filter, this amount becomes: $13.(13+1)/2 = 91$, and thus also from a computational point of view the advantage of making the separation has become clear.

5.5 The course-changing controller

5.5.1 Introduction

Although the course-changing controller is functionally separated from the actual track predictor, there are several arguments to combine this unit with the yaw filter, which is considered to be part of the track-prediction system. The principle arguments are:

- minimization of the controller's response to the wave influence by using the filtered signals, provided by the yaw filter, instead of the measured signals,

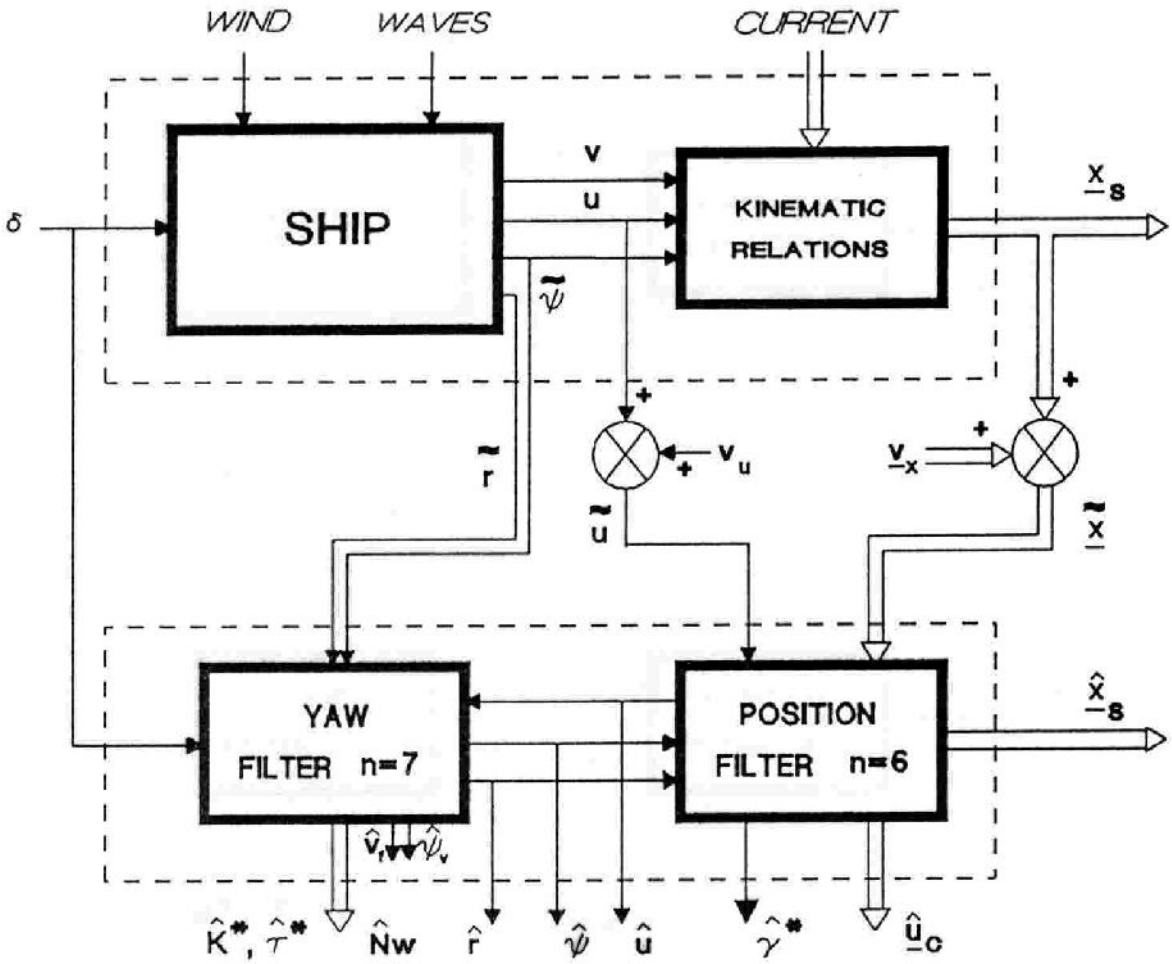

Fig. 5.9 Yaw and position estimation by two separate Kalman filters

- adjusting of the autopilot parameters on the basis of the on-line identification of the ship's dynamics, performed by the yaw filter.

This combination of the yaw filter with the course-changing controller will be discussed in Section 5.5.2

The integration of the yaw filter and the course-changing controller may be extended on the basis of the model-reference techniques, discussed in Section 4.6. In this way an integrated configuration is obtained for direct compensation of, among others, non-linearities in the rudder to rate-of-turn transfer. This model-reference approach will be discussed in Section 5.5.3.

5.5.2 Combination of the yaw filter with the course-changing controller

The course-changing controller described in Section 3.3.2.2 consists of two gains K_p , K_d and a rudder limiter δ_{max}, according to Figure 5.10.

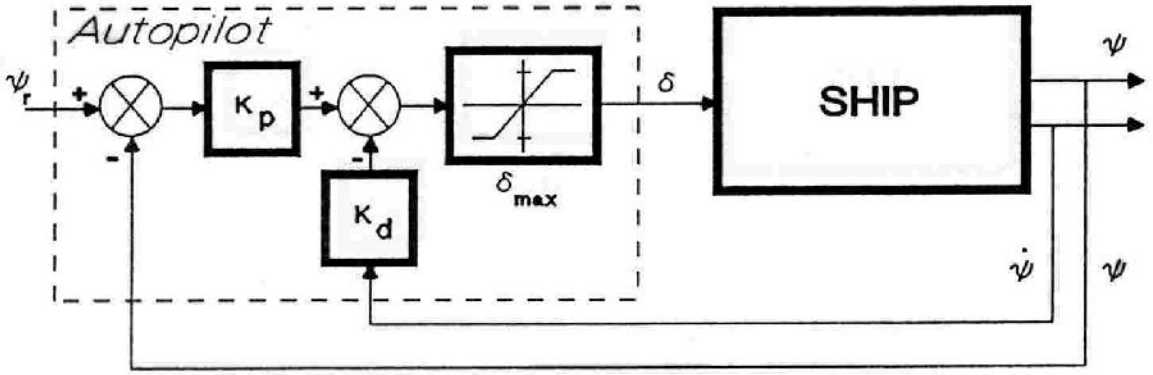

Fig. 5.10 Ship with a course-changing controller

The gains K_p and K_d may be chosen in such a way that a desired closed-loop response of the ship's actual heading ψ to the autopilot-setting ψ_r is obtained. If the transfer from rudder to rate of turn is approximated by the De Keizer model, given by:

$$\tau^* \frac{L}{u} \dot{r} + r = K^* \frac{u}{L} \delta \qquad (5.78)$$

a possible choice for K_p and K_d becomes:

$$K_p = \omega_n^2 \frac{\tau^*}{K^*} \frac{L^2}{u^2} \qquad (5.79)$$

$$K_d = \frac{L}{u} \frac{2 \zeta \sqrt{(K_p K^* \tau^*)} - 1}{K^*} \qquad (5.80)$$

which relate the autopilot gains to the natural frequency ω_n and damping ratio ζ of the closed-loop system (Van Amerongen, 1982).
According to this pole-placement scheme, besides the ship's forward speed u (provided by the position filter), the ship's normalized parameters K^* and τ^* have to be available. Moreover, for practical applications of the autopilot it is desirable to minimize the controllers response to the wave influence, which causes high-

frequency rudder motions (Van Amerongen, 1982).
From these demands it follows that the course-changing controller can be combined in a natural way with the yaw filter, which provides an estimation of the ship's rate-turn, heading and parameters.
The on-line estimation of the parameters K^* and τ^*, according to (5.27)-(5.28), provides the course-changing controller with an indirect-adaptive nature.

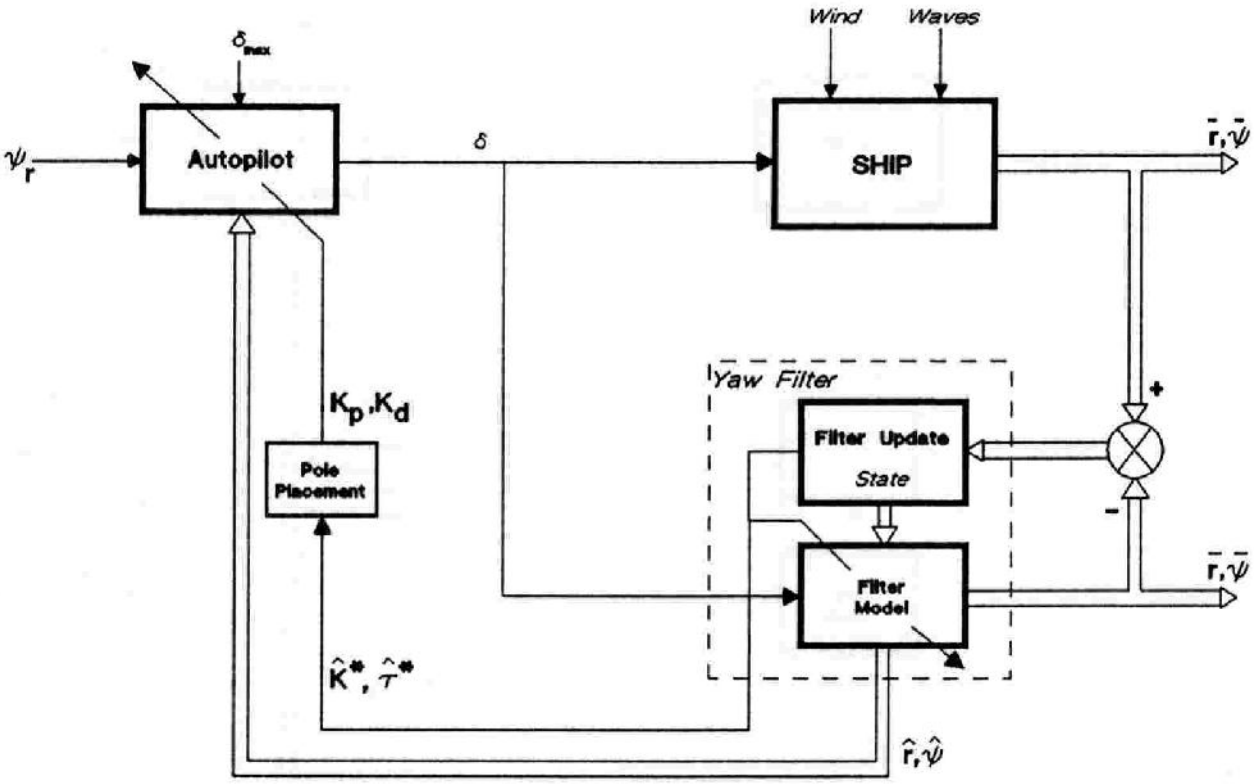

Fig. 5.11 Course-changing controller in combination with the yaw filter

5.5.3 The model-reference approach

In Figure 5.11 the yaw filter is used entirely for identification purposes, on the basis of which the parameters of the course-changing controller are adjusted. This adjustment is based upon the first-order De Keizer model of the rudder to rate-of-turn transfer. Because the parameters of this model depend on the ship's actual forward speed, part of the non-linear nature of the ship's yaw transfer is accounted for. However, additional non-linearities in the reversed spiral characteristic as well as small time constants of the ship have been disregarded. This will cause variations in the estimated parameters, which in principle could be used

for direct compensation according to the model-reference techniques discussed in Section 4.6. For this purpose the estimated parameters have to be separated into an average part, yielding the parameters of the reference model, and deviations from this average value, used for direct compensation. By adjusting the parameters of the course-changing controller on the basis of the reference-model parameters, a configuration is obtained for compensating both long-term parameter deviations and, if the adaptation is fast enough, short-term parameter deviations (causing direct compensation).

In this way a combination with the track predictor also becomes more promising, because this approach yields a more or less constant set of parameters for the prediction model.
To modify the yaw-filter structure for model-reference control, the discrete equations for the process (ship) and the model (Section 5.3) are reconsidered:

process:

$$r(k) = a_s(k-1)r(k-1) + b_s(k-1)\delta(k-1) + N_w(k-1) \qquad (5.81)$$

a priori:

$$\bar{r}(k) = \hat{a}_s(k-1)\hat{r}(k-1) + \hat{b}_s(k-1)\delta(k-1) + \hat{N}_w(k-1) \qquad (5.82)$$

To make the separation into long- and short-term parameter deviations, the discrete parameters of the model are written as:

$$\hat{a}_s(k-1) = a_R + (\hat{a}_s(k-1) - a_R) = a_R + \Delta\hat{a}_s(k-1) \qquad (5.83)$$

$$\hat{b}_s(k-1) = b_R + (\hat{b}_s(k-1) - b_R) = b_R + \Delta\hat{b}_s(k-1) \qquad (5.84)$$

$$\hat{N}_w(k-1) = 0 + (\hat{N}_w(k-1) - 0) \qquad (5.85)$$

with a_R and b_R "constant".
An equivalent form of the a-priori estimation may then be obtained by substituting (5.83)-(5.85) in (5.82):

$$\bar{r}(k) = a_R\hat{r}(k-1) + b_R\delta'(k-1) \qquad (5.86)$$

with the modified rudder signal:

$$\delta'(k-1) = \delta(k-1) + \Delta\hat{a}_s(k-1)/b_R\hat{r}(k-1) + \Delta\hat{b}_s(k-1)/b_R\delta(k-1) + \hat{N}_w(k-1)/b_R \qquad (5.87)$$

Eqs. (5.86) and (5.87) can be regarded as a model-reference type formulation of the Kalman-filter model for identification, where deviations of the estimated parameters from the reference-model parameters a_R and b_R (continuous-time: K_R^* and τ_R^*) are added to the input signal of the reference model (Figure 5.12).

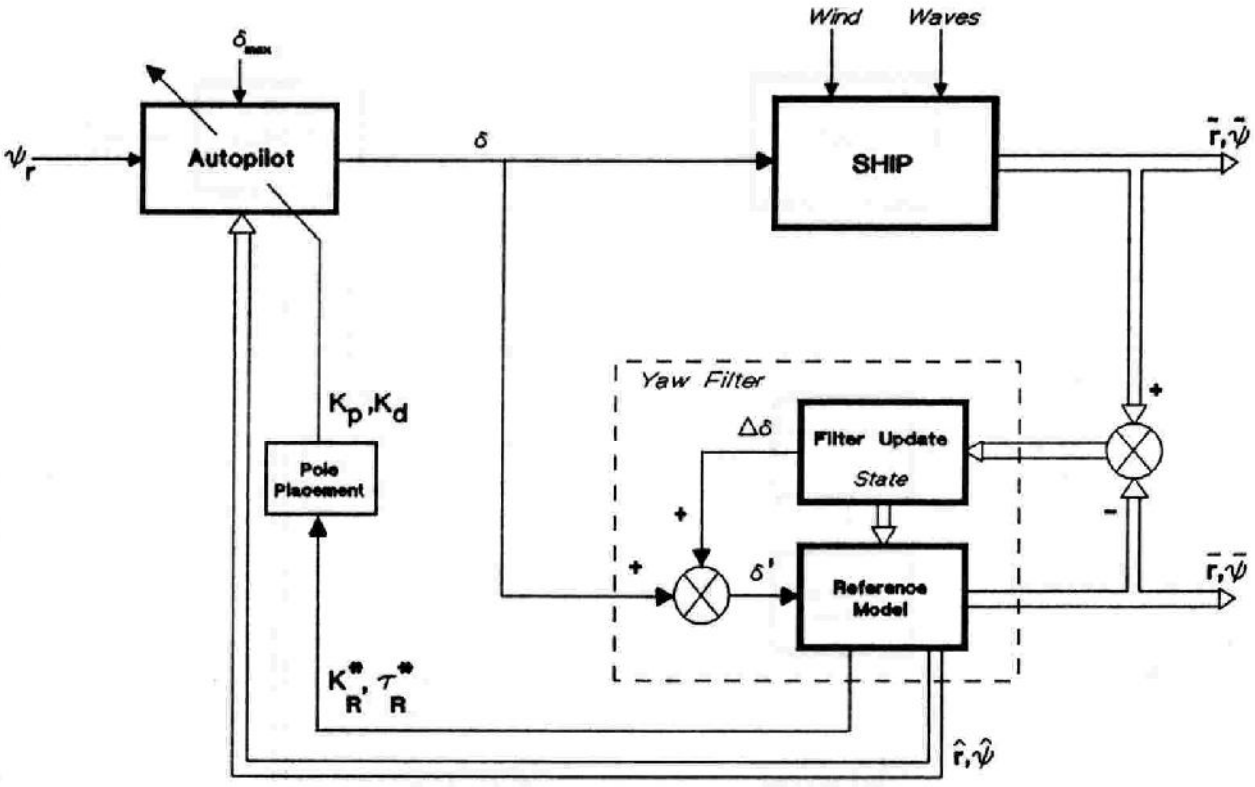

Fig. 5.12 Model-reference type identification

For the model-reference control structure, the ship's input signal $\delta(k)$ in (5.87) is modified to $\delta''(k)$, in such a way that the reference-model input $\delta'(k)$ in (5.86) transforms to (see also Figures 5.13 and 5.14):

$$\delta'(k-1) = \delta(k-1) \qquad (5.88)$$

So, by (5.87) and (5.88):

$$\delta(k-1) = \delta''(k-1) \qquad (5.89)$$
$$+ \Delta\hat{a}_s(k-1)/b_R\hat{r}(k-1) + \Delta\hat{b}_s(k-1)/b_R\delta''(k-1)$$
$$+ \hat{N}_w(k-1)/b_R$$

and thus:

$$\delta''(k-1) = \delta(k-1) \qquad (5.90)$$
$$- \hat{\Delta a}_s(k-1)/\hat{b}_s(k-1)\hat{r}(k-1) - \Delta\hat{b}_s(k-1)/\hat{b}_s(k-1)\delta(k-1)$$
$$- \hat{N}_w(k-1)/\hat{b}_s(k-1)$$
$$= \delta(k-1) - \Delta\delta(k-1)$$

This yields the modified filter structure of Figure 5.13, which by (5.88) is equivalent to the model-reference control structure of Figure 5.14.
In this way deviations between the ship's parameters a_s and b_s and reference model parameters a_R and b_R are compensated by an additional input signal $\Delta\delta$ for the ship.
Because the modification for model-reference control has been achieved by an addition to the common input signal $\delta(k)$ for both process (ship) and model (Figure 5.13), the equations for the Extended Kalman filter for state and parameter estimation remain unaffected.

Finally, the limitations on the rudder angle and speed, imposed by the steering machine (Section 2.3.4), may be incorporated into this structure by using the actual (measured) rudder angle as the input for the model, instead of the ordered rudder angle. For the model-reference type presentation of Figure 5.14 this is equivalent to subtracting the difference between ordered and actual rudder angle from the input of the model, by which again the condition for identical input for process and model is satisfied (Figure 5.15).
Resuming, the parameters of the course-changing controller may be adjusted on the basis of the parameters a_R and b_R of the "reference model". Short-term parameter deviations are compensated by an additional rudder angle, according to (5.90).
The determination of the reference-model parameters, especially in combination with the predictor, will be investigated more explicitly in the next section.

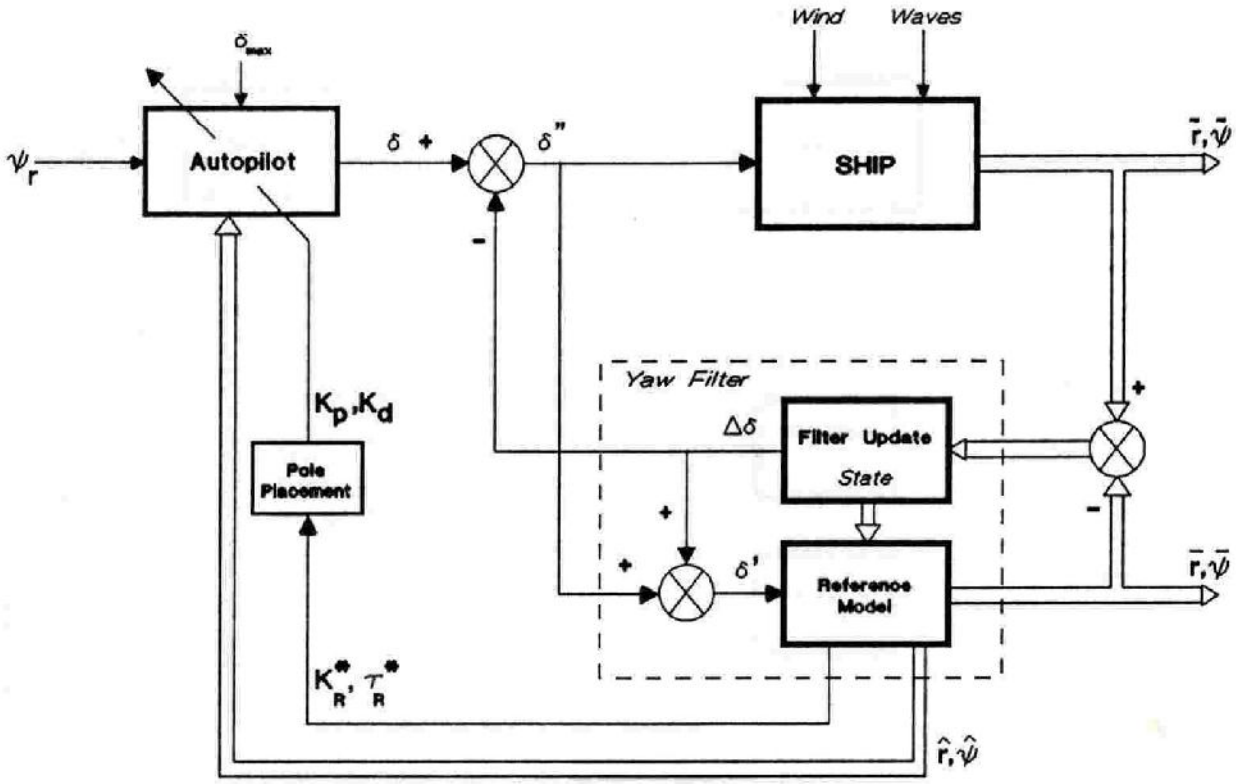

Fig. 5.13 Modified filter structure

5.6 The track predictor

In Chapter 3 a predictor structure was determined on the basis of a generalized track description, derived from the kinematic relations. The determination of the parameters of the resulting prediction model for the calculation of the predicted track and the problem of track adaptation (to provide the predictor with the desired closed-loop nature) will be discussed in this section.

5.6.1 Identification of the prediction model

The parameters of the prediction model are the gain K^* and the time constant τ^*, for the prediction of the normalized rate of turn r^*, and a constant γ^*, for the prediction of the normalized sway velocity v^* (Section 3.3.4). Further, an estimation of the ship's forward speed u is required for the correct gain scheduling of the

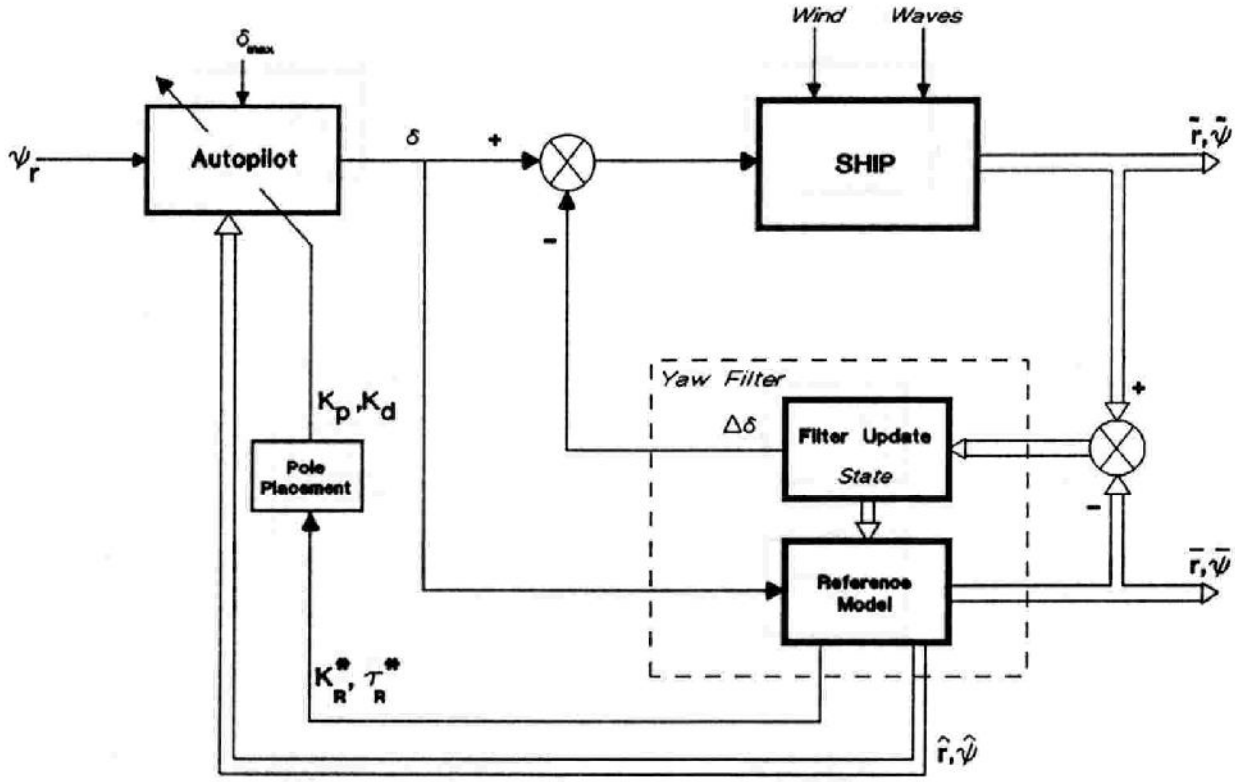

Fig. 5.14 Model-reference control

autopilot parameters.

The actual calculation of the predicted track is performed on the basis of the initial state of the ship, which is assumed to be known. Under this assumption the initial values of the different variables could be chosen zero for the comparison between real and predicted track.

These relevant variables for the predictor consist of the ship's heading ψ and position x_s, y_s.

For an on-line estimation of the yaw-model parameters K^* and τ^* and the states r and ψ, the yaw filter was designed (Section 5.3). An estimation of the ship's forward speed u, the sway constant γ^* and the position x_s, y_s is provided by the position filter, described in Section 5.4.

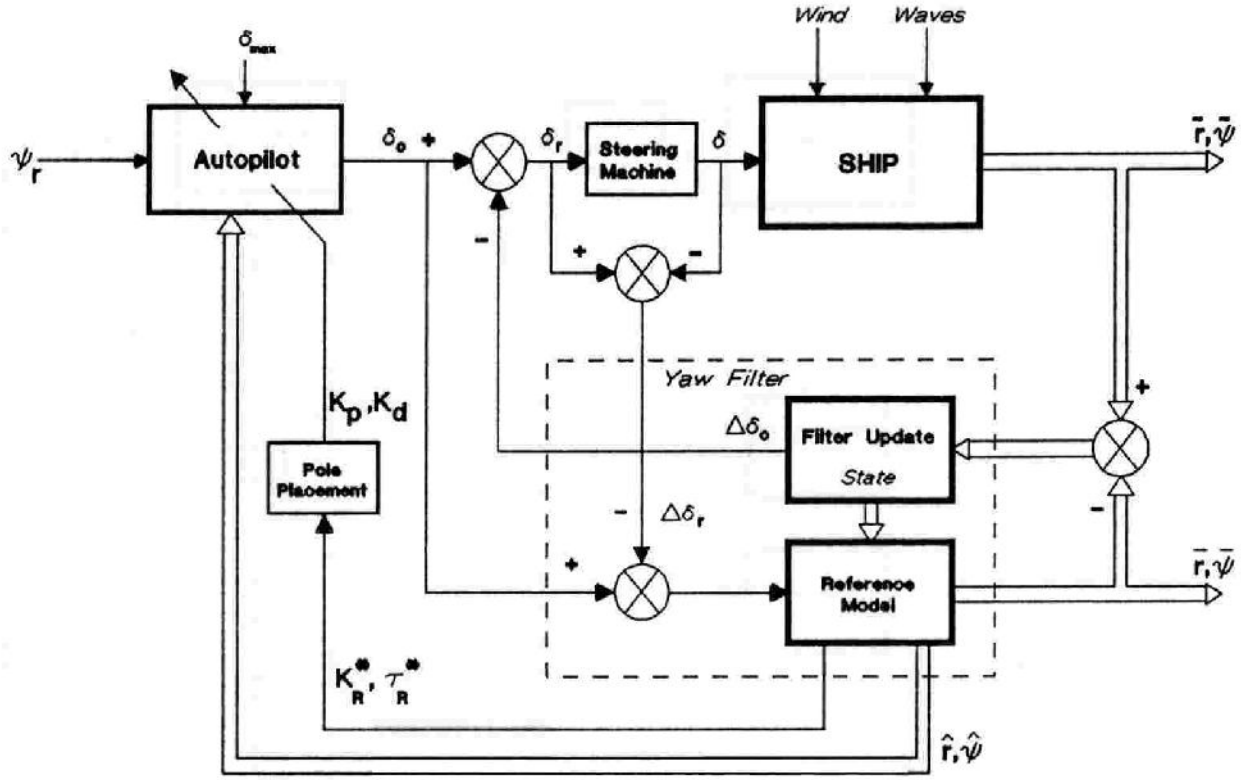

Fig. 5.15 Incorporation of the steering machine

The combination of these filters with the predictor and course-changing controller leads to the block-diagram of Figure 5.16.
In this figure the predicted track is calculated for a trial course setting ψ_t and rudder limit δ_{tmax}, whereas the actual autopilot settings are given by ψ_r and δ_{max}. The output of the track-prediction system for the trial settings consists of a set of predicted positions $\{\underline{x}_p\}$, starting from the actual position.

5.6.2 Adaptation of the predictor

The adaptation of the track predictor to changing conditions and disturbances (wind, current) may be divided into two parts:

- Adaptation of the prediction model parameters, to account for changing ship dynamics. This kind of adaptation may be considered as a "long term" adaptation to the changing (load) conditions. The aim of this adaptation is to improve the initial prediction of the ship's track, before the execution of a

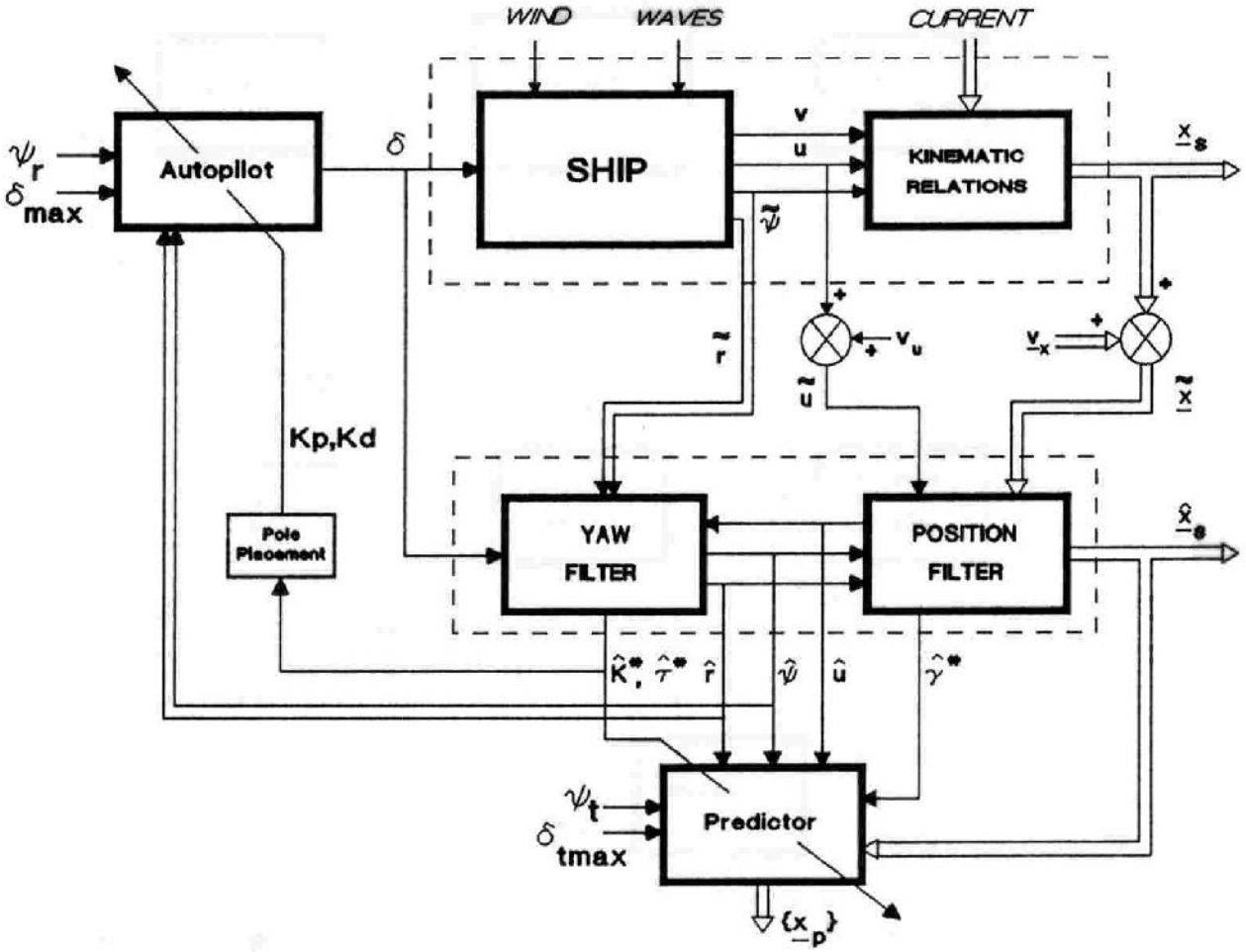

Fig. 5.16 Filters in combination with the predictor

manoeuvre, thus improving the navigator's cognitive anticipation (the open-loop element, discussed in Chapter 1).

- Adaptation of the predicted track during the execution of a manoeuvre, due to changing disturbances. Because this type of adaptation is performed on the basis of the observed difference between what is expected (predicted) and what is observed (measured), the navigator is assisted in his perceptive anticipation (closed-loop element).

5.6.2.1 Adaptation of the prediction model

Because the parameter-estimation part of the yaw filter is of an adaptive nature through the introduction of system noise, the structure of Figure 5.16 is also adaptive with respect to the predictor.
As an extension of this approach the structure of Figure 5.16 may be combined with the model-reference controller, described in Section 5.5.3. In this case the filter model, which provides the parameters for the prediction model, has become a reference model for the ship for the compensation of short-term parameter deviations. As pointed out in Section 5.5.3, a reasonable choice for the parameters of the reference model may be obtained by splitting the estimated parameters into an average part a_R and b_R , which ensures a "long-term" adaptation of the reference and prediction model, and a deviation from the average value $\Delta\hat{a}_s$ and $\Delta\hat{b}_s$, caused by, for instance, additional non-linearities. These parameter deviations from the average value may then be translated by Eq. (5.90) into an additional rudder angle $\Delta\delta$ for direct compensation (Figure 5.17).
The actual splitting of the estimated parameters into an average value and deviations from this value may be performed by filtering the estimated parameters, for instance for a_s:

$$a_R(k) = a_R(k-1) + K_R(\hat{a}_s(k) - a_R(k-1)) \qquad (5.91)$$

With the filter gain K_R the adaptation speed of the reference-model and thus the prediction-model parameters can be adjusted, with extreme values:

- $K_R = 0$, which implies no update of the reference-model and prediction-model parameters (yaw filter used entirely for compensation),
  The short-term parameter deviations, used for direct compensation by (5.90), then become:

$$\Delta\hat{a}_s(k) = \hat{a}_s(k) - a_R(k) = \hat{a}_s(k) - a_R(0) \qquad (5.92)$$

  with $a_R(0)$ the initial value of a_R.

- $K_R = 1$, which implies complete update of the reference-model and prediction-model parameters (yaw filter used entirely for identification). In this case the compensation part becomes:

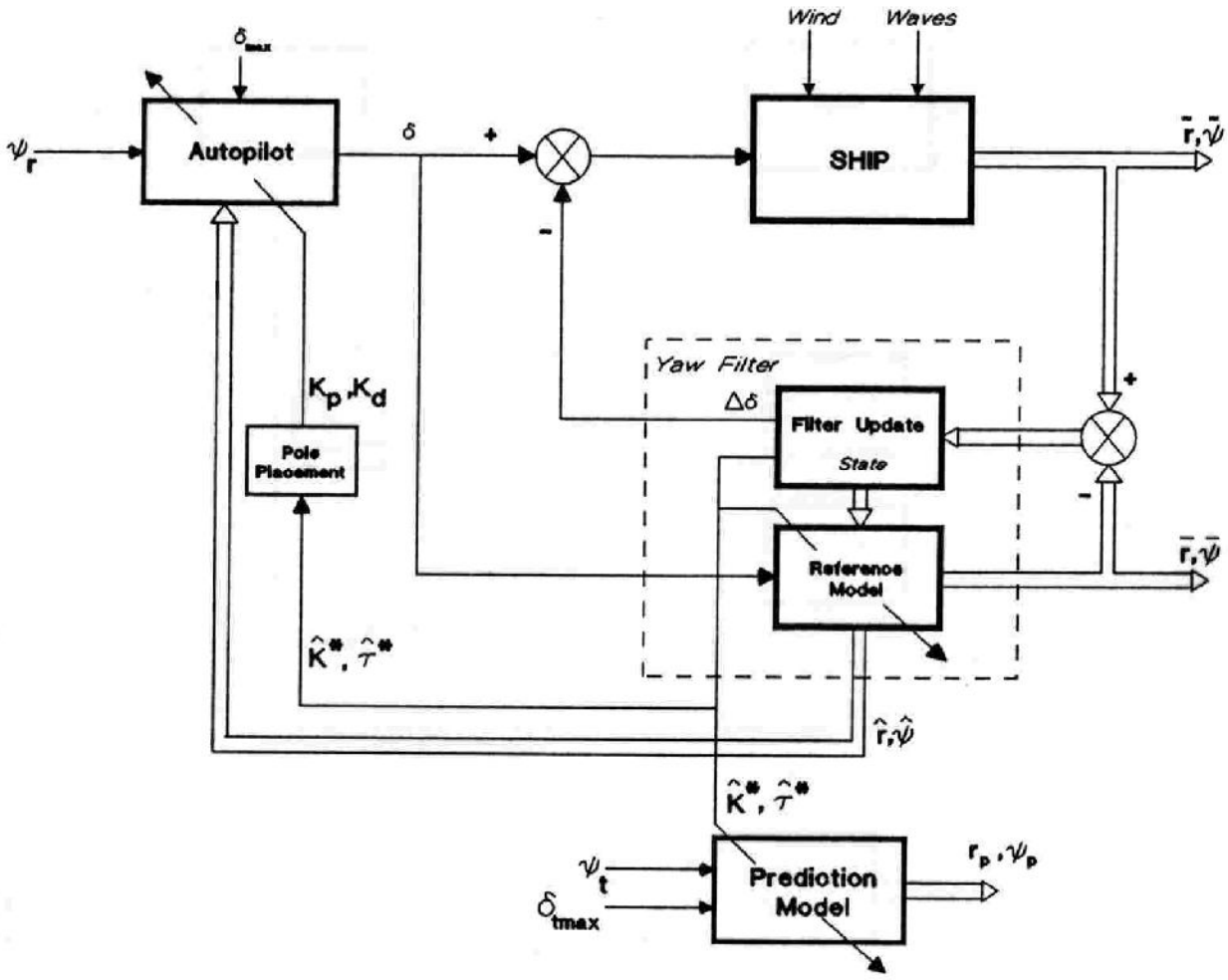

Fig. 5.17 Combination of predictor with model-reference control

$$\Delta\hat{a}_s(k) = \hat{a}_s(k) - a_R(k) = 0 \qquad (5.93)$$

and thus, by (5.90), $\Delta\delta = 0$

5.6.2.2 Track adaptation

The adaptation mechanism described in the previous section was intended to adjust the parameters of the prediction model to changing ship dynamics. Further, the estimated offset and short-term parameter deviations, due to wind influence, unmodelled dynamics and non-linearities may be compensated by the course-

changing controller of the model-reference type.
Although in this way the quality of the relatively simple prediction model is improved, deviations between real and predicted track will still occur during the execution of a manoeuvre. To account for these remaining deviations, a track-adaptation mechanism has to be designed which by definition should be independent of the prediction model and its parameters (otherwise this adaptation mechanism should be classified under the adaptation methods for model improvement).
For this model-independent adaptation of the predicted track, the general kinematic relations described in Section 3.2.2 are reconsidered for the real (with current influence) and predicted normalized x-coordinate of the track:

$$x_s^*(s^*) = \int_0^{s^*} \cos\psi \, d\sigma^* - \int_0^{s^*} \sin\psi \, v^* d\sigma^* + \int_0^{s_c^*} \cos\psi_c d\sigma_c^* \qquad (5.94)$$

$$x_p^*(s^*) = \int_0^{s^*} \cos\psi_p d\sigma^* - \int_0^{s^*} \sin\psi_p \, v_p^* d\sigma^* \qquad (5.95)$$

with ψ_c the current direction.
From these general relations it may be concluded that the principle causes of deviations between real and predicted track are:

- heading (rate-of-turn) deviations, caused by, for instance, wind influence,
- position deviations, caused by current influence.

These principle causes of deviations will be considered in more detail.

- *Rate-of-turn deviations*

For the direct adaptation of the predicted track, due to rate-of-turn deviations, a multiplicative relation between the real and predicted rate of turn is assumed. Under this assumption a simple, but efficient geometrical update mechanism for the predicted track will be shown to be feasible.
Thus it is assumed that the real and the predicted normalized rate of turn r^* as a function of the normalized travelled distance s^* are related to each other by:

$$r^*(s^*) = K_\rho r_p^*(s^*) \qquad (5.96)$$

with K_ρ a constant.
Noting that $r^*(s^*) = d\psi/ds^*$, this has the following effect on the kinematic relations (forward-speed part, x-coordinate):

$$x^*_{su}(s^*) = \int_0^{s^*} \cos\{ \int_0^{\sigma^*} K_\rho r^*_p(\sigma^*_2) d\sigma^*_2 \}\, d\sigma^* \qquad (5.97)$$

$$x^*_{pu}(s^*) = \int_0^{s^*} \cos\{ \int_0^{\sigma^*} r^*_p(\sigma^*_2) d\sigma^*_2 \}\, d\sigma^* \qquad (5.98)$$

which is difficult to interpret in terms of track adaptation.
To gain more insight into the effect of (5.97)-(5.98) on the difference between real and predicted track, these equations are transformed to the course domain by substituting:

$$ds^* = \frac{ds^*}{d\psi} d\psi = \frac{1}{r^*} d\psi \qquad (5.99)$$

and r^* has to be considered as a function of the new independent variable ψ.
This yields for the kinematic relations:

$$x^*_{su}(\psi) = \int_0^{\psi} \cos\varphi \frac{1}{K_\rho r^*_p(\varphi)} d\varphi = \frac{1}{K_\rho} \int_0^{\psi} \cos\varphi \frac{1}{r^*_p(\varphi)} d\varphi \qquad (5.100)$$

$$x^*_{pu}(\psi) = \int_0^{\psi} \cos\varphi \frac{1}{r^*_p(\varphi)} d\varphi \qquad (5.101)$$

The relation between x_{su} and x_{pu} becomes:

$$x^*_{su} = \frac{1}{K_\rho} x^*_{pu} \qquad (5.102)$$

and in an analogous way for the y-position:

$$y^*_{su} = \frac{1}{K_\rho} y^*_{pu} \qquad (5.103)$$

This implies that a direct adaptation mechanism for rate-of-turn deviations is provided by scaling the forward-speed part of the predicted track with a factor $1/K_\rho$.

The sway contribution to the real and the predicted track is given by:

$$x^*_{sv}(\psi) = -\int_0^\psi \sin\varphi \; \frac{v^*}{r^*} \, d\varphi \qquad (5.104)$$

$$x^*_{pv}(\psi) = -\int_0^\psi \sin\varphi \; \frac{v^*_p}{r^*_p} \, d\varphi \qquad (5.105)$$

Substitution of the drift equations:

$$v^* = \gamma^* r^* \qquad (5.106)$$

$$v^*_p = \gamma^*_p r^*_p \qquad (5.107)$$

in (5.104)-(5.105) yields:

$$x^*_{sv}(\psi) = \int_0^\psi \sin\varphi \; \gamma^* \, d\varphi \qquad (5.108)$$

$$x^*_{pv}(\psi) = \int_0^\psi \sin\varphi \; \gamma^*_p \, d\varphi \qquad (5.109)$$

According to this result, the sway contribution to the predicted track does not need to be updated for rate-of-turn deviations, because this contribution only depends on the estimated sway constant γ^*, an estimation of which is provided by the position filter.

For an on-line estimation of the scaling factor K_ρ , it is assumed that the predicted normalized rate of turn r^*_p is available as a function of the predicted heading ψ_p (which could be realized as a look-up table). The estimation of K_ρ may then be written as the determination of a constant, observed through the predicted normalized rate of turn:

$$K_\rho(k) = K_\rho(k-1) + w_k(k-1) \qquad (5.110)$$

$$\hat{r}^*(k) = r_p^*(\hat{\psi}(k)).K_\rho(k) + v_k(k) \qquad (5.111)$$

with system noise w_k to achieve adaptation and observation noise v_k to state the uncertainty in the ship's estimated normalized rate of turn:

$$\hat{r}^*(k) = \frac{\hat{r}(k)}{\hat{u}(k)}.L \qquad (5.112)$$

The estimations $\hat{r}(k)$ and $\hat{\psi}(k)$ are provided by the yaw filter and the estimated forward speed by the position filter.
The filter structure for the on-line determination of K_ρ is presented in Figure 5.18. In this figure K_k is the update gain for the track-scaling factor.

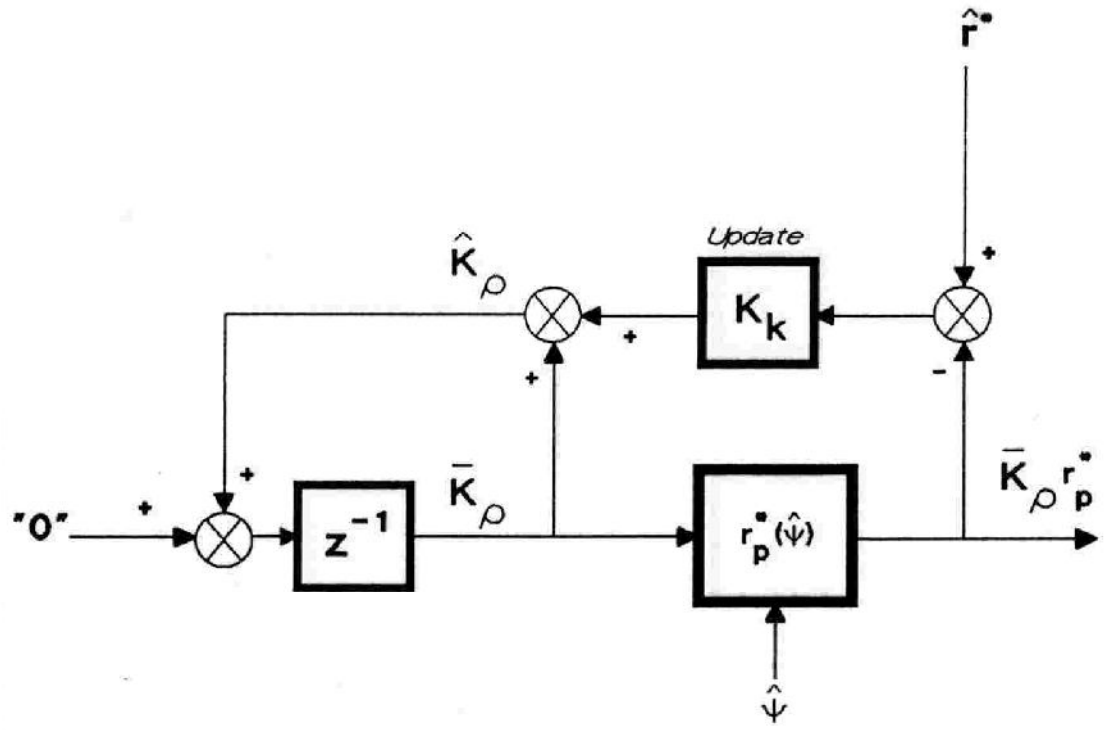

Fig. 5.18 Estimation of track-scaling factor K_ρ

- *Position deviations:*

As described in Section 3.4.2, the effect of uniform current may be separately added to the predicted track in the time domain by:

$$x_p(t) = x_{pu}(t) + x_{pv}(t) + \int_0^t \hat{u}_{cx} d\tau \qquad (5.113)$$

$$y_p(t) = y_{pu}(t) + y_{pv}(t) + \int_0^t \hat{u}_{cy} d\tau \qquad (5.114)$$

with a forward-speed contribution x_{pu},y_{pu} , a sway-speed contribution x_{pv},y_{pv} and $\hat{u}_{cx}$, $\hat{u}_{cy}$ the on-line estimated current speed in x, y direction, provided by the position filter.
The corresponding discrete equations are (again using an Euler approximation):

$$x_p(k) = x_{pu}(k) + x_{pv}(k) + k.T_s\hat{u}_{cx} \qquad (5.115)$$

$$y_p(k) = y_{pu}(k) + y_{pv}(k) + k.T_s\hat{u}_{cy} \qquad (5.116)$$

which constitute an additive update mechanism for the predicted track.
The overall structure for track adaptation is shown in Figure 5.19.

5.7 Review

In this chapter the techniques for optimal measurement filtering, presented in Chapter 4, have been applied to the track-prediction problem. This has resulted in the following filters:

- A Kalman filter for the filtering of the wave motions and an on-line identification of the yaw-model parameters (Section 5.3). For this filter the following signals have to be available:
  - the actual rudder angle δ,
  - the ship's rate of turn r,
  - the ship's heading ψ.

- A Kalman filter for the filtering of the ship's forward speed and position and estimation of the current influence (Section 5.4).

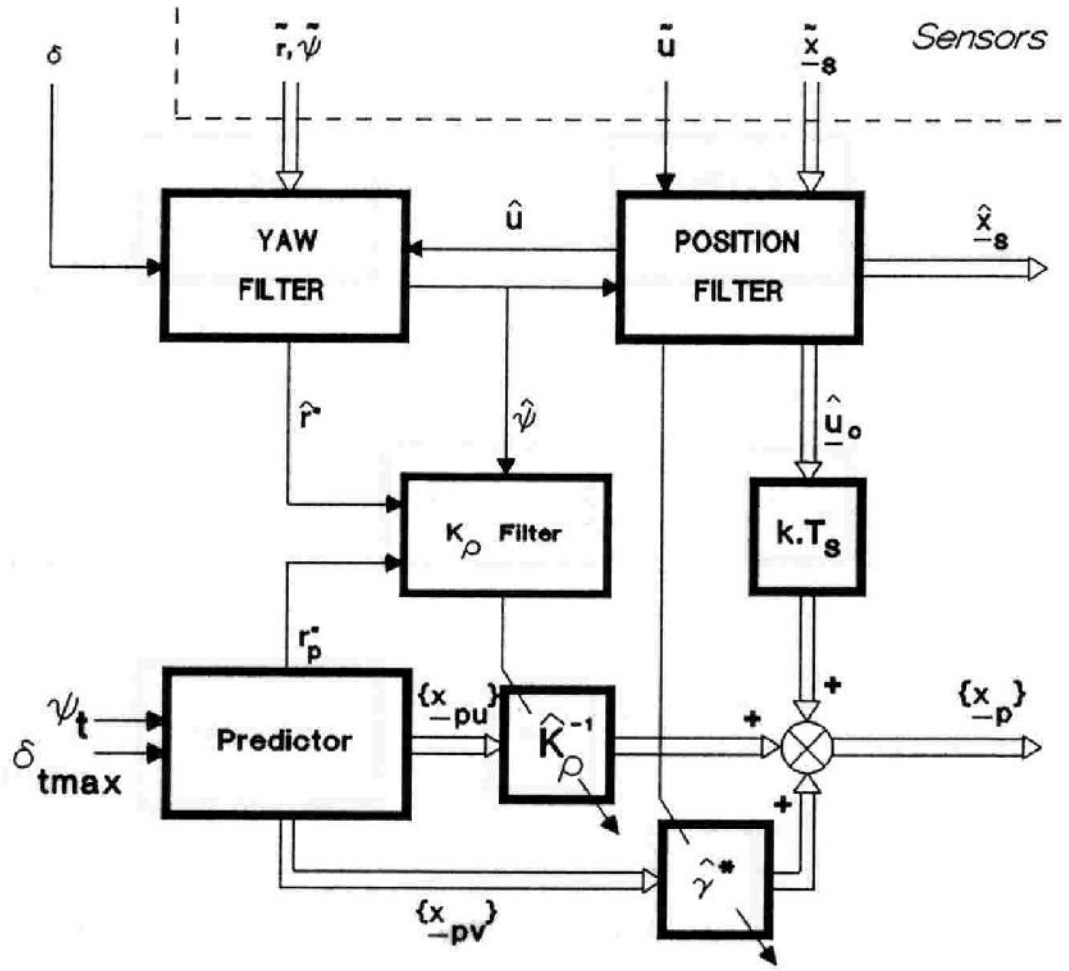

Fig. 5.19 Track adaptation: overall structure

The filter requires the following measurement information:
- the ship's forward speed u,
- the ship's position x_s, y_s.

Further, in Section 5.5 an extension of the course-changing controller has been proposed on the basis of the model-reference approach for direct adaptive control in combination with an Extended Kalman filter (based on the concept discussed in Section 4.6).
This allows a direct compensation of short-term parameter deviations.

By combining the on-line identification, performed by the yaw filter, with the predictor (Section 5.6.1), the prediction model is provided with an adaptive nature

(Section 5.6.2.1) to deal with, for instance, changing ship dynamics. In this way the quality of the prediction model and the resulting initial predicted track is improved.

Finally, in Section 5.6.2.2 a track-adaptation mechanism has been derived by reconsidering the general kinematic relations, presented in Section 3.2.2. On the basis of this approach the analysis of the track-adaptation problem could be split into a separate analysis for rate-of-turn deviations and position deviations. This has resulted in a scheme for direct adaptation of the predicted track during the execution of a manoeuvre to the changing conditions, without an explicit need for the complete recalculation of the prediction on the basis of the dynamic prediction model.

6 REALIZATION AND RESULTS

6.1 Introduction

In this chapter the realization of and the results obtained with an experimental track-prediction system are described. In this experimental set-up the different algorithms for identification, control and prediction, described in the preceding chapter, are implemented.
The experiments performed consist of:

- laboratory experiments to evaluate the performance of the algorithms,
- a manoeuvring-simulator experiment at the TNO Institute for Perception in Soesterberg. This experiment was carried out to evaluate the performance of the track predictor as a manoeuvring aid for the navigator.

The results of the various experiments will be presented after a global description of the chosen hardware and software configurations for the implementation of the experimental track PREdiction SYStem (PRESYS).

6.2 Implementation of PRESYS

6.2.1 Hardware

To determine the contribution of the track predictor to the navigational performance, a user interface had to be developed. On the functional level this user interface may be subdivided into an input part (console), for the input of user commands, and an output part (display), for the presentation of the predicted track. This yields the functional diagram of Figure 6.1, for the overall track-prediction system.

In this diagram the "Ship I/O" part stands for all the interaction to be performed between the ship's sensors and the navigation bridge.
In correspondence with this functional diagram a hardware configuration was chosen according to Figure 6.2. The configuration consists of a PDP 11/73 minicomputer for the implementation of the different modules for control and prediction, and an IBM PC/AT for the intelligent user interface.

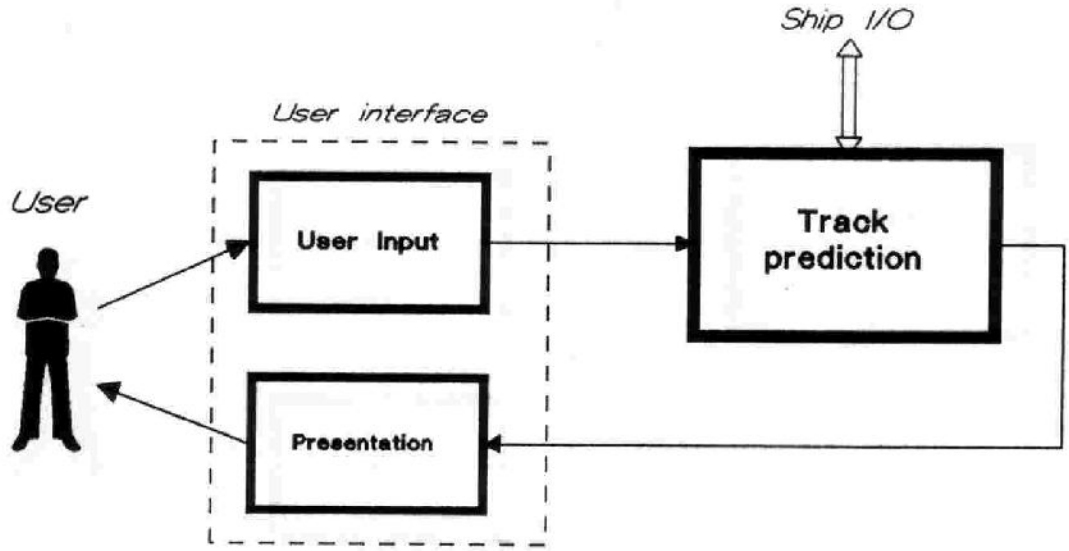

Fig. 6.1 The track-prediction system

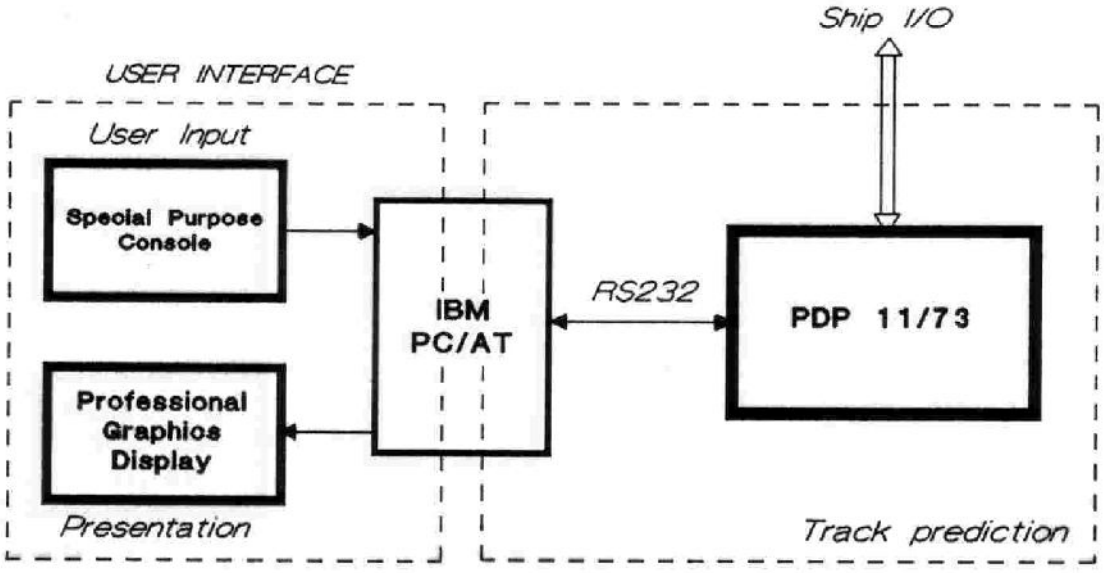

Fig. 6.2 Hardware configuration of PRESYS

The PDP 11/73 is provided with a hard disk and two floppy disk drives for data storage. For the interfacing to the ship's sensors the system is connected to the special-purpose ADIBUS interface. This interface consists of several A/D and D/A

converters and I/O ports for digital communication.
The IBM PC/AT is provided with a Professional Graphics Controller (resolution 480 x 640) in combination with a Professional Graphics Display for the presentation part and a special purpose user's console for the user input. For the typical man/machine related aspects of the user-interface design, the experience of the TNO Institute for Perception was called upon.

6.2.2. Software

The different tasks to be carried out by PRESYS on a real-time basis are:

- filtering and identification:
  on-line filtering of the measured signals and identification of the prediction-model parameters, according to the discrete filtering and identification algorithms described in the preceding chapter,
- control:
  automatic course changing and course keeping,
- prediction:
  calculation and adaptation of the predicted track,
- data logging:
  monitoring and storage of signals of interest on hard disk.

Further, the intelligent user interface (IBM PC/AT) monitors the input of user commands and is used to display the predicted track.
To realize these different tasks, the PDP 11/73 is provided with the multi-tasking operating system RSX 11M+, which has special facilities for real-time applications. In this way the different functions could be realized as separate FORTRAN tasks which are scheduled periodically. This enables an on-line substitution of, for instance, different prediction schemes to make a comparison between different algorithms. In addition, switching to an external autopilot or from an internal ship model to a real or externally simulated ship is quite easy. For an eventual final version of the track-prediction system, however, it will be more efficient to combine several modules into one task. In this single task the different calculations for filtering and control may be rearranged, not according to function but according to primary (*before* the rudder output) and secondary (*after* the rudder output) calculations. In this way the time delay of the control loop is decreased. Typical values of the different periods range from 0.4 seconds for the yaw filter and controller to 2 seconds for the position filter and the predictor.

The software of the IBM PC/AT is also mainly realized in FORTRAN, apart from some low-level communication routines for the PDP 11/73 and the user's console. Because all the functions connected with console handling and graphic presentation are performed by this intelligent user interface, the data exchange between the two computer systems is reduced to a minimum and can be performed on the basis of a serial RS232 link.
For the presentation part of the track predictor an integrated navigation display, as developed by the TNO Institute for Perception, was taken as the starting point. On this synthetic display, which was designed to enable one-man-bridge steering (Boer and Schuffel, 1985; Van Breda and Van de Kooij, 1985), navigation information is integrated with manoeuvring information.
For the combined presentation the total information on the display is divided into different categories, to which the prediction information is added. For the presentation on a colour display, the colours were chosen according to these different types of information.
More information on the realization of the user interface will be given in Section 6.4, where the manoeuvring-simulator experiment is described.

6.3 Simulation results

6.3.1 Simulation set-up

To test the experimental track-prediction system, various simulations were performed in a laboratory environment. These simulations range from:

- Simulations with the interactive simulation program PSI, to verify the algorithms for identification, prediction and control which were derived in Chapter 5 on the basis of the theory.
- Simulations with externally simulated dynamics of a ship, to test the PRESYS software and hardware (interfaces). The external ship model consisted of an analog part, for the simulation of the yaw dynamics, and a digital part for the calculation of the ship's position. The simulations were performed as a final test before the system was moved to Soesterberg for the experiments on the manoeuvring simulator.

For the simulations the disturbances were realized as:

- *Wind*: additional yaw moment, depending on the relative wind angle.
- *Waves*: high-frequency signal, added to the rate-of-turn signal according to Figures 2.13 and 2.14.
- *Current*: additional displacement, calculated from the current speed and direction, according to (2.71)-(2.72).

6.3.2 Performance of the yaw filter

To demonstrate the performance of the yaw filter as a combined state and parameter estimator, a zig-zag trial was performed with the simulated dynamics of the "R.O.V. Zeefakkel" (see also Section 3.5). In Figure 6.3 the results for the combined estimation scheme are compared to those obtained with a Parallel MRAS identification structure. For this simulation no a-priori knowledge on the parameters was assumed. The performance of the parameter-estimation part may be judged on the basis of the criterion function J_p:

$$J_p = \int_0^T \left(\frac{K^* - \hat{K}^*}{K^*} \right)^2 + \left(\frac{\tau^* - \hat{\tau}^*}{\tau^*} \right)^2 dt \qquad (6.1)$$

In Figure 6.3 the following signals are shown:

- $\tilde{r}$ the ship's rate-of-turn signal with wave influence,
- $\hat{r}$ the filtered rate-of-turn signal,
- K^*, τ^* the normalized parameters,
- $\hat{K}^*, \hat{\tau}^*$ the estimated normalized parameters,
- J_p the parameter criterion function, integrated with a time constant of 10 seconds instead of the pure integration as defined in Eq. (6.1)

To demonstrate the model-reference control application of the Extended Kalman filter, in Figure 6.4 a second simulation was performed with the simulated dynamics of a container vessel with a length of 200 m. and a cruising speed of 19 knots. The steering machine was simulated as described in Section 2.3.4, with a maximum rudder speed of 2.5 degrees/second.
The direct compensation was switched on after 250 seconds. This direct compensation forces the ship to follow the response of the reference model, analog to the principles of discrete MRAC discussed in Chapter 5. The parameters of the reference model are slowly adapted to the ship's dynamics by averaging the

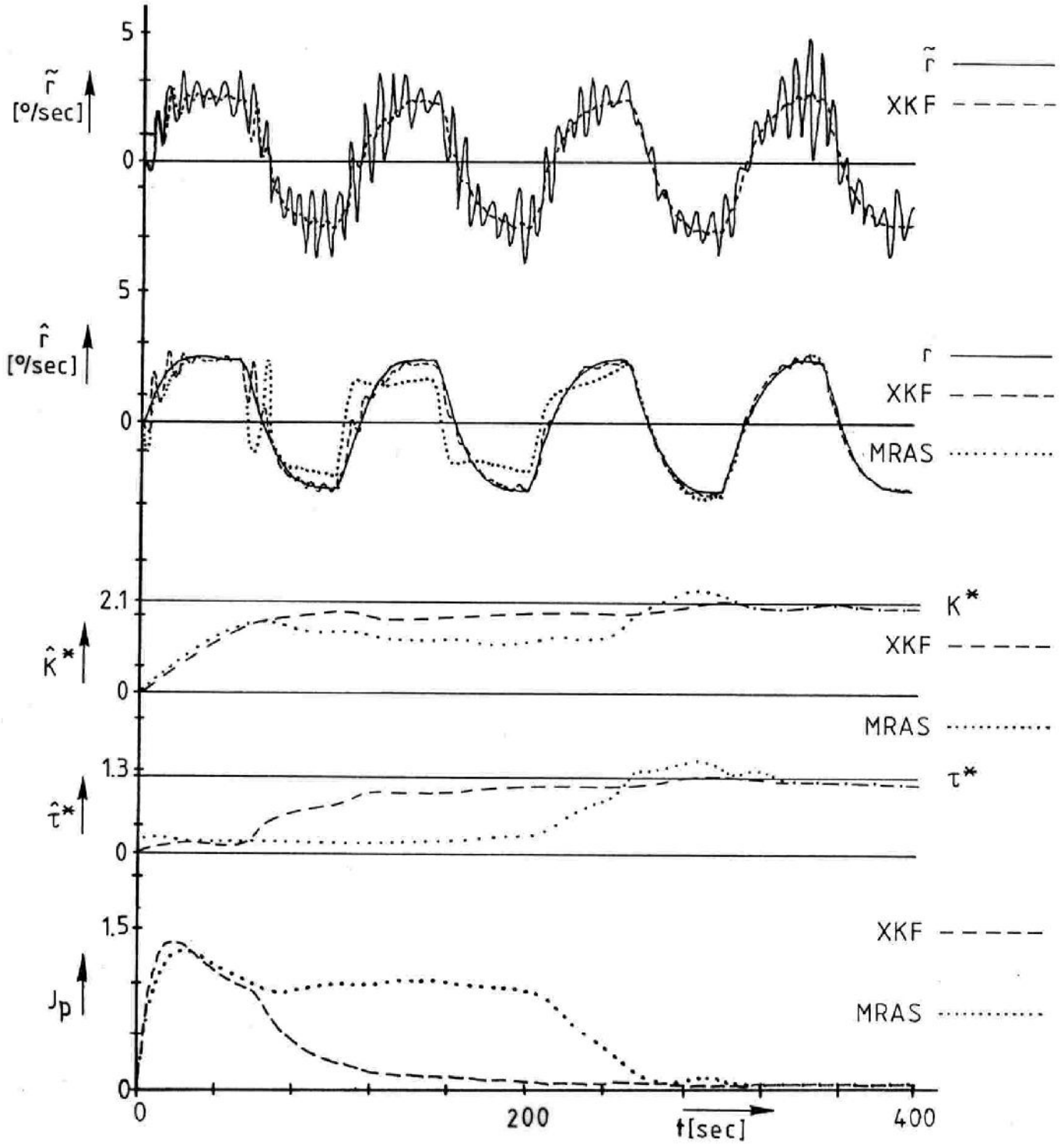

Fig. 6.3 Performance of the yaw filter

estimated parameters of the yaw filter, with initial values $K^*/4$ and $\tau^*/4$ (see also Section 5.6.2.1). In this way the prediction model, which receives its parameters from the reference model, finally becomes optimally adjusted to the ship's dynamics. This can be seen from the fact that towards the end of the simulation

almost no additional rudder angle (the difference between δ and δ_p) is required to compensate for the differences between ship and reference model.
To give an impression of the quality of the yaw prediction, a criterion function J_r is introduced. This criterion function is based on the principles of track correspondence, discussed in Chapter 3:

$$J_r(s^*) = \int_0^{s^*} (r_s^*(\sigma^*) - r_p^*(\sigma^*))^2 \, d\sigma^* \qquad (6.2)$$

with $r_s^*(\sigma^*)$ and $r_p^*(\sigma^*)$ the real and predicted normalized rate of turn as a function of the normalized travelled distance σ^*.
For a constant predicted speed U_p, the criterion function may be evaluated as a function of the time by:

$$J_r = \int_0^T (r_s^*(t) - r_p^*(\sigma^*(t)/U_p))^2 \, dt \qquad (6.3)$$

In Figure 6.4 the following signals are shown:

$\tilde{r}$	the ship's rate-of-turn signal with wave influence,
r_p	the predicted rate-of-turn signal,
δ	the actual rudder angle (compensation included after t = 250 seconds),
δ_p	the predicted rudder angle (without steering machine),
J_r	the criterion, integrated with a time constant of 100 seconds,
K^*, τ^*	the ship's normalized parameters,
K_R^*, τ_R^*	the normalized parameters of the reference model and the prediction model.

The performance of the yaw filter in combination with the course-changing controller, described in Section 5.5, is illustrated in Figure 6.5. In this simulation some course changes were performed in the presence of wind. The initial values of the reference-model parameters were again chosen as $K^*/4$ and $\tau^*/4$. Because the autopilot parameters K_p and K_d are calculated from these parameters by (5.79)-(5.80), the course-changing controller is initially not well adjusted to the ship's dynamics. This is clearly demonstrated by the first course change. Further, the rudder signal is rather noisy because the measured rate-of-turn and heading signals were used for the autopilot. After the first course change both the filtered signals were used and the direct compensation was switched on (at t = 350 seconds). The direct compensation again gives a great improvement of the quality

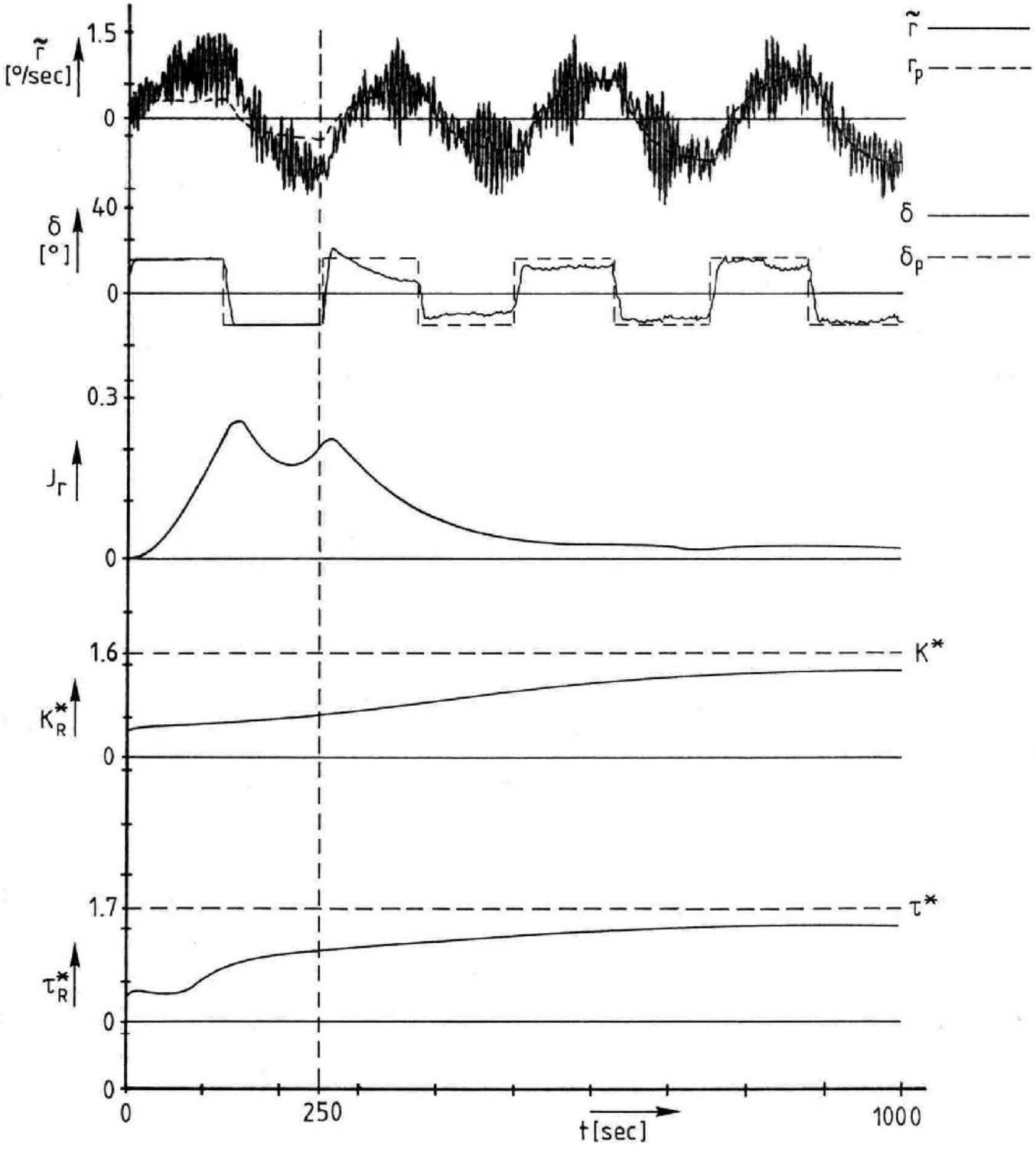

Fig. 6.4 Direct compensation with the yaw filter

of the yaw prediction, which can be seen by comparing the real and the predicted course error. The long-term adaptation of the prediction-model parameters to the ship's dynamics is illustrated by comparing the different course changes and the amount of rudder compensation to each other.

To prevent the drifting of the parameters because of the wave influence, the parameter adaptation is only switched on during the course changes. The offset estimation, which is used for compensation of the wind influence, is permanently switched on.
In addition to the signals shown in Figure 6.4, the real and predicted course errors ε and ε_p are shown.

6.3.3 Performance of the position filter

The filtering of the ship's observed position and the reconstruction of the current influence from the position fixes is illustrated by Figure 6.6.a,b. The zig-zag trial was performed with a hydrodynamic model of a container vessel. The position fixes were provided at an interval of 2 seconds with a standard deviation of 50 m. (which is more than the standard deviation of a satellite navigation system such as the Global Positioning System G.P.S.).
The adaptation of the filter to a changing current influence is demonstrated by "switching off" the current influence at t = 430 seconds. The current speed and direction were chosen 3 knots and 30 degrees.
The estimation of the forward speed was tested by changing the cruising speed from 19 knots to 10 knots at t = 760 seconds.
For the estimation of the drift speed, the sway velocity was modelled proportional to the rate of turn, as described in Chapter 5:

$$\hat{v} \approx \hat{\gamma}^{*} . L . \hat{r} = \hat{\gamma} . \hat{r} \qquad (6.4)$$

with $\hat{\gamma}$ the estimated sway constant and L the length of the ship.

In Figure 6.6.a the following signals are shown:

u_{cx}, u_{cy}	the current speed in x and y direction,
$\hat{u}_{cx}$, $\hat{u}_{cy}$	the estimated current speed in x and y direction,
$\hat{\gamma}$	the estimated sway constant,
u ,v	the ship's forward speed and sway speed,
$\tilde{u}$	the ship's observed forward speed,
$\hat{u}$, $\hat{v}$	the estimated forward speed and sway speed.

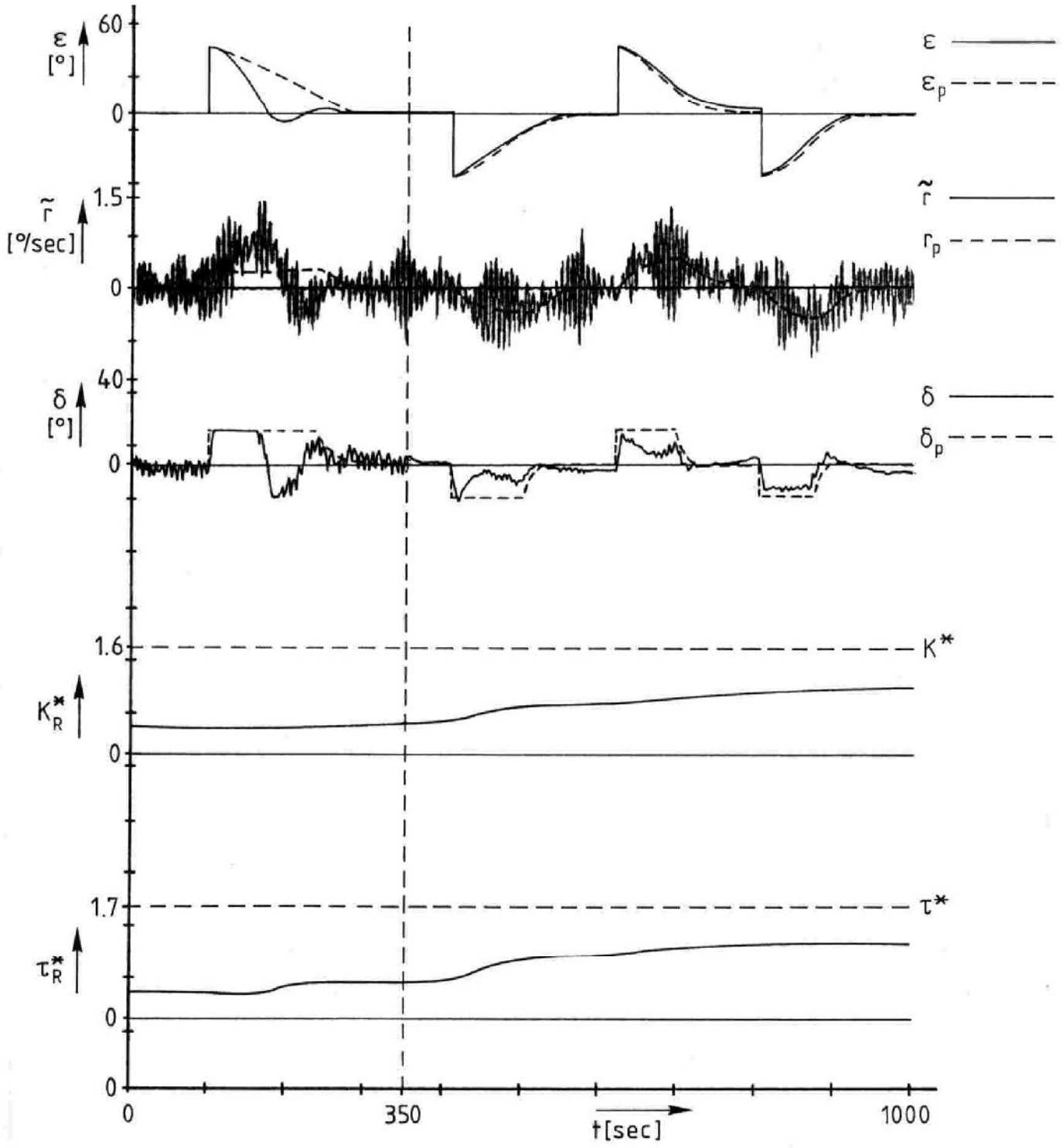

Fig. 6.5 Yaw filter in combination with the course changing controller

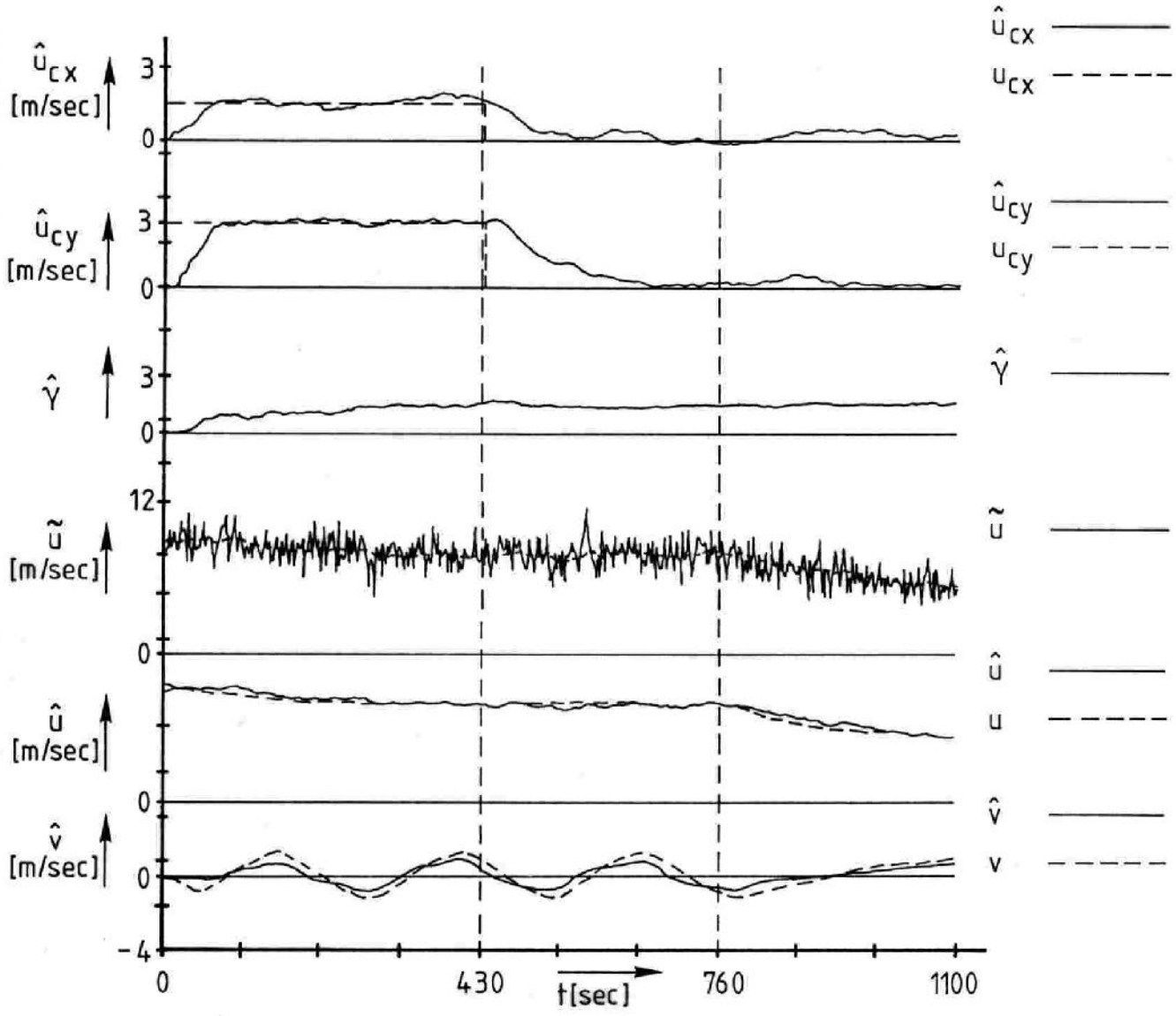

Fig. 6.6.a Estimation of the different speed components

The corresponding actual, observed and filtered tracks are presented in Figure 6.6.b.
In this figure

$\underline{\tilde{x}}_s$	is the observed track,
$\underline{\hat{x}}_s$	is the filtered track,
$\underline{x}_s$	is the ship's actual track.

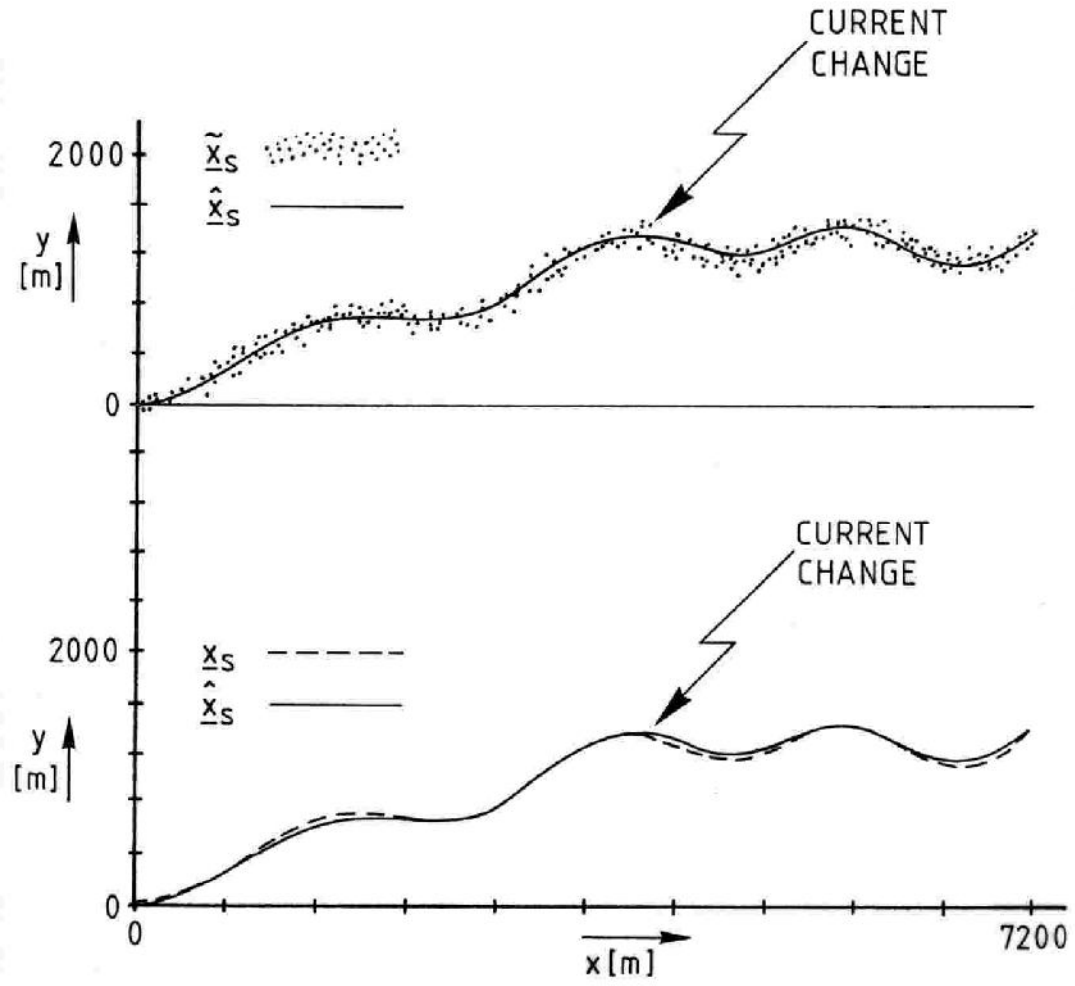

Fig. 6.6.b Observed and filtered track

6.3.4 Track prediction and adaptation

The predicted track is calculated on the basis of the estimated parameters of the yaw transfer, provided by the yaw filter. This initial predicted track is adjusted to rate-of-turn (wind influence) and position deviations (current influence) by the track-adaptation mechanism, described in Section 5.6.2.2. The calculation of the final predicted track therefore consists of three parts:

- Calculation of the initial prediction on the basis of the prediction model of the ship's dynamics (without current influence and disturbances). This yields the track $\underline{x}_0(i)$, $i = 1,...,N_p$, with N_p the number of predicted positions.

- Scaling of the predicted track for rate-of-turn deviations:
  $\underline{x}_\rho(i) = \underline{x}_0(i)/K_\rho$, $i = 1,....N_p$
  with the scaling factor K_ρ provided by the on-line estimation scheme, described in Section 5.6.2.2.
- Addition of current influence on the basis of the estimated current speed in x and y directions, provided by the position filter:
  $\underline{x}_p(i) = \underline{x}_\rho(i) + \underline{\hat{u}}_c.i.T_s$, $i = 1,....,N_p$

To demonstrate the track adaptation mechanism, two course changes of + and - 120 degrees were carried out under the influence of wind and current, with the direct compensation of the course-changing controller switched off.
The on-line estimation of the track-adaptation factors is presented in Figure 6.7.a for the two course changes.

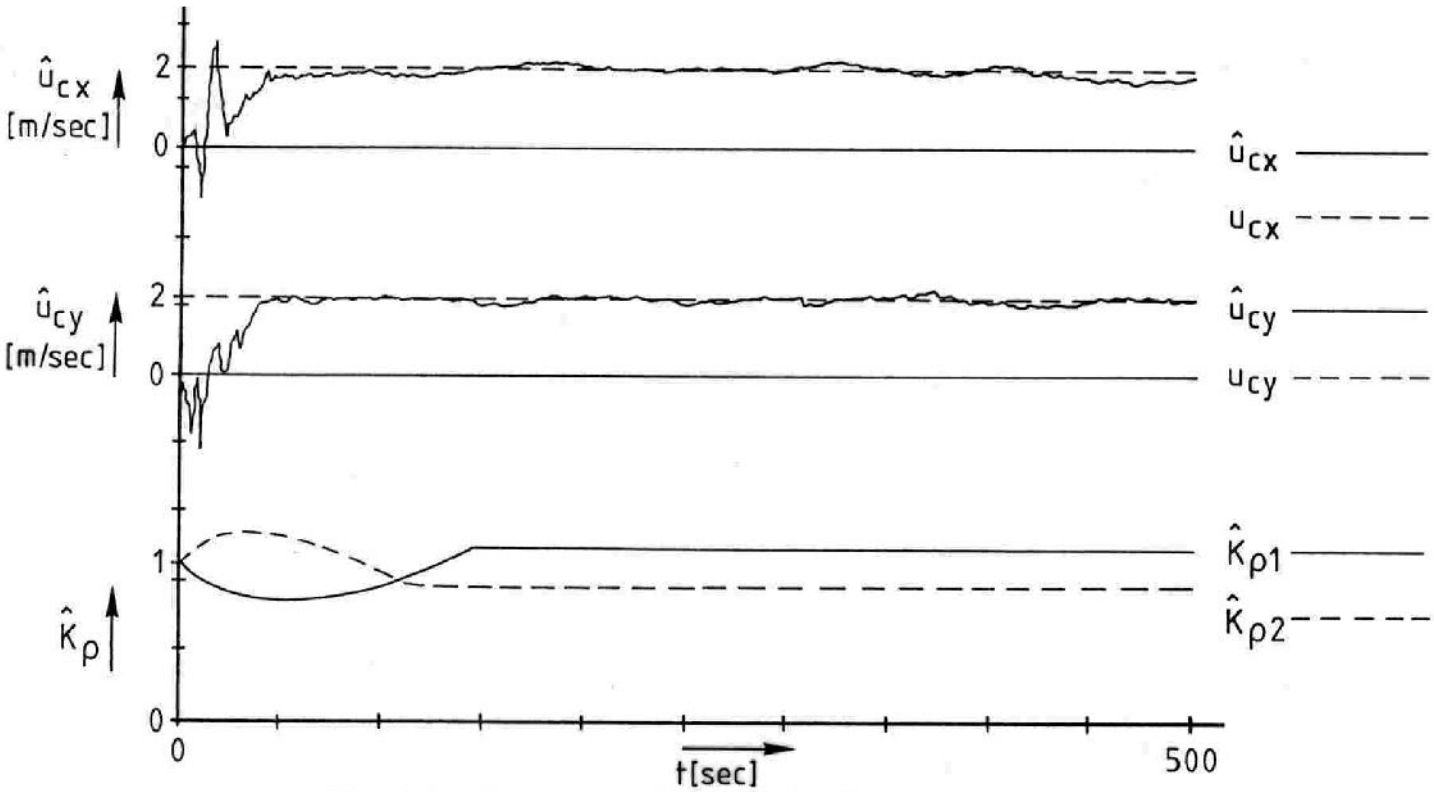

Fig. 6.7.a Estimation of the track adaptation factors

In Figure 6.7.a the following signals are shown:

u_{cx}, u_{cy}	the current speed in x and y direction,
$\hat{u}_{cx}$, $\hat{u}_{cy}$	the estimated current speed in x and y direction,
$K_{\rho 1,2}$	the estimated track-scaling factors for the 2 course changes.

The determination of the adapted predicted track from the initial prediction and the adaptation factors for wind and current is illustrated in Figure 6.7.b.

In this figure

$\tilde{\underline{x}}_s$	is the ship's observed track,
$\underline{x}_s$	is the ship's actual track,
$\underline{x}_p$	is the predicted track, adapted to wind and current influence,
$\underline{x}_0$	is the initial predicted track,
$\underline{x}_\rho$	is the predicted track, adapted to the wind influence.

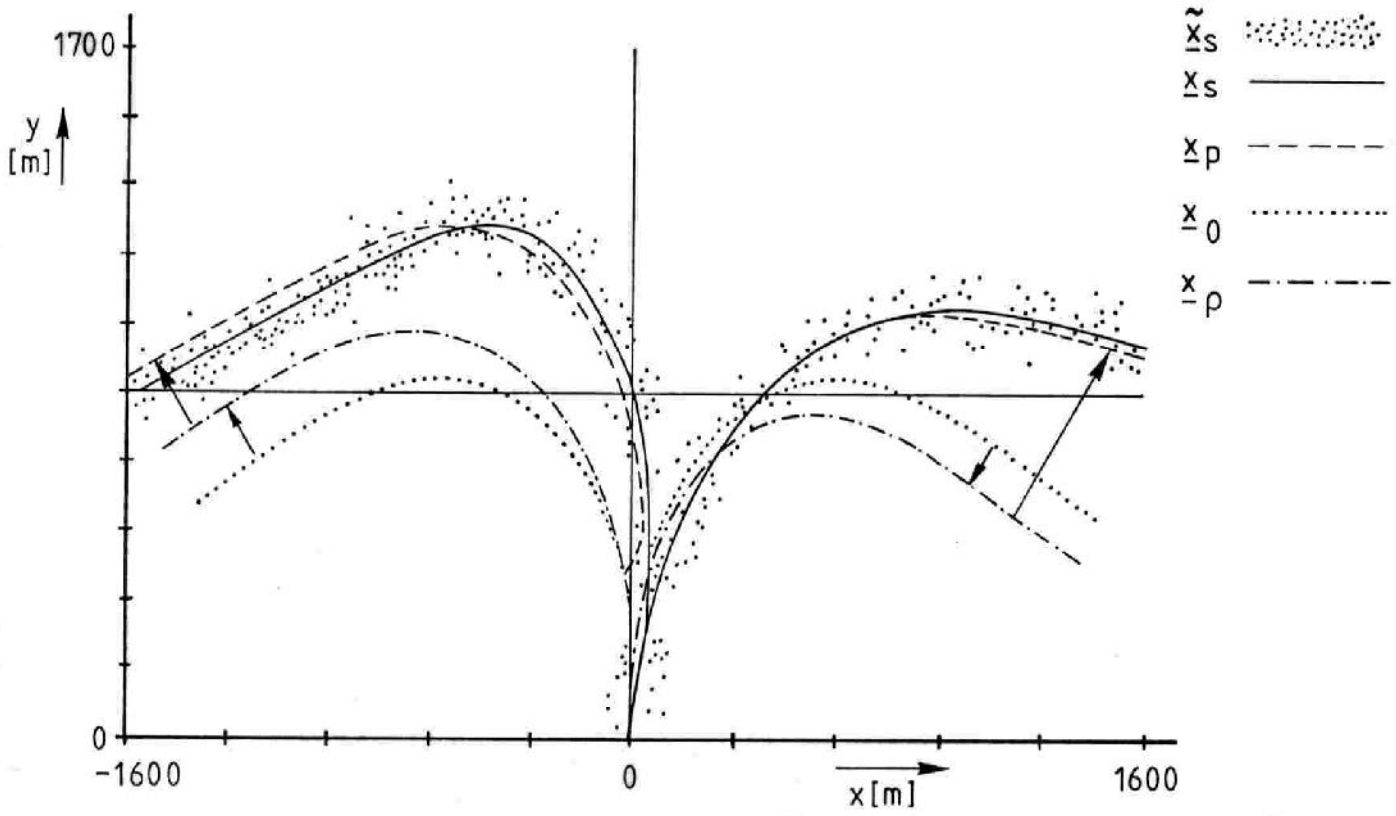

Fig. 6.7.b Track prediction and adaptation

6.4 Experiment on the manoeuvring simulator

6.4.1 Introduction

In 1985 investigations were carried out by the TNO Institute for Perception, regarding the feasibility of one-man-bridge ship steering. For this purpose a bridge set-up was designed with all the information, essential to manoeuvring and navigation, presented in an integrated way to the navigator (Van Breda and Van de Kooij, 1985). This bridge was called Bridge '90 (The bridge of the 1990's). The integrated information presentation consisted mainly of:

- A synthetic display (NAVDIS) on which both manoeuvring (heading, rate of turn, speed and rudder, according to Figure 6.8, part I) and navigation information (radar information concerning the ship's surroundings and other traffic and the planned track, according to Figure 6.8, part II) was presented.
- A Semi-Automatic Chart table, consisting of a conventional chart table on which the actual position of the ship was plotted automatically by means of a light dot.

An overview of the overall Bridge '90 mock-up is presented in Figure 6.9
In order to compare this Bridge '90 condition with one person on the bridge, with the conventional bridge condition with two people, a simulator experiment was set up, called the Bridge '90 experiment. For this purpose several tracking tasks were designed in a balanced way (Figure 6.10) under the following conditions:

- presence of other traffic
- presence of disturbances such as wind and current
- presence of an outside view
- presence of an extra monitoring task to measure the mental work load of the subjects under the different conditions.

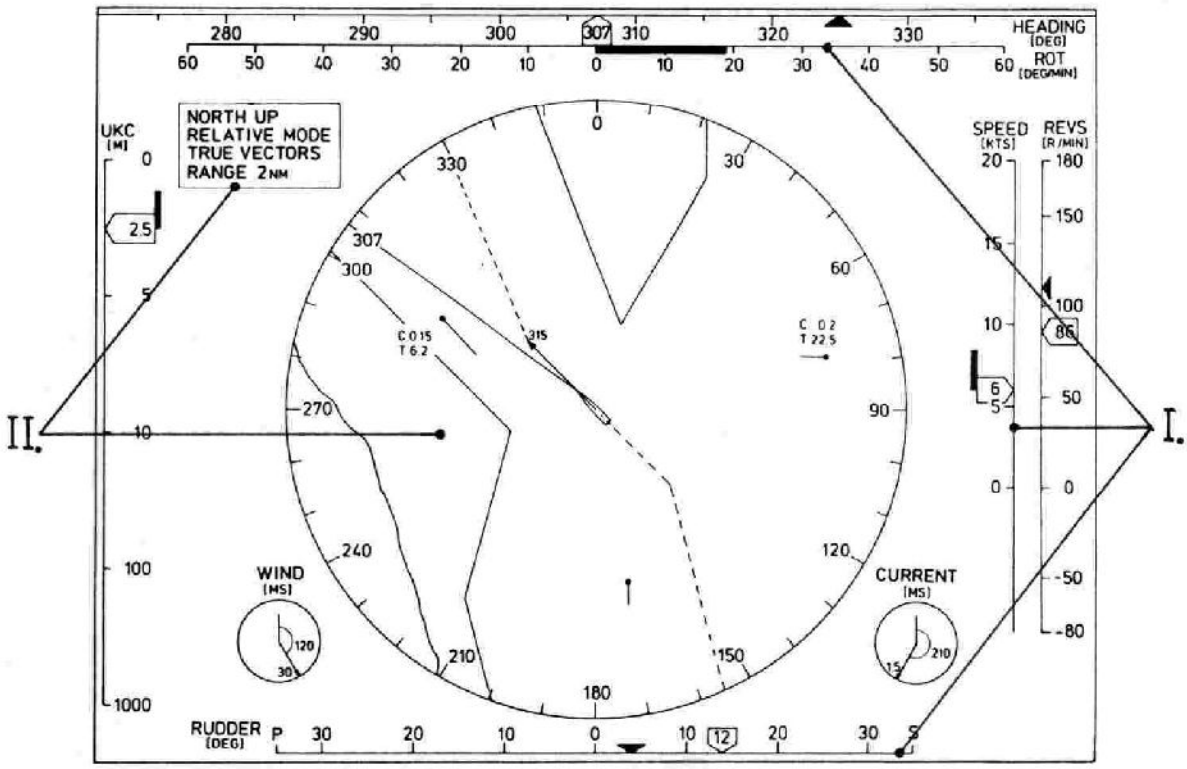

Fig. 6.8 The integrated navigation display NAVDIS

The experiment was carried out with 18 navigators who were instructed to sail the planned tracks ("reference tracks" in control terms) as accurately as possible. These tracks were to be sailed with a 40.000 DWT container vessel at an instructed speed of 19 knots.

A-posteriori analysis of the measured data, the results of which include the mean deviation of the reference track, showed that the subjects who had sailed under the Bridge '90 condition scored better than those who sailed under the conventional bridge condition (Boer and Schuffel, 1985).

In addition to this main conclusion, it became evident that the presence of an outside view was irrelevant for this kind of tracking experiments.

To evaluate the contribution of the experimental track-prediction system to the navigational performance it was decided that the track-predictor experiment could, just as the Bridge '90 experiment, be set up as a tracking experiment with the conditions adapted to this specific situation:

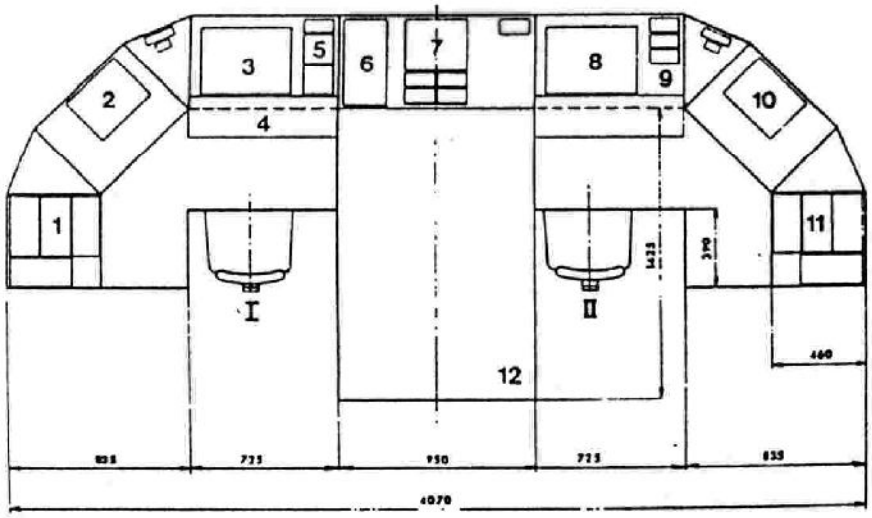

I. main position
II. back-up position

1. communications panel
2. Engine-Room supervision display
3. navigation and manoeuvring display
4. console
5. autopilot
6. telegraph
7. status-information display
8. back-up nav. man. display
9. back-up steering system
10. ER-supervision display
11. communications panel
12. semi-autom. chart table

Fig. 6.9 The Bridge '90 mock-up (Van Breda et al., 1985)

- absence of other traffic
- absence of an outside view
- presence of wind and current

The outcome of the experiment under these conditions should give a clear insight into the contribution of the track predictor to the accuracy with which the reference track could be sailed.
Before presenting the outcome of the actual simulator experiment (see also Passenier, 1988; Van Breda and Schuffel, 1989), the integration of the track-prediction system with the ship's bridge, according to Figure 6.9, will be described.

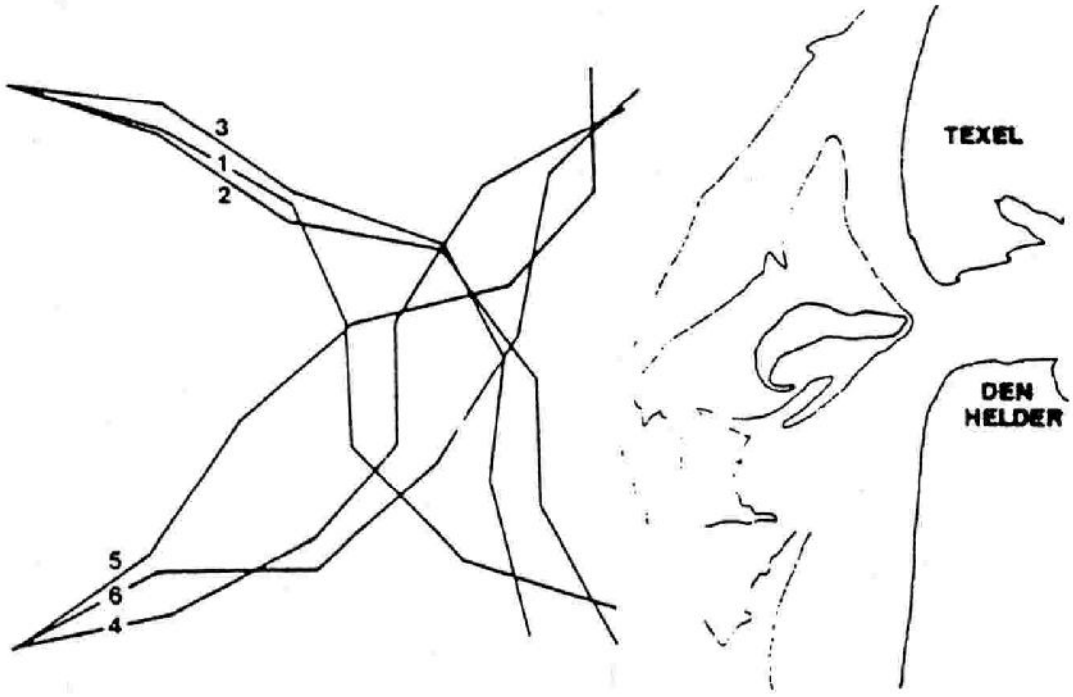

Fig. 6.10 The reference tracks for the Bridge '90 experiment

This integration consisted of:

- Integration of the prediction system with the user's consoles for navigation and manoeuvring on the ship's bridge (user input).
- Integration of the prediction information with the integrated navigation display of Figure 6.8 (user presentation).

6.4.2 Integration of the track predictor with the ship's bridge

The predictor input, which consists of settings of the trial heading and rudder limit, is closely related to the inputs of the course-changing controller. The predictor output (the predicted track) is to be related to the ship's surroundings and the planned track. This suggests the use of the predictor in an integrated environment; integration with respect to manoeuvring and navigation information. A combined user console for the trial manoeuvre settings as well as for the actual autopilot settings is a logical choice, whereas the predicted track is superimposed on an integrated display, as discussed in Section 6.4.1.

According to this integrated approach, the predictor could be implemented in the Bridge '90 mock-up according to Figure 6.11.

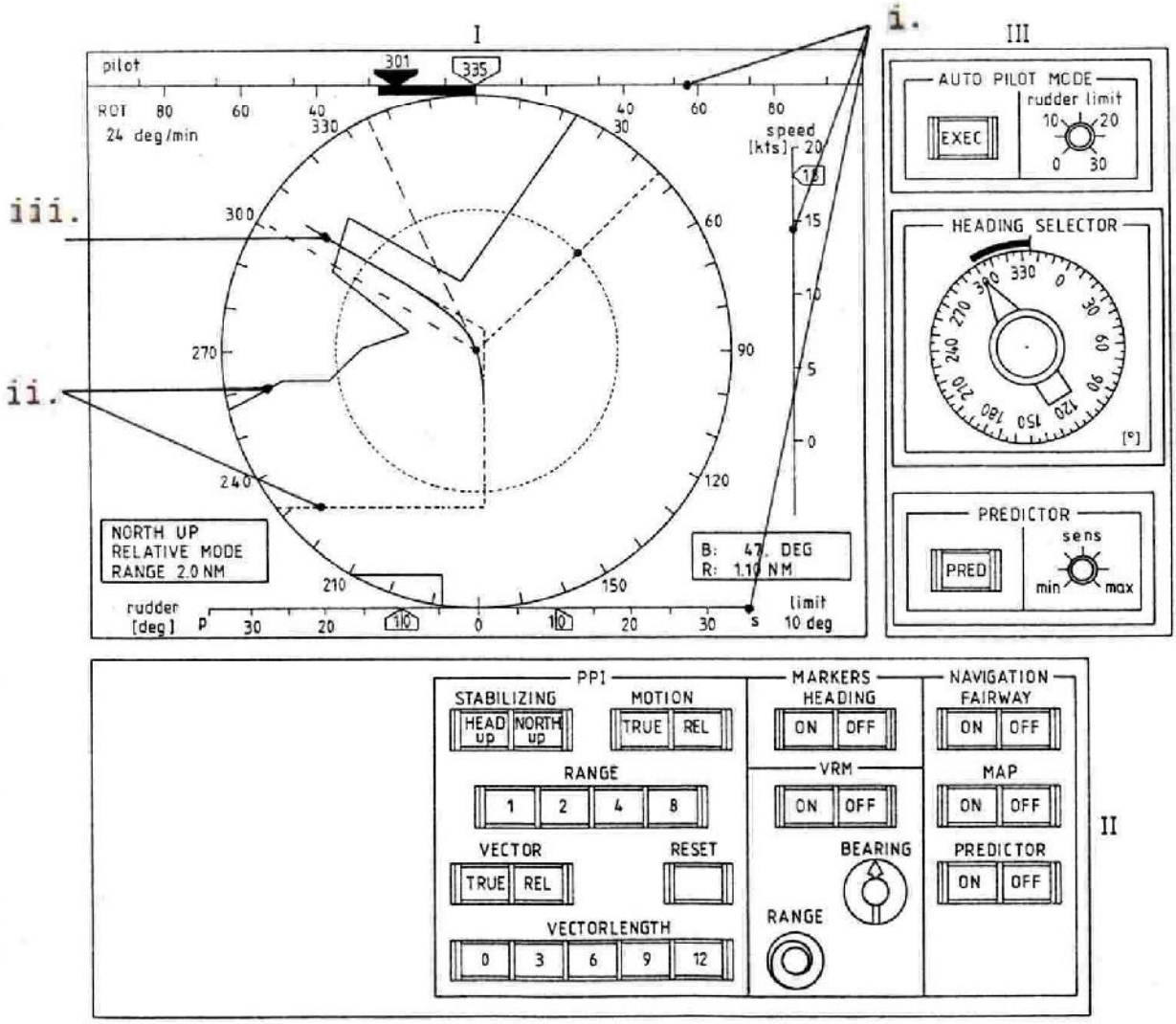

Fig. 6.11 Integrated Prediction and Navigation set-up

In this figure

I. is the integrated Manoeuvring/Navigation/Prediction Display with
   - manoeuvring information: heading, rate of turn, rudder and forward speed (i.),
   - navigation information: the ship's surroundings and the planned track (ii.),
   - prediction information: predicted track superimposed on the planned track (iii).

II. is the user console for the display consisting of:
- **Range input**: 1,2,4 or 8 nm,
- variable range marker (**VRM**) input which enables the plotting of targets on the radar screen,
- **On/Off** switches for the various markers (VRM, heading and trial heading marker).

III. is the combined user console for the predictor and the autopilot.
The **heading selector**, which is combined with a compass read out, is used together with the **rudder limiter** as the predictor input to calculate the predicted track, becoming the real autopilot settings after pressing the **EXECUTE** push button.

The logical consistency of this approach manifested itself during the experiments when the subjects had hardly any difficulties in using the predictor in combination with the autopilot during the different tracking tasks.

A general impression of the integration of the track predictor with the NAVDIS and the user's console in the ship's bridge and the interfacing with the manoeuvring simulator is given in Figures 6.12, 6.13 and 6.14.
More detailed information can be found in Appendix A.

Fig. 6.12 Integration of the predictor with the ship's bridge

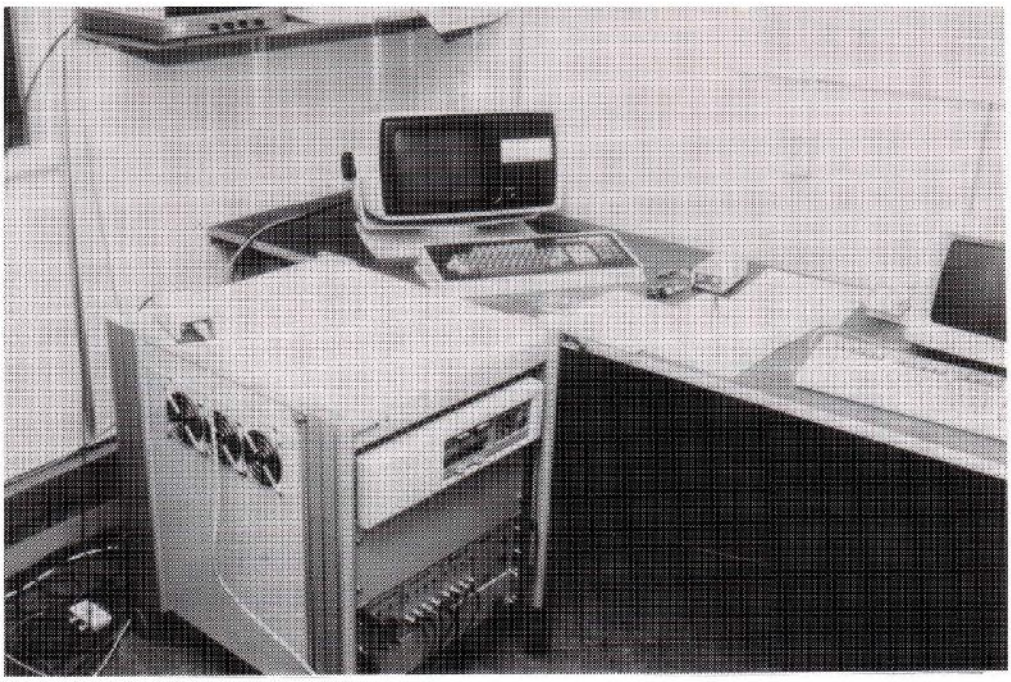

Fig. 6.13 The track-prediction computer

6.4.3 Set-up of the experiment

Based upon the experiences with the Bridge '90 experiment it was decided to design 6 tracks which were to be sailed by 12 experienced navigating officers in active service, in the age from 25 to 30.
The tracks were to be set up in such a way that the manoeuvring tasks would vary from easy to difficult, to get an indication of the contribution of the predictor for the different tasks.
In each track 5 course changes were incorporated, varying from 15 degrees (easy) to 105 degrees (difficult). The distance between the waypoints varied from 2 to 2.5 nm., to enable the ship to get a new "steady state" between the course changes.
The course changes were divided randomly over the waypoints of the 6 tracks, according to table 6.1.a,b:

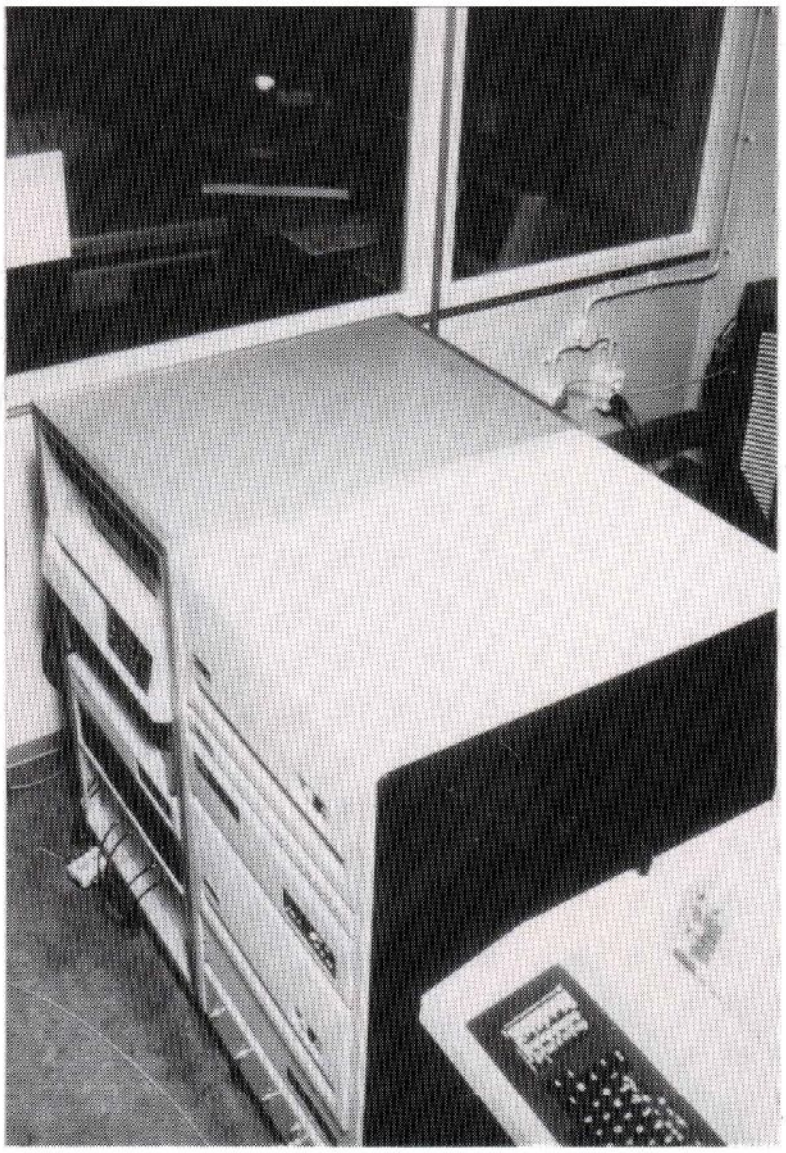

Fig. 6.14 The manoeuvring-simulator computers

Course change:	C1:	15 degrees
	C2:	30 degrees
	C3:	45 degrees
	C4:	75 degrees
	C5:	105 degrees

Table 6.1.a The different course changes

Tracks:	T1:	C4	C3	C2	C5	C1
	T2:	C1	C4	C5	C2	C3
	T3:	C3	C1	C5	C4	C2
	T4:	C5	C2	C4	C1	C3
	T5:	C2	C1	C3	C4	C5
	T6:	C3	C5	C1	C2	C4

Table 6.1.b The course changes divided over the tracks

To these tracks 9 buoys were added to enable the subjects to verify their position by means of the VRM.
The disturbances were chosen to be constant for each scenario according to Table 6.2:

	Speed		Direction
Current:	2.5	knots	South West
Wind:	7	m/s	North West

Table 6.2 The disturbances

Figure 6.15 gives a combined overview of the 6 scenarios (North up) which were located in the same area in which the Bridge '90 experiments were performed (see Figure 6.10).

To determine which types of information should be weighed against each other, the following demands have to be satisfied:

- The effect of the predictor should become clear in an "undisturbed" way. This implies that when 2 conditions are compared, one of them with the assistance of the track predictor, other factors which could influence this comparison (such as the type of presentation of the manoeuvring information, presence of the chart table) should be kept constant. In this way a mixed effect in the outcome of the comparison is avoided.

- The conditions should be realistic, which means realizable on a real ship in the near future.

The integration of the track predictor with the ship's bridge is described in Section 6.4.2 (integration with the autopilot, integration with radar information). It can be concluded that the most realistic environment in which the track predictor can

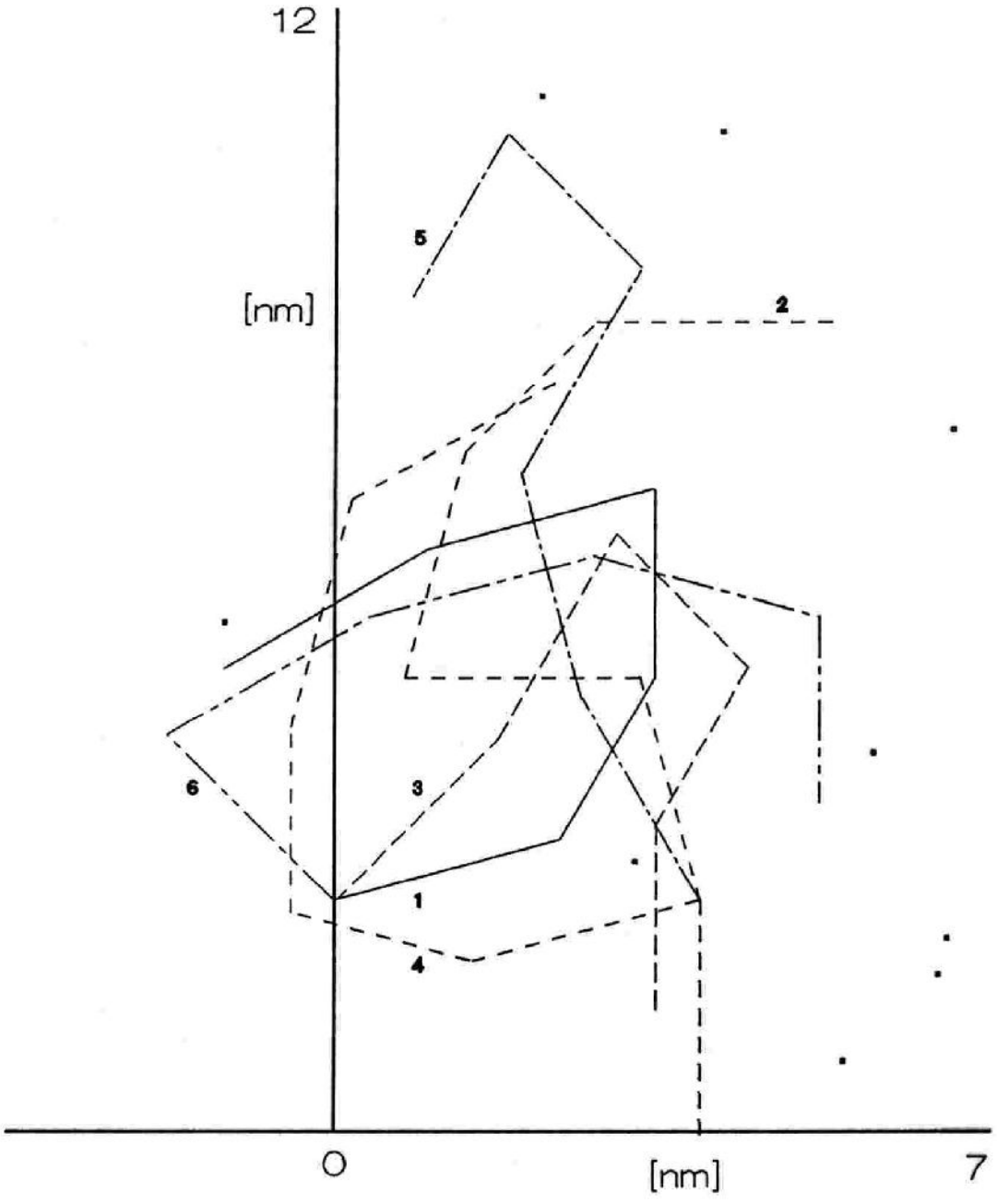

Fig. 6.15 Overall picture of the scenarios

be implemented is an integrated one, according to the type of Bridge '90. Therefore the starting point for the design of the different conditions has been the following:

- Integrated navigation display NAVDIS present, displaying the ship's manoeuvring and navigation (planned track) information.
- Semi-Automatic Chart table present, receiving its information from an integrated positioning system on board the ship (based, for instance, on the satellite navigation system G.P.S.). The chart table is intended to give the navigator an overall view of the manoeuvring area and can be used as a back-up system by plotting NAVDIS targets with the aid of the Variable Range Marker.

Because for this reference condition the planned track is made visible, the navigation method is comparable to a simplified version of parallel indexing (Shell, 1975; Spaans, 1979).

A good alternative for the track predictor could be the presentation of the own ship's ground-speed vector (Sheridan, 1966) on the NAVDIS, which can be regarded as a linear predictor (extrapolator), into which no rate-of-turn information is incorporated.
This condition surely is interesting both from a scientific and an economic point of view:

- Scientific viewpoint:
  What is the extra effect on the navigational performance of adding rate-of-turn information to this "linear predictor", resulting in the actual track predictor?
- Economic viewpoint:
  ARPAs with presentation of the ship's ground vector already exist and would be a less expensive solution than the track predictor.

Together with the reference condition of simplified parallel indexing, 3 conditions A,B and C were obtained to be evaluated on the basis of the simulator experiment (Figure 6.16.a,b,c):

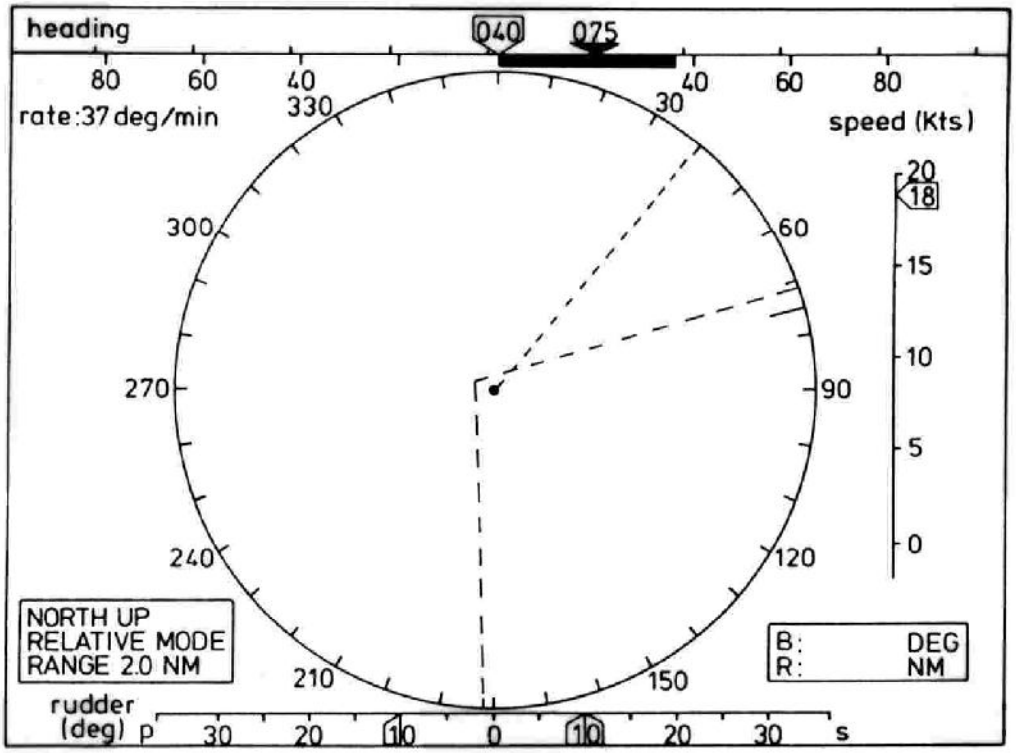

Fig. 6.16.a Condition A : simplified parallel indexing

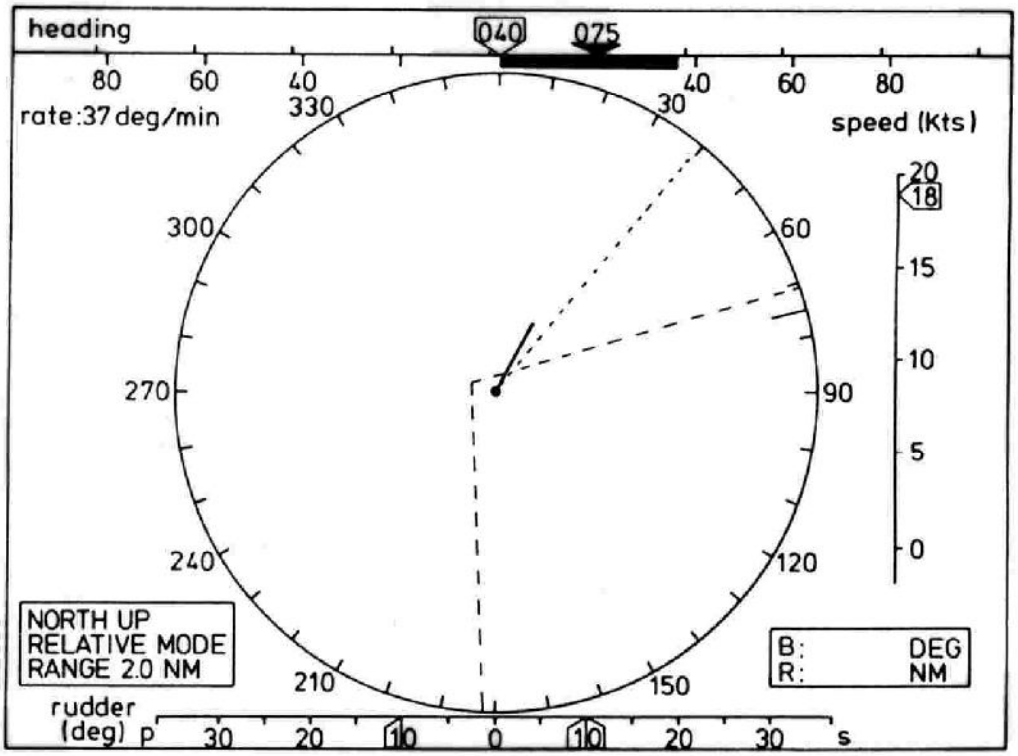

Fig. 6.16.b Condition B : ground-speed vector

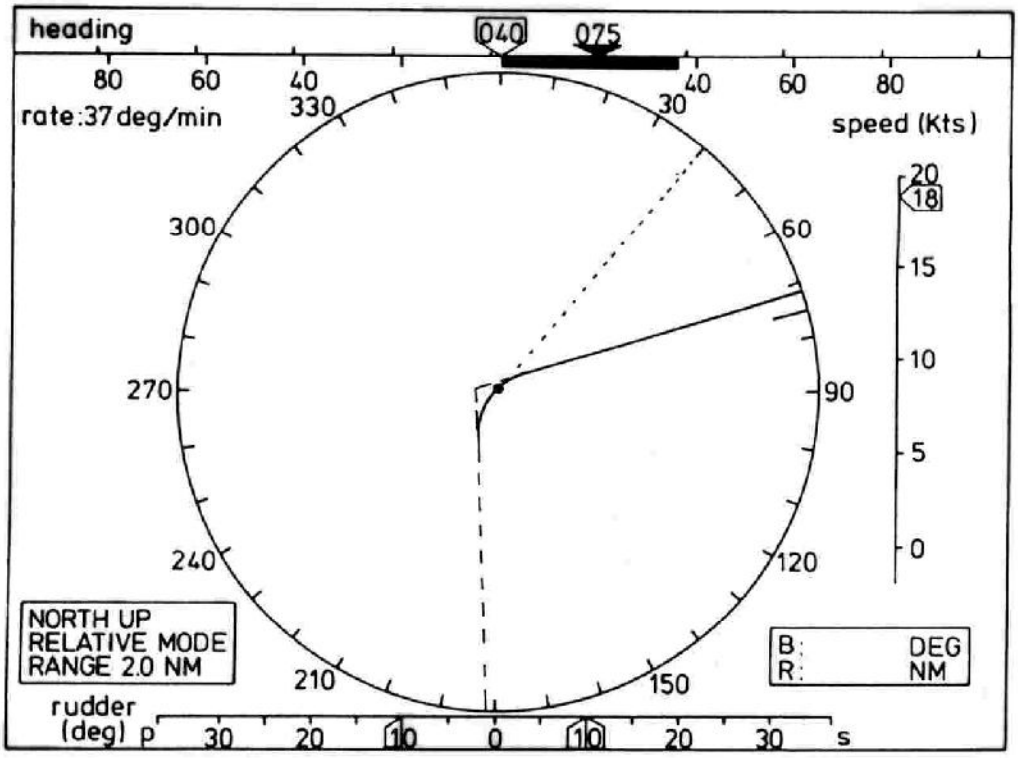

Fig. 6.16.c Condition C : track predictor

The 3 conditions were divided over the 12 subjects according to table 6.3, which was set up in such a way that undesirable learning effects would cancel out:

A B C B C A C A B : subject 1+2
B A C A C B C B A : subject 3+4

B C A C A B A B C : subject 4+6
A C B C B A B A C : subject 7+8

C A B A B C B C A : subject 9+10
C B A B A C A C B : subject 11+12

Table 6.3 Division of the 3 conditions over the subjects

6.4.4 Results

The experiments were carried out with a simulated (hydrodynamic) model of a 40.000 DWT container vessel, with a length of 226 m. This model will from now on be referred to as the "ship". More information about the dimensions of the ship, which had also been used for the Bridge '90 experiment, can be found in Appendix B.
Before carrying out the actual experiment (described in Section 6.4.4.2), first some preliminary tests (Section 6.4.4.1) were performed.

6.4.4.1 Preliminary tests

As a first test, the parameters of the ship's yaw dynamics were identified. This yielded the parameters of the reference model on the basis of which the autopilot and predictor parameters were calculated during the actual tracking experiment. The on-line identification was performed by the yaw filter on the basis of a zig-zag trial with a rudder deflection from +15 to -15 degrees.
The corresponding results are presented in Figure 6.17, which was realized by the Signal Monitor Program SMP.
In this figure the following signals are shown:

r_R the rate-of-turn signal of the reference model,
r the ship's rate-of-turn signal,
δ the actual rudder angle,
$\hat{K}^*, \hat{\tau}^*$ the estimated normalized parameters,
$\hat{N}_w$ the estimated offset.

Comparing the ship's response to the response of the parallel reference model gives a good indication of the performance of the parameter estimator. The parameter estimator has converged after approximately 5 minutes, resulting in (at a cruising speed of 19 knots and a ship's length of 226 m):

$$K^* = 1.6 \qquad \tau^* = 1.7$$

$$K = K^*.U/L = 0.07 \qquad \tau = \tau^*.L/U = 45 \text{ sec.}$$

During the actual experiment the adaptation of the reference-model parameters was switched off. By using direct compensation the ship is forced to follow the response of the reference model.

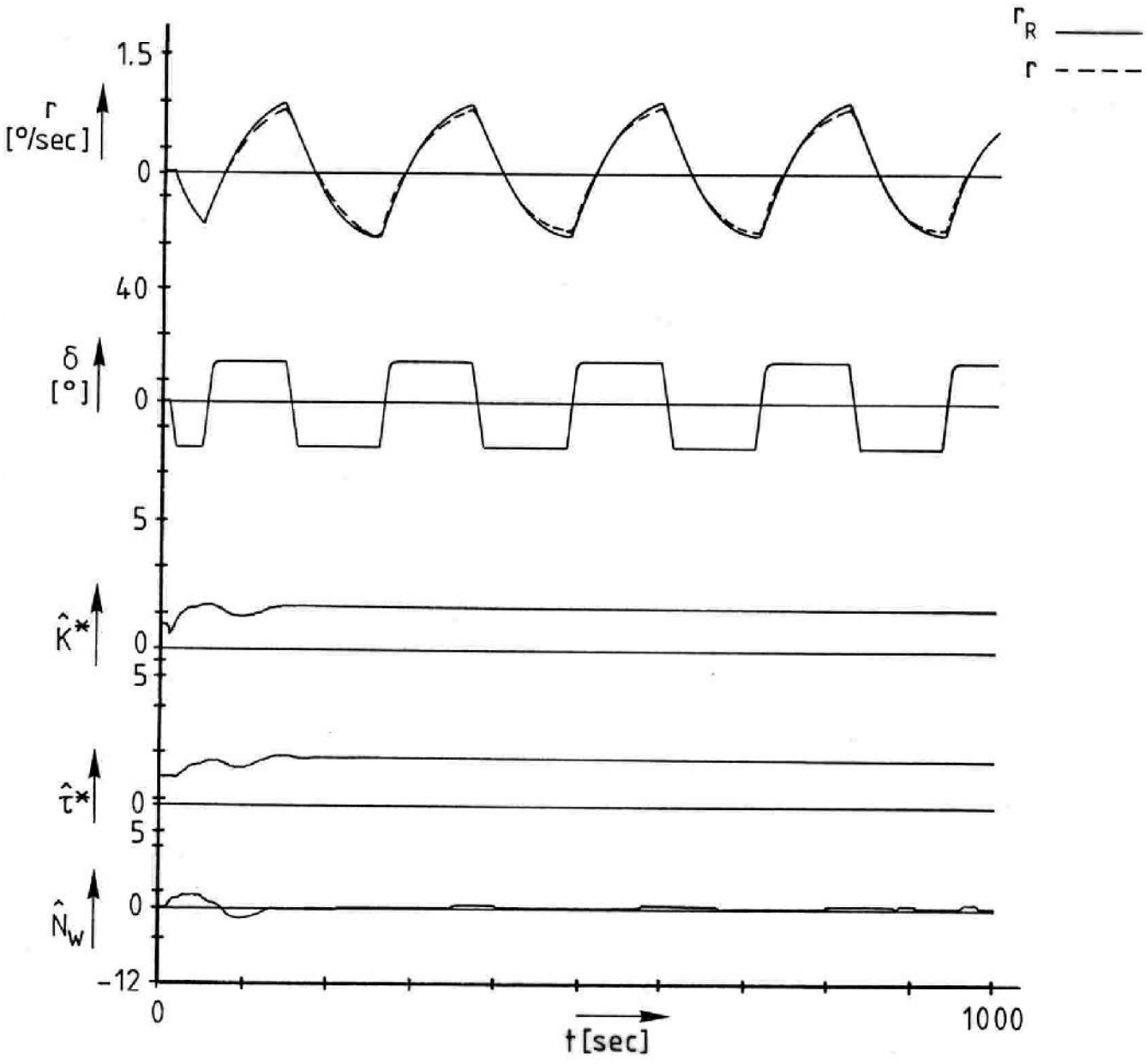

Fig. 6.17 Identification of the yaw dynamics

To test the behaviour of the autopilot with gain scheduling on the basis of the reference-model parameters, two course changes of +90 and -90 degrees were carried out for a rudder limit of 15 degrees. The results for the ship's rate of turn and course error are presented in Figure 6.18.

In this figure the following signals are shown:

r the ship's rate-of-turn signal,
δ the actual rudder angle (direct compensation included),
ε the course error.

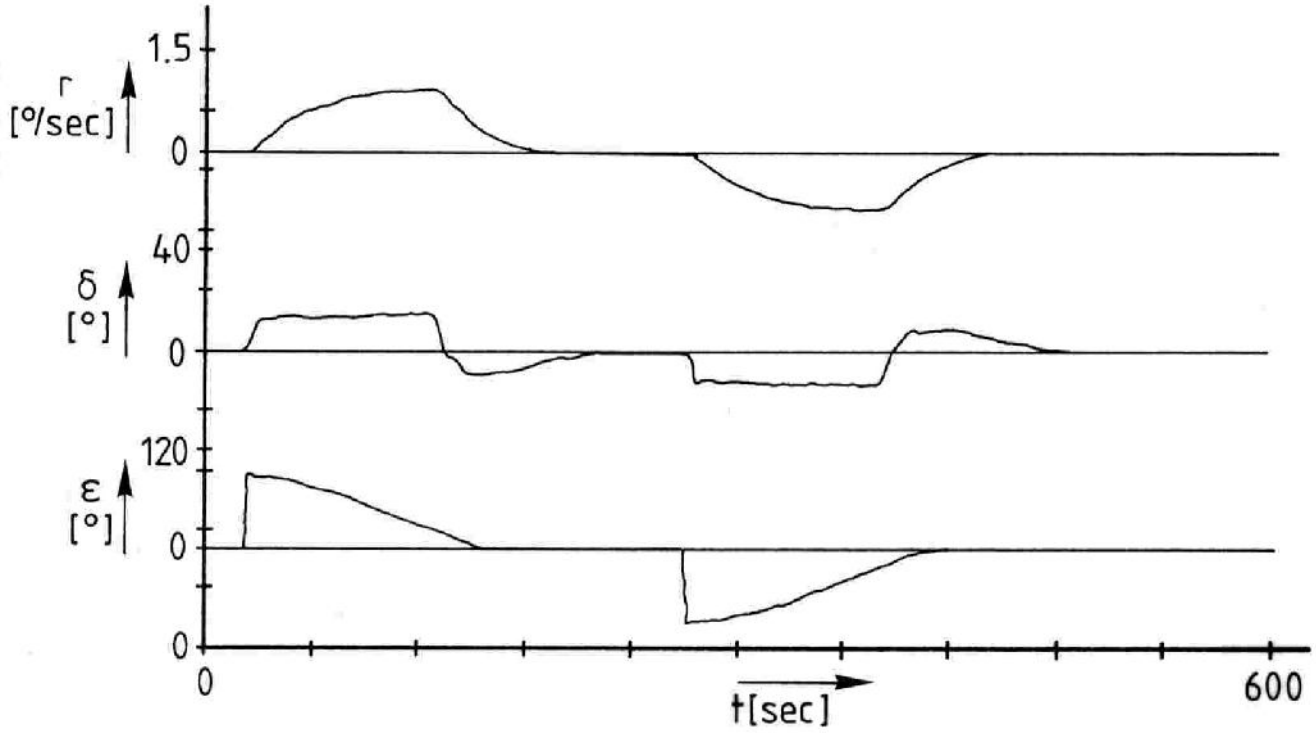

Fig. 6.18 Performance of the course-changing controller

The corresponding ship's path for the course change of 90 degrees is presented in Figure 6.19. In this figure the influence of the drift angle on the ship's track, due to the ship's sway velocity, is also made visible.

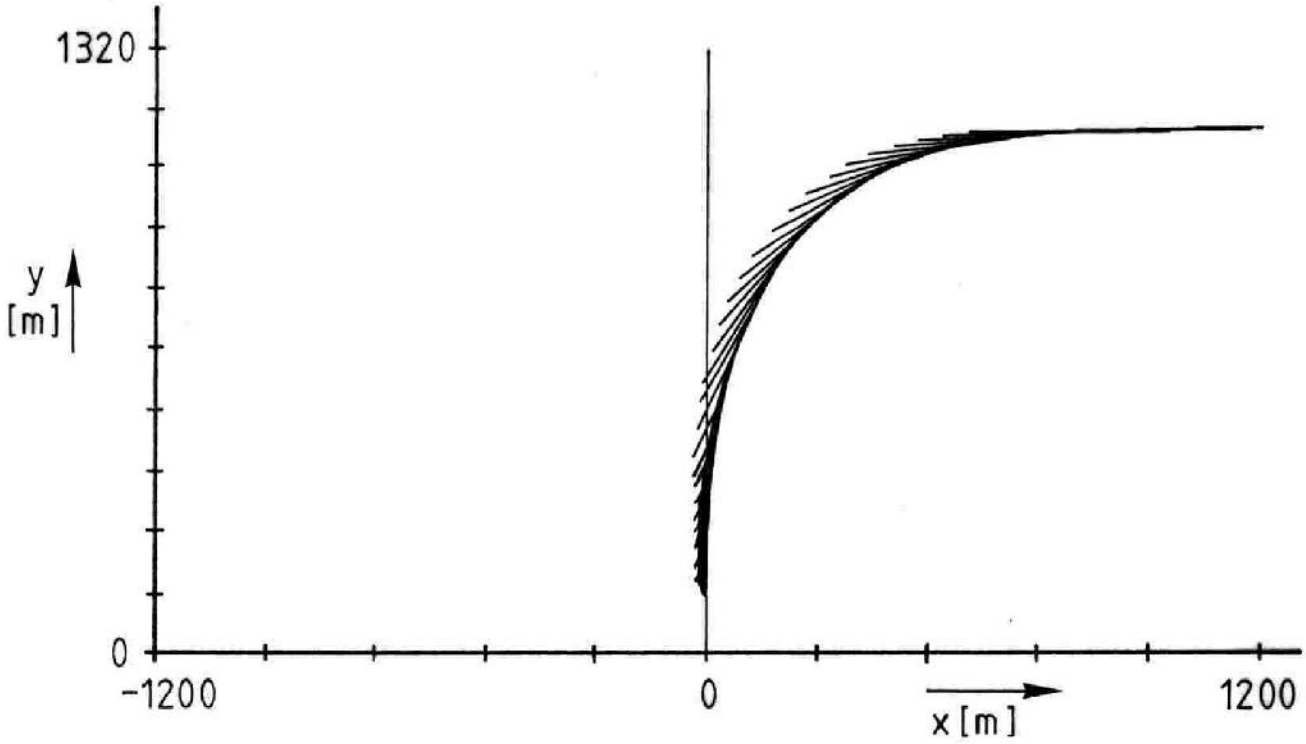

Fig. 6.19 Ship's path for a course change of 90 degrees

The reconstruction of the sway velocity from the position fixes by the position filter is illustrated in Figure 6.20 for a zig-zag trial.
In this figure $\hat{v}$ is the estimated sway velocity on the basis of the estimated sway constant $\hat{\gamma}$.

From Figure 6.20 it may be concluded that the estimated sway constant $\hat{\gamma}$ does not converge so well, probably due to unmodelled dynamics in the transfer from rate of turn to sway velocity. For the tracking experiment $\hat{\gamma}$ was fixed to a value of 2.26 (the dashed line in Figure 6.20), using the current-estimation part of the position filter to account for sway deviations between ship and model.
The current estimation by the position filter, and the resulting adaptation of the predicted track on the prediction display by the track-adaptation mechanism, were tested by switching on a strong current of 6 knots, direction 210 degrees, during sailing. The results are presented in Figure 6.21.a,b.

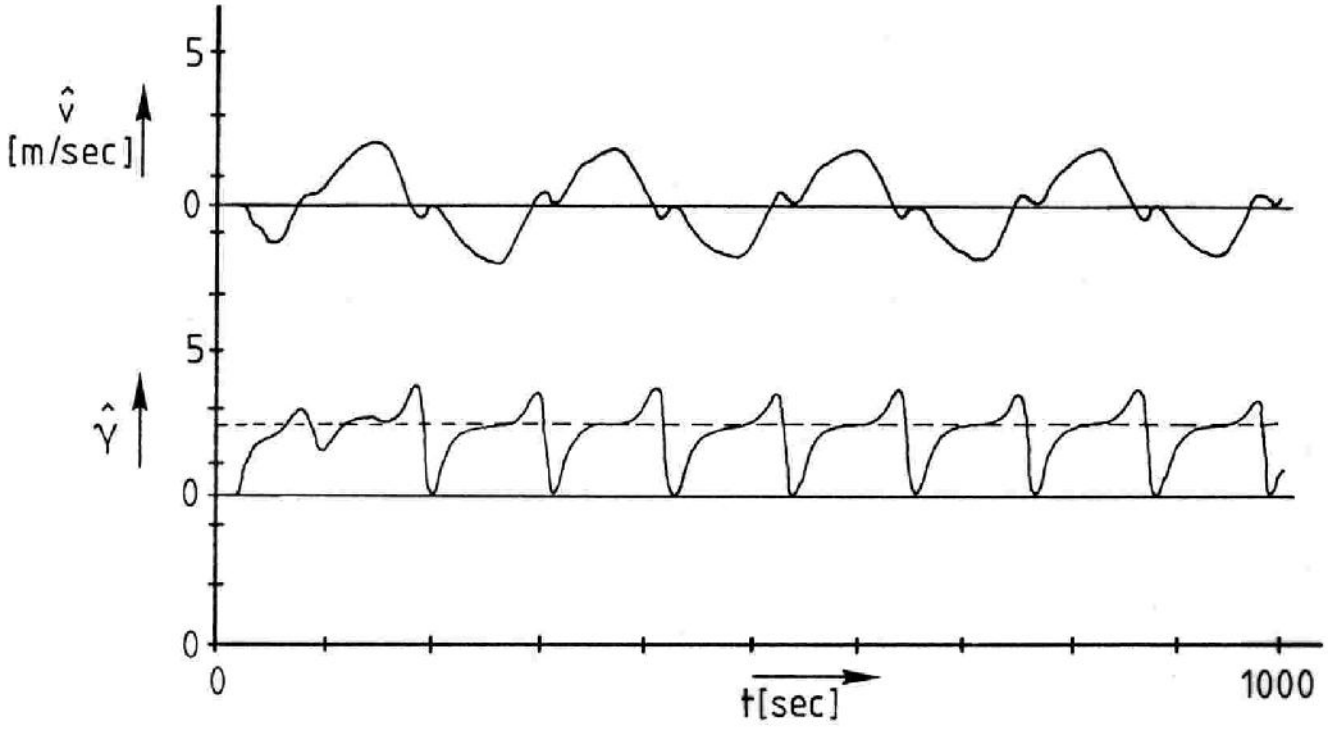

Fig. 6.20 Estimation of the sway velocity v

By using the heading selector, which is coupled to a trial marker on the NAVDIS, the navigator can directly determine the necessary course change to compensate for the current influence from Figure 6.21.b.

After the identification, autopilot and track-adaptation tests, a complete reference track was sailed by a nautical expert, who was consulted on the experiment. The track was sailed with the assistance of the predictor at a cruising speed of 19 knots (Figure 6.22.a,b). At the third course change additional current was switched on, activating the track-adaptation mechanism to enable compensatory actions by the navigator. Just before the last course change an evasive action was undertaken at a maximum rudder value of 40 degrees, after which the track predictor was used to get back on the reference track. This clearly illustrates the fact that the predictor is a manoeuvring aid to the navigator, instead of a track-keeping autopilot.

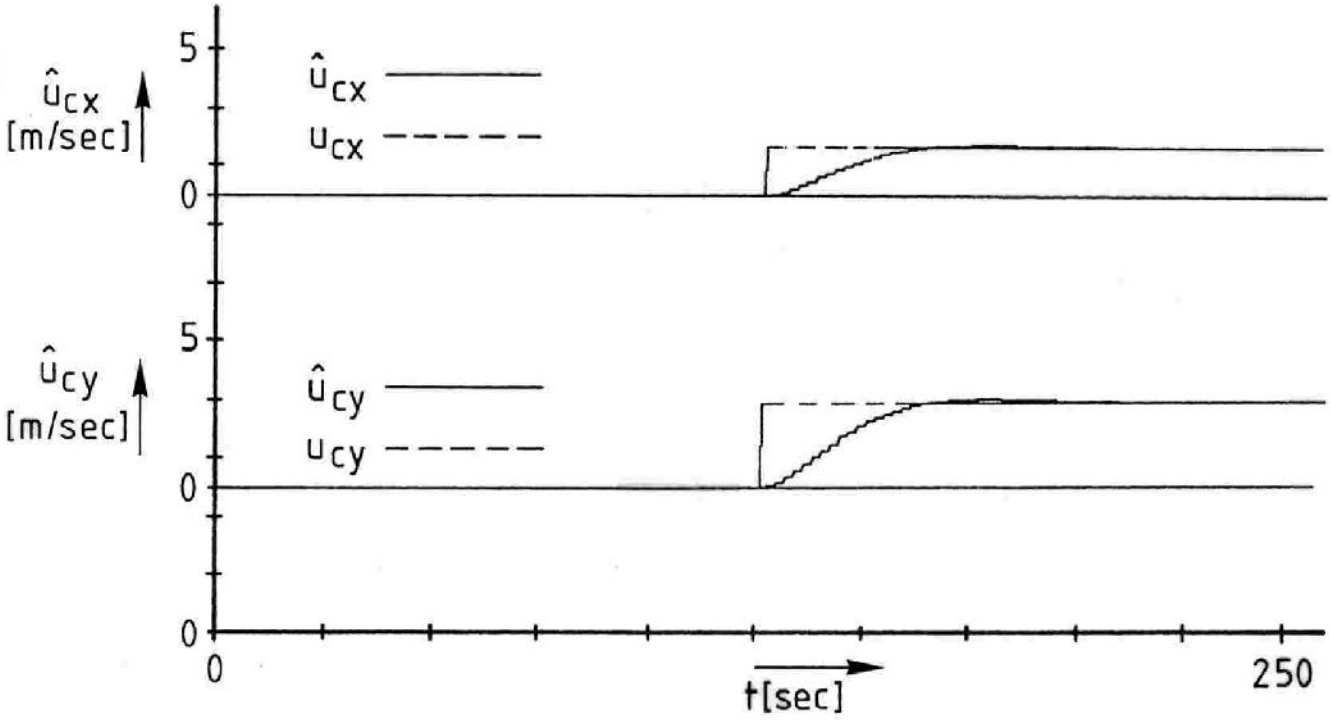

Fig. 6.21.a Current estimation by the position filter

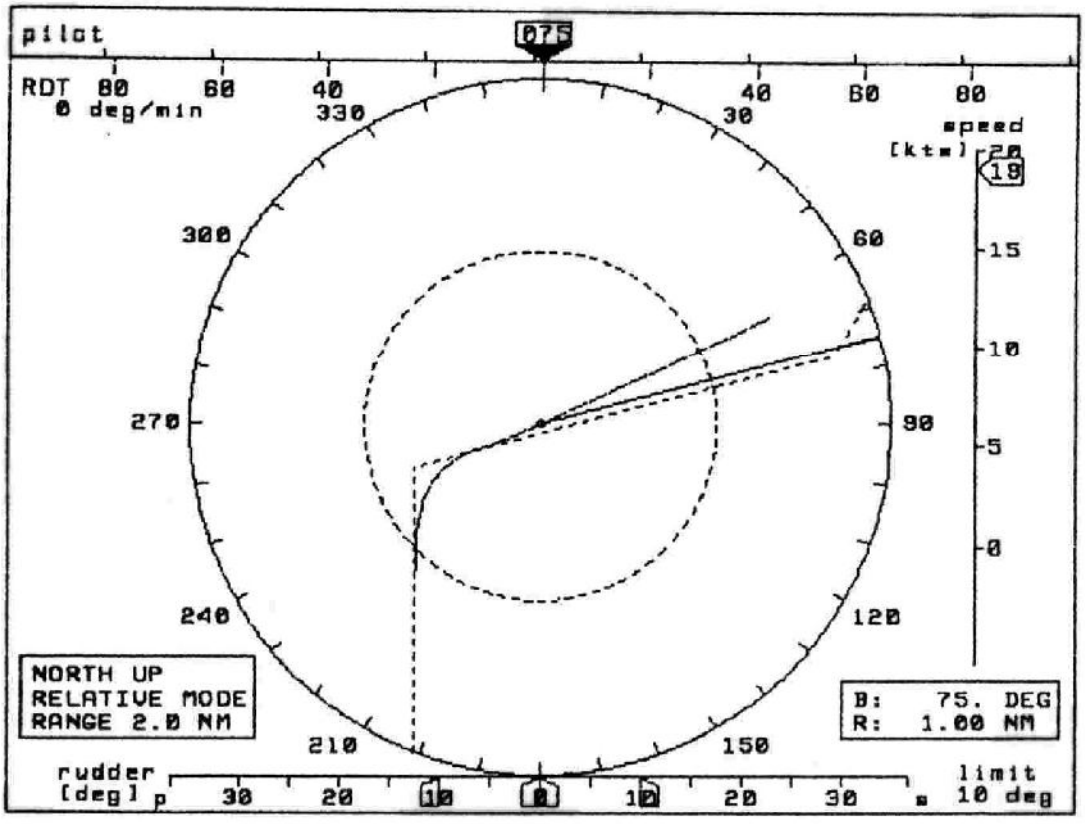

Fig. 6.21.b Resulting track adaptation on the predictor display

In Figure 6.22.a the course-error, rate-of-turn and rudder signals are presented for this trial. In Figure 6.22.b the reference track and the actual sailed track are presented. The compensations, carried out by the navigator after each course change, are a result of the track adaptation caused by the imperfect prediction of the sway velocity. Further, the estimated current influence, used for the track-adaptation mechanism, is recorded.

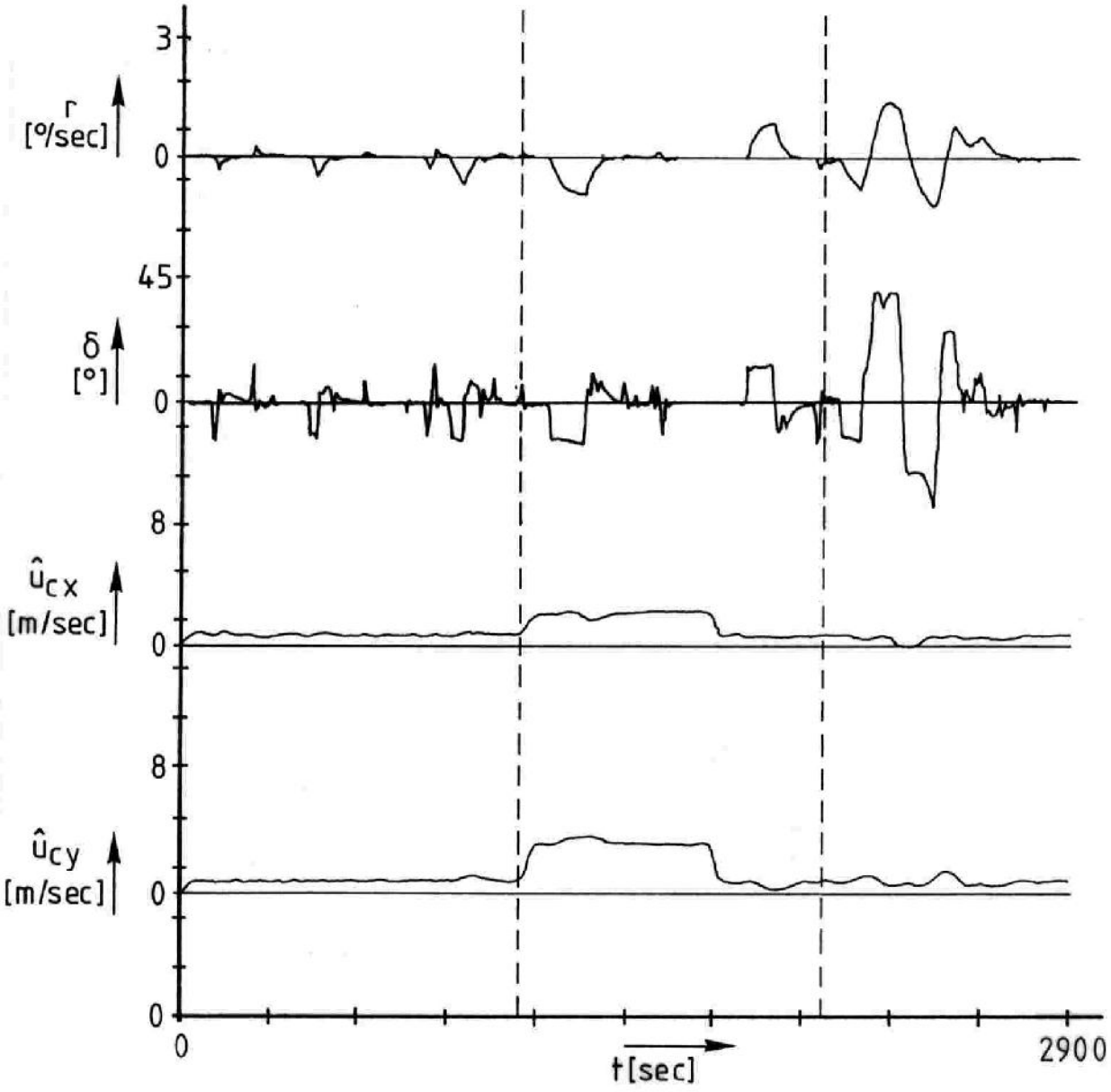

Fig. 6.22.a Recorded signals

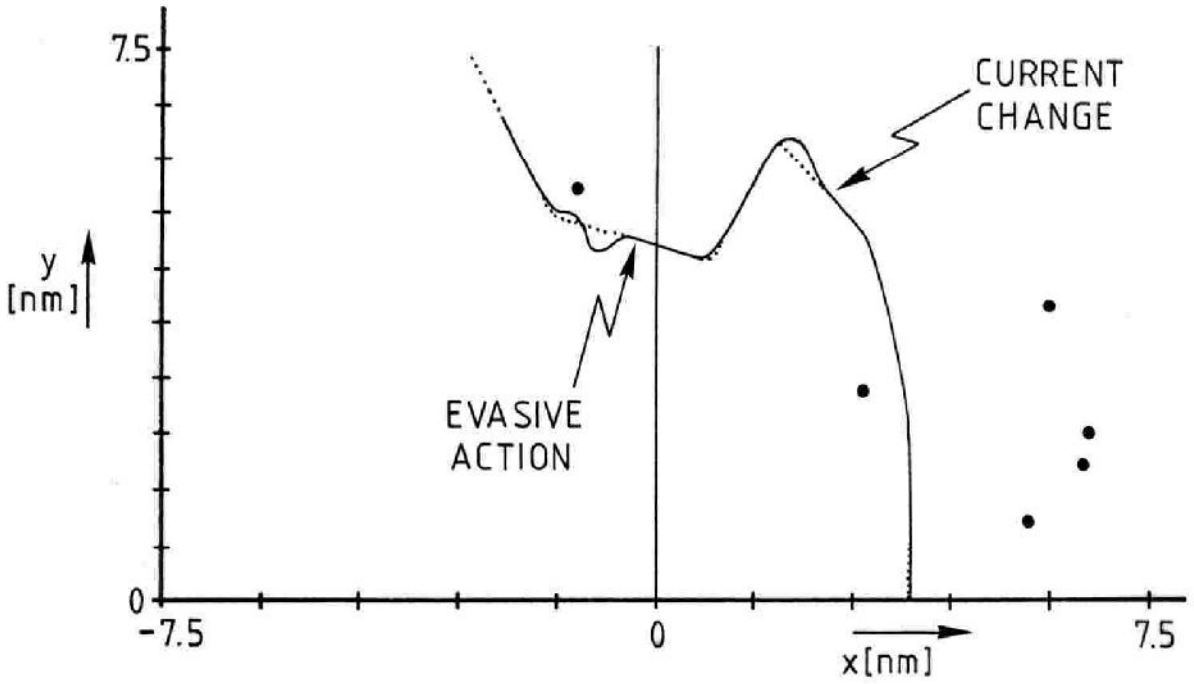

Fig. 6.22.b Reference track versus sailed track

6.4.4.2 Results of the tracking experiment

After consulting an expert in radar-assisted navigation from the "Hogere Zeevaartschool Vlissingen", some final alterations were carried out regarding the information presentation. At this stage the system became ready for the actual tracking experiment.

The 12 subjects were instructed to sail the reference tracks as accurately as possible, at a cruising speed of 9.5 m/s or 19 knots (corresponding to the Bridge '90 experiment). The rudder limit was fixed at 10 degrees, resulting in a nominal rate of turn of approximately:

$$r_{ss} = K^* \cdot \frac{U_{ss}}{L} \cdot \delta_{max} = 1.6 \cdot \frac{9.5}{226} \cdot 10 \cdot 60 \approx 40 \text{ deg/min}$$

The rudder limit was fixed to produce results which could be compared to each other, which would not be the case if the subjects were allowed to choose the rudder limit, and the resulting turning-circle diameter, according to their own preference.

To get a realistic comparison, information was provided before hand regarding the ship's rate of turn, forward speed and the resulting turning circles at different rudder angles and cruising speeds. Also information was given about the values of the disturbances (wind and current speed and direction).
In total 9 tracks were sailed by each subject, resulting in 9 x 12 = 108 tracks for the experiment. (Each track took approximately 40 minutes to sail.)
To give a visual impression of the obtained results, for each of the 3 information conditions A,B and C a representative track was determined, based on the mean deviation between the actual and the reference track. These results are presented in Figure 6.23.a,b,c, where the figure subscripts a,b and c correspond to the information conditions A,B and C.

To determine the accuracy for the sailing of a particular track, the root-mean-square (RMS) error with respect to the reference track was calculated according to (Poulton, 1974; Boer and Schuffel, 1985):

$$\text{RMS error} = \sqrt{\left(\frac{\sum_{i=0}^{i=N} (\underline{X}_i - \underline{M}_i)^2}{N} \right)} \qquad (6.5)$$

In this equation $(\underline{X}_i - \underline{M}_i)$ is the perpendicular lateral distance between the ship's position $\underline{X}_i$ and the reference trajectory $\underline{M}_i$ at interval i, with a total of N intervals (the data was sampled every 2 seconds). The RMS error was corrected for the ship's inherent manoeuvrability for the different course changes. This means that the ship's turning dynamics was accounted for in the calculation of the distance between ship and reference trajectory.
Averaging the RMS error over the 36 tracks which were sailed for each of the 3 conditions A,B and C yields a quantitative result which is a good basis for carrying out the comparison.

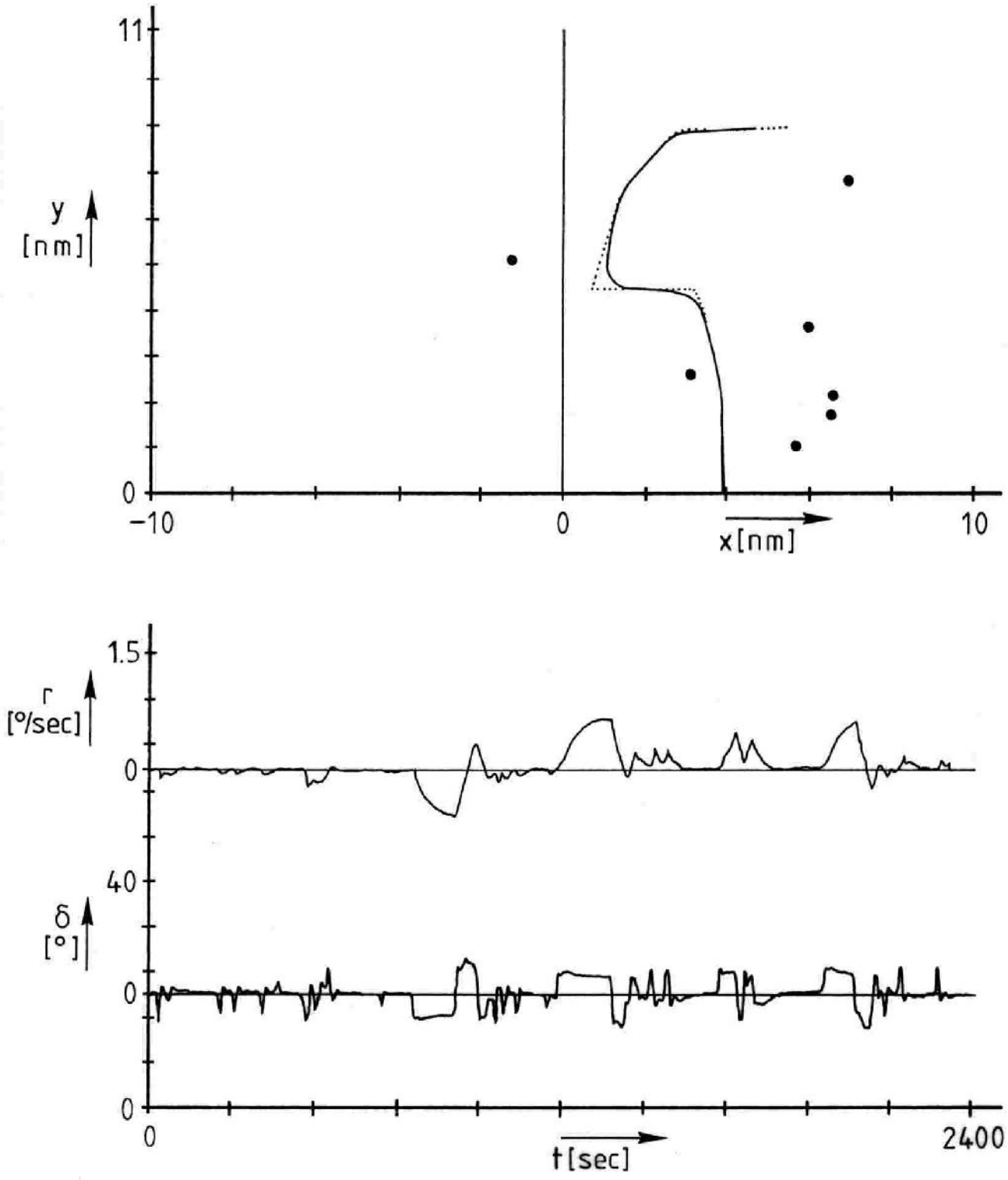

Fig. 6.23.a Results of the parallel-indexing trial

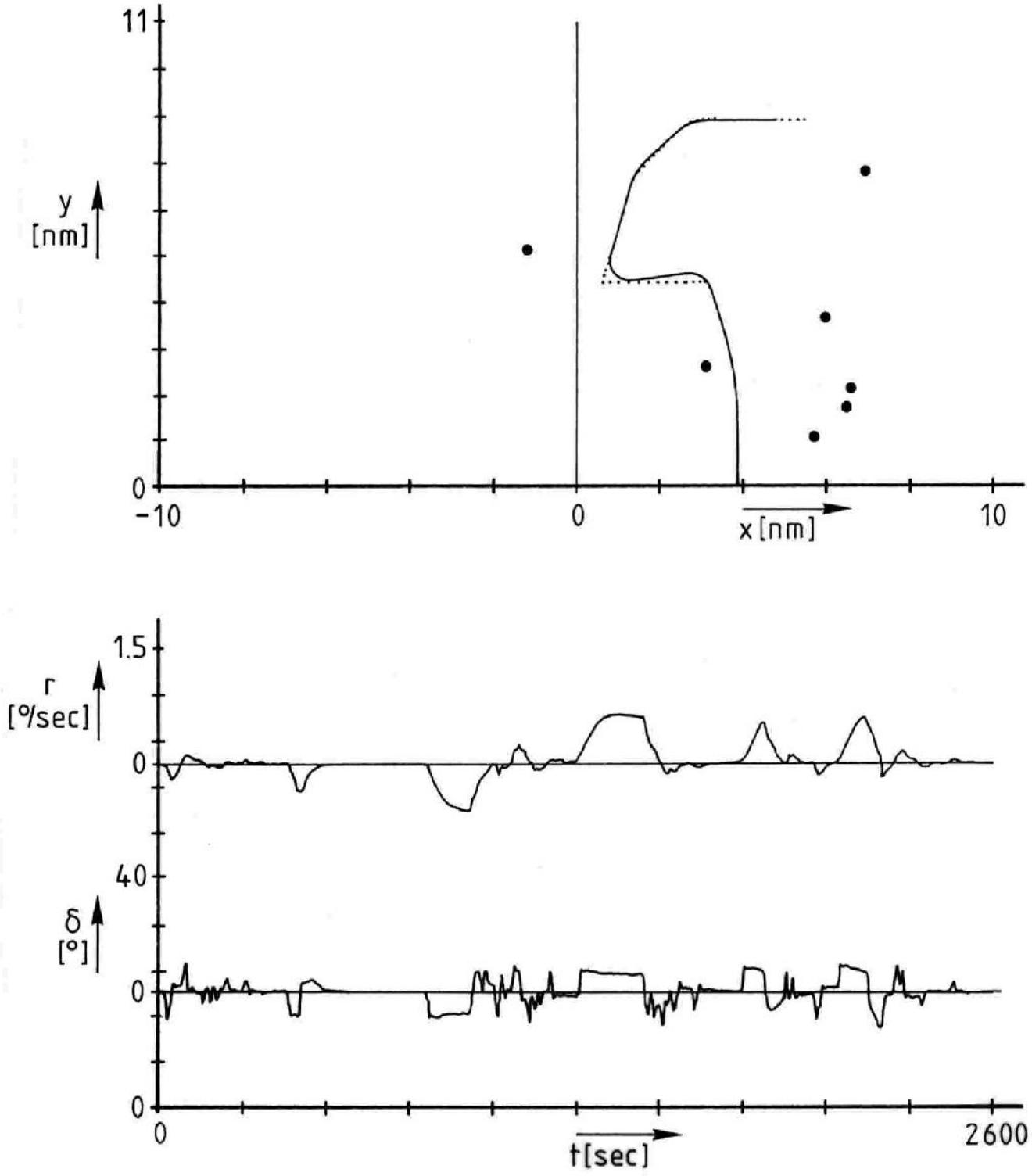

Fig. 6.23.b Results of the ground-speed vector trial

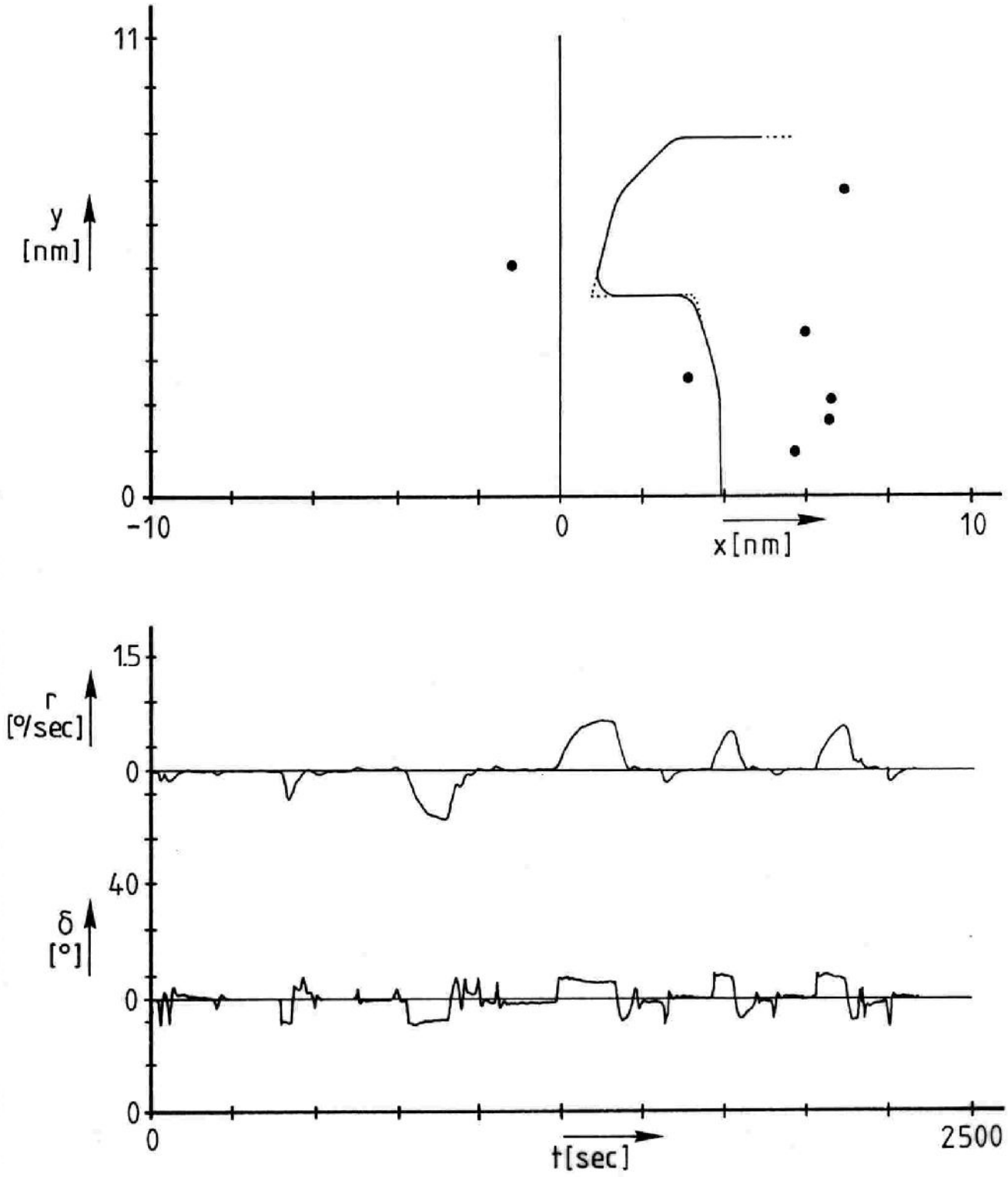

Fig. 6.23.c Results of the track-predictor trial

The results for the mean RMS error for the information conditions A,B and C are given in Table 6.4:

Condition	RMS [m]
A (parallel indexing) :	117
B (speed vector) :	95
C (track predictor) :	33

Table 6.4 Mean RMS error for the 3 conditions

with a very high level of significance ($p << .01$).
The level of significance of the effects for the 3 conditions was determined by performing an analysis of variance on the RMS error (Van Breda and Schuffel, 1989).
The results of Table 6.4 are evidence that the track predictor makes a significant contribution to the accuracy with which a reference track can be sailed: a decrease of the mean RMS error from 100 m., for conditions A and B, to 30 m. for condition C.
The analysis has also demonstrated a rather poor separation between the conditions A and B, although, on the average, the ground-speed vector condition scores slightly better than the parallel-indexing condition.

To take into account the learning effect, for each condition the mean RMS errors were determined for each replication of a particular condition: by each subject 9 tracks were sailed, divided over 3 conditions, thus each condition was repeated 3 times. The results for the RMS-error analysis for the replications are presented in Figure 6.24.
Due to the learning effect, there is a significant improvement for the conditions A and B after the 3 replications. However, a comparison of the final scores after the third replication still shows a significant improvement in accuracy for the predictor-assisted condition C.
From Figure 6.24 it also can be concluded that for the track-predictor condition the learning effect is relatively small and is more or less cancelled out at the second replication. This probably is an illustration of the fact that for predictor-assisted manoeuvring the navigator's acquired knowledge about the ship's manoeuvrability has become less relevant in regard to the navigational performance.

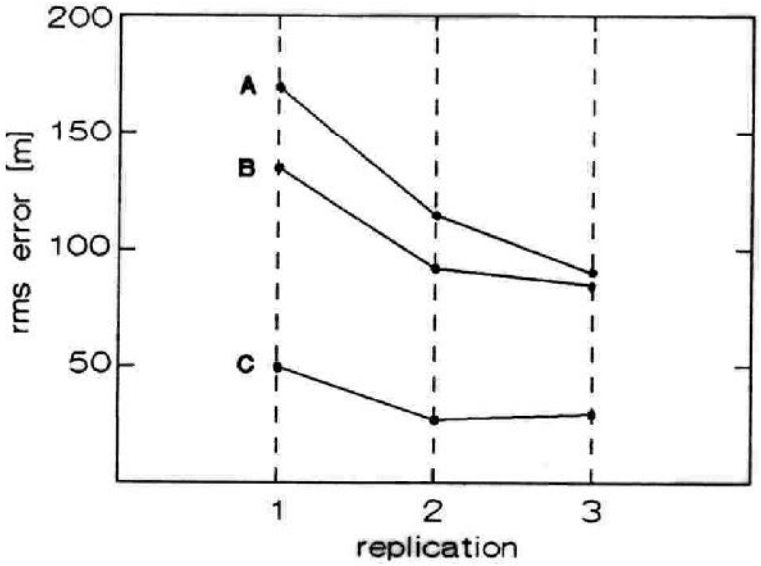

Fig. 6.24 RMS analysis according to replication

To evaluate the influence of the information conditions on the navigational performance for the different navigation tasks, in Figure 6.25 the results of Figure 6.24 were split up according to the magnitude of the course change:

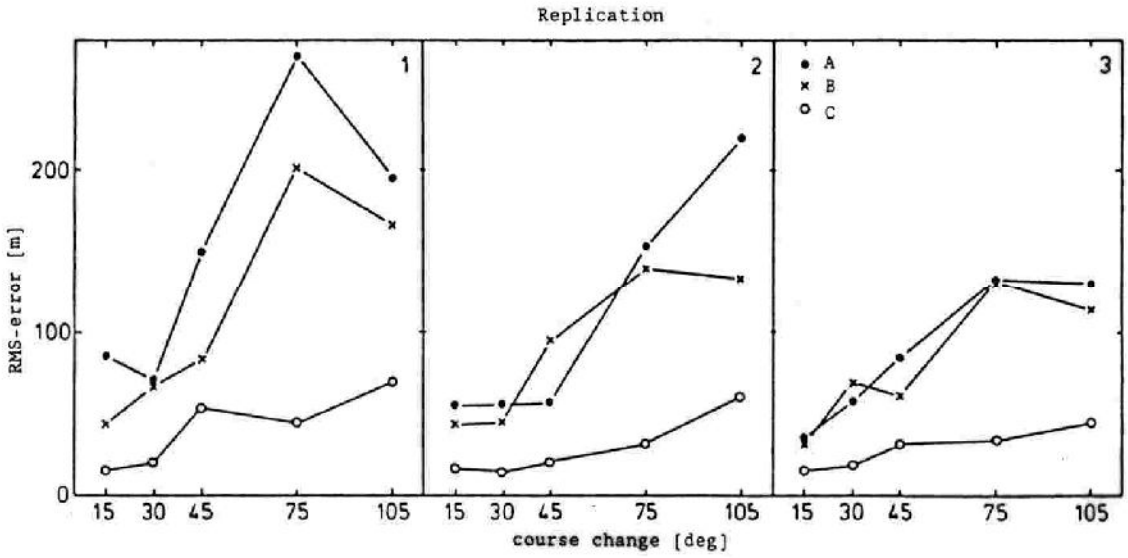

Fig. 6.25 RMS analysis according to course change and replication

The analysis shows a significant increase of the average RMS error as a function of the magnitude of the course change for all information conditions. From these results it also follows that the largest contribution of the track predictor, relative to the other information conditions, is to be expected for large course changes (>45 degrees). In this case the average track deviation (RMS error) is reduced by 70% for the track-predictor condition, compared to the parallel-indexing or ground-speed vector conditions.

To investigate the influence of the information conditions on the way in which the ship was controlled by the subjects, the variability of the recorded rate-of-turn signal was considered to be a measure (Van Breda and Schuffel, 1989).
A calculation of the standard deviation of this signal shows a small difference for the 3 conditions:

Condition	σ_r (deg/sec)
A (parallel-indexing) :	0.202
B (speed vector) :	0.202
C (track predictor) :	0.190

Table 6.5 Standard deviation of the rate-of-turn signal

This small difference might be explained by the fact that for the track-predictor condition (anticipating) steering corrections are performed by the navigator on the basis of even the smallest deviations between predicted and planned track.

7 CONCLUSIONS AND SUGGESTIONS

In this thesis the design of a track predictor for ships is reported. The principle purpose of the track predictor is to assist the navigator in his anticipating capabilities during manoeuvring, thus achieving safer navigation.
To determine a sufficiently accurate prediction model, a geometrical analysis was performed to determine the different variables which are relevant to the shape of the ship's track during manoeuvring. The underlying assumption for this approach was that the navigator's performance could be improved by presenting a predicted track with a shape identical to the ship's actual track.
As a result of the mathematical analysis, a geometrical relation was constructed, by which the shape of the ship's track is completely determined:

$$\underset{\sim}{x}_s^*(s^*) = \underset{\sim}{\Delta x}_u^*(r^*(s^*)) + \underset{\sim}{\Delta x}_v^*(r^*(s^*), v^*(s^*)) \qquad (7.1)$$

From this relation it could be concluded that for a correct prediction of the ship's track, with respect to the ship's surroundings, the ship's rate of turn r^* and sway velocity v^* (both normalized with respect to the forward speed) need to be correctly predicted as a function of the distance covered by the ship s^*.
This implies that the loss of forward speed during manoeuvring, which is the main cause of the time-domain manoeuvring models becoming non-linear, is not required to be explicitly predicted for a prediction of the ship's track. Therefore, regardless of the ship's forward-speed dynamics, a sufficient model to reflect the ship's turning dynamics in relation to the ship's track is given by the relations:

$$\tau^* \frac{dr^*}{ds^*} + r^* = K^* \delta \qquad (7.2)$$

$$v^* = -\gamma^* r^* \qquad (7.3)$$

A correct translation of the predicted track, to adjust the track to the distance covered by the ship since the prediction was calculated, was proven to be a translation of the track on the basis of a correspondence between the real and predicted course.

Further, it has been shown that a global adaptation of the predicted track to disturbing influences such as wind and current, could be obtained by a track-

adaptation mechanism on the basis of rate-of-turn and position deviations.

A suitable method for on-line identification of the prediction-model parameters and the disturbances on the basis of noise-corrupted measurements has been determined by a structural comparison of different, well-known, identification schemes. The common factor of these identification schemes is the calculation of a one-step-ahead predicted output, which is used for the update of the parameters. On the basis of optimal measurement interpretation, an alternative method has been proposed to base the model-prediction on the filtered process output:

$$\hat{y}(k) = \bar{y}(k) + K_y(k)(\tilde{y}(k)-\bar{y}(k)) \quad ; \quad 0 \leq K_y(k) \leq 1 \qquad (7.4)$$

with $K_y(k)$ determined according to the principles of discrete Kalman filtering. The identification algorithm with $\hat{y}(k)$ chosen according to (7.4) may be interpreted as a combined equation-error ($K_y(k) = 1$) and output-error identifier ($K_y(k) = 0$).

The advantages related to the choice of (7.4) are:

- improvement of the convergence speed of the parameter-estimation part, compared to the Parallel MRAS identification algorithm ($K_y = 0$),
- after convergence, considerable bias reduction, compared to the Series-Parallel MRAS or Least-Squares identification algorithm ($K_y = 1$),
- besides the estimation of the parameters, a noise-free estimation of the process state is obtained.

Adaptation to varying parameters is inherently achieved by assuming system noise to be added to the parameters, instead of the introduction of a forgetting factor λ, which is a more artificial way of stating permanent uncertainty about the estimated parameters.

Continuation of the structural analysis of the combined state and parameter estimation scheme showed a direct link with the field of Extended-Kalman filtering. On the basis of this analysis two Extended-Kalman filters were designed for the filtering of the wave motions and the estimation of the ship's yaw dynamics and for the filtering of the ship's position and estimation of the current influence.

Analogous to the relation between MRAS identification and control, a method has been proposed to use the Extended Kalman filter for adaptive model-following control. On the basis of this analogy, a direct compensation mechanism was

derived to compensate for rate-of-turn deviations between ship and model by the autopilot. The resulting control scheme shows a resemblance to the model-update technique proposed by Van Amerongen et al. (1980). The main difference lies in the method of updating the state of the reference model to improve the controller's performance.

Regarding the presentation of the prediction information to the navigator, a straightforward method was chosen of superimposing the predicted track on an integrated manoeuvring and navigation display, as designed by the TNO Institute for Perception. The input of user commands for the predictor could be obtained by a minor extension of the autopilot console. It appeared that, for this integrated approach, the track predictor could be added to the ship's bridge as a logical function between navigation (track planning) and manoeuvring (actual course changing).

Besides experiments in a laboratory environment to test the algorithms for prediction, identification and control, a manoeuvring-simulator experiment was conducted with the experimental track-prediction set-up at the TNO Institute for Perception in Soesterberg.
For this experiment, the track predictor was tested against more conventional methods of navigation such as Parallel Indexing and the presentation of a ground-speed vector.
To judge the influence of the different information conditions on the navigational performance, the experiment was focused on the tracking of various routes, with course changes varying from "easy" (15 degrees) to "difficult" (105 degrees). An analysis of the average route deviation for the different conditions showed the following:

The overall accuracy is improved by using the track predictor. The improvement of the navigational performance manifests itself especially for course changes larger than 45 degrees. In those cases the average route deviation was reduced with 70 %, compared to conventional conditions.

No significant differences were found between the ground-speed vector condition and the Parallel-Indexing condition. This suggests that the speed vector might be useful for the compensation of current influence during track-keeping between two waypoints, while for course changing rate-of-turn information becomes more important.

An analysis of variance of the rate-of-turn signal showed no significant differences for the three conditions, although a decrease of the variance was expected for the track-prediction condition. It seems however that for this condition additional (anticipating) compensatory steering actions are carried out by the navigator, on the basis of relatively small deviations between the desired track and the predicted track.

On the basis of these results it is concluded that the largest contribution of the track predictor is to be expected for large course changes (> 45 degrees). For most existing fairways with course changes up to 30 degrees (IMCO 1972), a less accurate but satisfactory result may also be obtained with the parallel-indexing or ground-speed vector navigation method, compared to the track predictor.
The attractiveness of the track predictor lies mainly in navigation in confined areas (terminal navigation) and emergency manoeuvring: in these situations large course changes are involved, while the effect of these course changes, leading the ship off the planned track, should be made clear to the navigator (avoidance of groundings). For the application of terminal manoeuvring, knowledge about the current and wind speed and direction may rather easily be incorporated into the track-prediction system as a-priori information.
For these conditions the combination of the track predictor with the "autopilot-assisted manual mode" as suggested by Van Amerongen (1982) might particularly be useful. Integration of this rate-of-turn control with the track predictor yields a configuration with which the future effect of the choice of rudder deflections, instead of course changes, may be judged by the navigator.
Further, to extend the usefulness of the track predictor for these situations, time and speed information becomes relevant (collision avoidance). For this purpose more research needs to be done on the predictability of the different relevant signals in the time domain, which requires a more complex prediction model.

Another possible application of the track predictor may be found in the manoeuvring with mine sweepers, where reference tracks with large course changes (180 degrees) are to be sailed as accurately as possible. For this application possible benefits are to be expected from a fully automatic path controller, which could be achieved by extending the integration of the track predictor with the course-changing controller.

Regarding a practical implementation of the track predictor, integration with an electronic sea chart offers a promising combination. A similar simulator experiment demonstrated the improvement of the navigational performance obtained with the electronic chart, when used on its own, to be marginal when compared to a conventional condition (Van Breda and Schuffel, 1989).

APPENDICES

Appendix A

Interfacing between the track predictor and the manoeuvring simulator

The experimental track-prediction system consists of 2 subsystems:

PDP 11/73 for real-time aspects such as:	
- on-line parameter estimation	(period 400 ms)
- autopilot (course-changing controller)	(period 400 ms)
- calculation and adaptation of the predicted track	(period 2 sec.)
- data logging	(period 2 sec.)

IBM PC/AT with Professional Graphics Controller for:
- user interaction (autopilot and radar settings)
- presentation of the manoeuvring information (NAVDIS)
- presentation of the predictor information

Information interchange between the 2 systems takes place on a serial basis, with a baud rate of 9600.

For the experiment these 2 systems were interfaced to the IZF manouevring simulator, consisting of:

- PDP 11/23	: supervisor
- PDP 11/34	: ship model (period 80 ms)
- Bridge set-up	: navigation display, SAC and user consoles

For the interfacing between the PDP 11/73 (prediction and control) and the manoeuvring simulator, a mixed analog/digital approach was chosen:

PDP 11/73 <--> PDP 11/34 (model) :		
analog interfacing:		
- 11/73 analog input:	- rate of turn	r [deg/sec]
	- forward speed	u [m/s]
	- actual rudder angle	δ [deg]
- 11/73 analog output:	- ordered rudder angle	δ_r [deg]

PDP 11/73 <--> PDP 11/23 (supervisor) :		
serial interfacing:		
- 11/73 serial input:	- ship's course	ψ [deg]
	- ship's position	x_s, y_s [m]

The IBM PC/AT for the user interaction was interfaced to 2 user consoles in the ship's bridge by means of the TNO NIC/NOC interface:

user console 1 :
- autopilot and predictor settings - compass read out

user console 2 :
- navigation display settings such as: - range input (1,2,4 or 8 nm) - Variable Range Marker input (range and bearing) - on/off switches for the various markers on the display

For the presentation of the Navigation Display NAVDIS the IBM Professional Graphics Controller RGB output was connected to a 19" colour display in the ship's bridge, thus completing the interfacing according to Figure A.1

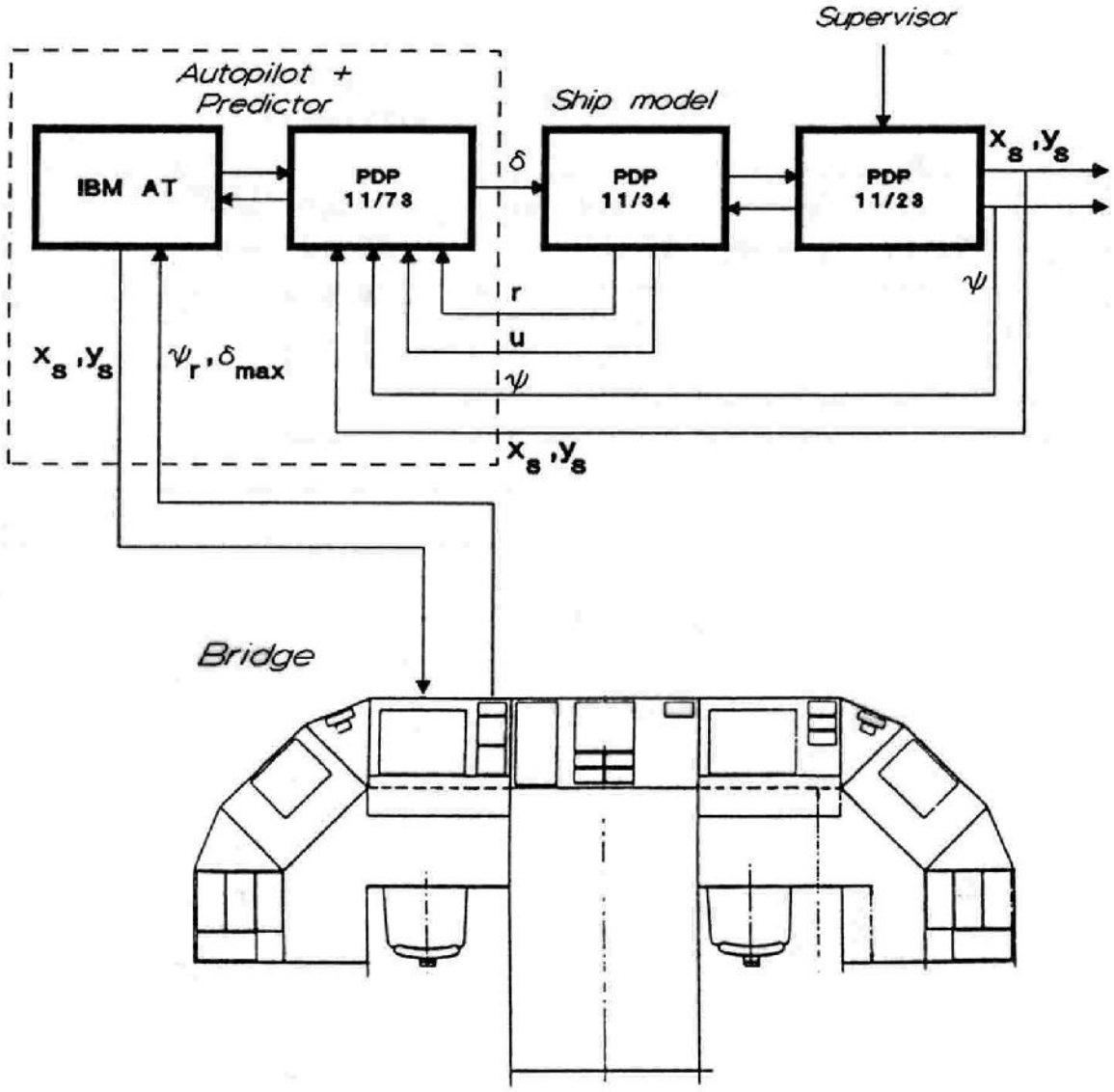

Fig. A.1 Interfacing between the track predictor and the simulator

Appendix B

The ship model

In this appendix specific information is given about the 40.000 DWT container vessel "STS Soesterberg", used for the manoeuvring-simulator experiment.

The principle dimensions are as follows:

Length over all:	225.87 m
Breadth:	30.50 m
Depth:	16.40 m
Draught:	11.20 m
Displacement:	40.000 DWT
Diameter propeller:	7.00 m
Power:	32.450 SHP
Service speed:	22 kn

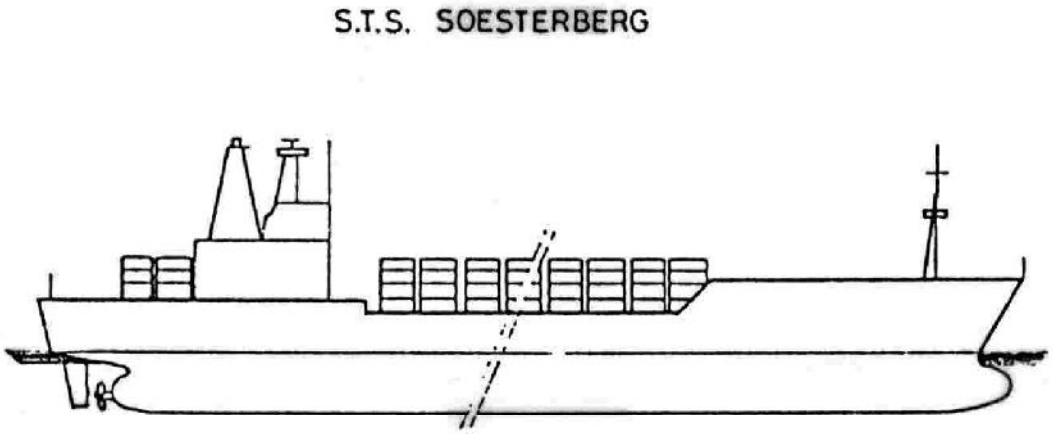

Fig. B.1 Sketch of the "own ship"

The ship's movements are related to a fixed, rectangular, clockwise turning axis system:

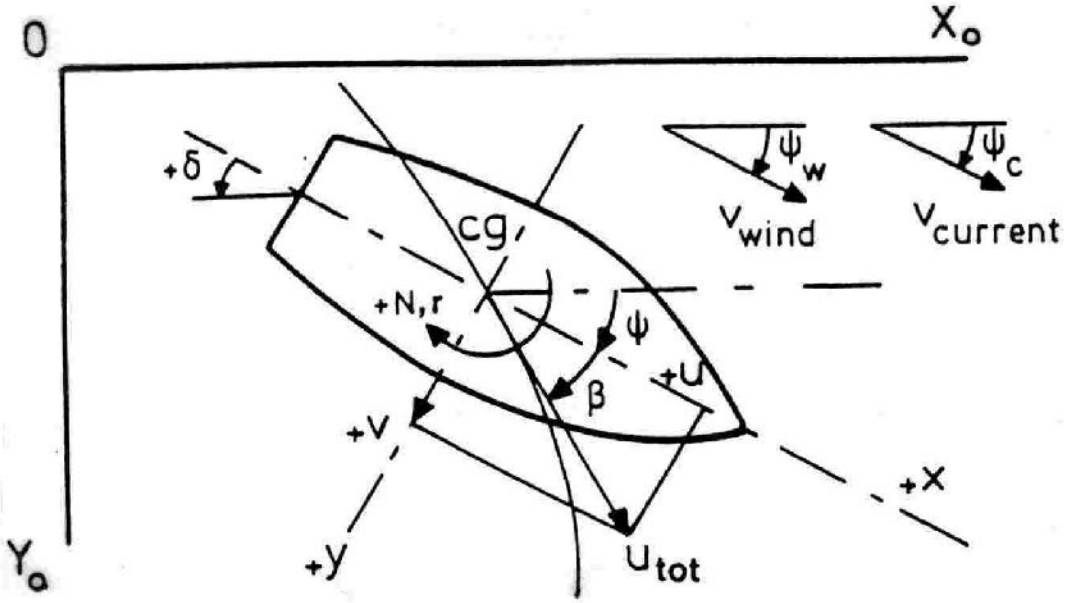

Fig. B.2 Coordinate system and definition of forces and velocities

REFERENCES

Abkowitz, M.A., "Lectures on Ship Hydrodynamics - Steering and Manoeuvrability", Hya Report no. Hy-5, 1964.

Amerongen, J. van, "Adaptive steering of ships - a model-reference approach to improved manoeuvring and economical course keeping", Ph. D. thesis, Delft University of Technology, p. XII, 195, April 1982.

Amerongen, J. van, "Digital model-reference adaptive control with applications to ship's steering", Proceedings 6th IFAC/IFIP Conference on Digital computer applications to process control, Dusseldorf, FRG, 1980.

Amerongen, J. van, C. de Keizer and W. Verhage, "Measurements of the speed of the ship using an automated Snellius method", Int. Shipbuilding Progress, Vol. 24, no. 273, 1977.

Amerongen, J. van, and H.R. van Nauta Lemke, "Recent developments in automatic steering of ships", The Journal of Navigation 39 (1986) no 3, pp. 349-362, 1986.

Arend, A.G.A van den, "Baanpredictor", Master's thesis, Control Laboratory, Delft University of Technology, 1979.

Bech, M., "The reversed spiral test as applied to large ships", Shipping world, Nov. 1968.

Bech, M., and L. Wagner Smitt, "Analogue Simulation of Ship Manoeuvres", Hya Report no. Hy-14, 1969.

Berlekom, W.B., "Simulator Investigations of Predictor Steering Systems for Ships", The Naval Architect, pp. 23-34, 1977.

Bernotat, R., "Prediction displays based on the extrapolation method", Displays and controls, Eds. Bernotat and Gartner, 1971.

Boer, J.P.A. and H. Schuffel, "De scheepsbrug in de jaren '90: Navigatieprestatie en mentale belasting van de wachtdoend officier", TNO Institute for Perception, Soesterberg, 1985.

Boonekamp, P.M.H., "Een baanpredictor voor schepen", Master's thesis, Delft University of Technology, 1978.

Bosch, P.P.J. van den, "PSI - Software Tool for Control System Design", Journal A, vol. 22, no. 2, pp. 55-61, 1981.

Breda, L. van and J.G.S. van de Kooij, "Beschrijving van de brugmockup-ups en simulator t.b.v. het project "Brug '90"", TNO Institute for Perception, Soesterberg, 1985.

Breda, L. van and H. Schuffel, "Het sturen van schepen met baanvoorspelling", TNO Institute for Perception, Soesterberg, 1989.

Breda, L. van and H. Schuffel, "Het sturen van schepen met de elektronische kaart", TNO Institute for Perception, Soesterberg, 1989.

Davidson, K.S.M., and L.I. Schiff, "Turning and course keeping qualities", Trans. SNAME, Vol. 54, 1946.

Dugard, L. and I.D. Landau, "Recursive output error identification algorithms: theory and evaluation", Automatica Vol. 16, pp. 443-462, 1980.

Eda H., and C.L. Crane, "Steering characteristics of Ships in Calm Water and Waves", 1965.

Eykhoff, P., "System identification - parameter and state estimation", John Wiley & Sons Ltd., 1974.

Gerritsma, J., "Scheepshydrodynamica - Golven", Report no. 473-K, Ship Hydrodynamics Laboratory, Delft University of Technology, 1979.

Groen, P., and Dorrestein, R., "Zeegolven", KNMI, Opstellen op oceanografisch en maritiem meteorologisch gebied, no. 11, Staatsdrukkerij, 's Gravenhage, 2976.

Heemink, A.W., "Storm surge prediction using Kalman filtering", Rijkswaterstaat Communications;no.46, Thesis Twente University of Technology, 1986.

Kalman, R.E., "A new approach to linear filtering and prediction problems", Trans. of the ASME, pp. 35-45, March 1960.

Kalman, R.E. and R.S. Bucy, "New results in linear filtering and prediction theory", Trans. of the ASME, pp. 95-108, March 1961.

Keizer, C. de, "Een multivariabel model van de Zeefakkel", Report Control Laboratory, Delft University of Technology, 1977.

Kelley, C.R., "Manual and Automatic Control", J. Wiley and Sons, London, 1968.

Klugt, P.G.M. van der, "Rudder roll stabilization", Ph. D. thesis, Delft University of Technology, p. XVI, 257, October 1987.

Kristiansen, S., "Analysis of ship casualities and its application in design", Proceedings of the International symposium on advances of Marine Technology, Oslo, 1980.

Lammers, H.C., "Towards the practical application of self-tuning adaptive control", Ph. D. thesis, Delft University of Technology, p. 287, January 1984.

Landau, I.D., "Unbiased recursive identification using model reference adaptive techniques", IEEE Trans. Autom. Control, Vol. AC-21, pp. 194-202, 1976.

Leeuwen, G. van, "A simplified non-linear model of a manoeuvring ship", Shipbuilding Laboratory, Delft University of Technology, Report no. 262, 1970.

Maybeck, P.S., "Stochastic models, estimation and control", Vol.I, Academic Press, New York, 1982.

Mendel, J.M., "Discrete techniques of parameter estimation: the equation error formulation", Marcel Dekker, New York, 1973.

Nanninga, J.G., "Ontwerp van een baanpredictor voor schepen", Master's Thesis, Control Laboratory, Delft University of Technology, 1974.

Nomoto, K., T. Taguchi, K. Honda and S. Hirano, "On the steering qualities of ships", Int. Shipbuilding Progress, Vol. 4, 1957.

Norrbin, N.H., "On the design and analysis of the zig-zag test on base of quasi linear frequency response", SSPA Report No. B104-3, 10th ITTC, London, 1963.

Passenier, P.O. and J. van Amerongen, "An adaptive track predictor for ships", Proceedings 8th Ship Control Systems Symposium, The Hague, The Netherlands, 1987.

Passenier, P.O., "Gebruikers-interactie met het baanpredictie-systeem", Interim report STW-project DEL37.0538, April 1987.

Passenier, P.O., "Tracking tasks using a track predictor", Report Control Laboratory, Delft University of Technology, 1988.

Passenier, P.O., "An adaptive track predictor for ships, realization and results", Proceedings IFAC workshop CAMS'89 on expert systems and signal processing in marine automation, Lyngby, Denmark, 1989.

Pierson, W.J., and L. Moskovitz, "A proposed spectrum for fully developed wind seas based on similarity theory of S.A. Kitaigorodskii", Journal of Geophysical Research, Vol. 69, December 1964.

Poulton, E.C., "Tracking skill and Manual Control", Academic Press, New York, 1974.

Reissenweber, M.G., "Baanpredictie voor schepen", Master's thesis, Control Laboratory, Delft University of Technology, 1975.

Schelling, C.H., "The influence of disturbances on the steering of a ship", Master's thesis, Control Laboratory, Delft University of Technology, 1977.

Schuffel, H., "Human control of ships in tracking tasks", Ph. D. Thesis, Katholieke Hogeschool Tilburg, p. 179, June 1986.

Shell, "Radarnavigatie; De parallel index plotting methode", Rotterdam, 1975.

Sheridan, T.B., "Three models of preview control", IEEE Transactions for Human Factors in Electronics, Vol. 7, p. 91-102, 1966.

Söderström, T. and P. Stoica, "System Identification", Prentice Hall International, Series in Systems and Control Engineering, 1989.

Spaans, J.A., "Parallel-Index Methode", Nautisch Technisch Tijdschrift De Zee, Rotterdam, 1979.

Wagner, B., "Windkräfte an Ueberwasserschiffen", Schiff und Hafen 12, Jahrgang 19, 1967.

ACKNOWLEDGEMENTS

The adaptive track predictor reported in this thesis is the result of a research project at the Control Laboratory of the Faculty of Electrical Engineering of the Delft University of Technology. The investigations were supported (in part) by the Netherlands Technology Foundation (STW).

I wish to thank Prof.ir. H.R. van Nauta Lemke and the Royal Netherlands Navy for enabling me to work on this project instead of being conscripted into the army.

I wish to acknowledge the cooperation with the TNO Institute for Perception. Especially, I wish to thank dr.ir. H. Schuffel and ing. L. van Breda for their enthusiastic support in preparing and carrying out the experiment on the manoeuvring simulator.

I wish to thank Mr. J.W.G. Vink and the navigators of the Hogere Zeevaartschool Vlissingen for their willingness to participate in the experiment.

I wish to acknowledge the fruitful discussions with the members of the STW users' commission every half year.

I wish to acknowledge the many valuable suggestions made by Prof.dr.ir. J. van Amerongen during the last five years and his efforts towards a successful completion of the project.

I wish to thank Prof.dr.ir. P.P.J. van den Bosch for the fruitful discussions and his encouraging me to complete this thesis.

I wish to thank Ms. J.B. Zaat-Jones for reviewing the manuscript and Mr. G. van Berkel, who has drawn part of the figures.

Last but not least, I wish to thank my parents for their support during my study and Renée for her optimism and patience during the writing of this thesis.

CURRICULUM VITAE

Peter Passenier werd op 29 september 1960 geboren te Sint Laurens.

- In 1978 behaalde hij het diploma Gymnasium β aan de Christelijke Scholengemeenschap Walcheren.

- Vanaf 1978 werd de studie Elektrotechniek aan de Technische Hogeschool Delft gevolgd, alwaar hij in 1984 afstudeerde.

- Van 1984 tot 1989 is Peter werkzaam geweest als wetenschappelijk medewerker in tijdelijke dienst bij het Laboratorium voor Regeltechniek in het kader van het STW project "Baanpredictie van schepen voor een veiliger navigatie".

- In september 1989 is hij in dienst getreden als wetenschappelijk medewerker bij het TNO Instituut voor Zintuigfysiologie te Soesterberg, afdeling Technische Menskunde.

STELLINGEN

behorende bij het
proefschrift van
P.O. Passenier

Delft, 28 november 1989.

1. Voor een optimaal gebruik van de baanpredictor dienen de baanpredictorconsole en de stuurautomaatconsole te worden gecombineerd tot een functioneel logisch geheel binnen een geïntegreerde manoeuvreer- en navigatieomgeving. Deze integratie van bedieningsmiddelen sluit conceptueel goed aan bij de geïntegreerde presentatie van predictie- en manoeuvreergegevens op het navigatiescherm.

2. Voor het aantonen van het effect van de baanpredictor op de navigatieprestatie van de mens is de mogelijkheid tot het uitvoeren van een gecontroleerd experiment in een realistische omgeving noodzakelijk. Vanwege deze vereiste controleerbaarheid en de benodigde grote hoeveelheid data voor een statistisch verantwoorde toetsing van de hypothese, is een "full scale" simulatorexperiment met proefpersonen te prefereren boven experimenten op zee.

3. *Equation-error* en *Output-error* identificatieschema's zijn te herleiden tot twee extreme vormen van gecombineerde toestands- en parameterschatting.

4. Het modelreferentie adaptief regelen met behulp van een Extended Kalman filter is analoog aan een regeling volgens het *model update* principe. Het verschil tussen beide methoden uit zich in de wijze waarop de toestand van het referentiemodel wordt aangepast aan de metingen.
   J. van Amerongen, "Digital model-reference adaptive control with applications to ship's steering", Proceedings 6th IFAC/IFIP Conference on Digital computer applications to process control, 1980

5. Introductie van (additieve) systeemruis op de parameters ter verkrijging van adaptatie bij parameterschatting is (volgens de principes van Kalman filtering) methodologisch beter verantwoord dan de introductie van een (multiplicatieve) vergeetfactor.

6. Baanpredictie is zinvol voor het vinden van de juiste baan.

7. Vanwege het multidisciplinaire karakter van de regeltechniek dient de regeltechnicus te beseffen dat zonder wederzijds aanvaarde definities van begrippen een gedachtenwisseling over begrippen kan ontaarden in een woordenwisseling zonder wederzijds begrip.

8. Het dragen van formele kleding tijdens een sollicitatiegesprek levert een nodeloos kleurloze waarneming van de sollicitant als informatiebron op.
Het dragen van vrijetijdskleding tijdens een dergelijke gelegenheid zou derhalve dienen te worden gestimuleerd.

9. Gezien het accent dat bij bepaalde vormen van sport op het routinematig verrichten van motorische handelingen wordt gelegd, dient men zich als trainer af te vragen of het op de lange termijn niet méér de moeite loont om met een robot, voorzien van enige elementaire vormen van kunstmatige intelligentie, in zee te gaan dan te proberen door middel van training de vereiste motorische routines bij een menselijke pupil te ontwikkelen.

10. Voor het verhogen van het inzicht van de gemiddelde leerling in de exacte vakken op het Voorbereidend Wetenschappelijk Onderwijs, dient meer aandacht te worden besteed aan het tonen van de onderlinge verbanden tussen en de historische ontwikkeling van de verschillende vakgebieden. Op deze wijze wordt voor de leerling het accent verplaatst van het moeten opstellen van verschillende beschrijvende modellen tussen vragen en antwoorden naar het kunnen opstellen van een verklarend model ten aanzien van de gepresenteerde theorie, met mogelijkheid tot extrapolatie naar andere, niet in het kader van het onderwijs vallende, gebieden.

11. Volgens de stelling van Gödel is artikel 3.7 van het promotiereglement, dat de promotoren na dienen te gaan of de stellingen van de promovendus verdedigbaar zijn, niet in alle gevallen uitvoerbaar.
E. Nagel en J.R. Newman, "Gödel's proof", 1958

12. Programmeren is rangschikken van iets en niets, van niets tot iets.